Modelling stromal FAK regulation of tumour growth, angiogenesis and progression

Batista, Silvia

Modelling stromal FAK regulation of tumour growth, angiogenesis and progression

Sílvia Batista

Thesis submitted for the Degree of Doctor of Philosophy

University of London

August 2012

Adhesion and Angiogenesis Laboratory

Centre for Tumour Biology

Barts Cancer Institute – A CR-UK Centre for Excellence

Queen Mary University of London

Charterhouse Square

London EC1M 6BQ

United Kingdom

DECLARATION OF AUTHORSHIP

I, Sílvia Batista, confirm that the work presented in this thesis is my own and the work of other persons has been properly cited and acknowledged.

Signed:

COPYRIGHT NOTICE

ABSTRACT

The growth of tumours within a whole organism depends on the tumour microenvironment. This involves both resident stromal cells, such as endothelial cells and fibroblasts, and also bone marrow derived stromal cells. Integrins and growth factor receptors are known regulators of the tumour stroma. Since focal adhesion kinase (FAK) is a downstream effector of both integrins and growth factor receptors it likely also plays an important role in the regulation of the tumour microenvironment.

Using adult mice where FAK is deleted ubiquitously after treatment with tamoxifen my data demonstrate that loss of stromal FAK inhibits tumour growth and angiogenesis but increases metastasis burden in experimental metastasis assays even when the tumour cells themselves still express FAK. Moreover, my data indicate loss of FAK in the bone marrow (BM) compartment and specifically in myeloid cells is sufficient to enhance tumour metastasis in experimental metastasis assays and in a spontaneous tumour model. In contrast loss of bone marrow FAK was not sufficient to affect primary tumour growth or angiogenesis. Taken together these data demonstrate that bone marrow derived FAK plays a significant but differential role in primary tumour growth and metastasis.

In a parallel study, I have developed a novel set of transgenic mice to enable us to dissect the mechanism of FAK function in primary tumour growth, metastasis and angiogenesis. I have generated point-mutant FAK knockin-knockout mice where mutant FAK is inducibly expressed (knockin) and endogenous FAK deleted (knockout) in specific cell types in adult mice. Here I show efficient deletion of mouse FAK and expression of FAK 861F mutant in tamoxifen-treated endothelial cells isolated from mice. Importantly the FAK 861F mutation in endothelial cells was sufficient to decrease tumour growth and angiogenesis *in vivo* suggesting that the FAK-P-Y861 phosphorylation site plays an important role in tumour growth and angiogenesis.

TABLE OF CONTENTS

LIST OF FIGURES

LIST OF TABLES

1. INTRODUCTION

1.1. Tumourigenesis

Tumourigenesis defines a multistep process that drives the progressive transformation of normal cells into highly proliferative derivatives. The most important characteristic of a cancer cell is the defect in regulation of normal cell proliferation and homeostasis. Hanahan and Weinberg (Hanahan and Weinberg, 2000; Hanahan and Weinberg, 2011) originally described at least six hallmarks of cancer: self-sufficiency in growth signals; insensitivity to growth inhibitory signals (evading growth suppressors); evasion of programmed cell death (apoptosis); limitless replicative potential; sustained angiogenesis (see **1.3**) and tissue invasion and metastasis (see **1.2**).

Although tumour cells proliferate under inappropriate conditions they do not necessarily proliferate faster than normal cells, rather their growth is not restrained to appropriate time and conditions. Genetic alterations in human cancers generally comprise activation of proto-oncogenes (into oncogenes) and inactivation of tumour suppressor genes. Oncogenes can induce expression of growth factors, growth factor receptors, signal transducers and transcription factors that allow the liberation of cancer cells from dependence of external growth signals. Tumour suppressors, on the other hand, limit cell growth and proliferation by activation of senescence or apoptosis programmes (Hanahan and Weinberg, 2000).

Normal epithelial cells cultured *in vitro* show contact inhibition through cell-to-cell and cell-to-substrata interactions that restrain their proliferation. Cancer cells lose this contact inhibition and are able to proliferate irrespective of interactions with other cells or substrata. *In vivo* extracellular matrix components (ECM) that form the cell basement membrane generate physical barriers that restrain and control proliferation (see **1.4**) (Eagle and Levine, 1967) . Cancer cells are capable of changing their extracellular matrix receptor profiles, i.e., integrins, thus controlling interactions with the ECM and switching cell behaviour from quiescent to motile and proliferative (Desgrosellier and Cheresh, 2010; Kren *et al*., 2007).

Finally it is accepted that to generate solid tumours cancer cells have to acquire unlimited replicative potential. Telomere shortening has been shown to induce replication-induced senescence and limit replicative potential. Perhaps for this reason telomerase (the enzyme responsible for telomere elongation) was shown to be expressed in 85% of tumours and appointed as a possible cancer therapy target (Martinez and Blasco, 2011).

1.2. Tumour metastasis

Metastasis is defined as the development of secondary tumours at a site that is distant from the location of the primary cancer (Coghlin and Murray, 2010). Traditionally this process has been viewed as a final step in tumour progression. The conventional description of the metastatic steps include: (1) extracellular matrix degradation and local invasion of host stroma by tumour cells; (2) intravasation into lymphatic or vascular vessels; (3) survival in the circulation; (4) extravasation into target tissues; (5) survival and colonisation of these tissues by metastatic tumour cells to form micrometastases and (6) proliferation and angiogenesis activation to form clinically detectable metastasis (Talmadge and Fidler, 2010).

Metastatic cell behaviour has been studied for decades and is still not fully understood. In order for cancer cells to invade the surrounding stroma they have to overcome cell-to-cell adhesion. Therefore one of the common concepts associated with metastasis is epithelial-to-mesenchymal transition (EMT) which is the process by which cells lose their epithelial characteristics, such as cell-to-cell adhesion and planar and apical polarity, to acquire mesenchymal features such as motility and invasiveness (Polyak and Weinberg, 2009). E-cadherin is a major mediator of cell-to-cell adhesion between normal epithelial cells (Aberle *et al*., 1996) and its expression has been shown to be lost during tumour metastasis in several human epithelial cancers (Birchmeier and Behrens, 1994). In mouse models, loss of E-cadherin expression was also shown to be coincident with the transition to invasive carcinoma and associated with early invasion and metastasis (Perl *et al*., 1998). β-catenin interacts with the cytoplasmatic tail of E-cadherin at the plasma membrane and by

linking it to the cytoskeleton is essential for E-cadherin function (Aberle *et al.*, 1996; Stappert and Kemler, 1994). Translocation of β-catenin from the adherens junction to the nucleus has been associated with the loss of membrane E-cadherin that, through activation of target genes, such as the E-cadherin gene repressor *SLUG,* and triggers EMT (Conacci-Sorrell *et al*., 2003). Loss of E-cadherin was analysed in human tissue samples of one of the most well studied epithelial tumours, colorectal cancer, that has a very defined histological progression from adenoma to carcinoma. These tumours have an epithelial growth pattern and only at the invasive front they resemble EMT. Together with plasma membrane loss of E-cadherin the authors have observed an increased nuclear localisation of β-catenin at the invasive front of the tumour, features that are absent in the central mass of the tumour. Interestingly growing metastases again showed membrane localisation of E-cadherin and β-catenin (Brabletz *et al*., 2001). This study suggests that the defects in cell-to-cell adhesion, observed in invasion, might be reversed in order to re-establish a metastatic growing tumour. Some authors had already suggested that tumour cells have to reverse EMT through a mesenchymal-epithelial transition (MET) after dissemination to be able to form a metastasis phenotypically similar to the primary tumour (Brabletz *et al*., 2005). These studies suggest cancer cells change their adhesion profiles thoughout the metastatic process.

Invasion of tumour cells into surrounding stroma is also accompanied by defects in the extracellular basement membrane. Tumour cells at the invasive front are capable of producing proteases that degrade ECM and facilitate invasion and dissemination into the circulation (Liotta, 1986). Tumour blood vessels, because of their leaky and haemorrhagic features (see **1.3**), can provide an escape route for cancer cells into the

blood system (Bergers and Benjamin, 2003). This step is called intravasation. An elegant study by Wickoff *et al* using *in vivo* confocal microscopy to track tumour cells showed that metastatic cancer cells have enhanced orientation towards blood vessels. This blood vessel intravasation is a critical step for metastasis (Wyckoff *et al.*, 2000). Alternatively tumour cells can also enter lymphatic capillaries due to their discontinuous junctions that make them highly permeable. The lymphatic system is used to filter excess extravascular fluid before it returns into the venous blood system. Once tumour cells enter the lymphatic vessels they can be drained into lymph nodes where they can form metastasis. Tumour cells can re-enter the blood circulation through the venous system or through the lymph node blood vessels. For that reason lymphatic spread can also constitute an indirect route for blood tumour cell dissemination (Chambers *et al*., 2002; Tammela and Alitalo, 2010). Lymph node metastasis is considered a negative prognostic factor in many cancer types (Pai *et al*., 2011; Tammela and Alitalo, 2010).

As stated above cancer cell dissemination can occur after local invasion, but, it has also been suggested to occur even before the tumours invade the surrounding stroma. Using two mouse models of invasive mammary carcinomas (BALB-NeuT and MMTV-PyMT) Husemann *et al*, have observed dissemination of tumour cells even before disruption of basement membrane in the primary hyperplastic lesions. Moreover analysis of 607 breast cancer patient samples found no correlation between number of disseminated tumour cells in the bone marrow, where metastasis are usually found, and primary tumour size (Husemann *et al.*, 2008). In the same line using a mouse model of PDAC to study the various stages of pancreatic cancer progression Rhim *et al* have shown, more recently, that EMT, migration, bloodstream

entry and seeding of the liver by tumour cells can occur in parallel or even before detectable tumour formation at the primary site (Rhim *et al*., 2012). These studies suggest cancer cell dissemination and metastasis might also be an early event in tumour progression and can perhaps explain two main clinical observations: (1) The appearance of metastatic lesions years after resection of small tumours without any detectable metastasis at the time of diagnosis (Pantel *et al*., 2008); (2) Patients who present with neoplasms at metastatic sites but with no detectable primary tumour. This accounts for 4 to 5 % of invasive cancers (Greco and Hainsworth, 2009). It has been shown in breast cancer that even patients with early stage tumours can relapse after surgery suggesting dissemination at early stages of tumour progression (Schmidt-Kittler *et al.*, 2003).

In order for disseminated cancer cells to form distant metastasis they have not only to acquire abnormal migration features but also stem cell like properties, i.e., the ability to self-renewal and initiate new tumours at distant sites. For this reason disseminated-cancer cells with self-renew capabilities have also been named cancer stem cells (CSCs) and were first identified in haematological malignancies such as acute myeloid leukaemia (AML). Bonnet and Dick have identified $CD34^{+}CD38^{-}$ subpopulations that could differentiate *in vivo* to reacquire the same leukaemic properties in mice as seen in patients (Bonnet and Dick, 1997). Several studies in breast, brain and colorectal cancer identified CSC populations that are able to initiate tumours *in vivo* (Al-Hajj *et al*., 2003; O'Brien *et al*., 2007; Shipitsin *et al*., 2007; Singh *et al*., 2004).

Importantly, because disseminated cancer cells have to be able to survive in the ciculation, extravasate into target organs and have self-renewal capabilities that allow them to initiate tumours, metastasis is an inefficient process. From the tumour cells that are able to disseminate into the circulation only a small percentage will develop metastases (Weiss, 1990). Using *in vivo* video microscopy to follow B16F1 tumour cells after tail vein injection Luzzi *et al* have demonstrated that even though about 80% of the cells are able to survive in the circulation and extravasate, only 1 in 40 can actually form micrometastases in the liver by day 3. More importantly only 0.01% of the injected cells can form macroscopic tumours by day 13 and about 36% remain as solitary cancer cells, majority of which were in a dormant state (Luzzi *et al*., 1998). These dormant cells remain in a state of low proliferation in micrometastasis or as solitary cells in a quiescence state until they are stimulated to proliferate again (Eyles *et al*., 2010; Suzuki *et al*., 2006). This is one of the major clinical challenges as tumour recurrence can occur several years after treatment of a primary tumour and these cells were shown to be resistant to chemotherapy (Meng *et al*., 2004; Naumov *et al*., 2003). The factors responsible for dormancy and reactivation of dormant cells are still under investigation but the microenvironment plays a crucial role. When Suzuki *et al* isolated disseminated tumour cells that were in a dormant state in metastasis free organs and implanted them into organs that are preferred sites of metastasis these cells reactivated their tumourigenicity (Suzuki *et al*., 2006). This study brings us back to Stephen Paget's 'seed and soil' hypothesis; that metastasis to a certain organ is not random but depends on the interactions with its microenvirnoment (Paget, 1889).

1.3. The stromal contribution to tumour progression

Tumours are complex masses of transformed and untransformed cells (stromal cells) that interact to facilitate tumour growth, invasion and dissemination of tumour cells. The stromal contribution in tumour progression was recently reviewed by Hanahan and Coussens as exemplified in **Fig. 1** (Hanahan and Coussens, 2012) and will be the main focus of my PhD thesis. I will concentrate on two main compartments within the stroma: the vascular compartment; and the bone marrow compartment from which infiltrating immune cells, cancer associated fibroblasts, vascular endothelial cells and blood vessel supporting cell progenitors can be derived (**Fig. 1**). In this chapter I will give a brief description of vascular and haematopoietic embryonic development and the main characteristics and functions of these two compartments in the maintenance of organism homeostasis. Then I will focus on the different modulation and role of vascular and haematopoietic compartments in the support of tumour angiogenesis, tumour growth and metastasis.

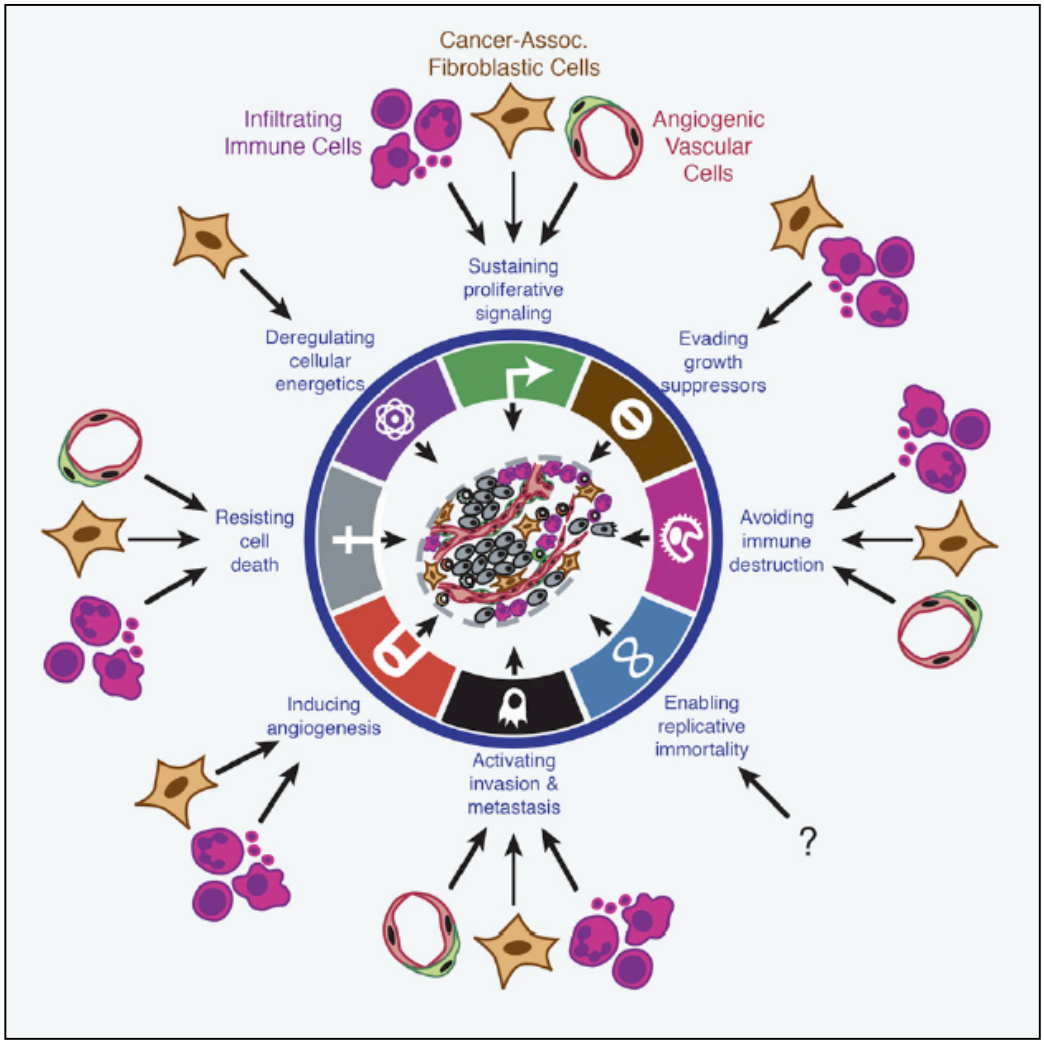

Figure 1: The stromal contribution in tumour progression.

Tumour stroma plays an essential role in all the steps during tumour progression. Hanahan and Coussens divided stromal cells into 3 main classes: infiltrating immune cells, cancer associated fibroblastic cells and angiogenic vascular cells. My PhD thesis will focus on the role of angiogenic vascular cells in tumour growth and angiogenesis and the function of bone marrow derived infiltrating immune cells in tumour growth and metastasis (Adapted from (Hanahan and Coussens, 2012)).

1.3.1. Vascular compartment

An Anatomical Study of the Motion of the Heart and of the Blood in Animals published by William Harvey in 1628 was the first description of the cardiovascular system. This is the first organ system that becomes functional in the vertebrate embryo. The two most basic components of the vascular system are endothelial and blood cells (Risau, 1997). Small blood vessels are composed mostly of endothelial cells (ECs) with few associated pericytes, medium size vessels are surrounded by pericytes and larger vessels are supported additionally by smooth muscle cells (SMCs) (Carmeliet, 2003).

A. Embryonic blood vessel development

Blood vessel development involves 2 processes: vasculogenesis and angiogenesis. Vasculogenesis occurs mainly during development and consists of the formation of blood vessels from undifferentiated ECs precursors, the angioblasts. After the primitive vascular network is established, sprouting of new capillaries from pre-existing ones can form blood vessels, a process known as angiogenesis. (Carmeliet, 2000; Risau, 1997).

I. Vasculogenesis

Vasculogenesis and haemangiogenesis are thought to begin in the yolk sac with the haemangioblast, a common precursor of both endothelial and haematopoietic stem cells (HSCs). In mice, the first mature embryonic blood cells are detected in blood islands of the yolk sac at embryonic stage E7.5 in which the central cells will give rise to embryonic haematopoietic cells whilst peripheral cells differentiate into endothelial cells that eventually determine the primitive vascular plexus (Carmeliet, 2000; Choi, 1998). Given their common origin, endothelial and embryonic haematopoietic stem cells express several common markers such as Tie-2 (Hamaguchi *et al*., 1999), CD-31 (Platelet endothelial cell adhesion molecule-1, (PECAM-1) (Baumann *et al*., 2004), CD144 (VE-cadherin) (Kim *et al*., 2005) and vascular endothelial growth factor receptor 2 (VEGFR-2/flk-1) (Shalaby *et al*., 1995). Angioblast differentiation is dependent on vascular endothelial growth factor (VEGF), VEGFR-2 and basic fibroblast growth factor (bFGF) (Carmeliet, 2000).

II. Angiogenesis

Angiogenesis occurs during development and in the adult organism and it can contribute to the pathogenesis of many disorders such as cancer, psoriasis and arthritis (Beck and D'Amore, 1997; Carmeliet, 2003). During development angiogenesis starts taking place from embryonic stage E8.5 onwards. Growth of new blood vessels from existing ones comprises 2 main steps: sprouting and intussusception. Sprouting angiogenesis involves migration and proliferation of endothelial cells in order to extend the new capillaries. Intussusception angiogenesis is the process by which existing blood vessels are split in order to generate new ones (Conway *et al*., 2001; Djonov *et al*., 2000).

Sprouting angiogenesis is divided into several steps that involve interactions between endothelial cells and mural cells and ECM components: (1) endothelial cell activation; (2) basement membrane degradation; (3) endothelial cell proliferation and migration; (4) tube cell formation, elongation and remodelling; (5) and maturation of blood vessels (**Fig.2**).

During endothelial cell activation existing vessels are dilated, a process that involves nitric oxide; vascular permeability promoted by VEGF (also named vascular permeability factor) is increased allowing the extravasation of plasma proteins that will form the scaffolding matrix necessary for the migration of endothelial cells; and angiopoietin-1 (Ang-1) interaction with the endothelial Tie-2 receptor inhibits excessive vascular permeability that would lead to vessel leakage and circulatory

collapse (Thurston *et al*., 2000). Basement membrane degradation is regulated by angiopoietin-2, an inhibitor of Tie-2 signalling. At this stage vessels become destabilised by losing interendothelial cell contacts and detachment of endothelial cells from the supporting muscle smooth cells (Gale and Yancopoulos, 1999). Matrix metalloproteinases (MMPs) degrade the extracellular matrix releasing growth factors sequestered within the matrix such as VEGF, bFGF and platelet derived growth factor (PDGF) that are important for endothelial cell proliferation and migration (Nelson *et al*., 2000). Once the basement membrane has been dissolved endothelial cells are free to proliferate, migrate and assemble into new vessels stimulated by the numerous pro-angiogenic factors such as VEGF, bFGF and Ang1 (Carmeliet, 2000). Cell adhesion molecules such as integrins, that will be described further, have an important role in endothelial cell migration and tube formation (Eliceiri and Cheresh, 1999). The maturation of vessels is initiated by the recruitment of pericytes and deposition of new basement membrane (Carmeliet, 2000; Kalluri, 2003). Signalling via transforming growth factor beta-1 (TGF-β1), Ang-1 and Tie-2 stabilises endothelial cell-pericyte interactions (Carmeliet, 2003).

Endothelial sprouts contain two populations of cells: tip cells and stalk cells. Tip cells are located at the tip whilst stalk cells are found along the vascular body. Sprouting angiogenesis is guided by the coordination between tip cell migration and stalk cell proliferation in response to VEGF (**Fig.2**).

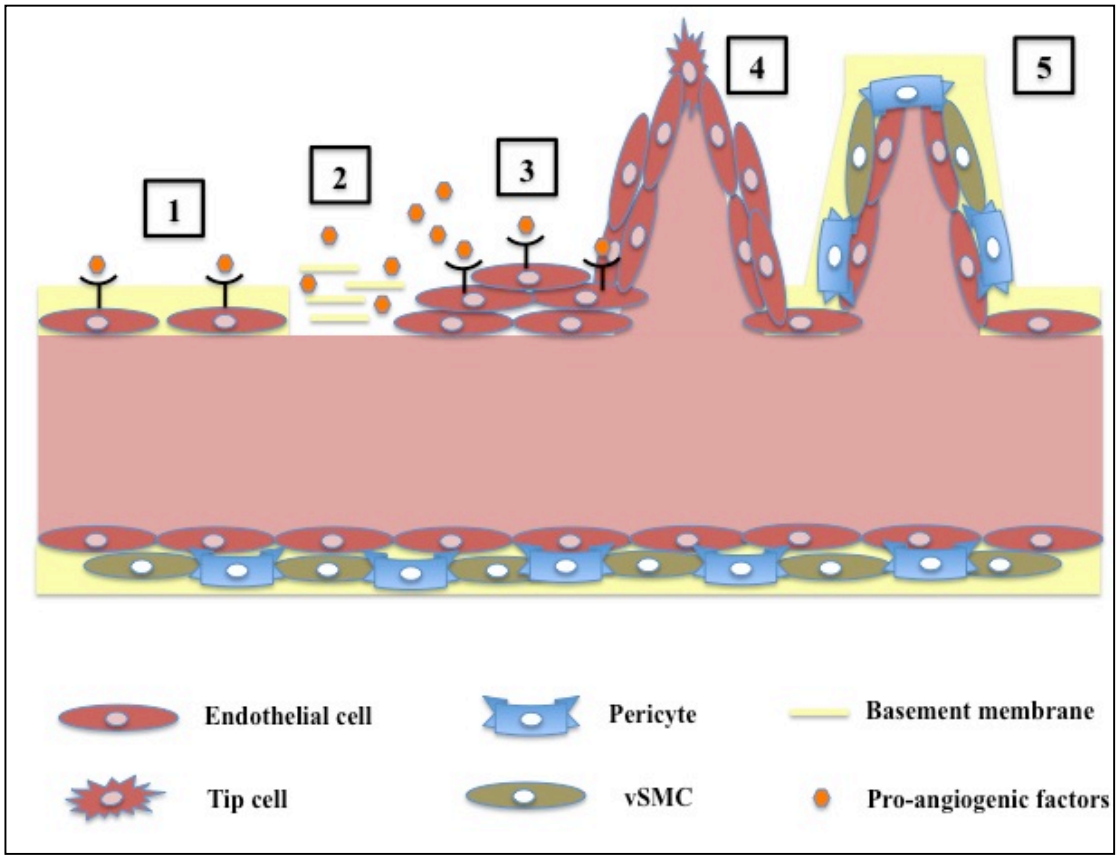

Figure 2: Sprouting angiogenesis

Sprouting angiogenesis involves: 1) endothelial cell activation, mainly dependent on VEGF; 2) basement membrane degradation by matrix metalloproteinases (MMPs) that releases growth factors such as VEGF and bFGF; 3) endothelial cell proliferation migration governed by specialised tip cells in response to pro-angiogenic factors such as VEGF; 4) tube cell formation, elongation and remodelling mediated by cell adhesion molecules such as integrins; 5) maturation of blood vessels by recruitment of pericytes and vascular smooth cells (vSMCs) and deposition of new basement membrane and stabilisation of endothelial-pericyte interactions by Ang-1 and TGF-β1.

B. Growth factor pathways in angiogenesis

Angiogenesis is dependent on the balance between pro- and anti-angiogenenic factors. Pro-angiogenic factors include vascular endothelial growth factor vascular endothelial growth factor (VEGF), platelet-derived growth factor (PDGF), fibroblast growth factor (FGF), angiopoietins and transforming growth factor β (TGF-β) (Adams and Alitalo, 2007; Carlson *et al*., 2001; Karsan *et al*., 1997; ten Dijke and Arthur, 2007). On the other hand, angiostatin that results from degradation of plasminogen; endostatin that is derived from collagen XVIII; and thrombospondin-1 are considered endogenous anti-angiogenic inhibitors (Folkman, 2006; Lawler, 2002). VEGF is considered the major regulator of blood vessel formation and for this reason its function and signalling in angiogenesis will be described separately (Leung *et al*., 1989; Yancopoulos *et al*., 2000).

I. Vascular endothelial growth factor and its receptors in angiogenesis

VEGF was initially designated vascular permeability factor due to its ability for increasing blood vessel permeability (Keck *et al*., 1989). VEGF knockout mice show defects in vasculogenesis with delayed, but not abortive, differentiation of endothelial and blood cells (Carmeliet *et al*., 1996). The VEGF protein family comprises seven members: VEGFs A-E and placenta growth factor (PIGF) (Robinson and Stringer, 2001). VEGF-A is the most studied isoform and has a pivotal role in angiogenesis by controlling endothelial cell proliferation, survival, migration, differentiation, tube formation, permeability and vessel maintenance (Carmeliet, 2005; Gerber *et al*., 1998;

Gupta *et al*., 1999). VEGF-A has five splicing variants: 121, 165, 183, 189 and 206. $VEGF_{165}$ and $VEGF_{121}$ are the most predominant forms produced by the majority of cell types. However $VEGF_{165}$, which ortholog in the mouse is $VEGF_{164}$, is considered pivotal since $VEGF_{164}$-transgenic mouse is the only one from all the splice variant-expressing transgenic mice that develops normally (Neufeld *et al*., 1999; Robinson and Stringer, 2001).

Three main VEGF receptors (VEGFRs) were identified: two receptor tyrosine kinases, VEGFR-1 or flt-1 and VEGFR-2 or flk-1, and a fms-like tyrosine kinase VEGFR-3 or flt-4 (Ferrara *et al*., 2003). VEGFR-1 is expressed in endothelial cells (Fong *et al*., 1995), haematopoietic progenitors (Hattori *et al*., 2002) and mature bone marrow derived cells such as myeloid cells (Clauss *et al*., 1996) and in smooth muscle cells (Wang and Keiser, 1998); VEGFR-2 is mainly expressed in endothelial cells (Ortega *et al*., 1997) but also in primitive and more mature haematopoietic cells (Matthews *et al*., 1991); and VEGFR-3 expression is restricted to lymphatic endothelial cells (Kaipainen *et al*., 1995). VEGF-A-C, E and PIGF act on blood vessels via VEGFR-1 and/or VEGFR-2, whereas VEGF-C-D are the main lymphangiogenesis drivers through VEGF receptor 3 (VEGFR-3)(Roy *et al*., 2006).

VEGFR-2 deficient mice fail to develop endothelial and haematopoietic cells whereas VEGFR-1 knockout mice form endothelial cells in embryonic and extra-embryonic tissues but fail to assemble them into normal vascular channels (Fong *et al*., 1995; Shalaby *et al*., 1995). Moreover VEGFR-2 has been shown to be important for endothelial cell proliferation differentiation and migration (Ortega *et al*., 1997). These studies suggest VEGFR-2 has a crucial role in endothelial cell development and

behaviour whereas VEGFR-1 seems to be more important in vascular remodelling. Interestingly, a soluble form of VEGFR-1 was shown to negatively regulate angiogenesis (Ambati *et al*., 2006; Ambati *et al*., 2007). The role of VEGFR-1 in haematopoietic cells will be described in **1.3.2D-I**.

VEGFR-2 signalling is considered the main driver of angiogenesis. Upon VEGF binding VEGFR-2 undergoes dimerisation and ligand-depend tyrosine phosphorylation results in activation of several mitogenic, chemotatic and pro-survival proteins such as phosphatidylinositol-3 kinase (PI3K), phospholipase C-γ (PLCγ), protein kinase C (PKC), focal adhesion kinase (FAK), Ras proteins and mitogen-activated protein kinase (MAPK) among others (Ferrara *et al*., 2003; Zachary and Gliki, 2001). Many of these pathways are common to integrin signalling (see **Fig. 5**). A co-receptor for VEGFR-2 was also shown to have a role in blood vessel formation. It was named neuropilin-1 and was first identified in neurons as a semaphorin receptor and implicated in neuronal guidance. Neuropilin-1 was shown to increase binding of VEGF to VEGFR-2 that resulted in increased VEGF-mediated chemotaxis (Soker *et al*., 1998).

C. Tumour Angiogenesis

I. Angiogenic switch

In normal tissues angiogenesis is normally repressed and only occurs in processes such as wound healing. On the other hand for a tumour to grow, it needs oxygen and nutrient supply as well as an efficient way of removing toxic metabolic products. As a consequence tumours develop their own vasculature by activating the so called "angiogenic switch". Tumour angiogenesis results mainly from an imbalance of angiogenic signals in favour of pro-angiogenic signals (Bergers and Benjamin, 2003; Fidler and Ellis, 1994; Naumov *et al*., 2006). Hypoxia is the first physiological regulator of the angiogenesis switch. As the tumour mass grows, some of the cells (usually the ones in the centre of the tumour) will start to be deprived of oxygen due to the increased distance of diffusion from the existing vessels, becoming hypoxic (Bertout *et al*., 2008; Thomlinson, 1977). This will lead to activation of Hypoxia Inducible Factor 1 (HIF-1) in the tumour and tumour-associated cells that in turn will result in up-regulation of the pro-angiogenic factors such as VEGF, iNOS (inducible nitric oxide synthase), bFGF, PDGF and epithelial growth factor (EGF) that will activate quiescent endothelial cells to form new blood vessels (**Fig.3**) (Calvani *et al*., 2006; Jensen *et al*., 2006; Liao and Johnson, 2007; Yoshida *et al*., 2006).

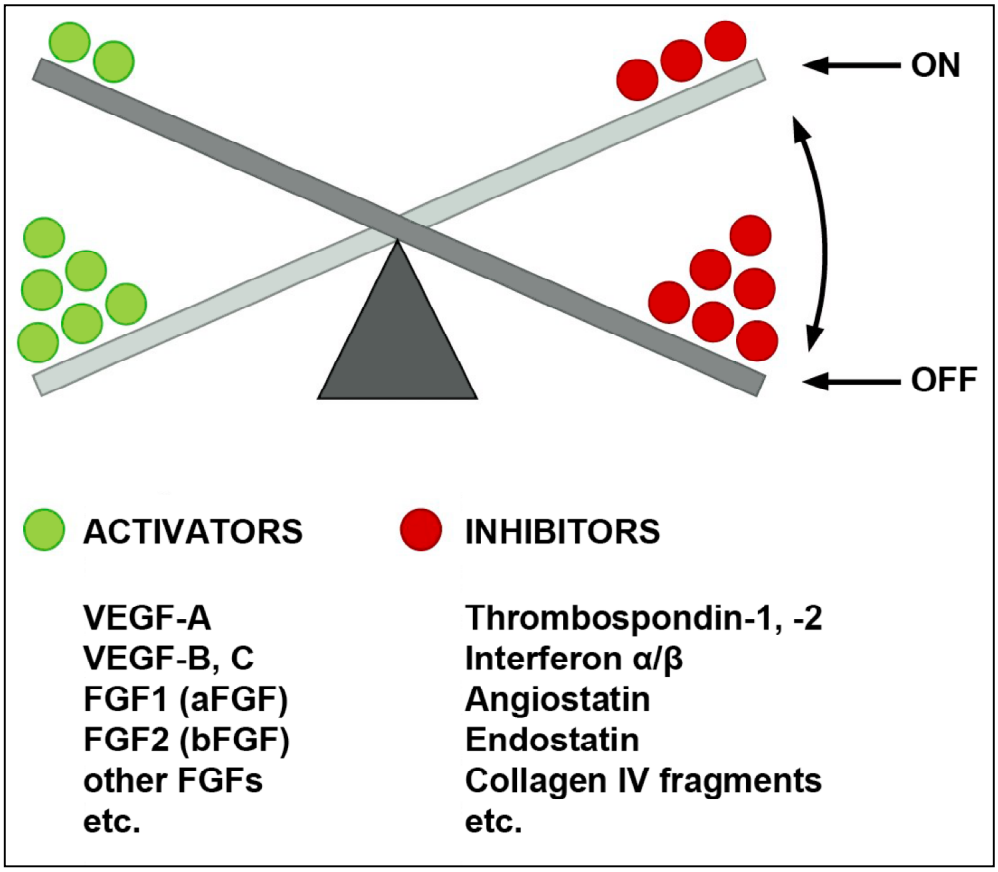

Figure 3: The angiogenic switch

In normal tissues angiogenesis is regulated by a balanced production of pro- and anti-angiogenic factors and it is normally repressed. Tumour angiogenesis results mainly from an imbalance in the angiogenic signals in favour of pro-angiogenic factors such as vascular endothelial growth factor (VEGF) and basic fibroblast growth factor (bFGF) (Adapted from Weinberg, 2007).

II. Tumour vasculature features

In contrast to normal vasculature, tumour blood vessels are irregularly shaped, dilated and tortuous presenting a chaotic organisation and forming a vascular plexus that is more leaky and haemorrhagic in part due to the elevated production of VEGF (Bergers and Benjamin, 2003). These features contribute to poor blood flow into the tumour and subsequent low drug delivery rates. The increased leakiness also allows easier escape of tumour cells into the circulation (De Bock *et al*., 2011). One of the emerging cell types involved in the leaky phenotype of tumour blood vessels has been the pericyte or mural cell. In general these cells are less abundant and more loosely attached to the tumour vasculature (Bergers and Song, 2005). Pericyte proliferation and recruitment to blood vessels is not only dependent on the PDGFB-PDGFRβ axis but also on the endothelial localisation of PDGFB. Disruption of this axis by genetic ablation of PDGFB in mice results in haemorrhagic tumour blood vessels that are hyperdilated and show low pericyte coverage (Abramsson *et al*., 2003).

D. Anti-angiogenic therapy and vessel normalisation

Given the crucial role of blood vessels in tumour growth and cancer cell dissemination anti-angiogenic therapy approaches have been developed for many types of cancer. The main principle of anti-angiogenic therapy is that destruction of tumour blood vessels in combination with chemotherapy would destroy both the blood vessels feeding the tumour and the cancer cells themselves thereby inhibiting cancer growth and spread.

The known role of VEGF in endothelial cell migration, survival, proliferation and permeability made it the prime target for anti-angiogenic therapy (De Bock *et al*., 2011). Bevacizumab, a humanised monoclonal anti-VEGF antibody, was the first Food and Drug Administration-approved anti-angiogenic drug in monotherapy or in combination with chemotherapy. This was based on the efficacies shown in metastatic renal cancer and in combination with standard chemotherapy for the treatment of metastatic colorectal cancer (Hurwitz *et al*., 2004; Yang *et al*., 2003). It likely seems contradictory that a drug that destroys tumour vasculature can have efficacy with chemotherapeutic drugs that need access into the tumour. However anti-VEGF therapy was shown in animal studies to decrease tumour interstitial fluid pressure that in turn increased drug perfusion into the tumour (Dickson *et al*., 2007; Tong *et al*., 2004). In fact tumour blood vessels showed increased pericyte and basement membrane coverage after anti-VEGF therapy (Tong *et al*., 2004). These observations have led to the concept of 'vessel normalisation' whereby reduction, but not total loss of tumour blood vessels in combination with reduced tortuosity and increased vessel stability may be beneficial for chemotherapy delivery. Since tumour vasculature is

abnormal it is suggested that anti-angiogenic therapy should be used in a therapeutic 'window' where the structure and function of blood vessels are improved and the balance between pro-angiogenic and anti-angiogenic molecules is restored resembling 'normal' angiogenesis. The main problem with vessel normalisation is that the maintenance of a balance between pro- and anti-angiogenic mediators is not easy to sustain (Jain, 2005).

E. Resistance to anti-angiogenic therapy and metastasis

Despite the promise of anti-angiogenic therapy, resistance has become a major issue and survival benefits are still modest (Broxterman *et al*., 2003). Using a mouse model of pancreatic cancer Casanovas *et al* have shown that although treatment with anti-VEGFR2 antibody induces an initial stasis in tumour growth, restoration of blood vessel density is observed possibly due to hypoxia-dependent up-regulation of other pro-angiogenic factors such as bFGF (Casanovas *et al*., 2005). Another study has highlighted the importance of hypoxia in the recruitment of bone marrow derived cells to promote neovascularisation and invasion and a role for VEGF in the inhibition of this perivascular tumour invasion. These data suggest blocking the VEGF pathway could enhance metastasis (Du *et al*., 2008). Moreover an increase in tumour hypoxia appears to be associated with increased invasion and metastasis following anti-angiogenic therapy (Ebos *et al*., 2009; Narayana *et al*., 2009; Paez-Ribes *et al*., 2009). Together these lines of data suggest that a better understanding of the molecular basis of angiogenesis and the consequences of anti-angiogenic therapy are required.

1.3.2. Bone marrow compartment

A. Embryonic haematopoiesis

Haematopoietic stem cells (HSCs) are the basis of the entire adult blood system. In 1957 E. Donnan Thomas performed the first stem cell transplant in human twins and validated intravenous injection of bone marrow cells as a strategy for long-term repopulation of blood cells (Thomas *et al*., 1957). The multipotency property of HSCs was first shown in the early 1960s with the origin of myeloid multilineage colonies in the spleen after bone marrow transplant into irradiated mice (Till and McCulloch, 1961; Becker *et al*., 1963).

In humans and mice blood cells emerge primarily in the extraembryonic yolk sac until the onset of the systemic blood flow. Initially haematopoietic progenitor cells migrate to the embryonic liver and this becomes the central organ for blood cell production during most of *in utero* development. At later embryonic stages liver-derived cells seed in the bone marrow and spleen. In humans bone marrow sustains haematopoiesis throughout life whereas in mice this function is performed by both the bone marrow and spleen (Yoder, 2002). As described previously (see **1.3.1A**), in mice the mesodermal precursor, the haemangioblast, develops into both haematopoietic and endothelial cells (Choi, 1998). Embryonic haematopoiesis starts in the yolk sac at embryonic stage E.7-7.5 with large nucleated erythrocytes (erythroblasts), some macrophage progenitors and megakaryocytes surrounded by a layer of endothelial cells forming the so-called blood islands. At the beginning of embryonic stage E7.5-E8 erythroid and myeloid (granulocytic and monocytic) progenitors appear whereas only at embryonic stage E8.5 erythroid-myeloid-lymphoid progenitors are found in

the yolk sack. HSCs are detected in the intra-embryonic aorta-gonado-mesonephros (AGM) at embryonic stage E10.5 and slightly later (E11-E11.5) in the yolk sac, placenta and foetal liver. The liver becomes the main reservoir of HSCs until mid gestation (E17), after which time these cells colonise the bone marrow, the main reservoir in adults (Boisset and Robin, 2012; Yoder, 2002).

Cellular niches that regulate cell self-renewal, differentiation and quiescence compose adult bone marrow. These cellular niches are basically functional compartments that support the function of cells within bone marrow through several different signals such as growth factors, cytokines and also cell-to-cell and cell-to-ECM contacts. Two main cellular niches have been identified: The haematopoietic stem cell niche and the immune cell niche (Mercier *et al*., 2012). Regulation of these two niches is one of the focuses of my PhD data.

B. Haematopoietic stem cell niche

As described before HSCs are pluripotent cells that have the capacity to undergo self-renewal and can differentiate into specific lineages. They can be isolated from the bone marrow based on cell surface markers, the most commonly used being the lineage-marker negative $SCA^{+}KIT^{+}CD31^{-}CD48^{-}CD150^{+}$. The hallmark of this long self-renewal capacity is the maintenance of HSCs in a quiescent/slow cycling state Here the bone marrow microenvironment plays an essential role and disrupting interactions between HSCs and bone marrow stroma leads to HSC activation and mobilisation from bone marrow. Two main compartments, vascular and

mesenchymal, that contribute to this HSC homeostasis will be described briefly (Cheshier *et al*., 1999; Mercier *et al*., 2012; Wilson *et al*., 2008).

I. Vascular contribution to the HSC niche

Given the common origin of endothelial cells and HSCs it is not surprising that a large proportion of $CD150^+$ HSCs are found attached to the fenestrated endothelium of bone marrow sinusoids (Del Fattore *et al*., 2010; Mazo *et al*., 1998). Bone marrow endothelial cells express factors that stimulate haematopoiesis such as granulocyte colony-stimulating factor (G-CSF); macrophage colony-stimulating factor (M-CSF); granulocyte-macrophage colony stimulating factor (GM-CSF); stem-cell factor and interleukin-6 (IL-6). In addition they also express adhesion molecules such as E-selectin; P-selectin; VCAM-1; ICAM-1 and also molecules that facilitate cell homing such as E-selectin and CXC-chemokine ligand 12 (CXC12) (Mazo *et al*., 1998; Mercier *et al*., 2012). Bone marrow endothelial cells are necessary for self-renewal and repopulation of HSCs after irradiation (Butler *et al*., 2010). In fact, cell lines and primary endothelial cells isolated from yolk sac or AGM, as opposed to endothelial cells from non-haematopoietic organs, have the ability to maintain HSCs *in vitro* (Li *et al*., 2004). This suggests endothelial cells isolated from haematopoietic organs present particular features that are essential for HSC maintenance.

II. Mesenchymal contribution to the HSC niche

Mesenchymal stem cells also reside in the bone cavity and can give rise to bone marrow mesenchymal stromal cell (MSCs) lineages such as chondrocytes, osteoblasts, fibroblasts, adipocytes, endothelial cells and myocytes (Del Fattore *et al*., 2010). Endothelial cells are surrounded by perivascular MSCs that support haematopoiesis and interact directly with HSCs (Le Blanc and Mougiakakos, 2012). Long-term HSCs are found attached to N-cadherin expressing osteoblasts. Increasing N-cadherin expressing osteoblasts results in increased bone marrow HSCs suggesting these cells are important for the regulation of HSC niche size (Zhang *et al*., 2003). A specific population of MSCs that express the marker nestin was identified around bone marrow blood vessels and adrenergic nerve fibres and found to be important for HSC maintenance. Depletion of nestin-positive cells resulted in decreased HSC homing and increased release of HSCs from bone marrow (Mendez-Ferrer *et al*., 2010). It is still not clear if these nestin expressing cells are a subtype of CXCL12-abundant reticular (CAR) cells that surround bone marrow sinusoids or are located near endosteum and were found to associate with HSCs. Disruption of interactions between HSCs and CAR cells reduces bone marrow HSC numbers (Sugiyama *et al*., 2006).

C. Immune cell niche

Besides the role in immune cell development, bone marrow can also host mature immune cell types.

I. Lymphocytes

Lymphocytes constitute 3 main lineages: Natural Killer (NK) cells, T cells and B cells. NK cells are short-lived cells and are classified as innate immune cells due to their ability to respond quickly to injury without prior sensitisation, whereas T and B cells were classified in the adaptive immune response because of their memory capacity, i.e., ability to generate long-lived progeny after first stimulation with an antigen (Sun and Lanier, 2011). T and B cells use recombination activation gene (RAG) enzymes for rearrangement of their receptor genes. This feature is commonly exploited in murine studies. Mice deficient in RAG1 or RAG2 are generally used to distinguish T and B cells from other immune cell functions. These mice lack mature T and B cells, however they present normal numbers of NK and myeloid cells (Mombaerts *et al*., 1992; Shinkai *et al*., 1992).

Lymphopoiesis is compartmentalised, with B and NK cells development occurring mainly in the BM whereas the majority of the T cells develop in the thymus (see **Fig.4**). However all cell types originate from a common precursor identified in the BM, clonogenic lymphocyte restricted progenitor cell (CLP), that is characterised by the expression of interleukin 7 receptor (IL-7R). T cells are subject to a final lineage decision in the thymus to form mature CD4 (helper) and CD8 (cytotoxic) T cells. Cell surface markers can define these cells: CD3 for the T cells; B220 for the B cells;

NK1.1 and NG2D for the NK cells (Pear and Radtke, 2003; Rosmarin *et al*., 2005; Sun and Lanier, 2011).

NK and CD8 T cells can rapidly degranulate and secrete IFN-γ, following antigen receptor triggering, which is particularly important in viral infections but also in responses against tumours (Sun and Lanier, 2011).

II. Myeloid cells

The term *myeloid* comes from the Greek word marrow and indeed myeloid cells represent the main cell type in the bone marrow compartment and one of the most studied during my PhD. This cell population comprises polymorphonuclear cells (PMN) or granulocytes, monocytes (Mon), macrophages (extravasated blood monocytes) and dendritic cells (DCs). These cells are characterised by rapid turnover and phagocytic activity. Granulocytes, or PMNs, are the most abundant myeloid cell type in the blood and their names come from the multilobulated shape of the nucleus (PMN) and storage of granules in the cytoplasm (granulocytes) that can be released upon inflammation. Together with monocytes the main function of PMNs is to eliminate pathogens and components of damaged tissue using phagocytosis (Fiedler and Brunner, 2012; Rosmarin *et al*., 2005). Both cell types also play an important role in adaptive immune responses by suppressing T cell responses. This has generated the concept of myeloid-derived suppressor cells (MDSCs). On the other hand DCs have the ability to activate specific T cells during inflammatory responses. For this reasons the myeloid cell population plays a pivotal role in the regulation of immune cell responses (Auffray *et al*., 2009; Ueha *et al*., 2011).

As for lymphopoiesis, myelopoiesis starts in haematopoietic stem cells and it is viewed as an hierarchical process by which these HSCs give rise to several committed progenitor cells (see **Fig. 4**). A common myeloid progenitor (CMP) will give rise to the committed progenitors granulocyte-monocyte progenitor (GMP) or to a megakaryocyte-erythroid progenitor (MEP). GMP develop into progenitors committed to the 4 main types of granulocytes: eosinophil lineage-commited progenitors (EoP) that will develop into eosinophils; basophil/mast cell progenitors (BMCP) that will give rise to mast cell (MCP) progenitors that differentiate into mast cells and basophil progenitors (BaP) that will develop into basophils; and finally a still unknown progenitor that differentiates into neutrophils (Fiedler and Brunner, 2012). In the case of monocytes/macrophages and DCs a macrophage DC progenitor (MDP) that shares markers of CMP and GMP will differentiate into monocytes and common DC precursors (CDP) that will give rise to different types of DCs (Ueha *et al*., 2011).

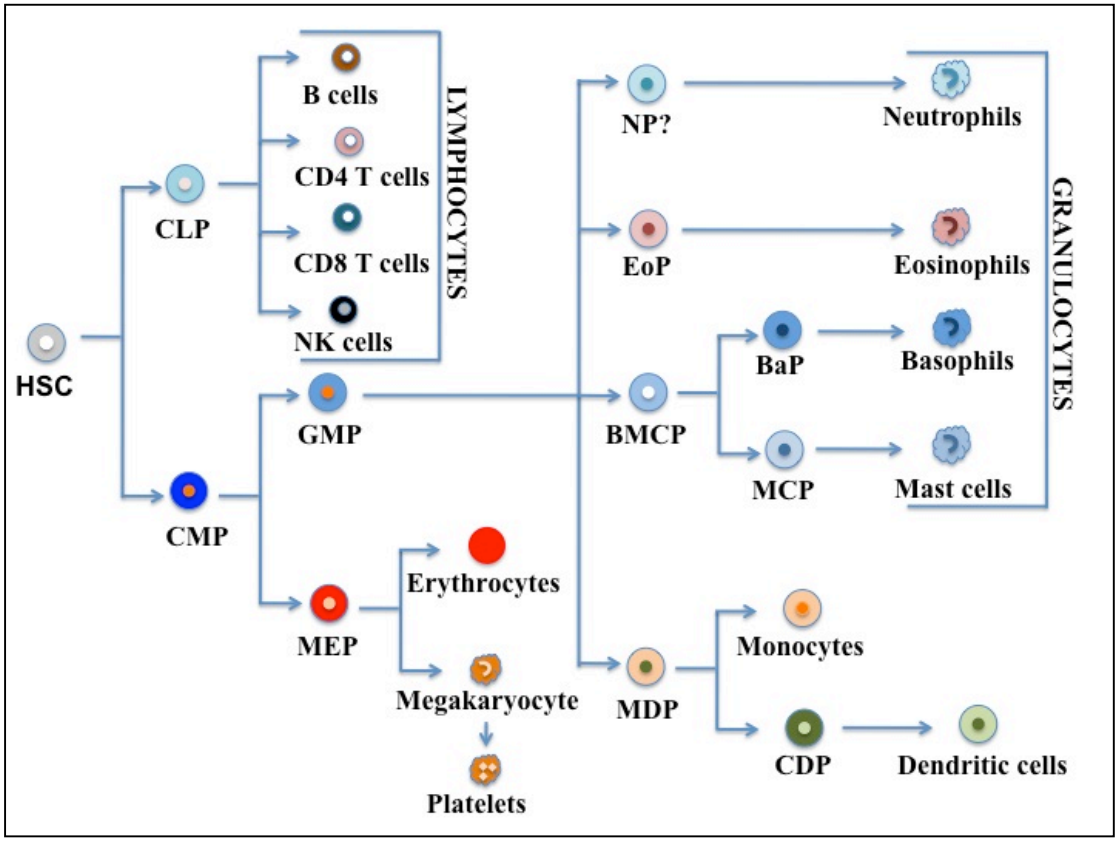

Figure 4: Lymphocyte and myeloid cell development

The common progenitor of lymphopoiesis and myelopoiesis is HSCs that give rise to several committed progenitor cells such as the common lymphocyte (CLP) and the common myeloid (CMP) progenitors. CLP differentiates into NK, B and T cells. The latter are subject to a final lineage decision in the thymus to form mature CD4 (helper) and CD8 (cytotoxic) T cells. CMP give rise to megakaryocyte-erythroid (MEP) and granulocyte-monocyte (GMP) progenitors. MEP develops into megakaryocytes and erythrocytes whereas GMP differentiates into an eosinophil lineage-commited progenitor (EoP) that gives rise to eosinophils; basophil/mast cell progenitor (BMCP) that differentiates into mast cell progenitor (MCP) that develops into mast cells and basophil progenitor (BaP) that gives rise to basophils; and a still unknown progenitor (NP) that differentiates into neutrophils. On the other hand an intermediate macrophage DC progenitor (MDP) that shares markers of CMP and GMP differentiates into monocytes and common DC precursors (CDP) that in turn give rise to different types of DCs.

- **Granulocytes**

The most abundant type of granulocytes and 50-70% of total blood leucocytes are neutrophils. For that reason most studies of granulocyte function are based mainly on neutrophils. Neutrophils are constantly produced in the bone marrow and circulate in the bloodstream until they are required for an immune response. Macrophage stimuli activate endothelial cells to facilitate the passage and guidance of neutrophils to sites of infection. The main function of neutrophils is phagocytosis and destruction of pathogens mainly by release of cytotoxic granules. These cells produce cytokines such as tumour necrosis factor α (TNF-α), interleukin 1 (IL-1), interferons (IFNs), toxic substances and reactive oxygen species. They also have the capacity to regulate the activation of macrophages, T cells and more neutrophils. Their main expression markers, in mouse, are CD11b and Ly6G (Fiedler and Brunner, 2012).
Granulocyte-monocyte colony stimulating factor (GM-CSF) is the main chemoattractant for neutrophils *in vivo* and has been shown to have an anti-apoptotic effect in these cells causing neutrophilia (Khajah *et al*., 2011; Wengner *et al*., 2008).

Recently neutrophils were classified into 2 categories: N1 and N2; mainly due to the plasticity of these cell-types in tumours. N1 neutrophils have an anti-tumoural activity and are characterised by low levels of arginase; their ability to activate cytotoxic T cells (CTL) and their ability to kill tumour cells. On the other hand N2 neutrophils that are mainly differentiated in response to the immunossupressive cytokine TGF-β, have a pro-tumoural effect and are characterised by high expression of arginase, VEGF, MMP-9 and other pro-tumourigenic molecules (Fiedler and Brunner, 2012; Piccard *et al*., 2012).

Eosinophils are usually resident in organs such as the gastrointestinal tract, mammary glands and bone marrow where they contribute to tissue and immune homeostasis. Basophils and mast cells are less abundant in the circulation and are mainly responsible for allergic reactions due to their production of histamine (Fiedler and Brunner, 2012).

- **Monocytes/macrophages and dendritic cells**

Monocytes and dendritic cells are also known as the mononuclear phagocyte system (MPS). DCs represent 5%, whereas *bona fide* monocytes represent 95% of MPS. In mouse these cells are identified by their expression of cell surface markers such as CD115 or CD11b and according to the variable expression of Ly6C marker can be subdivided into different subsets: $CD115^+$; $Ly6C^+$ and $CD115^+Ly6C^-$. $CD115^+$; $Ly6C^+$ cells are called inflammatory monocytes, represent 80-90% of blood monocytes and are also characterised by their expression of the chemokine receptor CCR2, adhesion molecule L-selectin and low expression of chemokine receptor CX3CR1. These cells are recruited to inflamed tissues and produce high levels of TNF-α and IL1. $CD115^+Ly6C^-$ cells are also termed patrolling monocytes and are characterised by lack of expression of CCR2 or L-selectin but high expression of CX3CR1 and lymphocyte-function associated antigen 1 (LFA-1). The name of these cells comes from their ability to crawl along the luminal face of the endothelium and extravasate rapidly in response to tissue damage (Auffray *et al*., 2009; Geissmann *et al*., 2010).

The development of blood monocytes is dependent on monocyte colony stimulating factor (M-CSF or CSF-1). One important feature of these cells is that, whereas

myeloid progenitor cells proliferate in response to CSF-1, terminally differentiated macrophages become refractory to these proliferative signals (Auffray *et al*., 2009). Macrophages (extravasated monocytes) were classified into two main statuses of activation: M1 'classically' activated; and M2 'alternatively' activated macrophages. M1 macrophages are involved in responses of type I helper T cells (Th1) when stimulated with IFN-γ and are characterised by elevated expression of the major histocompatibility complex (MHC) class II, release of pro-inflammatory cytokines such as IL-12, IL-23 and TNF-α, generation of ROS and nitric oxide (NO), and a capacity for killing cells and pathogens. In contrast M2 macrophages differentiate in response to IL4 and IL13 and are involved in the responses of type II helper T cells (Th2). Their main features are low expression of MHC class II and elevated expression of arginase and release of anti-inflammatory cytokines such as IL-10. These cells are involved in immune suppression and tissue-remodelling processes such as wound healing (Chioda *et al*., 2011; Qian and Pollard, 2010).

DCs can be subdivided into classical dendritic cells (cDCs) and plasmocytoid dendritic cells (PDC). cDC although present in human circulation, are rare in mouse blood. They are specialised antigen processing and presenting cells, and when immature, have a high phagocytic capacity. Mature cDCs, in contrast, are high cytokine producers. On the other hand PDCs are long-lived cells that are present in the bone marrow and all peripheral organs. PDCs are specialised in viral infection responses due to their ability to produce IFNs but can also present antigens and control T-cell responses (Geissmann *et al*., 2010).

- **Myeloid-derived suppressor cells**

Myeloid-derived suppressor cells (MDSC) are an heterogeneous population of cells that comprise myeloid progenitor cells and immature myeloid cells. These cells are a major focus of my PhD thesis. They are expanded in pathological conditions such as infection, inflammation and cancer and their main function is suppression of T cell responses. These cells represent 20-30% of mouse bone marrow and 2-3% of spleen. They are a mixture of myeloid cells with characteristics of monocytes and granulocytes and are generally described by the co-expression of mouse markers detected by antibodies against CD11b and Gr1 ($CD11b^{+}Gr1^{+}$). Gr1 recognises monocyte/macrophage and neutrophil markers Ly6C and Ly6G respectively, whereas CD11b is mainly a monocyte/macrophage marker. MDSCs are usually subdivided into monocytic-like, when they present a mononuclear morphology, and are $CD11b^{+}Ly6G^{+/-}Ly6C^{+}$, or granulocytic/neurophil-like when they present with multilobulated nuclei and are $CD11b^{+}Ly6G^{+}Ly6C^{lo}$. These cells can produce immunossupressive substances such as arginase, inducible nitric oxide synthase (iNOS) and/or reactive oxygen species (ROS) (Gabrilovich and Nagaraj, 2009; Ostrand-Rosenberg and Sinha, 2009). MDSC were shown to block *in vitro* proliferation of T cells (Bronte *et al*., 2000; Mazzoni *et al*., 2002). More*over in vivo* depletion of MDSCs restored T cell proliferation and responses (Bronte *et al*., 2000). Other authors have demonstrated that these cells are capable of repressing NK cell cytotoxicity *in vitro* and *in vivo* in tumour bearing hosts (Li *et al*., 2009; Liu *et al*., 2007). The main activators of MDSC expansion are cyclooxygenase 2, stem-cell factor (SCF), IL-6, M-CSF, GM-CSF and VEGF. Janus kinase protein (JAK) and signal transduction and activator of transcription 3 (STAT-3) are the main regulators

of MDSC expansion (Gabrilovich and Nagaraj, 2009). JAK2/STAT-3 activity in myeloid cells was shown to prevent their differentiation into mature cells *in vitro* (Nefedova *et al*., 2004). Importantly Kortylewiski and colleagues have demonstrated that genetic or pharmacological inhibition of STAT-3 in mice enhances the anti-tumoural function of dendritc cells, T cells, NK cells and neutrophils (Kortylewski *et al*., 2005).

D. Growth factor and chemokine signalling in BMDCs

Bone marrow derived cell homing and mobilisation into distant tissues via the circulation is regulated by several cytokines, chemokines and growth factor signalling pathways. It is dependent on interactions with cells and extracellular matrix that comprise the surrounding stroma. The complex integration between extracellular and intracellular signals from different cell types is important to maintain the haematopoietic homeostasis and to allow efficient responses in conditions of stress such as infection. Survival and proliferation of HSCs is dependent on lineage-specific cytokines. Good examples are colony-stimulating factors (CSFs) such as monocyte-granulocyte (GM-CSF), monocyte (M-CSF) and granulocyte (G-CSF); these are CSFs that can stimulate proliferation of myeloid cells (Hercus *et al*., 2009).

Given the complexity of the cytokine, chemokine and growth factor signalling in haematopoiesis I will focus on three signalling pathways that have also been widely associated with bone marrow derived cell activity, especially myeloid cell recruitment in cancer: VEGF/PIGF-VEGFR-1, CXCL12-CXCR4/7, CCL2-CCR2 (Barreda *et al*., 2004; Duda and Jain, 2010; Duda *et al*., 2011; Zhang *et al*., 2010b).

I. VEGF/PIGF-VEGFR1

The role of VEGF and its receptors in angiogenesis has already been described in this thesis (see **1.3.1B-I**). VEGFR- 2 deficient mice fail to develop haematopoietic cells and Flk-1 expression was shown in haematopoietic stem cells (Shalaby *et al*., 1995; Ziegler *et al*., 1999). However Flk-1 positive haematopoietic stem cells failed to reconstitute lethally irradiated adult mice. This suggests VEGFR-2 is important for embryonic haematopoiesis but not for the function of hematopoietic stem cells in the adult mouse bone marrow (Haruta *et al*., 2001). Inhibition of VEGFR-1 but not VEGFR-2 decreased haematopoietic recovery in mice after 5-fluorouracil-induced depletion of cycling haematopoietic cells. Moreover PIGF was shown to restore haematopoiesis after myelossupression. PIGF that signals through VEGFR-1 increased VEGFR-1^{+} HSCs differentiation, mobilisation and reconstitution of haematopoiesis (Hattori *et al*., 2002). Migration of monocytes in response to VEGF-A and PIGF had already been shown to be dependent upon VEGFR-1 activation in these cells (Barleon *et al*., 1996).

The requirement of VEGFR-1 for the recruitment of bone marrow derived cells for growing tumours and metastases is not fully understood. Some studies indicate that blocking VEGFR-1 does not affect infiltration of BMDCs in tumours or spontaneous metastases (Dawson *et al*., 2009), whereas others show that VEGFR-1 is important in the formation of pre-metastatic niches by BMDCs (Kaplan *et al*., 2005)**.**

VEGFR-1 is considered to be a kinase impaired receptor tryrosine kinase, i.e., it is poorly phosphorylated upon ligand binding and its ability to phosphorylate other

substrates is also low. As a consequence VEGFR-1 activation and homodimerisation results in activation of a limited number of signalling pathways such as p44/42 MAP kinase (Rahimi, 2006). However most of signalling studies were performed in endothelial cells and it is not clear whether this phenomenon is common to all cell lineages.

II. Chemokine and chemokine receptors

Chemokines are a family of small cytokines that have leukocyte chemoattracting properties. Based on the position of four conserved cysteine residues they are divided into 4 main families: CXC, CXC3, CC and C. There are more than 50 known chemokines. Chemokines interact with more than twenty C-C and CXC seven-trans-membrane receptors coupled to G-proteins. They are composed of three extracellular and three intracellular loops surrounded by an N-terminus outside the cell surface and a C-terminus in the cytoplasm. The heterotrimeric G-proteins are coupled to one of the intracellular loops of the receptor and that mediates ligand binding and activation of signalling transduction pathways. Most chemokine receptors can bind with high affinity to more than one chemokine ligand and CCs are considered more promiscuous than CXCs in this context. On the other hand, many chemokines can also bind other receptors (Choi *et al*., 2012; Duda *et al*., 2011; Sun *et al*., 2010).

- **CXCL12-CXCR4/7**

CXCL12, also named stromal-derived growth factor-1 (SDF-1), is expressed in several tissue types and has two major isoforms, α and β, even though other isoforms have been identified. CXCL12-α is found in the majority of organs, undergoes rapid proteolysis in blood and is the predominant isoform secreted by bone marrow stromal cells and endothelial cells. CXCL12-β is expressed in highly vascularised organs such as kidneys, liver and spleen due to its ability to promote angiogenesis and is more resistant to proteolysis in blood (Sun *et al*., 2010).

CXCL12, mainly CXCL12-α, binds to two main receptors: CXCR4 and CXCR7. CXCR4 is highly expressed in haematopoietic stem cells in bone marrow, in monocytes, B cells and T cells in peripheral blood and it was also found to be expressed in cancer cells where its expression levels correlate with occurrence and extent of metastasis (Choi *et al*., 2012; Hinton *et al*., 2010; Muller *et al*., 2001; Sun *et al*., 2010). CXCR7 is mainly expressed in T cells and B cells but was also found in tumour cell lines and endothelial cells associated with tumours (Burns *et al*., 2006; Miao *et al*., 2007; Sun *et al*., 2010).

Upon CXCL12 binding CXCR4 forms homodimers and activation of signalling pathways such as phosphoinositide 3-kinase (PI3K)/Akt, focal adhesion kinase (FAK), nuclear factor kappa B (NF-κB) and mitogen activated protein kinase (MAPK) amongst others that regulate cell survival, proliferation and chemotaxis (Choi *et al*., 2012; Duda *et al*., 2011). Many of these pathways are common to receptor tyrosine kinase and integrin signalling (**Fig.5**). CXCR7 signalling, upon CXCL12 binding, is less well understood. It is thought CXCR7 can form heterodimers with CXCR4 that change the conformation of the latter and abrogate its

signalling. On the other hand CXCR7 can signal though PLC/MAP kinase pathway to increase cell survival (Choi *et al*., 2012; Duda *et al*., 2011; Sun *et al*., 2010).

CXCL12-CXCR4 axis is crucial for haematopoietic homeostasis. CXCL12-abundant reticular (CAR) cells in bone marrow stroma were found to associate with CXCR4-HSCs. CXCL12-CXCR4 signalling plays a pivotal role in maintenance of the quiescent HSC pool. Disruption of this signalling pathway resulted in reduced bone marrow HSC numbers (Sugiyama *et al*., 2006). Expression of CXCL12 by bone marrow stroma and interaction with CXCR4 receptor in neutrophils provides also a key bone marrow retention signal. Attenuation of CXCR4 leads to increase mobilisation of neutrophils into the circulation (Eash *et al*., 2010). G-CSF-mediated mobilisation of haematopoietic progenitor cells (HPCs) into the circulation coincided with N-terminal cleavage of CXCR4 in bone marrow HPCs, increase in SDF-1 degradation proteases and decreased accumulation of SDF-1 in bone marrow (Levesque *et al*., 2003). In other studies G-CSF was shown to decrease CXCL12 expression in bone marrow stromal cells such as osteblasts and decrease their activity resulting in HPC mobilisation into the circulation (Semerad *et al*., 2005). Moreover treatment of mice with G-CSF resulted in down-regulation of CXCR4 specifically in $Gr1^+$ cells that consequently increased their mobilisation to peripheral blood (Kim *et al*., 2006). Increases in SDF-1 production in tumours were shown to increase recruitment of bone marrow derived cells (Du *et al*., 2008; Jin *et al*., 2006a).

- **CCL2-CCR2**

CCL2, also called monocyte chemoattractant protein (MCP-1) due to its ability to attract monocytes *in vitro*, can also be a chemoattractant for T cells, NK cells and dendritic cells. CCL2 is expressed in a wide range of cell types such as fibroblasts, macrophages, lymphocytes, astrocytes, mast cells, endothelial cells and osteoblasts. Importantly it is also expressed in many cancer cell types such as prostate, lung, breast, melanoma, ovary and colorectal amongst others (Zhang *et al*., 2010a; Zhang *et al*., 2010b).

CCL2 binds with high affinity to the seven-trans-membrane G-protein coupled receptor CCR2. This receptor is mainly expressed in haematopoietic cells such as macrophages, non-haematopoietic cells such as fibroblasts, endothelial cells and mesenchymal stem cells and also in some cancer cells (Zhang *et al*., 2010b). CCR2 expression has been found to correlate with prostate cancer progression and metastasis (Lu *et al*., 2007). The signalling pathways activated upon CCL2 binding to CCR2 are very similar to the ones described for CXCL12-CXCR4 (Zhang *et al*., 2010a; Zhang *et al*., 2010b).

Mobilisation of monocytes from the bone marrow compartment is dependent on CCR2 activation by its ligands CCL7 and CCL2. CCR2 is highly expressed in $Ly6C^+$ monocytes and mice deficient in this chemokine receptor show decreased $Ly6C^+$ monocyte blood numbers and increased retention of these cells in the bone marrow compartment. Activation of CCR2 is also important for the mobilisation of $Ly6C^+$ monocytes from blood to inflamed tissues. (Tsou *et al*., 2007). GM-CSF can also activate the CXCL2-CCR2 axis to increase neutrophil mobilisation. (Eash *et al*.,

2010). CCR2 expression in $Gr1^+$ monocytes is important for their recruitment to metastatic sites by tumour or stromal-derived CCL2 and will be described further in **1.3.2F** (Qian *et al*., 2011).

E. Role of BMDCs in tumour growth and angiogenesis

Tumour progression is accompanied by enhanced haematopoiesis. Tumour-stromal interactions are not static; in fact many stromal cells are recruited from the bone marrow compartment. BMDCs are constantly recruited to tumours to differentiate into endothelial cells, pericytes, cancer-associated fibroblasts (CAFs) and various immune infiltrating cells during tumour development (Joyce and Pollard, 2009).

Tumour angiogenesis, as described before, is one of the hallmarks of cancer and depends on the proliferation and migration of endothelial cells. Growing evidence points to the importance of circulating endothelial progenitor cells (CEPs), highly proliferative cells derived from the bone marrow that have the ability to differentiate into mature endothelial cells when recruited to angiogenic sites, in angiogenesis and in the growth of certain tumours. The extent to which CEPs are incorporated in the tumour vasculature especially in humans is still controversial (Ahn and Brown, 2009; Rafii *et al*., 2002). Nevertheless, in animal studies, Lyden and colleagues (Lyden *et al*., 2001) have shown contribution of both VEGFR-2+ CEPs and VEGFR-1+ myeloid cells in xenograft tumour growth and angiogenesis. Other studies have suggested a minimal or absent contribution of BM-derived cells to tumour endothelium (Gothert *et al*., 2004; Larrivee *et al*., 2005). In human samples BM stem cells were shown to contribute to the tumour endothelium but at extremely low levels (Peters *et al*., 2005).

Recent studies have also highlighted the role of bone marrow derived mesenchymal cells that have the capacity of differentiating into mesenchymal tissues such as bone, cartilage and fat in supporting tumour angiogenesis. These cells have been shown to be possible precursors of pericytes expressing markers such as: α-smooth muscle actin (α-SMA), neuron-glia 2 (NG-2), platelet-derived growth factor receptor β (PDGFR-β) and tie-2, (Bexell *et al*., 2009; De Palma *et al*., 2005; Rajantie *et al*., 2004), or cancer-associated fibroblasts (CAFs) exhibiting sustained expression of stromal-derived growth factor 1 (SDF-1) (Mishra *et al*., 2008). These bone marrow derived mesenchymal cells seem to act as paracrine inducers of angiogenesis secreting VEGF (Beckermann *et al*., 2008), MMP-9 (Bergers and Song, 2005) or SDF-1 (Mishra *et al*., 2008). These cells are recruited to the tumours by growth factors such as VEGF, PDGF, EGF (Beckermann *et al*., 2008) and HIF-1 (Du *et al*., 2008).

In the past the increased infiltration of tumours by immune cells was thought to be a consequence of failed attempts of cancer cell destruction. More recently, several lines of evidence have shown that, in fact, many of these cells have tumour-promoting functions (Joyce and Pollard, 2009). De Palma and colleagues described a specific type of monocyte that expresses Tie-2 and has a pro-angiogenic function. In mouse models pharmacological or genetic disruption of the Ang2-Tie2 axis in Tie-2 expressing monocytes impaired the association of these cells with tumour endothelium and decreased tumour growth and angiogenesis (De Palma *et al*., 2005; De Palma *et al*., 2003; Mazzieri *et al*., 2011). Pro-angiogenic functions were also attributed to granulocytes such as neutrophils, due to their ability to produce MMP-9 (Nozawa *et al*., 2006), and mast cells (Soucek *et al*., 2007).

Macrophages are the most studied BMDC type that has been associated with cancer progression. Tumour associated macrophages (TAMs) have been associated with decreased survival and poor prognosis in some cancers such as lung (Chen *et al*., 2005), thyroid (Ryder *et al*., 2008) and hepatocellular carcinoma (Zhu *et al*., 2008). TAMs generally resemble M2 type macrophages and can express VEGF, EGF, FGF, MMPs and other molecules that can affect tumour cell proliferation, angiogenesis and extracellular matrix degradation (Sica *et al*., 2008). In fact some studies have shown that skewing TAM polarisation from M2 to M1 type can lead to vessel normalisation and decreased tumour growth and metastasis (Rolny *et al*., 2011). More recently Friedlender *et al* have also defined tumour-associated neutrophils (TANs) as N2 type neutrophils with a pro-tumoural function that is controlled by TGF-β. Blocking this cytokine resulted in infiltration of TANs with an anti-tumour function (Fridlender *et al*., 2009).

Another BMDC type that has been associated with poor prognosis in cancer patients is a population of $CD4^{+}CD25^{hi}FOXP3^{+}$ regulatory T cells (Tregs). These cells have been observed in blood, primary tumour microenvironment and lymph nodes and have a role in immune suppression in tumours (Curiel *et al*., 2004).

Finally, MDSCs were first described as a population of immature myeloid cells that increased in the blood of cancer patients and their circulation levels correlated with clinical stage and metastasis burden (Almand *et al*., 2001; Diaz-Montero *et al*., 2009). Their role in immune suppression has been demonstrated to contribute to increased tumour growth in several *in vivo* models (Bronte *et al*., 2000; Li *et al*., 2009; Mazzoni *et al*., 2002). Moreover Shojae *et al* have shown that granulocytic MDSC, through

expression of a mitogen for endothelial cells (Bv8), also have a pro-angiogenic function in tumours and are responsible for refractoriness to anti-VEGF therapy (Shojaei and Ferrara, 2008; Shojaei *et al*., 2007).

F. Role of BMDCs in tumour metastasis

In line with Paget's 'seed and soil' hypothesis (Paget, 1889) is the concept of a 'pre-metastatic niche'. Kaplan and colleagues suggest that VEGFR-1$^+$ haematopoietic-derived progenitor cells form clusters that home to tumour specific pre-metastatic sites and that preventing the formation of these clusters, by removing VEGFR-1$^+$ cells from the BM or using anti-VEGFR-1 antibodies, prevents tumour metastasis. These cells facilitate cancer cell invasion in the new microenvironment by their enhanced MMP-9 expression that is important for extracellular matrix remodelling. Bone marrow VEGFR-1$^+$ cell alpha4beta1 ($\alpha4\beta1$ or VLA-4) integrin binding by fibronectin is responsible for integrin activation and MMP-9 expression (Kaplan *et al*., 2005). Another study has also shown that MMP9 production from VEGFR-1$^+$ endothelial cells and macrophages in the lung is stimulated by tumour cells, and that this determined metastasis formation (Hiratsuka *et al*., 2002). More recently colonisation of lung by cancer stem cells was demonstrated to be dependent on periostin (an ECM component) production by stromal fibroblasts (Malanchi *et al*., 2012). These studies give examples of BMDC functions such as ECM remodelling that are involved in tumour metastasis.

As for primary tumours the role of myeloid cells in tumour metastasis has been extensively demonstrated. Primary tumours produce VEGF-A, TNF-α and TGF-β

that induce expression of chemoattractants such as S100A8 and S100A9 in metastatic sites that, in turn, attract myeloid cells. Once at metastatic sites myeloid cells secrete migration-stimulating factors such as TNF-α and chemokine macrophage inflammatory protein-2 (MIP-2) (Hiratsuka *et al*., 2006). Chen and colleagues have recently demonstrated that recruitment of macrophages and their interaction with tumour cells triggers anti-apoptotic signals in cancer cells and thus facilitates their seeding and metastasis (Chen *et al*., 2011). Another study had already linked BMDCs interaction with tumour cells as a determinant to overcome dormancy in a model of bone metastasis. BMDC-tumour cell interaction increased recruitment of monocytic osteoclast progenitors that elevated osteoclast activity and bone reabsortion to facilitate metastasis (Lu *et al*., 2011).

Increased numbers of MDSCs have also been clinically correlated with metastasis burden (Diaz-Montero *et al*., 2009). One of the main features in the contribution of these cells to tumour metastasis, as described before for the primary tumours, is the ability to suppress cytotoxic T and NK responses. Their expansion in metastatic sites decreases T cell activation, proliferation and cytotoxicity as it was shown in liver metastasis from mouse models of pre-invasive pancreatic and advanced colorectal cancer. Moreover MDSC expansion can also increase the development of regulatory T cells that further increase the immune suppressive microenvironment and facilitate metastasis (Connolly *et al*., 2010). Increased hypoxia within the primary tumour has also been shown to increase recruitment of MDSCs to metastatic sites generating an immuno-suppressive niche that comprised defective NK cell populations and favoured metastasis (Sceneay *et al*., 2012).

MDSCs can also have other functions that directly contribute to tumour metastasis besides their immune suppression effects. Yang *et al* have demonstrated $CD11b^{+}Gr1^{+}$ cell recruitment at the invasion front of tumours using a mouse model of mammary carcinoma that forms metastases in the lung (MMTV-PyMT). These cells were shown to produce of MMPs, such as MMP2, 13 and 14, that might be responsible for the increased metastasis observed. Interestingly the MMTV-PyMT mouse model used had a specific type II TGF-β deletion in mammary epithelial cells that makes it more aggressive and metastatic showing the tumour suppressor activity of this cytokine. However, in this study $CD11b^{+}Gr1^{+}$ cells were shown to produce high levels of TGF-β that was found at the invasive front of both mouse and human mammary tumours suggesting TGF-β has both tumour suppressor and tumour promotion functions depending on the cell type where it is expressed (Yang *et al*., 2008). Qian *et al* have shown, also using the MMTV-PyMT model, that $Gr1^{+}$ monocytes are recruited to pulmonary metastases, but not to primary tumours through the interaction of $Gr1^{+}$ monocyte chemokine receptor, CCR2, with tumour or stromal-derived CCL2. Pharmacological disruption of this interaction decreased metastasis. Importantly tumour cell extravasation and pulmonary seeding were dependent on production of VEGF by these $Gr1^{+}CCR2^{+}$ monocytes (Qian *et al*., 2011). MMP-9 production by $CD11b^{+}Gr1^{+}$ cells has also been described as a main determinant for vascular remodelling in pre-metastatic lung and increased metastasis in the 4T1 breast tumour model (Yan *et al*., 2010). Granulocytic $CD11b^{+}Gr1^{+}$ cells (neutrophils) in two different studies were associated with increased colonisation of metastatic sites by disseminated tumour cells. It was suggested that neutrophils interact with tumour cells and form bridges that facilitate cancer cell interaction with target metastatic tissue (Huh *et al*., 2010; Spicer *et al*., 2012). Gao *et al* have demonstrated that monocytic

$CD11b^{+}Gr1^{+}$ cells recruited to pre-metastatic lungs, in the MMTV-PyMT mouse model, expressed an ECM proteoglycan named versican. This ECM proteoglycan was responsible for decreasing tumour cell phospho-Smad2 levels and this in turn induced a mesenchymal-to-epithelial transition important for cell proliferation and colonisation of metastatic cells. Importantly, versican knockdown in the bone marrow was sufficient to decrease lung metastasis (Gao *et al*., 2012).

1.4. Cell adhesion in tumour progression

Many of the processes in tumour progression involve changes in ECM-to-cell and cell-to-cell interactions that provide not only physical support, but also activate complex signalling cascades that regulate tumour development and metastasis. As cancer progresses cells acquire pro-invasive and migratory capabilities. Degradation of extracellular matrix is a crucial step in invasion. In this context cell adhesion proteins play a pivotal role. Proteins involved in the pro-invasive behaviour include epithelial cadherins, matrix metalloproteinases and include also a family of cell surface receptors named integrins (Ramsay *et al*., 2007) that will be the main focus of this section. Importantly I will describe the most relevant studies implying that endothelial and BMDC integrins play major roles in tumour progression.

1.4.1. Integrins

Integrins are a family of heterodimeric, transmembrane proteins that mediate both ECM-to-cell and cell-to-cell interactions. In mammals there are 24 known integrins that result from the non-covalent association of 18 different types of α-subunits with 8 different types of β-subunits. Some integrins recognise the tripeptide sequence RGD present in ECM proteins such as fibronectin and vitronectin, or are cell adhesion receptors for laminins or collagen. There are also some that are leukocyte-specific receptors that bind to counter receptors of the Ig superfamily like intercellular cell adhesion molecule (ICAM) and vascular cell adhesion molecule 1 (VCAM-1). These interactions occur via the extracellular domains of integrins (Hynes, 1999; Hynes,

2002). The cytoplasmatic tails of integrins are associated with several adaptor proteins such as talin, vinculin and paxillin. These proteins are responsible for mediating the interaction with the actin cytoskeleton and with signalling molecules such as focal adhesion kinase (FAK). All of these interactions are responsible for the formation of focal adhesions, the molecular bridges that connect the intracellular and extracellular environments. In culture, most integrins will assemble into clusters known as focal contact sites (Romer *et al*., 2006).

1.4.2. Integrin signalling

Integrins are responsible for the modulation of many aspects of cell behaviour such as proliferation, survival/apoptosis, shape, polarity, motility, gene expression and differentiation. Importantly, many of the integrin-signalling molecules, such as FAK, are common to the signalling pathways triggered by both growth factors and cytokines through receptor tyrosine kinases (RTK) (**Fig.5**). In fact, many of the cellular responses to growth factors (such as EGF or PDGF) are dependent on cell adhesion to the substrata via integrins (Hynes, 2002; Ramjaun and Hodivala-Dilke, 2009; Sieg *et al*., 2000).

Integrins can transmit signals in two directions, inside-out and outside-in. Inside-out integrin signalling occurs when the intracellular signals influence the binding of an extracellular ligand to the integrin. These inside-out signals can lead to integrin conformational changes that, in turn, increase integrin intrinsic affinity for a specific ligand. Ligand binding induces integrin clustering that recruits cytoplasmatic signalling molecules to focal contacts triggering outside-in signals (Ginsberg *et al*.,

2005). Development of focal contacts requires the association of integrins with adaptor proteins such as vinculin, talin and paxillin that mediate the interaction with several protein kinases. Some of the protein kinases required for integrin-mediated cellular response are Src family protein kinases (SFK) such as Src, FAK, phosphatidylinositol 3-kinase (PI3K) and integrin-linked kinase (ILK) (Geiger *et al*., 2001).

Integrin and receptor tyrosine kinase signalling is transduced into 3 main pathways (as represented in **Fig.5**): (1) signalling via FAK and SFKs; (2) signalling via ERK/mitogen activated protein kinase (MAPK); (3) signalling via nuclear factor kappa B (NF-κB). One of the major events in integrin signalling is the recruitment of FAK and SFKs and activation of PI3K by FAK. Signalling downstream of PI3K can in turn activate Akt and small GTPases like Rac that induce changes in the cytoskeleton, cell contractility, cell migration, invasion and gene expression. FAK can also activate ERK signalling and this, together with signalling downstream of Rac, regulates cell proliferation, migration and survival. The third pathway that can be activated through integrin signalling downstream of Rac is the NF-κB pathway that can lead to cell migration and protection from apoptosis (Larsen *et al*., 2006; Ramjaun and Hodivala-Dilke, 2009).

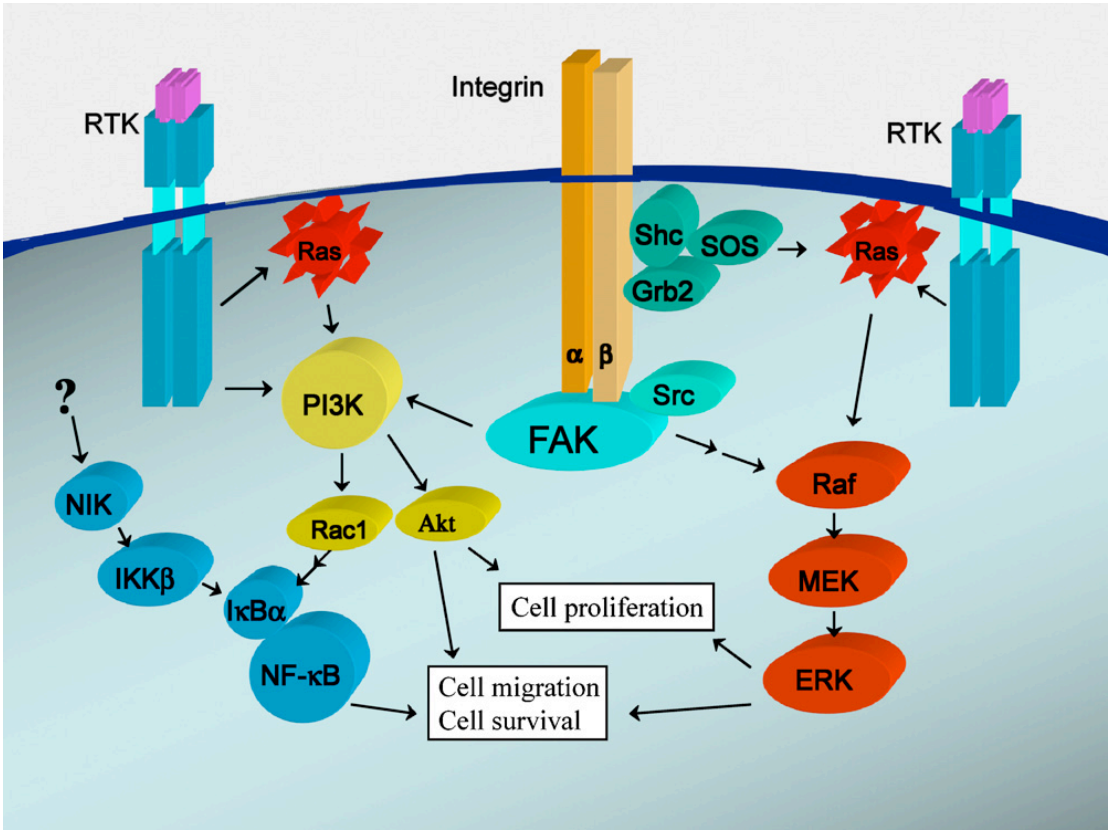

Figure 5: Integrin and receptor tyrosine kinase signalling pathways

Many signalling molecules downstream of integrins are common to the downstream signalling of receptor tyrosine kinases (RTK). The 3 main signalling pathways are: 1) signalling via FAK and SFKs; 2) signalling via ERK/MAPK; 3) signalling via NF-κB. Activation of integrin and receptor tyrosine kinase signalling can induce changes in cell proliferation, cell survival and also cell migration and invasion (adapted from (Ramjaun and Hodivala-Dilke, 2009).

1.4.3. Integrins in tumour progression

The role of integrins in tumour cell invasion and migration has been extensively studied. The most well studied integrins in cancer are αvβ3, αvβ5, α5β1, α6β4, α4β1 and αvβ6 because of their expression in cancer cells. Many epithelial integrins have been associated with solid tumour progression because of their retention in the tumour tissue (α6β4, α6β1, αvβ5, α2β1 and α3β1). Importantly integrins such as αvβ3, α5β1 and αvβ6 are usually expressed at low levels in the epithelia but are up-regulated in tumours. On the other hand, expression of integrin α2β1 decreases in tumours (Desgrosellier and Cheresh, 2010). Specific ablation of β1 integrin in pancreatic β cells in the RIP-Tag2 mouse model of pancreatic β-cell carcinogenesis resulted in impaired tumour growth due to reduced proliferation and increased senescence in tumour cells. On the other hand, disseminating tumour cells were increased even though they were not shown to elicit metastasis (Kren *et al*., 2007). However antibodies against α5β1 integrin have been shown to decrease tumour growth in xenograft mouse models (Bhaskar *et al*., 2007). Another study using a small peptide for inhibition of α5β1 together with a chemotherapeutic agent (5-fluorouracil) in a colon cancer mouse model has shown a benefit in tumour growth, metastasis and survival of the animals (Stoeltzing *et al*., 2003).

Integrin αvβ6 expression has been associated with epithelial-to-mesenchymal transition and autocrine TGF-β signalling in colon cancer cell lines. It was also shown to increase migration of these cells on fibronectin. More importantly high αvβ6 expression was associated with a reduction in median survival of patients with colorectal carcinoma (Bates *et al*., 2005). αvβ6 inhibitors were shown to decrease

xenograft tumour size *in vivo*, but did not affect tumour cell proliferation *in vitro* suggesting a positive role for stromal αvβ6 in tumourigenesis (Van Aarsen *et al*., 2008).

Integrin αvβ3 has been shown to correlate with patient outcome in cervical cancer (Gruber *et al*., 2005), lymph node metastasis in pancreatic cancer (Hosotani *et al*., 2002) and to control metastasis in human breast cancer (Felding-Habermann *et al*., 2001). More recently Desgrosellier *et al*, by injecting human pancreatic cancer cell lines with different αvβ3 expression levels in mice, have shown that expression of this integrin increases lymph node metastasis *in vivo* and anchorage-independent survival and growth of these cell lines *in vitro*. This study has suggested a role for αvβ3 in cell adhesion independent tumour cell survival (Desgrosellier *et al*., 2009).
Based on these studies inhibitors have been developed against αvβ3 and αvβ5 integrins and some of them are already in clinical trials: cilengitide is an inhibitor of both αvβ3 and αvβ5 that has shown modest anti-tumour activity in phase II clinical trials when used as a monotherapy for treatment of recurrent glioblastoma multiforme (Reardon *et al*., 2008). When added to standard chemoradiotherapy in patients with newly diagnosed glioblastoma the results met the endpoints for progression free survival and overall survival (Stupp *et al*., 2010). However in a small phase II clinical trial (16 patients) in patients with non-metastatic castration resistant prostate cancer cilengitide had no clinical activity (Alva *et al*., 2012). Our laboratory has demonstrated that low doses of αvβ3- and αvβ5-inhibitors can promote tumour growth in xenograft mouse models (Reynolds *et al*., 2009). The real clinical benefit of integrin inhibitors is still under investigation.

1.4.4. Role of endothelial integrins in tumour angiogenesis

Eight heterodimeric integrins have been found in endothelial cells. The α5β1 and αv-integrins (αvβ3 and αvβ5) recognise RGD-containing ligands such as vitronectin, fibronectin or von Willebrand factor, while α1β1 and α2β1 are predominantly collagen receptors but can also bind to laminin and α3β1, α6β1 and α6β4 are primarily laminin receptors (Hodivala-Dilke *et al*., 2003). Both genetic ablation and antagonist studies of α5β1, showed a vital role for this integrin in supporting angiogenesis (Kim *et al*., 2000; Yang *et al*., 1993). Antibodies and small peptides against α5β1 integrin have been shown to decrease angiogenesis *in vitro* and in mouse models *in vivo* (Bhaskar *et al*., 2007; Stoeltzing *et al*., 2003). The α1β1 and α2β1 antagonist studies also showed an important role for these integrins in angiogenesis (Funahashi *et al*., 2002; Senger *et al*., 1997). Our lab has recently shown that endothelial genetic ablation of either α6 (Germain *et al*., 2009) or α3 (da Silva *et al*., 2010) increases tumour angiogenesis pointing to an anti-angiogenic role for these two integrins.

The αv-integrins historically have been associated with endothelial sprouts (Eliceiri and Cheresh, 1999). Integrin αvβ3 is increased on tumour-associated vessels of human carcinomas (Max *et al*., 1997). However, our laboratory has demonstrated that mice lacking either β3, or β3 and β5, are not only viable and fertile having no defects in developmental angiogenesis but also present enhanced tumour growth and angiogenesis when these integrins are absent in the stromal compartment (Reynolds *et al*., 2002). Moreover we have also shown that low doses of αvβ3 and αvβ5 inhibitors

can actually promote tumour growth and VEGF-mediated angiogenesis. The pro-angiogenic effects of these inhibitors at low doses were attributed to changes in VEGFR-2 trafficking that in turn increase endothelial cell migration to VEGF (Reynolds *et al*., 2009).

1.4.5. BMDC integrins in tumour progression

BMDC integrins can regulate the release of these cells from the bone marrow and interactions with tumour cells, both of which play important roles in tumour progression. (Hiratsuka *et al*., 2006; Kaplan *et al*., 2005; Lu *et al*., 2011; Petty *et al*., 2009). Three main types of integrins are expressed in bone marrow derived cells: β1and β3 integrins whose expression is also found in other non-haematopoietic cell types; and β2 integrins whose expression is restricted to haematopoietic cells (Soligo *et al*., 1990). Although β2 expression has no apparent function in bone marrow homing, α4β1 integrin has been implicated in this process (Papayannopoulou *et al*., 2001). α4-integrin deficient haematopoietic progenitor cells accumulate in blood soon after deletion and accumulate progressively in the spleen as well. After bone marrow transplant, homing of α4-null cells to the bone marrow, but not spleen, is impaired (Scott *et al*., 2003). This is in contrast with results from β1 integrin conditional knockout in the haematopoietic system where no effect in bone marrow homing, haematopoiesis or lymphocyte trafficking was observed (Brakebusch *et al*., 2002). By transplanting RAG2 knockout mice with α4 integrin deficient bone marrow Banerjee *et al* have shown that thymic and gut lymphoid repopulation was impaired possibly due to a defect in BM-derived progenitor homing after transplantation. In addition, the

authors have demonstrated a defect in B-cell responses such as impaired immunoglobulin (Ig) M and IgE (Banerjee *et al*., 2008).

α4β1 integrin interaction with its ligand VCAM-1 has been extensively studied in myeloid populations (Hiratsuka *et al*., 2006; Kaplan *et al*., 2005; Lu *et al*., 2011; Petty *et al*., 2009). For example, neutrophil α4β1 is responsible for the adhesion to VCAM-1 in the bone marrow stroma and endothelium. Inhibition of either α4β1 or VCAM-1 leads to the release of neutrophils from bone marrow. Signalling of SDF-1 (CXCL12) through CXCR4 in neutrophils also increases α4β1-VCAM-1 adhesion and blocking both CXCR4 and α4 has synergistic effects on bone marrow neutrophil release (Petty *et al*., 2009).

α4β1-VCAM-1 interactions have also been associated in several processes in tumour progression. Jin *et al* have shown that α4β1 expression in circulating progenitor cells mediates the homing of these cells through interaction with VCAM-1 and fibronectin expressed in tumour active remodelling neovasculature (Jin *et al*., 2006b). The same group suggested that monocyte α4β1 is also important for their adhesion to tumour endothelium and extravasation into tumours to promote angiogenesis. Antagonists of α4β1 prevented adhesion of monocytes to endothelium and their subsequent colonisation of tumours *in vivo* that, in turn, resulted in decreased tumour angiogenesis (Jin *et al*., 2006c). Chen and colleagues have demonstrated macrophage α4β1 triggers anti-apoptotic signals in cancer cells through binding to tumour VCAM-1 and thus facilitates cancer cell seeding and metastasis (Chen *et al*., 2011). Another study showed that VCAM-1 expression in tumour cells and interactions with α4β1 integrin in BMDCs increased recruitment of monocytic osteoclast progenitors

that elevated osteoclast activity and bone reabsortion to facilitate metastasis (Lu *et al*., 2011).

BMDC β3 integrin has also been linked to cancer. Platelet $\alpha_{IIb}\beta3$ has been shown to be associated with bone metastasis in a mouse model of injected melanoma cells. In this study B16 melanoma cells were injected via the intra-cardiac route into β3-null and WT mice. β3-null mice displayed reduced metastasis to the bone. In addition, mice transplanted with β3-null bone marrow showed a similar protection to metastasis implying a BMDC involvement in the phenotype. Inhibition of platelet $\alpha_{IIb}\beta3$ also prevented B16 bone metastases (Bakewell *et al*., 2003). Feng and colleagues have described a requirement for $\alpha v\beta3$ expression on bone marrow derived cells for wound healing and tumour-associated angiogenesis (Feng *et al*., 2008). However, work from our laboratory has shown that VEGF-induced angiogenesis is increased in mice after β3-null BM transplantation and that vessels derived from β3-deficient BM are more likely to be non-functional (Watson *et al*., 2009).

1.5. Focal adhesion kinase

One of the central players in integrin and growth factor receptor signalling is FAK (see **Fig.5**), also known as protein-tyrosine kinase (PTK-2) (Sieg *et al*., 2000). It was originally identified by Kanner and colleagues (Kanner *et al*., 1990) as pp125, one of several proteins that were highly phosphorylated in Src-transformed cells. After being characterised in chicken as a cytoplasmatic protein-tyrosine kinase it was named focal adhesion kinase due to localisation at focal adhesions (Schaller *et al*., 1992). Increased FAK expression has been associated, at least in some cases, with enhanced tumour malignancy and poor prognosis (Aronsohn *et al*., 2003; de Vicente *et al*., 2012; Park *et al*., 2010).

1.5.1. Focal adhesion kinase structure and signalling

FAK is ubiquitously expressed and has several binding partners. Interactions with other proteins can trigger phosphorylation cascades but can also result in alterations at the transcription level (Frame *et al*., 2010; Golubovskaya and Cance, 2011; Mitra and Schlaepfer, 2006). On the other hand FAK fragments and related proteins have also been identified (Avraham *et al*., 1995; Lim *et al*., 2012; Schaller *et al*., 1993). This suggests FAK structure regulation has an essential role in the signalling cascades activated.

A. FAK domains and signalling

FAK is a 125-kDa protein with a central tyrosine kinase domain flanked by N-terminal and C-terminal domains (**Fig.6**) (Mitra *et al*., 2005).

I. FAK promoter

FAK promoter contains p53 and nuclear factor kappa B (NF-κB) binding sites. The p53 binding to FAK promoter was shown to repress FAK activity whereas NF-κB binding induced FAK expression *in vitro* (Golubovskaya *et al*., 2004). Analysis of human breast and colon primary tumours showed a correlation between increased FAK expression and p53 mutations. Isolated tumour-derived p53 mutants were unable to inhibit FAK expression *in vitro* as opposed to *wild type* p53. This study highlights a new role for p53 in tumourigenesis by regulating FAK expression (Golubovskaya *et al*., 2008). A recent study has demonstrated that proteosome inhibitor bortezomib can downregulate FAK promoter activity and thereby reduce cancer cell migration and increase apoptosis. The authors have shown that this repression of FAK transcription was independent of p53. Instead reduction of NF-κB binding to the FAK promoter seemed to be the main mechanism responsible for bortezomib-dependent FAK downregulation (Ko *et al*., 2010).

II. N-terminal or FERM domain

The N-terminal domain is also termed FERM (protein 4.1, ezrin, radixin and moesin homology) and has been associated with signalling from receptor tyrosine kinases such as PDGFR and EGFR (Sieg *et al*., 2000). This domain binds directly to the

cytoplasmatic tail of β1 integrin and is thought important for β1 integrin signalling (Schaller *et al*., 1995). The FERM domain also has a negative regulatory role in FAK activation. The N-terminus of FAK has been shown to bind directly to the FAK catalytic domain and to have an autoinhibitory effect on FAK catalytic activity and phosphorylation (Cooper *et al*., 2003; Dunty and Schaller, 2002). Importantly a crystal structure study has suggested that the FERM domain sequesters the Tyr397 autophosphorylation and Src recruitment site blocking FAK activation (Lietha *et al*., 2007).

Crystal structure analysis has subdivided FERM into three subdomains F1, F2 and F3 (Ceccarelli *et al*., 2006). Lim *et al* have identified p53 binding in the F1 subdomain, nuclear localisation signals (NLS) in the F2 subdomain and connections to Mdm2 and proteosomal degradation in the F3 subdomain. Moreover the authors have shown all the three sub-domains contribute to the regulation of p53 degradation and cell survival. FAK FERM nuclear localisation is important for Mdm2 binding and functions as a scaffold between p53 and Mdm2 to increase p53 ubiquitination (Lim *et al*., 2008a). Other studies have shown that FAK inactivation triggers p53 and p21 growth arrest and that the FERM domain is required for p53 enhanced degradation (Golubovskaya *et al*., 2005; Graham *et al*., 2011). Ossovskaya *et al* have identified nuclear exporting sequences (NES) in the F1 subdomain and then in the catalytic domain (Ossovskaya *et al*., 2008). This suggested that the FERM domain might be involved in transferring signals from the nucleus to the cytoskeleton and membrane-bound proteins.

III. FAK major autophosphorylation site

Located at the juncture of the N-terminal and catalytic domains is the major site for FAK autophosphorylation, Tyr-397 (Y397). This phosphorylation is a critical regulatory event that modulates the catalytic activity of FAK and triggers the physical association of FAK with SFKs such as Src and Fyn, via their SH2 domains (Cobb *et al*., 1994; Schaller *et al*., 1994; Xing *et al*., 1994) or alternatively other signalling proteins such as PI3K, Shc adaptor protein, phospholipase-Cγ, growth-factor-receptor-bound protein-7 (Grb7) and p120 RasGAP (Mitra *et al*., 2005). FAK-P-Y397 phosphorylation is required for both integrin- and growth factor-stimulated cell migration (Sieg *et al*., 2000; Sieg *et al*., 1999).

IV. FAK catalytic domain

FAK-P-Y397 autophosphorylation and Src binding are the major events in FAK activation. The FAK Src complex can then trans-phosphorylate tyrosines 576 and 577 (Y576 and Y577) that are located within the putative activation loop of the kinase domain (**Fig.6**). Src phosphorylation of these 2 tyrosines promotes maximal FAK catalytic activation. Both FAK-P-Y397 autophosphorylation and the activation loop sites (Y576 and Y577) were found to be crucial for adhesion-induced FAK activation and FAK enhanced cell spreading and migration (Calalb *et al*., 1995; Owen *et al*., 1999).

V. FAK C-terminal or FAT domain

The C-terminus of FAK is also termed focal adhesion targeting (FAT) domain, as the 159 amino acids within this region were found to be essential for focal adhesion localisation of FAK (Hildebrand *et al*., 1993). The binding site for paxillin is located within the C-terminus of FAK and overlaps the FAT region (Hildebrand *et al*., 1995). Paxillin was shown to bind to the same region of β-integrins (Schaller *et al*., 1995) as FAK and also to vinculin (Turner *et al*., 1990). Given the co-localisation of these proteins at focal adhesions, and the overlap between the paxilllin binding site and FAT domain, paxillin was proposed as a mediator of FAK localisation to focal adhesions. However, replacement of the terminal 13 residues of FAK disrupts paxillin binding but not localisation to focal adhesions suggesting the existence of other mediators for focal adhesion targeting of FAK (Hildebrand *et al*., 1993; Hildebrand *et al*., 1995). Talin binds the C-terminus of FAK and was proposed as an upstream mediator of FAK activation by integrins (**Fig.6**) (Chen *et al*., 1995).

The C-terminus of FAK also contains 2 proline rich motifs, which are thought to interact with SH3 domains in target proteins such as $p130^{Cas}$ (Cas) (Polte and Hanks, 1997). It has been proposed that FAK and Src can synergistically phosphorylate the substrate domain of Cas in response to integrin ligation, creating binding sites for the SH2 domain of the Crk adaptor protein. Cas/Crk downstream signalling can lead to Rac-mediated cell migration (Chodniewicz and Klemke, 2004; Mitra and Schlaepfer, 2006).

Paxillin (Y30 and Y118) and Cas are two of the main phosphorylation targets of the FAK Src complex. Their phosphorylation results, ultimately, in the activation of Rho-dependent GTPases such as Rac and increase in cell motility (Roy *et al*., 2002; Ruest *et al*., 2001; Schaller *et al*., 1999).

Src can also phosphorylate tyrosines 861 (Y861) and 925(Y925) that lie in the C-terminal domain of FAK (**Fig.6**). FAK-P-Y861 phosphorylation is associated with an increase in SH3-domain-mediated binding of Cas to the proline regions within the FAK C-terminus that is thought to be crucial for H-Ras mediated transformation (Lim *et al*., 2004). Importantly, FAK-P-Y861 phosphorylation has been implicated in VEGF signalling (Abu-Ghazaleh *et al*., 2001; Eliceiri *et al*., 2002). FAK-P-Y925 phosphorylation creates an SH2-binding site for the GRB2 adaptor protein. GRB2 binding to FAK can lead to the activation of ERK/MAPK cascade (Mitra *et al*., 2005; Mitra *et al*., 2006b).

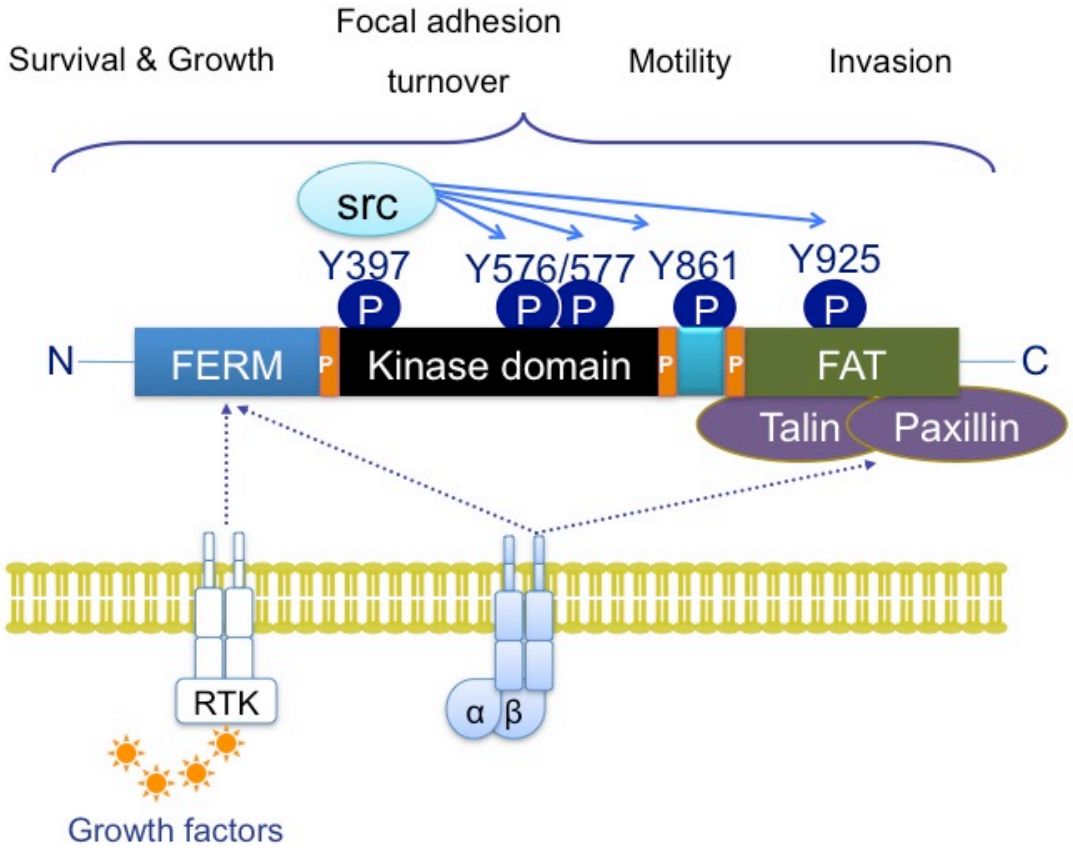

Figure 6: FAK structure and signalling

FAK is composed of a kinase domain, 3 proline rich regions (P) flanked by N-terminal and C-terminal domains. The N-terminal domain is termed FERM and directs interactions with growth factor receptor tyrosine kinase (RTK) and integrins. The C-terminus contains FAT that is required for focal adhesion targeting and 2 proline rich domains that interact with SH3 domains in target proteins such as Cas. FAK is recruited to sites of integrin clustering through interactions between its C-terminal and integrin-associated proteins such as talin and paxillin. This results in rapid FAK-P-Y397 autophosphorylation and Src binding. Within the complex, Src can then transphosphorylate FAK in other residues within the kinase (Y576 and Y577) and the C-terminal (Y861 and Y925) domains of FAK. FAK Src complex is responsible for the phosphorylation of other proteins and activation of signalling cascades that control survival/growth, focal adhesion turnover, motility and invasion.

B. FAK related non-kinase

Schaller and colleagues identified a non-catalytic isoform of FAK termed FAK related nonkinase (FRNK) that is identical in sequence to the C-terminal of FAK at both the nucleotide and amino acid levels (Schaller *et al*., 1993). An alternative promoter that resides in an intron of FAK positioned between the 3' exon coding sequences for the catalytic domain and 5' exon coding sequences for the C-terminal domain of FAK controls expression of FRNK (Nolan *et al*., 1999). In contrast to FAK, FRNK is expressed selectively in SMCs and appears to be up-regulated following vascular injury (Nolan *et al*., 1999). FRNK seems to act as an endogenous inhibitor of FAK and its overexpression inhibits cell spreading, migration and growth factor signalling (Hauck *et al*., 2001; Richardson and Parsons, 1996; Taylor *et al*., 2001).

C. FAK proteolysis

Some studies have shown that FAK and other focal adhesion proteins such as paxillin and talin can be cleaved by proteases such as calpain. The FAK calpain cleavage site lies between the two C-terminal proline-rich regions and results in an N-terminal fragment between 80-90 KDa and a C-terminal fragment of around 35 KDa. Importantly calpain proteolysis is required to regulate adhesion dynamics in motile cells (Carragher *et al*., 1999; Chan *et al*., 2010; Franco *et al*., 2004). More recently Lim *et al* have shown that inhibition of calpain resulted in decreased survival signals after oxidative stress such as Akt phosphorylation and Bcl2/Bax ratio. Survival was rescued by transfection of the N-terminal fragment in myofibroblasts *in vitro*. This

suggests the N-terminal fragment that results from calpain cleavage might have a pivotal role in cell survival in stress conditions (Lim *et al*., 2012).

D. Related adhesion focal adhesion kinase, Pyk2

Avraham and colleagues have identified another member of the focal adhesion protein kinase family, Pyk2, also termed related adhesion focal tyrosine kinase (RAFTK) that has close homology with FAK and shares a similar domain structure (FERM, kinase, proline rich and FAT domains) as well as common phosphorylation sites. Pyk2 can be activated through stimuli that increase intracellular calcium levels (the reason why it was also termed calcium-dependent protein tyrosine kinase (CADTK)). Unlike the ubiquitous expression of FAK, Pyk2 is mainly expressed in cells of the endothelium, central nervous system and haematopoietic lineages. FAK is localised at focal adhesions through its FAT domain in adherent cells whereas Pyk2 exhibits a perinuclear localisation (Avraham *et al*., 2000; Avraham *et al*., 1995). This difference in localisation of both proteins is thought to be responsible for the weak α5β1-mediated activation of Pyk2 in response to fibronectin binding, when compared with FAK (Klingbeil *et al*., 2001). Pyk2 deficient mice are viable and fertile however this protein was found to be essential for macrophage migration and function (Okigaki *et al*., 2003). Pyk2 was implicated in the reduction of the vascular endothelial cell-cell adhesion mediated by VE-cadherin. Upon loss of VE-cadherin, the reduced cell-cell adhesion is accompanied by an increase in β-catenin phosphorylation that is dependent on the activation of Pyk2. This signalling is important for endothelial cell integrity modulation (van Buul *et al*., 2005).

1.5.2. Focal adhesion kinase in mouse development

FAK expression is detected in early mouse embryos and is distributed throughout all cell types at the time of neurulation. Following neural tube closure, FAK expression becomes particularly abundant in the developing vasculature (Polte *et al*., 1994). FAK deficiency in mice is embryonic lethal at embryonic day E8.5 due to defects in late gastrulation related to an impaired mesoderm migration. This phenotype was similar to fibronectin-deficient mice suggesting an important role for FAK in mediating integrin-fibronectin interactions at this stage of development. Interestingly FAK deficient cells displayed an increased number of focal adhesions suggesting that FAK may be involved in focal adhesion turnover during cell migration (Furuta *et al*., 1995; Ilic *et al*., 1995).

1.5.3. FAK as a positive regulator in tumour progression

FAK is located at human chromosome 8q24term (Agochiya *et al*., 1999) and is overexpressed in many epithelial human cancers such as breast (Cance *et al*., 2000), colorectal (de Heer *et al*., 2008), thyroid (Owens *et al*., 1996), prostate (Tremblay *et al*., 1996), oral cavity (de Vicente *et al*., 2012), liver (Cai *et al*., 2009), stomach (Park *et al*., 2010) and ovary (Judson *et al*., 1999) and also in tumours of mesenchymal origin such as glial cells (Jones *et al*., 2001; Wang *et al*., 2000).

FAK signalling can promote changes in cell shape and the formation of invadopodia that promote an invasive cell phenotype (Hauck *et al*., 2002) and was shown to be up-

regulated in pre-invasive or invasive breast and colon cancer patient tissue samples (Cance *et al*., 2000). Analysis of FAK, paxillin and Src expression in colorectal cancer samples showed equivalent levels of the three proteins in liver metastases when compared with the primary tumours. Moreover high levels of both FAK and Src within tumour cells were indicative of poor prognosis and tumour recurrence (de Heer *et al*., 2008).

In mouse studies, specific deletion of FAK in keratinocytes suppressed chemically-induced skin tumour formation associated with increased keratinocyte cell death (McLean *et al*., 2004). Several mouse studies have shown that FAK is important for breast cancer tumourigenesis, progression and metastasis (Luo *et al*., 2009; Mitra *et al*., 2006a; Provenzano *et al*., 2008). Specific deletion of FAK in the mammary epithelium retarded tumour formation, growth and metastasis to the lung in the Polyoma middle T (MMTV-PyMT) tumour mouse model. Furthermore loss of FAK in these mice resulted in reduced Cas, Src and ERK1/2 phosphorylation (Provenzano *et al*., 2008).

1.5.4. FAK inhibitors

The positive role of FAK in tumour progression led to the development of small molecule inhibitors of FAK catalytic activity as anti-tumour agents. Novartis developed 2 ATP-competitive agents that decrease FAK-P-Y397 phosphorylation: TAC-544 and TAE-226. Both exhibit nanomolar inhibitory activity against FAK. However, TAE-226 can also inhibit Pyk2 and other receptor tyrosine kinases such as insulin-like growth factor 1. The anti-tumour activity of TAE-226 was shown in ovary and cancer models (Lim *et al*., 2008b). More recently Kurio *et al*, using human breast cancer xenograft mouse models that metastasise to the bone, have shown that TAE-226 not only decreased tumour growth but also bone metastasis increasing survival. The authors have also shown an effect of this compound in inhibiting osteoclasts *in vitro* and *in vivo* that is one of the mechanisms involved in bone metastasis (Kurio *et al*., 2011).

Pfizer developed another ATP-competitive agent, PF-228 that seems to be more selective in the inhibition of FAK-P-Y397 phosphorylation. Given the hypothesis of Pyk2 compensation for the loss of FAK, Pfizer developed PF562, 271 which has been shown to have inhibitory activity against both FAK and Pyk2. The anti-tumour activity of PF562, 271 was demonstrated in prostate, pancreatic, glioblastoma and lung xenotropic tumour models (Lim *et al*., 2008b). More recently Stokes *et al* have tested the efficacy of PF562, 271 in metastasis using an orthotopic mouse model of pancreatic carcinoma. First of all the authors have shown that the compound has an effect in decreasing proliferation not only of tumour cells but also stromal cells such

as cancer associated fibroblasts and macrophages *in vitro*. PF562, 271 decreased tumour growth, invasion and metastasis and also the numbers of tumour associated macrophages and fibroblasts *in vivo* (Stokes *et al*., 2011). A new small reversible small oral inhibitor was developed, PND-1186. Studies have demonstrated that the compound inhibits FAK-P-Y397 phosphorylation and downstream substrate p130Cas in orthotopic breast tumours, however the study does not mention any analysis of Pyk2 or other tyrosine kinases. They show efficacy in primary tumour and metastasis in the same model and also a decrease in inflammatory cell infiltration (Walsh *et al*., 2010). Most inhibitors are still on phase I clinical trials and there is no information on their clinical efficacy yet.

1.5.5. FAK as a negative regulator in tumour progression

Even though most of the evidence points towards a positive role for FAK in tumour progression, it has been over a decade since the first studies indicating a negative role for FAK in tumour progression appeared. A small study from Ayaki and colleagues analysed 10 matched samples of human normal colorectal mucosa, primary colorectal carcinoma and liver metastases. Even though tumours showed higher FAK levels than the normal colorectal mucosa the matched liver metastasis had significantly lower FAK levels than the tumours. Paxillin on the other hand was significantly up-regulated in tumours and metastasis when compared with normal colorectal mucosa (Ayaki *et al*., 2001). The same theory had been presented in another study using *in vitro* and in *vivo* mouse models. The authors demonstrated that downregulation or dephosphorylation of FAK was required and sufficient for EGF-induced detachment

of extracellular matrix and increased cell motility and invasion *in vitro*. Moreover when tumour cells expressing FRNK were injected in mice genomic PCR from several tissues suggested an increased dissemination of these cells (Lu *et al*., 2001). Other studies have also proposed weakening adhesion strength of integrins as an important factor for induction of cell motility (Lynch *et al*., 2005).

A more robust analysis on the prognostic value of FAK levels was performed in 162 resected cervical cancer specimens. Even though FAK expression was found up-regulated in tumour cells when compared with normal cervical epithelium, weak FAK expression was significantly correlated with poor overall survival. Importantly this weak expression was also significantly associated with pelvic lymph node metastasis and recurrent disease (Gabriel *et al*., 2006).

More recently Zheng *et al* have highlighted FAK dephosphorylation at FAK-P-Y397 and FAK inhibition by activated Ras as important events in promoting Ras-induced cell migration, invasion and metastasis. The authors claim ERK-dependent FAK phosphorylation at serine 910 primes FAK for dephosphorylation at FAK-P-Y397 by molecules downstream of Ras signalling. Tail vein injection of tumour cells with mutated FAK-P-Y397 or FRNK in mice resulted in increased numbers of Ras-mediated metastases *in vivo* (Zheng *et al*., 2009).

1.5.6. Endothelial FAK in angiogenesis

The high levels of FAK in the developing vasculature and the vascular defects observed in FAK deficient mice point to a possible role for FAK in angiogenesis (Furuta *et al*., 1995; Ilic *et al*., 1995) but the exact role of FAK in pathological angiogenic processes, such as tumour angiogenesis, is still not well understood.

FAK was found to be up-regulated in microvascular endothelial cells in malignant astrocytoma tumour biopsy samples. Using an endogenous inhibitor of FAK (FRNK), endothelial cell migration and tube formation of brain microvascular endothelial cells was inhibited suggesting a role for FAK in tumour angiogenesis (Haskell *et al*., 2003).

An *in vitro* study demonstrated that VEGF-A-induced migration of porcine aortic endothelial cells expressing VEGFR-2 requires the activation of PI3K, which depends on FAK activation by VEGF-A (Qi and Claesson-Welsh, 2001). Eliceri and colleagues have shown that VEGF-A-induced FAK-P-Y861 phosphorylation promotes the formation of a FAK/αvβ5 complex in endothelial cells, which is inhibited in Src-deficient mice (Eliceiri *et al*., 2002).

Transgenic mice that constitutively overexpress chicken FAK in vascular endothelial cells under the control of the Tie2 promoter (an enhancer that drives gene expression throughout embryogenesis and adulthood in endothelial cells) showed enhanced angiogenesis during skin wound healing and in response to ischaemia (Peng *et al*.,

2004). Moreover endothelial-specific FAK deletion using Cre-loxP technology with Cre expression driven by the Tie2 promoter does not affect early embryogenesis but leads to late embryonic lethality at embryonic stage E13.5 due to defects in vascular development that are responsible for haemorrhage and oedema (Shen *et al*., 2005).

Weiss and colleagues have crossed the FAK floxed mice with a tamoxifen-inducible Cre under the control of the 5'endothelial enhancer of the stem cell leukaemia locus (End-SCL-Cre-ER(T)) to induce specific FAK deletion in endothelial cells in adult mice. Surprisingly in this mouse model, endothelial-specific FAK deletion shows no vascular phenotype and no changes in angiogenic responses. The authors attribute this to a compensatory effect of Pyk2 for the loss of FAK (Weis *et al*., 2008). However our laboratory has demonstrated that by crossing FAK floxed mice with a different tamoxifen inducible Cre line, where Cre expression is driven by the endothelial-specific Pdgfb promoter (Claxton *et al*., 2008), endothelial FAK deletion in the absence of Pyk2 compensation decreased tumour growth and angiogenesis (Tavora *et al*., 2010). Dual inhibition of FAK and Pyk2 using the TAE226 inhibitor have shown an effect in repressing neoangiogenesis *in vitro* and in a mouse model *in vivo* (Schultze *et al*., 2010).

More recently Chen *et al* have also highlighted a role for endothelial FAK in VEGF-induced vascular permeability. Using genetic mouse strategies and pharmacological inhibition with PF562, 271 (FAK-P-Y397 and Pyk2 inhibitor) the authors claim FAK FERM domain association with VE-Cadherin leads to FAK activation and FAK kinase-dependent phosphorylation of β-catenin. This results in VE-cadherin/β-catenin dissociation and endothelial junction breakdown required for VEGF-induced

permeability. They also show that the effects of FAK inhibition in VEGF-induced permeability are independent of Src (Chen *et al*., 2012). In line with this another study has revealed a role for endothelial FAK in cancer cell homing and metastasis. The authors induced hyperpermeability in mice lungs *in vivo* by injecting Lewis Lung Cell (LLC) carcinoma cells, VEGF or tumour cell conditioning medium. They have shown increased levels of FAK phosphorylation and E-selectin in these areas of hyperpermeability. Moreover E-selectin was shown to be necessary for metastatic cancer cell homing and metastasis *in vivo* and inhibition of FAK by using a mouse model with FRNK overexpression in endothelial cells decreased E-selectin expression, cancer cell homing and metastasis (Hiratsuka *et al*., 2011).

1.5.7. Bone marrow derived FAK

The role of FAK in bone marrow is less understood even though FAK identification and most of the signalling and functional studies were performed in fibroblasts that can also be derived from the bone marrow compartment (Hsia *et al*., 2003).

A recent study has demonstrated FAK levels are increased in HSCs when compared with lineage progenitors and mature blood cells. HSC numbers were found increased when FAK was deleted in the bone marrow compartment in a Cre inducible conditional knockout under the expression of an interferon- inducible promoter (Mx1-Cre). These mice showed more dividing and fewer quiescent HSCs. By using competitive transplant assays where FAK depleted bone marrow cells were transplanted with competitor WT bone marrow cells into lethally irradiated WT mice

the authors showed FAK depleted bone marrow cells have long-term engraftment capacity. Importantly this study also suggests FAK levels in both HSCs and bone marrow stroma are necessary to regulate the HSC pool and long-term engraftment (Lu *et al*., 2011). On the other hand, using the same mouse model (MxCre) Vemula *et al* have shown that loss of FAK results in impaired erythropoiesis and myelopoiesis *in vivo*. They have also demonstrated that FAK depletion in erythroid and myeloid populations *in vitro* impaired cytokine induced growth and survival. FAK deficient myeloid cells also showed reduced migration and adhesion in extracellular matrix proteins such as fibronectin and SDF-1. Recruitment of myeloid cells to sites of inflammation *in vivo* was also deficient in a model of acute peritonitis (Vemula *et al*., 2010).

Glodek *et al* have highlighted a role for FAK in CXCL12-induced chemotatic and pro-adhesive responses in haematopoietic precursor cells. FAK knockdown in human pro-B acute lymphoblastic leukaemia (proB-ALL) cells resulted in decreased CXCL12-induced adhesion to VCAM-1 without impairing VLA-4 function and consequently reduced chemotaxis to this cytokine (Glodek *et al*., 2007).

When bone marrow cells are incubated with GM-CSF there is an up-regulation of FAK *in vitro* that might contribute toward maturation of monocytes/macrophages and granulocytes (Kume *et al*., 1997). Indeed FAK deletion in the myeloid population resulted in decreased monocyte recruitment to sites of inflammation *in vivo*. Primary bone marrow macrophages isolated from these mice showed adhesion and motility defects. Interestingly combined loss of FAK and Pyk2 resulted in more severe defects in invasion than either molecule alone (Owen *et al*., 2007). Another study has shown

that FAK, downstream of α5β1 integrin, promotes haptotaxis towards fibronectin and chemotaxis towards M-CSF in macrophages. In contrast, paxillin is important for chemotaxis downstream of α4β1 integrin and independent of FAK in macrophages (Abshire *et al*., 2011). Using a similar mouse model Kasorn *et al* have shown that FAK null neutrophils have defects in complement-mediated phagocytosis and pathogen killing capacity *in vitro* and *in vivo*. FAK deficiency also reduced adhesion to fibronectin and ICAM-1 but not to VCAM-1 and did not affect neutrophil transendothelial migration (Kasorn *et al*., 2009). Other studies suggested endothelial FAK is important for neutrophil transendothelial migration (Parsons *et al*., 2012).

1.6. Introduction summary

Tumour microenvironment has been recognised as being pivotal in regulation of cancer progression. Stromal-cancer cell interactions are dependent on integrin and growth factor receptor signalling activation. Focal adhesion kinase, being downstream of both growth factor receptors and integrins and for the recognised overexpression in many human cancers, has emerged as a promising anti-cancer target. However recent data have suggested FAK can also act as a negative regulator in tumour progression and raised concerns about the use of FAK inhibitors. These drugs are likely to affect both cancer and stromal compartments. The role of stromal FAK in tumour progression is less understood.

Bone marrow derived cell recruitment has been recognised as important not only in primary tumours but also in the formation of pre-metastatic niches. This recruitment is also dependent on integrin and cytokine signalling. FAK has shown to be important in inflammatory responses from myeloid cells but the role of FAK in cancer bone marrow derived cell recruitment has not been studied.

The complexity of the molecular basis of FAK function is likely important in the control of different signalling pathways. Exploring the role different phosphorylation sites of FAK play in tumour progression *in vivo* might give insights into the mechanism of FAK regulation of stromal-cancer cell interactions.

1.7. Research aims

1) Study the effect of stromal FAK deletion in adult mice during tumour growth, tumour angiogenesis and metastasis.

2) Investigate the effect of FAK deletion in the bone marrow compartment in tumour growth, tumour angiogenesis and metastasis.

3) Elucidate the importance of different FAK phosphorylation sites in the regulation of tumour angiogenesis, progression and spread.

2. MATERIALS AND METHODS

2.1. Antibodies

Rat anti-mouse CD31 (BD Biosciences, Oxford, UK), rat anti-endomucin antibody (clone V.7C7, Santa Cruz Biotechnology, CA, USA), mouse monoclonal anti-FAK (clone 77/FAK – BD Biosciences, Oxford, UK), rat anti-Gr1 (clone RB68C5 - BD pharmigen, Oxford, UK), rat anti-mouse Gr1 antibody functional grade purified (eBiosciences, Hatfield, UK), rat anti-mouse IgG2b κ isotype control antibody functional grade purified (eBiosciences, Hatfield, UK), Myc-Tag (9B11) mouse monoclonal antibody (Cell Signaling Technology, Boston, USA), rabbit anti-mouse large T-cell antigen (Santa Cruz Santa Cruz Biotechnology, CA, USA) anti-chicken FAK antibody (provided by Jun-Lin Guan, University Michigan, USA), mouse anti-HSC70 (Santa Cruz Biotechnology, CA, USA), anti-FcγRII/III (ABD Serotec, Kidlington, UK), anti-CD102 (ABD Serotec, Kidlington, UK), Rat IgG2a isotype control (Santa Cruz Biotechnology, CA, USA), mouse IgG2a isotype control (Dako, Cambridgeshire, UK), Alexa Fluor 546 goat anti-rat IgG (Invitrogen, Paisley, UK), anti-rat Alexa-Fluor-488 (Invitrogen, Paisley, UK), Polyclonal rabbit anti-mouse-HRP (Dako, Cambridgeshire, UK), Magnetic beads coated with sheep anti-rat (Dynal-Invitrogen Bead Separation, Oslo, Norway). Anti-mouse CD16-32 (Fc block), anti-mouse CD45-efluor450, anti-mouse Ly6G-FITC, anti-mouse Ly6C-APC, anti-mouse CD11b-PE, anti-mouse CD3-PECy5, anti-mouse CD4-FITC, anti-mouse CD8-APC, mouse haematopoietic lineage-efluor450, anti-mouse CD117 (cKit)-APC, anti-mouse Ly6-A/E (Sca-1)-PerCP-Cy5.5, anti-mouse CD34-efluor700, anti-mouse CD135 (Flt3)-PE and anti-mouse CD16-32-FITC were all purchased from eBiosciences (Hatfield, UK).

2.2. Extracellular matrix reagents

Fibronectin and Collagen type I were purchased from Millipore, Watford, UK.

2.3. Mice

2.3.1. Generation of RERTn$^{ERT/ERT}$Cre; FAK$^{fl/fl}$ mice

In order to study the effect of stromal FAK deletion in adult mice and to overcome the early embryonic lethality of the constitutive deletion of FAK (Ilic *et al*, 1995) we have generated global inducible-FAK knockout mice.

Previously characterised RERTn$^{ERT/+}$Cre mice (Barriere *et al*., 2007; Guerra *et al*., 2003) were obtained from Mariano Barbacid Laboratory (Centro de Investigaciones Oncologicas, Madrid, Spain) and bred in order to generate RERn$^{ERT/ERT}$Cre homozygous mice. In these mice Cre is expressed under the promoter of the large unit of RNA polymerase II being generated in the majority of the cells and thus we used them as a tool to delete target genes inducibly in adult mice.

FAK flox/flox (FAK$^{fl/fl}$) mice were obtained from Jane Robinson (Sanger Institute, Cambridge, UK). FAK$^{fl/fl}$ allele was generated by gene targeting mouse embryonic stem (ES) cells that resulted in the insertion of loxP sites flanking the exon that encodes the FAK amino acids 413/444 (McLean *et al*., 2004). These mice were crossed with the RERTn$^{ERT/ERT}$Cre mice in order to generate RERTn$^{ERT/ERT}$Cre;FAK$^{fl/fl}$ on a mixed C57BL6/129 background (**Fig.7**).

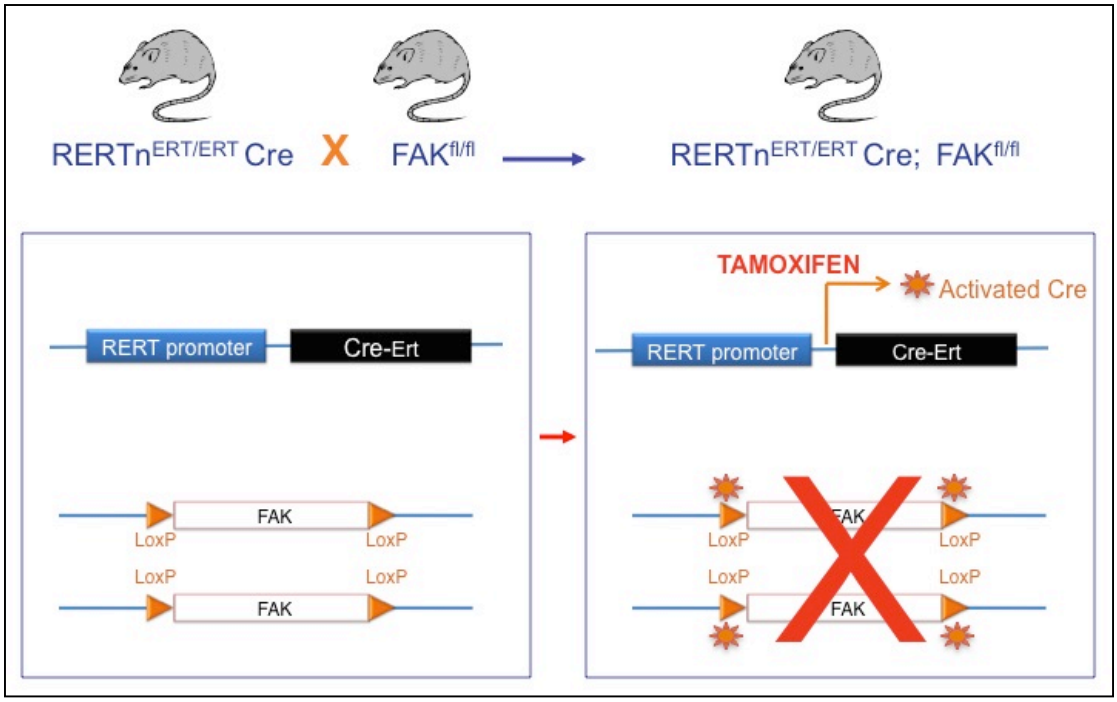

Figure 7: Generation of ubiquitous inducible-FAK deficient mice

Upon tamoxifen treatment, Cre recombinase under the expression of the large subunit of RNA polymerase II promoter RERT allows the recombination of the LoxP sites. This will allow for the excision of mouse FAK in all RERT positive cells.

2.3.2. RIP-Tag2 mice

RIP-Tag2 mice are transgenic for the rat insulin promoter II gene linked to the large-T antigen of SV40 (RIP-Tag) (Hanahan, 1985). RIP-Tag2 mice develop pancreatic β-cell hyperplasia by 9 weeks of age and by 16 weeks of age develop highly vascularised solid pancreatic insulinomas accompanied by lymph node and liver micrometastasis (Lopez and Hanahan, 2002).

2.3.3. Generation of Pdgfb-iCreER;FAK$^{fl/fl}$;R26FAK$^{KI/KI}$ mice

In order to study the effect of the different FAK phosphorylation sites on tumour growth and angiogenesis we are generating point-mutant FAK knockin mice in the mouse Rosa26 locus (R26$^{FAKKI/KI}$ mice).

For that purpose we have used different chicken FAK constructs provided initially from Margaret Frame's laboratory (Beatson Institute for Cancer Research, Glasgow, UK) described in **Table 1**.

Table 1: Point-mutant chicken FAK constructs

Construct name	WT aminoacid	Construct aminoacid
WT (control)	Tyrosine (Y) 397 Lysine 454 Tyrosine (Y) 861	Tyrosine (Y) 397 Lysine 454 Tyrosine (Y) 861
397F	Tyrosine (Y) 397	Phenylalanine (F) 397
397E	Tyrosine (Y) 397	Glutamic acid (F) 397
KD	Lysine 454	Arginine 454
397E/KD	Tyrosine (Y) 397 Lysine 454	Phenylalanine (E) 397 Arginine 454
861F	Tyrosine (Y) 861	Phenylalanine (F) 861

A. Targeting embryonic stem cells

Chicken FAK constructs were cloned into the pRosa26-1 vector by Dr. Bernardo Távora generating the genetic targeting construct shown in **Fig.8**. This targeting vector consists of a neomycin-resistant cassette adjacent to a STOP codon both of which are flanked by loxP sites. Downstream of this lies the WT or mutant chicken FAK followed by an IRES-GFP insert (**Fig.8**). Theoretically the c-myc tag and GFP should act as reporters of WT or mutant chicken FAK.

Figure 8: Chicken FAK targeting construct into mouse Rosa26 locus

A neomycin-resistant cassette adjacent to a STOP codon (NeoR STOP) both of which flanked by loxP sites precedes the chicken FAK construct that is tagged with c-myc on the C-terminus and is followed by IRES-GFP insert. Two homologous regions to the mouse Rosa26 locus to allow homologous recombination into mouse embryonic stem cells flank this entire sequence.

I. <u>Expansion and linearisation of the targeting vectors</u>

Targeting vectors were expanded by transformation of Stbl3 chemically competent bacteria (Invitrogen, Paisley, UK). 0.2 µl of plasmid DNA was added to 100 µl of Stbl3 chemically competent bacteria and incubated on ice for 30 min. The cells were then subjected to a heatshock at 42ºC followed by 2 min recovery on ice. Finally the cells were shaken for 1h at 37ºC at 225 rpm in a shacking stage incubator and plated in Luria-Bertani (LB) broth (1% (w/v) tryptone, 0.5% (w/v) yeast extract and 1% (w/v) sodium chloride) with 1.5% (w/v) agar plates supplemented with 100 µg/ml of

ampicilin (Sigma, Dorset, UK) in distilled water (filter sterile) at the dilutions of 1:10 -1:100.

Ampicilin resistant colonies were grown in 250 ml of LB supplemented with 100 µg/ml of ampicilin and DNA isolated using the EndoFree Maxi Kit (Qiagen, West Sussex, UK). Isolated DNA was then analysed with different restriction enzymes (SacII, PacI/AscI, EcoRV, BamHI, Hind III and Pac/EcoRV) to rule out any recombination event.

Each targeting construct (220µg) was then digested overnight at 37ºC with 20 µl of SacII enzyme (New England Biolabs Hertfordshire, UK), 25 µl of buffer 4 (New England Biolabs Hertfordshire, UK) and distilled water up to a volume of 250 µl. Running 20 µl of reaction in a 0.8% agarose gel assessed the efficiency of digestion. In the case of an efficient digestion, without any undigested DNA bands, the linearised DNA was purified by phenol/chlorophorm extraction. Equal volumes of saturated phenol (Sigma, Dorset, UK) were added to the DNA samples before vortexing and centrifugation at maximum speed (12000 g) for 3 min at 4ºC. The supernatant was carefully transferred to a clean tube making sure that no interphase or phenol got into the new tube and an equal volume of 1:1 phenol:chlorophorm:isoamylic alcohol (Sigma, Dorset, UK) was added. Samples were vortexed and centrifuged for 3 min at maximum speed at 4ºC. The upper aqueous phase was transferred to a new tube and equal volume of chlorophorm (BDH laboratory Supplies, Poole, UK) was added previous to the vortexing and centrifugation at maximum speed for 3 min. This procedure was repeated once. DNA on the upper aqueous phase was precipitated with 0.1 volume of 3M sodium acetate (BDH laboratory Supplies, Poole, UK) pH 5.2 and 2 volumes of of 100% ethanol

(Fisher Scientific, Leicestershire, UK) at -80 ºC overnight or at least for a few hours. DNA was pelleted with centrifugation at maximum speed for 30 min at 4ºC and washed once with 70% ethanol. After centrifugation for 15 min at maximum speed at 4ºC pelleted DNA was air dried and ressuspended in Tris-EDTA (TE) to a concentration of 1 mg/ml.

II. Electroporation of mouse ES cells

Four to five 25µl aliquots of each linearised targeting vector were frozen, labelled and sent to Ian Roswell in the Transgenic Unit in Claire Hall Laboratories where these targeting vectors were used to electroporate mouse ES cells. The mouse ES cells used were from hybrid 129S6.C57BL6J mice (Transgenic facility CRUK) and were maintained on primary embryonic fibroblast cells with the addition to the media of Leukaemia Inhibitory Factor (LIF), at 1000 units/ml, to prevent differentiation and maintain pluripotence.

Constructs were electroporated into 5 x 10^6 - 10^7 ES cells. Selection was applied 24 hours after electroporation with the addition of 200µg/ml G418 in ES cell medium. After 8-10 days colonies were clearly visible. Colonies were picked from the plates into wells of a 96-well microtitre plate, cultured and, when they reached confluence, half of the cells were frozen and half were transferred to the corresponding well of a further 96-well plate to extract DNA for the screening of homologous recombinants by Southern blot analysis. Screening by Southern blotting is important to confirm the homologous recombination of constructs within the Rosa 26 locus and determine if any random integrations have occurred. Any clones with random integrations should not be used further.

B. Screening and confirmation of homologous recombinants by Southern Blot analysis

I. Southern blot reagents

Cell lysis buffer (Clare Hall Laboratories) - 10 mM Trizma base/Trizma hydrochloride (pH 7.5), 10 mM EDTA, 10 mM NaCl, 0.5% Sarcosyl and 2 mg/ml proteinase K (add fresh).

TE buffer - TE buffer is composed by 10 mM Trizma base/Trizma hydrochloride (pH 7.5) (Sigma, Dorset, UK) and 1mM EDTA (BDH laboratory Supplies, Poole, UK).

DNA loading buffer - The 10X loading buffer was prepared by mixing 20X SSC:glycerol 1:1, 0.3% bromophenol blue (Sigma, Dorset, UK) and 0.3% xylene cyanide (Sigma, Dorset, UK).

TBE - The 10X TBE solution used is composed by 108 g/l Trizma base, 55g/l orthoboric acid (Sigma, Dorset, UK) and 20 mM EDTA.

10X Nick translation buffer - 0.5M Tris-HCl (pH 7.4), 50 mM $MgCl_2$ (Sigma, Dorset, UK), 0.1 M βME (Sigma, Dorset, UK). Stored at -20°C.

Phosphate buffer – 316 ml of 0.5M $Na_2H_2PO_4.H_2O$ (Fisher Scientific, Leicestershire, UK) added to 684ml of 0.5M $Na_2HPO_4.7H_2O$ (Fisher Scientific, Leicestershire, UK) to make 1L of 0.5M sodium phosphate pH 7.2.

Church & Gilbert Solution - 0.25M phosphate buffer, 7% SDS (Sigma, Dorset, UK), 1mM EDTA.

II. DNA preparation and digestion for Southern blot analysis

Cells from an ES cell colony transferred to a well of a 96-well plate (see **2.3.3A-II**) were grown to confluence (3-4 days). Media was removed from each well and cells were washed twice with PBS (200µl/well). 50µl of cell lysis buffer was added to each well, the plate sealed and incubated overnight at 60ºC in a humid atmosphere. After the lysis plate was frozen at -80ºC and sent in dry ice to our laboratory. After thawing the plate 50µl of isopropanol (BDH Laboratory supplies, Poole, UK) was added to each well and DNA precipitated by a short gentle vortex. The plate was then centrifuged at 1200g for 30 mins and the wells emptied by inverting the plate onto tissue paper. The pellet was washed once with 70% ethanol and re-centrifuged at 1200g for 15 min. The DNA pellet was then air dried, ressupended in the following restriction enzyme mix and left overnight at 37ºC:

Enzyme (EcoRV)	2 µl (40 units)
10X buffer	3 µl
RNase	0.2 µl (50 µg/ml final)
Spermidine	0.75 µl (1mM final)
100X BSA	0.3 µl
dH_2O	23.75 µl
Total	30 µl

The enzyme and buffers were purchased from New England Biolabs, Hertfordshire, UK, RNase was purchased from Sigma, Dorset, UK. Spermidine was purchased from Sigma, Dorset, UK and diluted in distilled water to 4 mM.

The initial screen was performed using EcoRV digested DNA. On the following day an additional 1 µl of EcoRV was added to each well and the samples were left 3-4h at 37ºC.

For the confirmation screen of expanded clones 10 µg of DNA were digested with EcoRV and AvrII separately using the same restriction mixed described.

III. Electrophoresis

Digested DNA samples were mixed 1:10 with 10 X DNA loading in preparation for electrophoresis on 0.8% agarose gels. Agarose gels were prepared by microwaving agarose (Gibco BRL, Paisley, UK) with a volume of 1X TBE (10X TBE diluted in distilled water) adequate to the size of the tray used. All gels were supplemented with ethidium bromide (0.2 µg/ml) (Sigma, Dorset, UK) before polymerising in a sealed tray with 1 or more combs at room temperature (RT). Gels were placed in a gel tank (Scotlab-Anachem, Luton, UK) flooded with TBE 1X and samples loaded using yellow tips. Gels were run at 25 volts overnight. Five µl of Hyperladder I (Bioline, London, UK) was used to determine the Kb size of DNA fragments. Bands were visualised under UV light and photographed using an EagleEye Still Video System (Stratagene, Cedar Creek, TX, USA).

IV. Transfer DNA from agarose gels to nylon membranes

After electrophoresis agarose gels were photographed alongside a ruler, in order to measure the distance from the wells to the DNA ladder fragments. Efficient digestion can be seen by observing long even streaks of DNA with a distinct band at around 2 Kb. Gels were immersed in 2 volumes (1000 ml) of HCl 0.1N (BDH Laboratory supplies, Poole, UK) with gentle shaking during 15 minutes in order to depurinate the DNA. The step of depurination (random Creation of apurinic sites in the double-strand DNA) is important to fragment the DNA and allow for efficient transfer. Gels were then transferred to 2 volumes (1000 ml) of NaOH 0.4N (Fisher Scientific, Leicestershire, UK) and shaken for 15 minutes in order to denature the DNA into single strands and allow efficient probe hybridization after transfer. Gels were then ready to be assembled into a transfer stack to allow for DNA to be transferred to nylon membranes by capillary action (**Fig.9**).

Southern blot transfer was set up as follows: a platform was placed in a tray with 500 ml of 0.4N NaOH. A layer of Whatman paper was used as a wick for the 0.4N NaOH that was placed in the bottom tray. The gel was then placed on top of the Whatman paper and the Zeta probe membrane (previously immersed in 0.4N NaOH) (Bio-Rad Laboratories, Hertfordshire, UK) on top of the gel. The edges of the gel were sealed with Parafilm in order to prevent a short-circuit of the transfer (i.e. so that the 0,4N NaOH transfer buffer passes directly through the gel carrying the transfer of the DNA present in the gel onto the Zeta-probe membrane). Three layers of Whatman paper were laid on the membrane, followed by a stack of paper towels to create a gradient

that facilitates the transfer. A weight was placed in the top of the paper towels to maintain firm contact and reassure an homogeneous transfer. The DNA was transferred overnight. Finally nylon membrane was removed from the stack, UV-crosslinked (12000 μJ) and then neutralised with 2X SSC, 0.2M Tris-HCl, pH 7.5. Membranes were air dried and stored at RT until required.

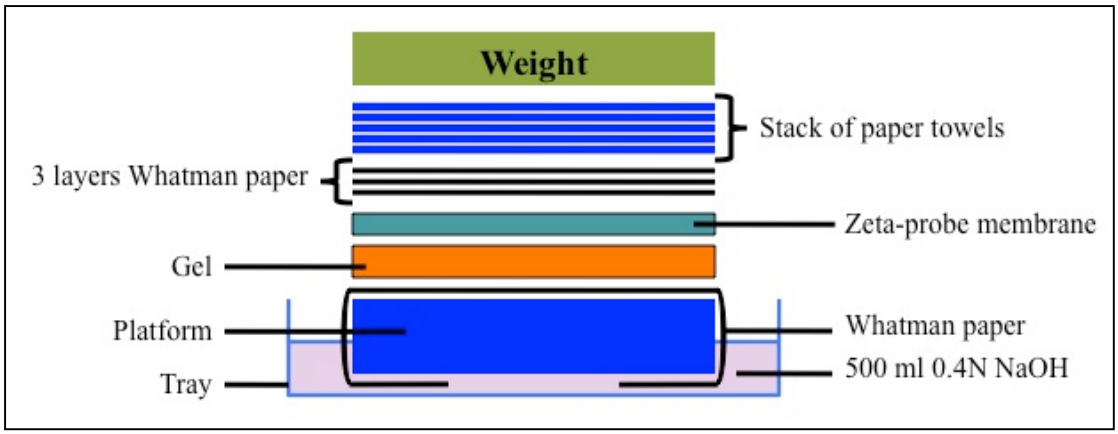

Figure 9: Diagram of Southern blot transfer set up.

A Whatman paper is placed on the top of a platform in contact with 500 ml of 0.4N NaOH inside a tray. The gel and membrane are then placed on top of the Whatman paper in this order. Three layers of Whatman paper are laid on the membrane plus a stack of paper towels creating a gradient that facilitates the transfer of DNA from the gel to the membrane by capillarity. A weight is place on the top of the transfer setting in order to maintain firm contact, stabilise it and guarantee an homogeneous transfer.

V. Isolation and preparation of DNA probes

DNA was analysed using three different probes: Probe A, Probe B and Probe C. This section will describe sequence and hybridisation sites of each probe, probe isolation and labelling.

- **Probe A – 5'R26 external probe**

Probe A is a 369 bp fragment, which was isolated from the pTopoRosa26pr2+ (provided by David Stevenson, Beatson Institute, Glasgow, UK), contains an ampicillin resistant cassette and is generated by EcoRI digestion (highlighted in red). The sequence is:

GAATTCGCCCTTGAGATAGGAACTGGAAAACCAGAGGAGAGGCGTTCAGGAAGATT
ATGGAGGGGAGGACTGGGCCCCCACGAGCGACCAGAGTTGTCACAAGGCCGCAAGA
ACAGGGGAGGTGGGGGGCTCAGGGACAGAAAAAAAAGTATGTGTATTTTGAGAGCA
GGGTTGGGAGGCCTCTCCTGAAAAGGGTATAAACGTGGAGTAGGCAATACCCAGGC
AAAAAGGGGAGACCAGAGTAGGGGGAGGGGAAGAGTCCTGACCCAGGGAAGACATT
AAAAAGGTAGTGGGGTCGACTAGATGAAGGAGAGCCTTTCTCTCTGGGCAAGAGCG
GTGCAATGGTGTGTAAAGGTAGCTGAGAAGGGCGAATTC

Probe A hybridises in the Rosa 26 locus outside the homologous recombination region of the targeting vector (**Fig. 10**). It was used in the first screen and confirmation of the targeted ES cells.

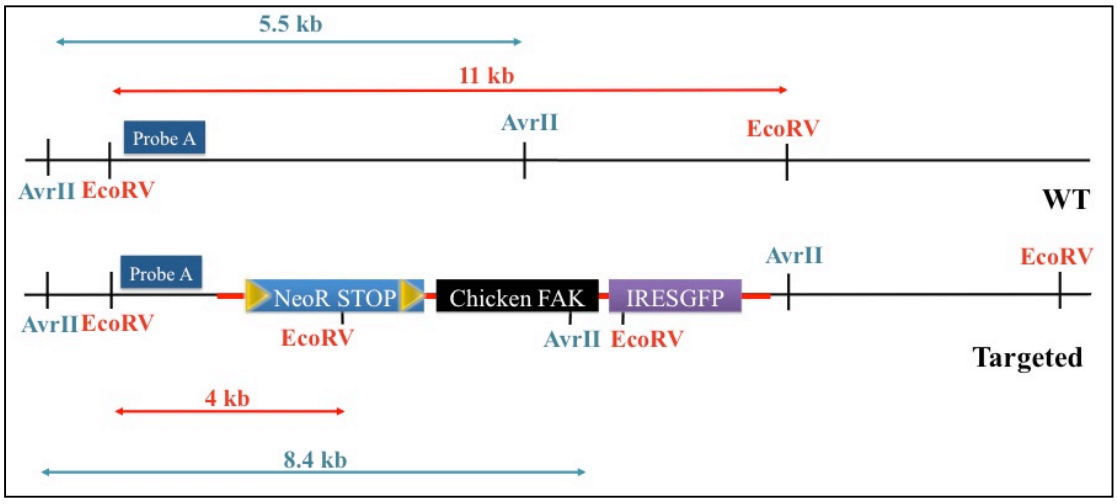

Figure 10: Schematic of Probe A hybridisation and predicted EcoRV and AvrII fragment sizes.

EcoRV predicted fragments after hybridisation with probe A are 9 Kb for the WT allele and 4 Kb for the targeted allele. AvrII predicted fragments are instead 5.5Kb for the WT allele and 8.4 Kb for the targeted allele.

- **Probe B – GFP internal probe**

Probe B is a 752 bp fragment isolated from the pEGFP-N2 vector, contains a kanamycin resistant cassette and is generated by double digestion with BamHI and NotI (highlighted in red). The sequence is:

GGATCCACCGGCCGGTCGCCACCATGGTGAGCAAGGGCGAGGAGCTGTTCACCGGG
GTGGTGCCCATCCTGGTCGAGCTGGACGGCGACGTAAACGGCCACAAGTTCAGCGT
GTCCGGCGAGGGCGAGGGCGATGCCACCTACGGCAACTGACCCTGAAGTTCATCTG
CACCACCGGCAAGCTGCCCGTGCCCTGGCCCACCCTCGTGACCACCCTGACCTACG
GCGTGCAGTGCTTCAGCCGCTACCCCGACCACATGAAGCAGCACGACTTCTTCAAGT
CCGCCATGCCCGAAGGCTACGTCCAGGAGCGCACCATCTTCTTCAAGGACGACGGC
AACTACAAGACCCGCGCCGAGGTGAAGTTCGAGGGCGACACCCTGGTGAACCGCAT
CGAGCTGAAGGGCATCGACTTCAAGGAGGACGGCAACATCCTGGGGCACAAGCTGG
AGTACAACTACAACAGCCACAACGTCTATATCATGGCCGACAAGCAGAAGAACGGCA
TCAAGGTGAACTTCAAGATCCGCCACAACATCGAGGACGGCAGCGTGCAGCTCGCC
GACCACTACCAGCAGAACACCCCCATCGGCGACGGCCCCGTGCTGCTGCCCGACAA
CCACTACCTGAGCACCCAGTCCGCCCTGAGCAAAGACCCCAACGAGAAGCGCGATC
ACATGGTCCTGCTGGAGTTCGTGACCGCCGCCGGGATCACTCTCGGCATGGACGAG
CTGTACAAGTAAAGCGGCCGC

Probe B hybridises only in the targeting vector in the GFP insert and was used to confirm that this region is present in the targeted clones (**Fig. 11**).

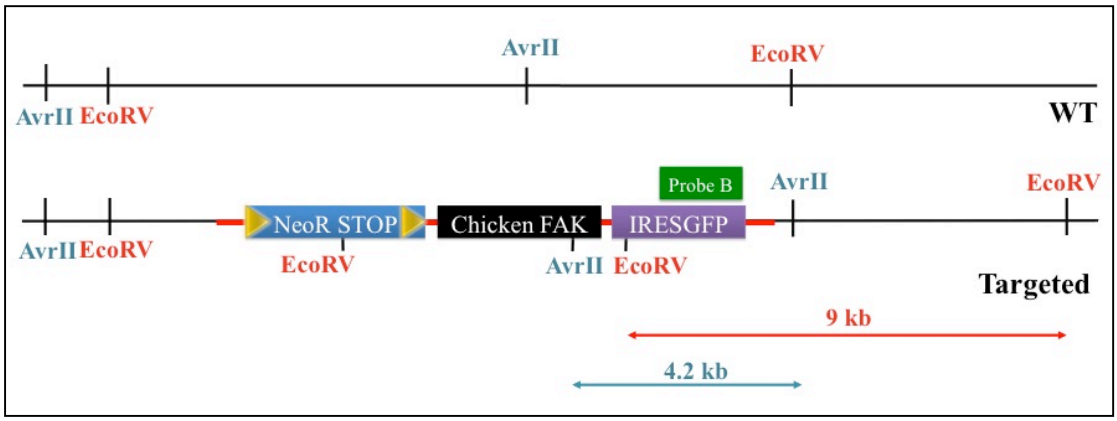

Figure 11: Schematic of Probe B hybridisation and predicted EcoRV and AvrII fragment sizes.

EcoRV and AvrII predicted fragments after hybridisation with probe B are 9 Kb and 4 Kb respectively for the targeted allele. Probe B does not hybridise in the WT allele.

- **Probe C – Neo internal probe**

Probe C is a 483 bp fragment isolated from the pTopoNeo vector, contains an ampicillin resistant cassette and was generated by digestion with EcoRI (highlighted in red). The sequence is:

GAATTCGCCCTTATGAACTGCAGGACGAGGCAGCGCGGCTATCGTGGCTGGCCACG
ACGGGCGTTCCTTGCGCAGCTGTGCTCGACGTTGTCACTGAAGCGGGAAGGGACTG
GCTGCTATTGGGCGAAGTGCCGGGGCAGGATCTCCTGTCATCTCACCTTGCTCCTGC
CGAGAAAGTATCCATCATGGCTGATGCAATGCGGCGGCTGCATACGCTTGATCCGGC
TACCTGCCCATTCGACCACCAAGCGAAACATCGCATCGAGCGAGCACGTACTCGGAT
GGAAGCCGGTCTTGTCGATCAGGATGATCTGGACGAAGAGCATCAGGGGCTCGCGC
CAGCCGAACTGTTCGCCAGGCTCAAGGCGCGCATGCCCGACGGCGATGATCTCGTC
GTGACCCATGGCGATGCCTGCTTGCCGAATATCATGGTGGAAAATGGCCGCTTTTCT
GGATTCATCGACTGTGGCAAGGGCGAATTC

Probe C hybridises only in the targeting vector in the neomycin resistant cassette and was used to confirm that this region is present in the targeted clones (**Fig. 12**).

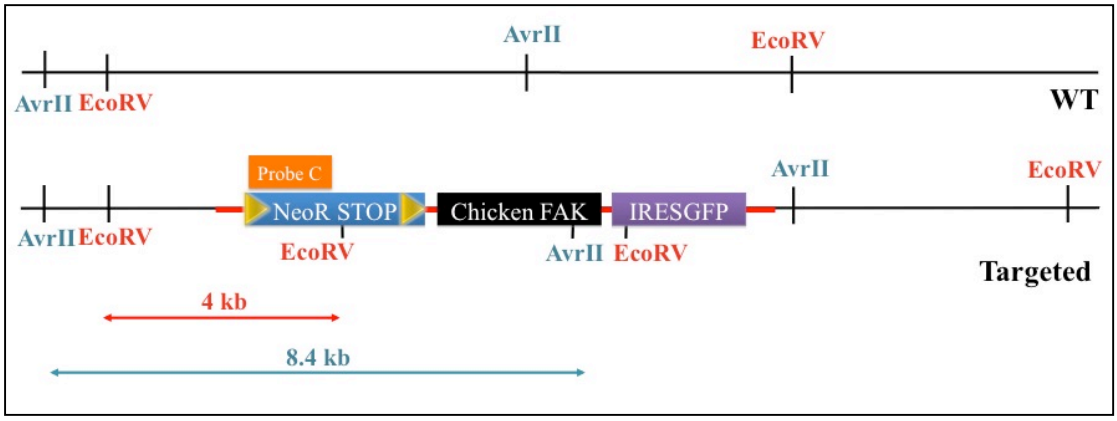

Figure 12: Schematic of Probe C hybridisation and predicted EcoRV and AvrII fragment sizes.

EcoRV and AvrII predicted fragments after hybridisation with probe C are 4 Kb and 8.4 Kb respectively for the targeted allele. Probe C does not hybridise in the WT allele.

- **Probe isolation**

The probes were prepared by digesting the 10 µg of the plasmid vector with the respective restriction enzymes at 37ºC overnight:

Table 2: Digestion recipes for Probes A, B and C.

Probe A		Probe B		Probe C	
pTopoRosa26pr2+	10 µg	pEGFP-N	10 µg	pTopoNeo	10 µg
EcoRI	2.5 µl	BamHI	2.5 µl	EcoRI	2.5 µl
EcoRI buffer	2.5 µl	NotI	2.5 µl	EcoRI buffer	2.5 µl
H_2O to a total	25 µl	Buffer 3	2.5 µl	H_2O to a total	25 µl
		BSA	0.25 µl		
		H_2O to a total	25 µl		

All enzymes and buffers were from New England Biolabs, Hertfordshire, UK.

On the following day the digested DNA was run on a 0.8% agarose gel (see **2.3.3B-III**) and the band that corresponded to the probe expected size was cut from the gel under the wavelength UV light and purified using the DNA gel extraction kit (Qiagen, West Sussex, UK) and eluted in 30 µl. The probe concentration was measured on the Nanodrop.

- **Probe labelling**

Probes isolated were radioactively labeled using the Random primer labeling of DNA probes protocol: 10-500 ng of DNA (isolated as described previously), 2 µl of 3 mg/ml random hexamer primers (Invitrogen, Paisley, UK), 1 µl of 1N NaOH and water to 9 µl final volume were mixed and left at RT for 5 min. Then 2 µl of 1M Tris-HCl (pH 7.5), 1.5 µl of 10X nick translation buffer, 5 µl of 300 µm each of dATP, dGTP, and dTTP (Roche, Welwyn Garden City, UK), 6.5 µl of α-32P dCTP and 1 µl

of Klenow (5 units) (New England Biolabs, Hertfordshire, UK) were added to a final volume of 25 µl. This mixture was incubated at RT for 2 hours (for optimum incorporation of label) or 37°C for 30 minutes. The unincorporated nucleotides were removed by running a spin column (Qiagen nucleotide extraction kit, Qiagen, West Sussex, UK) and the probe was eluted in 100 µl of TE. The probe was boiled 10 mins at 100°C and snap cooled for 3 mins on ice.

VI. Hybridisation, exposure and developing

Membranes from step **IV** were pre-hybridised in Church & Gilbert solution (Church and Gilbert, 1984) at 65°C with rotation over 3 hours with DNA face in contact with the solution. The 100 µl of probe labeled in **V** were added to Church & Gilbert solution and membranes hybridised overnight with rotation at 65°C. On the following day membranes were washed 3 times 1 hour each in 20 mM phosphate buffer, 1% SDS and 1 mM EDTA. Membranes were then exposed in phospho imager cassettes for at least 24h, and phospho imager plates developed in Tryphoon 8610 Variable Imager (GE Healthcare, Amersham, UK).

VII. Striping and re-probing membranes

After initial hybridisation with Probe A membranes were striped and re-probed with the Probes B and C. The membranes were striped by washing in NaOH 0.4N for 5 min and the reactions stopped by immersing membranes in 2X SSC. This procedure was repeated 3 times. To check that the stripping had worked membranes were exposed to phospho imager plates for a minimum of 24 hours and only used for subsequent hybridisation when the plates showed that no probe remained on the membranes.

C. Blastocyst injection and generation of chimeras

All clones that showed homologous recombination and no random inserts were prepared for karyotyping (Clare Hall Transgenic Department). Clones with normal karyotypes have a better chance of yielding viable chimeras and subsequent germline transmission after blastocyst injection. 15-20 targeted ES cells with normal chromosome counts (>70%) were microinjected into day 4 fertilised mouse embryos (blastocysts). Following injection, embryos were transferred into day 3 plugged pseudopregnant foster mice, which gave birth 18 days later. Coat colour could be determined one week after birth. Given that the ES clones were from male 129S6.C57BL6J (agouti/black) mice and the recipient blastocysts were C57 black chimerism can be predicted in male with agouti/black coat colour.

D. Breeding chimeras for germline transmission

High percentage agouti chimeras were bred to C57BL/6 mice. Because hybrid 129S6.C57BL6J ES cells (agouti/black) were used to generate the chimeras, germline tranmission can occur in either agouti or black mice in colour. However an agouti progeny is likely to have germline transmission given that only the ES cells had the agouti colour. The progeny were tail snipped and screened by Southern blotting for germline transmission. DNA was extracted from the tail snips as detailed in **2.4.2B** and Southern blots performed as described before. Sequencing of the mutation site was also performed according with point **2.4.3G** and **2.4.5** to confirm that chicken FAK mutation from the original constructs persisted *in vivo*.

E. Generation of Pdgfb-iCreER;FAK$^{fl/fl}$;R26$^{FAKKI/KI}$ mice

Any mice that displayed germline transmission were heterozygous for the targeted allele (R26$^{FAKKI/+}$). Thus R26$^{FAKKI/+}$ mice were intercrossed to generate homozygous knockin mice (R26$^{FAKKI/KI}$).

Pdgfb (Platelet-derived growth factor b) is highly expressed in endothelial cells (Hellstrom *et al*., 1999). To begin to generate inducible endothelial-specific point-mutant FAK knockin-knockout mice we utilised the Pdgfb-iCreER mice provided by Marcus Fruttiguer (Institute of Ophthalmology, UCL, London, UK). In these mice CreERT2 results from the fusion of Cre recombinase with a triple mutant estrogen receptor, allowing the production of an inactive form of Cre recombinase that becomes active only in the presence of tamoxifen. Downstream of the CreERT2 sequence was cloned an internal ribosomal entry site (IRES) followed by the coding sequence of enhanced green fluorescent protein (EGFP). The previous construct was recombined in the open-reading frame of the Pdgfb gene in a phage artificial chromosome (PAC), which was subsequently used to generate transgenic mice by pronuclear injection (Claxton *et al*., 2008). Pdgfb-iCreER mice were bred with FAK$^{fl/fl}$ mice to generate FAK$^{fl/fl}$ and Pdgfb-iCreER+;FAK$^{fl/fl}$ mice. These mice were and are now being bred with the R26$^{FAKKI/KI}$ mice to generate Pdgfb-iCreER+;FAK$^{fl/fl}$;R26$^{FAKKI/KI}$ mice and control FAK$^{fl/fl}$; R26$^{FAKKI/KI}$ mice. This produces an inducible knockin/knockout system that allows the mutant chicken FAK expression and simultaneously endogenous mouse FAK deletion in endothelial cells, after tamoxifen treatment in adult mice.

2.4. Genotyping, PCR and DNA electrophoresis

2.4.1. Reagents

A. Tail lysis buffer

Tail lysis buffer is composed by 50 mM of Trizma base/Trizma hidrochloride (pH 8.5) (Sigma, Dorset, UK), 10 mM of EDTA (pH 8.0), 100 mM NaCl (BDH Laboratory Supplies, Poole, UK) and 0.2% SDS. 0.1 mg/ml of proteinase K (Roche, Welwyn Garden City, UK) were added fresh before lysis.

B. TBE, TE buffer and DNA loading buffer

Please see section **2.3.3B-I.**

2.4.2. DNA extraction from ear/tail snips

Mice were ear or tail sniped for genotyping by PCR or tail snipped for Southern blot analysis.

A. Ear/tail snips for PCR genotyping

Ear and tail snips were also used for genotyping by PCR. Tissue samples were digested overnight in a 96-well plate at 56°C in 100μl (0.1 mg/ml PK) of tail lysis buffer. The DNA was precipitated by adding an equal volume of isopropanol and centrifuging the plate at 2600 rpm for 20-30 min. The supernatant was removed by carefully inverting the plate and the DNA pellet was dried at 56-70°C for a 2-4h. The DNA was then ressuspended in 200 μl of TE.

B. Tail snips for Southern blot analysis

Tail snips used for Southern blot analysis were digested overnight at 56°C in at least 500 μl (0.1 mg/ml PK) of tail buffer. On the following day NaCl was added to a final concentration of 1.65M. Samples were then centrifuged at maximum speed for 5-10 min, supernatant decanted and tissue debris discarded. An equal volume of isopropanol was then added and the solution inverted to precipitate the DNA. The DNA precipitates were then pelleted out by centrifuging at maximum speed for 20-30 min. DNA pellets were then washed once in 70% ethanol. After a further 10-15 min centrifugation at top speed the ethanol was removed and DNA pellets were air dried and ressuspended in 20-30 μl of TE buffer each. The concentration of each DNA sample was measured in the nanodrop.

C. Quick DNA extraction from tissue

This was performed according to the manufacture instructions using the DNA extraction kit (Sigma, Dorset, UK).

2.4.3. Polymerase chain reaction (PCR)

PCR was used to genotype all the mice.

A. Primer concentration

All PCR primers (Invitrogen, Paisley, UK) were stored as a stock solution of 100 μM in TE buffer at -20°C. Working dilution used for all reactions was 10 μM.

B. RERTn$^{ERT/ERT}$Cre PCR

PCR analysis for RERTn$^{ERT/ERT}$ Cre genotyping was carried out using the following oligonucleotide primers:

Polr2aF_14B5: 5' – **CCAGATGACAGCGATGAGGA** – 3'

Polr2aR_10B6: 5' – **CCTCTCTGAGCCTCAATTAAGCAG** – 3'

ESR1f_10B7: 5' – **TGAGTAACAAAGGCATGGAGCA** – 3'

For each reaction 1µl of DNA was added to 21 µl of Megamix (Cambio, Cambridge, UK) and 1 µl of each primer (10 µM).

The PCR conditions were the following: 5 min at 94°C; 35 cycles of 1 min at 94 °C, 1 min at 60°C and 30 sec at 72°C; 7 min at 72°C and finally rest at 4°C.

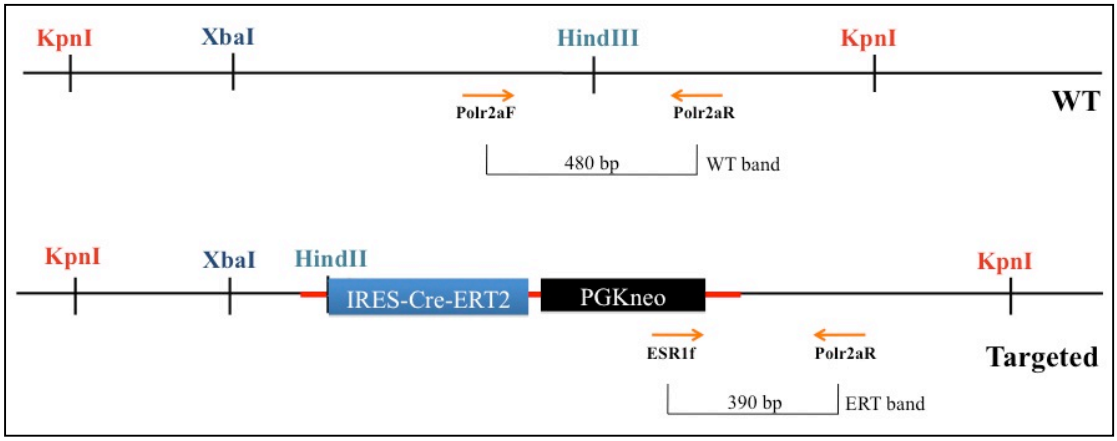

Figure 13: Diagram of primer localisation in the large subunit of RNA polymerase II & expected band sizes for RERTn$^{ERT/ERT}$Cre PCR

Polr2af and Polr2ar primers generate a wild type band (+) of 480 bp. ESR1f and Polr2ar primers generate a ERT band of 390 bp.

C. FAK$^{fl/fl}$ (LP2) PCR

PCR analysis for LP2 genotyping was carried out using the following oligonucleotide primers:

LP2as: 5' – **TTAATAAGACCAGAGGACTCAGC** – 3'

LP2h: 5' – **GGAAGAAGCTTGTATACTGTATG** – 3'

LP2s: 5' – **ATTGTGCTATACTCACATTTGGA** – 3'

For each reaction 1µl of DNA was added to 21 µl of Megamix and 1 µl of each primer (10 µM).

The PCR conditions were the following: 5 min at 94°C; 35 cycles of 1 min at 94 °C, 1 min at 56°C and 1 min at 72°C; 7 min at 72°C and finally rest at 4°C.

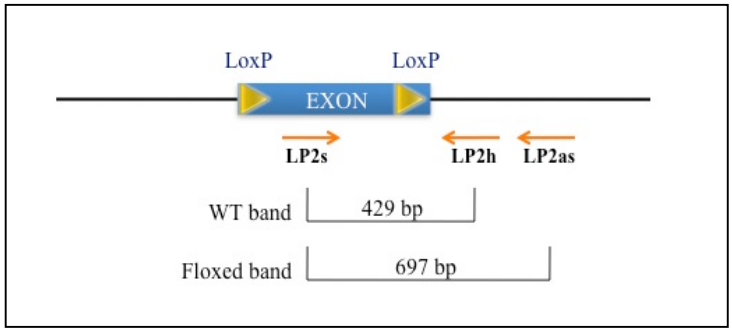

Figure 14: Diagram of primer localisation & expected band sizes for FAK$^{fl/fl}$ (LP2) PCR

The product is a doublet for LP2/+, being the upper band (697 bp) of the doublet for the LP2 and the lower band of the doublet (429 bp) for the wild type (+).

D. RIP-Tag2 PCR

PCR analysis for RIP-Tag2 genotyping was carried out using the following oligonucleotide primers:

Tag P1: 5' –**GGACAAACCACAACTAGAATGCAGTG**– 3'

Tag P2: 5' – **CAGAGCAGAATTGTGGAGTGG**– 3'

β2-microglobulin P1: 5' – **CACCGGAGAATGGGAAGCCGAA**– 3'

β2-microglobulin P2: 5' –**TCCACACAGATGGAGCGTCCAG**– 3'

For each reaction 1μl of DNA was added to 21.5 μl of Megamix (Cambio, Cambridge, UK) and 0.75 μl of each Tag P1 and Tag P2 primers (10 μM) and 0.5 μl of each β2-microglobulin and β2-microglobulin P2 primers (10 μM).

The PCR conditions were the following: 5 min at 94°C; 35 cycles of 1 min at 95 °C, 30 sec at 60°C and 2 min at 72°C; 7 min at 72°C and finally rest at 4°C.

Tag P1 and Tag P2 will generate a band of 449 bp of length whilst β2-microglobulin P1 and β2-microglobulin P2 will generate a band of 295 bp that will be used as a DNA positive control.

E. Pdgfb-iCreER PCR

PCR analysis for Pdgfb-iCreER genotyping was carried out using the following oligonucleotide primers:

PdgfbCre F: 5' – **GCCGCCGGGATCACTCTC** – 3'

PdgfbCre R: 5' – **CCAGCCGCCGTCGCAACT** – 3'

For each reaction 1µl of DNA was added to 22 µl of Megamix and 1 µl of each primer (10 µM).

The PCR conditions were the following: 5 min at 94°C; 35 cycles of 30 sec at 94 °C, 1 min at 57.5°C and 1 min at 72°C; 10 min at 72°C and finally rest at 4°C.

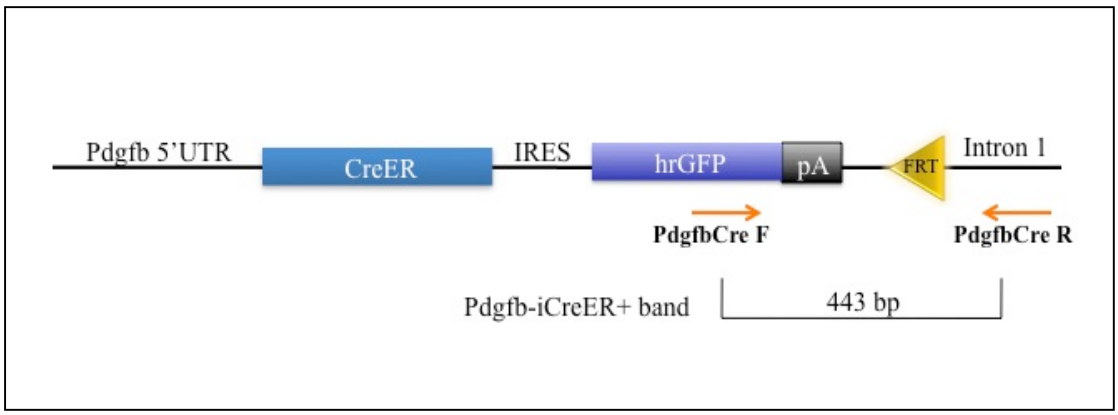

Figure 15: Diagram of primer localisation & expected band sizes for Pdgfb-iCreER

The 2 primers generate a product (443 bp) only for Pdgfb-iCreER+.

F. R26$^{FAKKI/KI}$ genotyping PCR

After the Southern blot screen confirmed correct targeting in the Rosa 26 locus (see **2.3.3D**), PCR was used routinely to genotype R26$^{FAKKI/KI}$ mice and was carried out using the following oligonucleotide primers:

Rosa 1 (Forward WT): 5' – **GTTATCAGTAAGGGAGCTGCAGTGG** – 3'

Rosa 2 (Reverse WT): 5' – **GGCGGATCACAAGCAATAATAACC** – 3'

Rosa 3 (Reverse Targeted): 5' – **AAGACCGCGAAGAGTTTGTCCTC** – 3'

For each reaction 1µl of DNA was added to 21 µl of Megamix and 1 µl of each primer (10 µM).

The PCR conditions were the following: 5 min at 94°C; 35 cycles of 30 sec at 94 °C, 1 min at 59.5°C and 30 sec at 72°C; 10 min at 72°C and finally rest at 4°C.

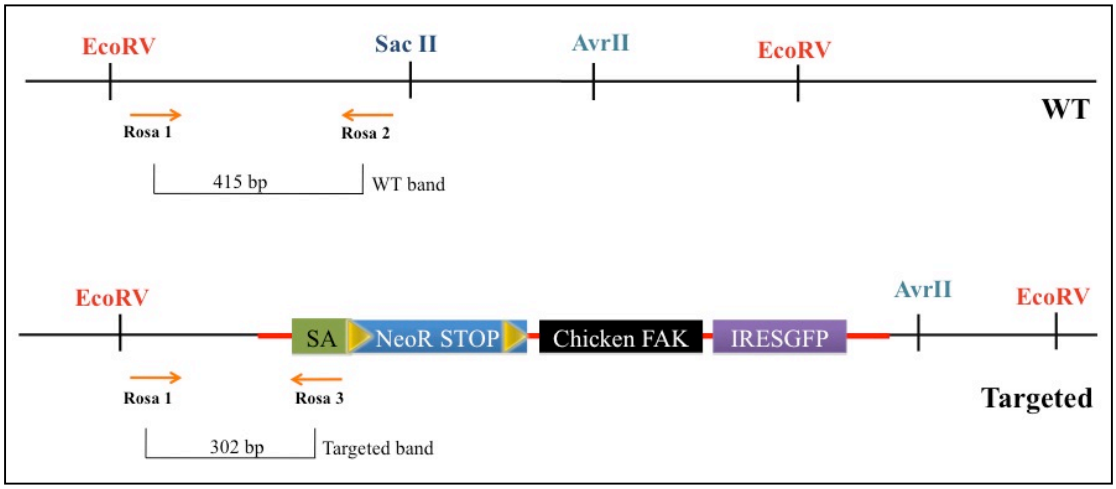

Figure 16: Diagram of primer localisation & expected band sizes for R26$^{FAKKI/KI}$ PCR

Rosa1 and Rosa 2 generate a wild type band (+) for Rosa 26 targeting of 415 bp. Rosa 1 and Rosa 3 generate a 302 bp band for targeted Rosa 26 locus.

G. R26$^{FAKKI/KI}$ sequencing PCR

After the Southern blot analysis a sequencing of the mutation sites was performed. For the 397 and 454 sites the PCR was carried out using the following oligonucleotide primers:

397mut fw2: 5' – **CCTTGAAATCAGGAGATCCTACG** – 3'

397mut rev: 5' – **GCCGCTCACCGTTCTCAATC** – 3'

For each reaction 1µl of DNA was added to 22 µl of Accuprime Mix (Invitrogen, Paisley, UK) and 1 µl of each primer (10 µM).

The PCR conditions were the following: 5 min at 94°C; 35 cycles of 30 sec at 94 °C, 30 sec at 60°C and 2 min at 68°C; 7 min at 68°C and finally rest at 4°C.

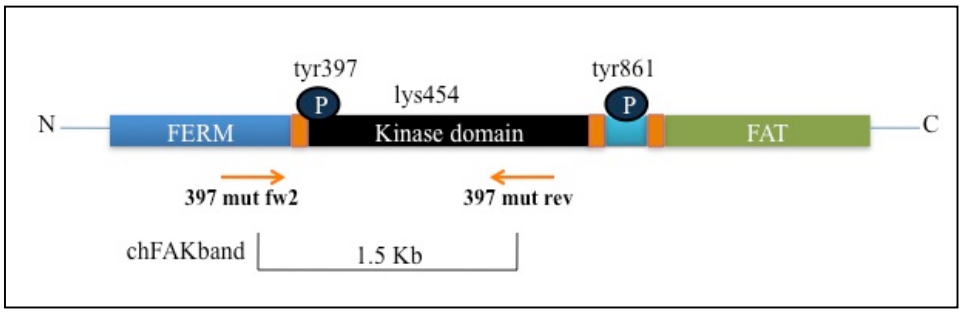

Figure 17: Diagram of primers localisation and expected band sizes for R26$^{FAKKI/KI}$ sequencing PCR

The reaction generates a 1.5 Kb band for the chicken FAK knockin and no band for the mouse FAK.

2.4.4. Electrophoresis

All PCR products were separated in a 2% agarose gel at 100 volts (see **2.3.3B-III**).

2.4.5. Sequencing

Five μl of sequencing PCR products (from **2.4.3G**) were run in 1 % agarose gels (see **2.3.3B-III**) at 120 volts. PCR products were purified using the PCR purification kit (Qiagen, West Sussex, UK). DNA was eluted in 30 μl of TE and sent for sequencing at the Queen Mary University sequencing service. For sequencing the Tyr397 and Lys454 sites 397mut fw2 and 397mut rev primers were used (see **2.4.3G**).

2.5. Flow cytometry

2.5.1. Cell isolation for flow cytometry

A. Blood cell isolation for flow cytometry

Mice were anaesthetised by inhalation with isoflurane (Abbot, Maidenhead, UK) and blood collected in 1/10 of 0.5M EDTA by heart puncture, centrifuged at 1600 rpm for 5 min at RT, washed in PBS and cells passed through a 70 μm cell strainer. After another centrifugation supernatant was discarded and 1 ml of Red Blood Cell Lysis Buffer (Sigma-Aldrich, Dorset, UK) was added to the cell pellet, incubated for at least 5 min to lyse the red blood cells before being diluted with 10 ml of FACS buffer (PBS + 0.1% FCS) and passed through another 70 μm cell strainer in order to remove the lysed cloths. Cells were washed twice in 10 ml of FACS buffer and counted.

B. Spleen cell isolation for flow cytometry

Mice were sacrificed by cervical dislocation and their coats sprayed with 70% ethanol. Mice were then transferred into sterile conditions, sprayed again with 70% ethanol and skin opened in the left of the peritoneal cavity with mice facing up to reveal the spleen. Spleen was forced through a 70 μm cell strainer, centrifuged at 1600 rpm for 5 min at RT and cells washed with PBS. After another centrifugation supernatant was discarded and 1 ml of Red Blood Cell Lysis Buffer was added to the cell pellet, incubated for at least 5 min to lyse the red blood cells before being diluted with 10 ml of FACS buffer (PBS + 0.1% FCS) and passed through another 70 μm cell strainer in order to remove the lysed cloths. Cells were washed twice in 10 ml of FACS buffer and counted. Cell surface phenotypes were determined by direct

immunofluorescence staining with conjugated anti-mouse antibody (Ab) and analysed using the BD LSRII software.

C. Lung cell isolation for flow cytometry

Mice were sacrificed by cervical dislocation and their coats sprayed with 70% ethanol. Mice were then transferred into sterile conditions, sprayed again with 70% ethanol and chest cavity opened to reveal heart and lungs. The later were mashed and digested in 2mg/ml of collagenase I (Gibco BRL, Paisley, UK) for 20min at 37°C. Digested lungs were forced through a 70 μm cell strainer, centrifuged at 1600 rpm for 5 min at RT and cells washed with PBS. After another centrifugation supernatant was discarded and 1 ml of Red Blood Cell Lysis Buffer was added to the cell pellet, incubated for at least 5 min to lyse the red blood cells before being diluted with 10 ml of FACS buffer (PBS + 0.1% FCS) and passed through another 70 μm cell strainer in order to remove the lysed cloths. Cells were washed twice in 10 ml of FACS buffer and counted. Cell surface phenotypes were determined by direct immunofluorescence staining with conjugated anti-mouse Ab and analysed using the BD LSRII software.

D. Bone marrow cell isolation for flow cytometry

Mice were sacrificed by cervical dislocation and their coats sprayed with 70% ethanol. Under sterile conditions, the skin of the lower limbs was removed, femurs removed and muscle trimmed away. One femur per mouse was used for flow cytometry analysis. Femur heads were removed with sharp scissors and the bone marrow of each femur was gently flushed out in 10 ml PBS into a 15 ml falcon using a 10 ml syringe and a 25 gauge needle. The bone marrow suspension was passed

through a 70 μm cell strainer centrifuged at 1600 rpm for 5 min at RT and cells washed with PBS. After another centrifugation supernatant was discarded and 1 ml of Red Blood Cell Lysis Buffer was added to the cell pellet, incubated for at least 5 min to lyse the red blood cells before being diluted with 10 ml of FACS buffer (PBS + 0.1% FCS) and passed through another 70 μm cell strainer in order to remove the lysed cloths. Cells were washed twice in 10 ml of FACS buffer and counted. Cell surface phenotypes were determined by direct immunofluorescence staining with conjugated anti-mouse Ab and analysed using the BD LSRII software.

2.5.2. Cell staining for flow cytometry

A. Blood, spleen and lung cell staining

Cells from blood, spleen and lung were aliquoted in a 96-well plate ($5x10^5$ cells per well in max 150 μl medium), centrifuged at 1600rpm for 5 min at 4ºC, supernatant discarded, pellet resuspended in 150 μl FACS buffer/well, cells centrifuged 1600rpm for 5 min at 4ºC, supernatant discarded and pellet resuspended pellet in 50ul/well anti-mouse CD16-32 (Fc block) (eBiosciences, Hatfield, UK) diluted 1:200 in FACS Buffer. Cells were incubated for 15min at 4ºC and 50ul/well antibody mixes of the following antibody mixes (1:200 final dilution) were added:

Stain A	**Stain B**
CD45-efluor450	CD45-efluor450
Gr1-FITC	CD4-FITC
Ly6C APC	CD8-APC
CD11b-PE	CD3-PECy5
	NK1.1-PE

A tube with each single colour antibody was prepared for compensation. Cells were incubated 30 min at 4ºC in the dark, centrifuged at 1600 rpm 5 min at 4ºC, supernatant discarded and washed twice in FACS buffer. Cell pellet was ressuspended in 2% formaldehyde in PBS (100ul/well), stored at 4^0C in the dark and samples analysed using the BD LSRII software until 48h after staining.

B. Bone marrow cell staining

Cells from bone marrow were stained separately for analysis of bone marrow cell progenitors. Cells were aliquoted in a 96-well plate ($1x10^6$ cells per well in max 150 μl medium), centrifuged at 1600rpm for 5 min at 4ºC, supernatant discarded. For stain A, pellet resuspended in 150 μl FACS buffer/well, cells centrifuged 1600rpm for 5 min at 4ºC, supernatant discarded and pellet resuspended pellet in 50ul/well Fc block (diluted 1:100 in FACS Buffer). Cells were incubated for 15min at 4ºC and 50ul/well of antibody mixes antibody mixes (1:100 final dilution) were added. For stain B pellet was ressuspended directly in 50ul/well of antibody mixes (1:100 final dilution).

Stain A	**Stain B**
CD45-efluor450	Lineage mix-e450
Gr1-FITC	c-kit-APC
Ly6C APC	Sca1-PercpCy5.5
CD11b-PE	CD34-Alexa 700
	Flt3-PE
	CD16/32-FITC

A tube with each single colour antibody was prepared for compensation. Cells were incubated 30 min at 4ºC in the dark, centrifuged at 1600 rpm 5 min at 4ºC, supernatant discarded and washed twice in FACS buffer. Cell pellet was ressuspended in 2% formaldehyde in PBS (100ul/well), store at 4^0C in the dark and samples analysed using the BD LSRII software until 48h after staining.

2.5.3. Gating and flow cytometry analysis

Single colours were run first to compensate for leaking fluorescence from one colour to another. Samples were acquired from live, excluding the duplets and 30,000-50,000 events were collected within the CD45+ population for Stain A, B of blood, spleen and lung and stain A of bone marrow. For bone marrow progenitor analysis samples were acquired from live, excluding the duplets and 30,000 events were collected within the lineage negative population. Each cell type was identified based on surface expression of different markers as represented in **Table 3** and **Table 4**.

Table 3: Flow cytometry analysis of mature immune cells

Cell type	Markers
Granulocytic $CD11b^{+}Gr1^{+}$	$CD45^{+}CD11b^{hi}Gr1^{hi}Ly6C^{lo}$
Monocytic $CD11b^{+}Gr1^{+}$	$CD45^{+}CD11b^{hi}Gr1^{lo+int}Ly6C^{hi}$
CD8 T cell	$CD45^{+}CD3^{+}CD8^{+}$
CD4 T Cell	$CD45^{+}CD3^{+}CD8^{+}$
NK cell	$CD45^{+}NK1.1^{+}$
NK T cells	$CD45^{+}CD3^{+}NK1.1^{+}$

$^{+}$positive, ^{hi}high, ^{lo}low

Table 4: Flow cytometry analysis of haematopoietic progenitors

Cell type	Markers
HSC	Lin^{-} $ckit^{+}$ $Sca1^{+}$
CMP	Lin^{-} $ckit^{+}$ $Sca1^{-}$ $CD16/32^{-}$ $CD34^{+}$
GMP	Lin^{-} $ckit^{-/lo}$ $Sca1^{-}$ $CD16/32^{+}CD34^{+}$
CDP/MDP	Lin^{-} ckit $^{int/lo}$ $Sca1^{-}$ $CD16/32^{+}$ $Flt3^{+}$

HSC (Haematopoietic stem cells), CMP (common myeloid progenitor), GMP (granulocyte/monocyte progenitor) CDP (common dendritic progenitor)/MDP (monocyte/dendritic cell progenitor).
$^{+}$positive, ^{int}intermediate, $^{-}$negative, ^{lo}low.

2.6. Cell Culture

All procedures were carried out under sterile conditions in a tissue culture hood.

2.6.1. Cell culture media and other cell culture reagents

A. B16 tumour cells growth media

B16F0 (melanoma, derived from C57black6) and B16F10 (melanoma, derived from C57black6) tumour cells were grown in Dulbecco's Modified Medium (DMEM) (Invitrogen, Paisley, UK) supplemented with 10% foetal calf serum (FCS) (Biosource, Bethesda, UK).

B. Endothelial cell medium (MLEC medium)

The endothelial cells were cultured routinely in MLEC medium which is composed of: 50:50 mix of Dulbecco's Modified Medium low glucose with Hams-F12 medium (PAA, Somerset, UK), supplemented with 0.1 mg/ml of heparin (Sigma, Dorset, UK), 100U/ml penicillin/streptomycin 100X (pen/strep) (Invitrogen, Paisley, UK), 2 mM glutamine (Invitrogen, Paisley, UK) and 20% FCS. This solution was filter sterilised using a 0.2 mm disposable bottle top filter and the sterile media supplemented with 50 μg/ml of endothelial mitogen (ABD Serotec, Kidlington, UK). Media were stored at 4°C.

C. Aortic ring medium

Aortic rings were grown in DMEM supplemented with 2.5% FCS with or without growth factors.

D. Flask coating solution

For endothelial cell culture tissue culture plastic was pre-coated using the following components:

0.1% gelatin: 0.1 % (w/v) porcine skin 300 bloom gelatin (Sigma, Dorset, UK) in distilled water and autoclaved 30 min at 65°C. Stored at 4°C.

Human Plasma Fibronectin : 1 mg/ml human plasma fibronectin in sterile PBS-A dissolved at room temperature. Stored at -80°C. The aliquots are thawed at 37°C before use and stored at 4°C for up to 3 weeks.

Pure Col™ 3 mg/ml (Nutacon, Leimuiden , Netherlands).

E. Collagenase solution

0.1% (w/v) collagenase solution was prepared by dissolving 0.2g of type I collagenase (Gibco Invitrogen, Paisley, UK) in 50 ml of PBS-ABC (plus calcium and magnesium) at 37°C for 1 hour. After adding equal volume of PBS-ABC, the solution was filtered using a 0.2 mm filter (BD Falcon, Bedford, MA, USA).

F. Antibody and magnetic beads solution for cell sorting

Anti-FcγRII/III antibody solution for negative sort: 1:1000 in PBS. Used 5 ml per T75 flask. Left at 4°C until used (approx. 20 min).

Anti-CD102 (ICAM-2) antibody solution for positive sort: 1μg/ml in PBS. Used 5 ml per T75 flask. Left at 4°C until used (approx. 20 min).

Anti-Rat Dynabeads solution: 1:500 in MLEC medium. Used 5 ml per T75 flask. Left at 4°C until used (approx. 1hour).

G. 4-Hydroxytamoxifen solution

4-hydroxytamoxifen (OHT) (Sigma, Dorset, UK) was diluted to 1 mM in 95% ethanol.

2.6.2. Mouse melanoma cell lines

A. B16F0 and B16F10 tumour cell growth

The B16F0 and B16F10 melanoma cells (C57/BL6) were used in the mouse tumour experiments. These cells were cultured in uncoated T175 flasks in DMEM 10% FCS at 37°C, 10% CO_2 and split 1:10-1:12. There were approximately $7.5x10^6$ cells/T175 flask at 80% confluency.

2.6.3. Primary endothelial cell culture

Primary endothelial cell culture was performed as described previously (Reynolds and Hodivala-Dilke, 2006).

A. Coating tissue culture flasks

Tissue culture flasks for endothelial cell culture were pre-coated prior to cell seeding. The coating solution was prepared by mixing 0.1% (w/v) gelatin with 30 μg/ml of PureCol and 10 μg/ml human plasma fibronectin. The coating solution was added to the flasks according with the size (10 ml/T125, 5 ml/T75, 3 ml/T25, 2 ml/6-well, 1 ml/24-well) and flasks incubated for at least 30 min at 37°C up to 16h at 4°C. The excess coating solution was aspirated off immediately before seeding the cells and washed briefly with a small volume of medium to neutralise acidity.

B. Collagenase treatment of lungs

Mice were sacrificed by cervical dislocation and their coats sprayed with 70% ethanol. Mice were then transferred into sterile conditions, sprayed again with 70% ethanol and chest cavity opened to reveal heart and lungs. Lung-derived cells were prepared as follows: lungs were transferred to a 10 cm dish and immersed in Hams-F12 supplemented with pen/strep placed on ice; fat removed with forceps; washed briefly in 70% ethanol; transferred to a new plate containing MLEC medium; minced with scalpels to produce a "pate"; "pate" were collagenase treated in 10 ml of freshly prepared 0.1% (w/v) collagenase in a 50 ml falcon tubes at 37°C for 2 hours. The digested lungs were then transferred to a petri dish and homogenised by syringing up and down 4-5 times, using a 20 ml syringe with a 19.5 gauge needle. The solution was passed through a cell 70 μm strainer (BD Falcon, Bedford, MA, USA) into a 50 ml falcon tube and 20 ml of MLEC medium added trough the strainer. The solution was centrifuged for 5 min at 1200 rpm and the supernatant removed leaving approximately 5 ml of liquid and the cell pellet in the tube. The pellet was carefully ressuspended and the cell suspension plated into a coated T75 tissue culture flask containing 10 ml of MLEC medium. The cells were cultured at 37°C, 10% CO_2 for 24h. On the following day cells were washed in PBS 3 times to remove residual red blood cells and the medium replaced. 3-5 sets of lungs from identical genotypes were used per preparation.

C. Negative sort

The lung-derived cells include many cells types such as endothelial cells, macrophages and fibroblasts. To remove macrophages "negative sorts" were performed. This involved: incubating the adherent cells in MLEC medium at 4°C for 20 min to chill the cells in order to avoid endocytosis and maintain the receptors at the surface of the cells; incubating the cells in a fresh change of MLEC medium with anti-FcγRII/III antibody solution to bind macrophages at 4°C for 30 min; one wash in PBS; incubating cells in anti-rat Dynabeads solution at 4°C for 30 min; and 3 washes in PBS. The attachment of beads to macrophages (small round cells) was confirmed using an inverted phase contrast microscope. Cells were then trypsinised with 2.5 ml of trypsin stock (25% Trypsin-EDTA from Gibco, Invitrogen, Paisley, UK), for approximately 2 min or until all cells have detached; trypsin inactivated with the addition of 9.5 ml of MLEC medium; cells were transferred to a 15 ml falcon tube and placed in a magnetic sorter. Bead-bound macrophages attached to the side of the tube over a period of 5 min were discarded and the non-bead bound cells were transferred to a new tube; centrifuged at 1200 rpm for 5 min; ressuspended in 12-15 ml of MLEC medium and plated in a pre-coated T75 flask.

The medium was changed every 2 days and once colonies of approximately 20 cells appeared, the positive sort to enrich for endothelial cells was carried out.

D. Positive sort

This step separates the endothelial cells from the remaining mixed cell population (specially fibroblasts), using an antibody against an endothelial cell marker ICAM-2, anti-CD102.

Positive sort involved: incubating the adherent cells in MLEC medium at 4°C for 20 min to chill the cells in order to avoid endocytosis and maintain the receptors at the surface of the cells; incubating the cells in a fresh change of MELC medium with anti-CD102 solution to bind endothelial cells at 4°C for 30 min; one wash in PBS; incubating cells in anti-rat Dynabeads solution at 4°C for 30 min; and 3 washes in PBS. The attachment of beads to endothelial cells was confirmed using an inverted phase contrast microscope. Cells were then trypsinised with 2.5 ml of trypsin stock, for approximately 2 min or until all cells have detached; trypsin inactivated with the addition of 9.5 ml of MLEC medium; cells were transferred to a 15 ml falcon tube and placed in a magnetic sorter. Non-bead bound cells were discarded and bead-bound endothelial cells attached to the side of the tube over a period of 5 min were ressuspended in 5ml of MLEC medium and plated in a pre-coated T25 flask.

MLEC medium was changed every 2 days and a second positive sort was performed once the T25 flasks were confluent. If most of the cells had beads attached, these were plated in T75 flasks after the second positive sort.

E. Splitting endothelial cells

Once endothelial cells reached 80-90% of confluence they were split 1:2. A maximum of 4-5 passages were done before endothelial cells began to differentiate.

2.6.4. Ex vivo aortic ring assay

Ex vivo aortic ring assays were performed as described previously (Masson *et al*., 2002; Reynolds *et al*, 2004). Briefly, the Pdgfb-iCreER+;$FAK^{fl/fl}$;$R26^{FAK861F/861F}$ and control $FAK^{fl/fl}$;$R26^{FAK861F/861F}$ mice were killed by cervical dislocation and the chest cavity opened. Lungs and heart were removed to reveal the thoracic aortae. Thoracic aortae were removed by grasping it at the end nearest the heart and separating aortae from spine using fine optical scissors. Aortae were placed in a petri dish with Optimen and transferred to a dissected microscope (housed in a sterile air-flow hood). Four aortae per genotype were usually taken per experiment. Aortae were prepared as follows: periaortic tissue (fat, blood and connective tissue) or damaged parts of the aortae were removed carefully using fine forceps and surgical blades; cleaned aortae were placed in a drop of Optimem medium (Invitrogen, Paisley, UK) supplemented with 100 U/ml of pen/strep to prevent drying out and cut into 20-30 rings of 0.5 mm per aorta using surgical blades; incubated in Optimem overnight at 37°C, 10% CO_2; after 16 hours rings were embedded in 50μl of a matrix composed of 1.2 mg/ml Collagen type I, 1.1 ml of 10X DMEM and sterile distilled water to a total volume of 10 ml; matrix allowed to polymerise; 150μl of DMEM 2.5% FCS added to each well supplemented with 30 ng/ml of VEGF and 1μM of hydroxytamoxifen, with the respective controls non-supplemented. Media was changed every 2 days and sprouts counted in the inverted microscope between 5-22 days post embedding.

2.7. Gene expression analysis

2.7.1. Endothelial RNA cell isolation and reverse transcription of RNA to make complementary cDNA

A. Endothelial cell RNA isolation and cDNA preparation

Pdgfb-iCreER+;$FAK^{fl/fl}$;$R26^{FAK861F/861F}$ and control $FAK^{fl/fl}$;$R26^{FAK861F/861F}$ mice endothelial cells were seed into 6 cm petri dishes at approximately 50-60% of confluency and grown in MLEC medium with or without 500 nM of 4-hydroxytamoxifen for 48h. The cells were then positive sorted (see **2.6.3D**) ressuspended in PBS, centrifuged at 1200 rpm and washed again in PBS. The supernatant was removed and the lysis performed using lysis buffer provided in the microRNA kit (Qiagen, West Sussex, UK). After lysis, bead-bound cells were centrifuged at 1200 rpm for 5 min, pellet discarded and supernatant kept. Total RNA was extracted using miniRNA kit (Qiagen, West Sussex, UK) and subjected to reverse transcription using the High Capacity cDNA archive kit (Applied Biosystems) according to the manufacturer's instructions. cDNA was synthesised from 0.1-1 mg purified RNA. As a control chicken RNA was also extracted from embryos using the same microRNA kit and cDNA was made using the same protocol.

B. Real time quantitative PCR (qPCR) for gene expression levels in endothelial cells

Two sets of test primers were used, chicken FAK specific primers and mouse FAK specific primers, as well as one set of control primers (actin).

Chicken FAK primers (Invitrogen, Paisley, UK):

chFAKleft - 5'-**ATTGCTGCTAGGAACGTGCT**-3'

ChFAKright - 5'- **GCCAAAGTCACCCAATTTCA**-3'

Mouse FAK primers (Invitrogen, Paisley, UK):

musFAKleft - 5'- **AACAGCTATTTGATTTCTTCTCAAAGT**-3'

musFAKright - 5'- **TCTTTTGCTAGATGCTAGGTATCTGT**-3'

Actin primers (Invitrogen, Paisley, UK):

Actin F - 5'-**AAGGCCAACCGTGAAAAGAT**-3'

Actin R - 5'-**GTGGTACGACCAGAGGCATAC**-3'

Real-time quantitative PCR (qPCR) reactions were performed in triplicate. Each 20 μl reaction contained 2-5 ng cDNA, 10 μl Platinum® SYBR Green® qPCR SuperMix-UDG with Rox (Invitrogen, UK), 300 nM of test primers or 50 nM (Actin) forward and reverse primers and nuclease free H_2O in an individual well of a 96-well plate. The following conditions were used to run the PCR amplification process: 50°C for 2 mins, denaturation at 95°C for 10 mins followed by 40 cycles at 95°C for 15 secs and 1 min annealing/extension at 60°C. Data analyses were accomplished using the StepOne Plus Real Time PCR machine (Applied Byosystems, Foster City, USA). Data was normalised to endogenous actin and fold changes in gene expression were calculated using the comparative CT method.

2.8. Protein analysis by Western Blotting

2.8.1. Cell lysis

A. Whole kidney cell lysis

Mice were sacrificed by cervical dislocation and their coats sprayed with 70% ethanol. One kidney from each animal was removed and immediately snap frozen directly in liquid nitrogen. Samples were stored at -80°C prior to processing. Tissue was placed in mortar containing liquid nitrogen and grinded to a fine powder with the pestle before 1ml lysis buffer (3% SDS, 60mM sucrose, 65mM Tris-HCl pH6.8) was added. DNA was sheared the by passing the homogenate through a 21 gauge needle attached to a syringe. Homogenate was transferred to an eppendorf tube, boiled for 10 min at 95°C and centrifuged for 10 min at 12, 000rpm. If supernatant was not clear It it was removed to fresh eppendorf and centrifuged again. Only clear supernatants were transferred to a fresh eppendorf and stored in 25 µl aliquots at -80°C prior to use.

B. Whole bone marrow cell lysis

For whole bone marrow cell lysis cells were extracted from femurs of animals, as it is described in **2.5.1D**, washed in PBS and lysed at RT with sample buffer: 10% (w/v) SDS, 20% glycerol (v/v), 312.5 mM Tris. Lysates were sonicated (3 times 5 sec) and prepared for protein quantification prior to storage in 25 µl aliquots at -20°C.

C. Endothelial cell lysis

For most Western blotting procedures in endothelial cells, except for detection of c-myc the following cell lysis protocol was used: endothelial cells were grown to 70-80% confluency and lysed with RIPA buffer (Millipore, Watford, UK): 2%Triton X100, 25 sodium deoxycholate, 0.2%SDS, 316mM NACl, 20 mM Trizma base/Trizma hydrochloride (pH7.3), 2mM EGTA supplemented with 1:100 dilution of protease inhibitor cocktail set III (100 mM AEBSF hydrochloride, 80 µM Aprotinin, 5 mM Bestatin, 1.5 MM E-64 protease inhibitor, 2 mM Leupeptin hemisulfate and 1mM pepstatin A) (Calbiochem, Nottingham, UK) and phosphatase inhibitor cocktail set II (200 mM Imidazole, 100 mM Sodium Fluoride, 115 mM Sodium Molybdate, 100 mM Sodium Orthovadate and 400 mM Sodium Tartrate dihydrate) (Calbiochem, Nottingham, UK), for 10 min on ice. After lysis cells were scrapped off the plate, transferred to a cold eppendorf and centrifuged at 10, 000 rpm for 10 min at 4°C. The supernatants were transferred to a new cold eppendorf, sonicated at 4°C (3 times 5 sec) and prepared for protein quantification prior to storage in 50 µl aliquots at -20°C.

D. Cell lysis for c-myc Western blot

For c-myc detection endothelial cells were grown to 70-80% confluency and lysed with125 mM Tris-Cl (pH 6.8), 5 mM EDTA, 5 mM EGTA (Sigma, Dorset, UK) in distilled water, supplemented with 1:100 dilution of protease inhibitor cocktail set III, for 10 min on ice. After lysis cells were scrapped off the plate, transferred to a cold eppendorf and centrifuged at 10, 000 rpm for 10 min at 4°C. The supernatants were transferred to a new cold eppendorf, sonicated at 4°C (3 times 5 sec) and prepared for protein quantification prior to storage in 25 µl aliquots at -20°C.

2.8.2. Protein quantification

Protein concentrations were quantified using the Bio-Rad DC Protein Assay kit (Bio-Rad Laboratories, Hertfordshire, UK), a colorimetric assay based on Lowry assay (Lowry *et al*, 1951). Protein standards were prepared by diluting a 4 mg/ml BSA solution in the appropriate lysis buffer to obtain solutions with concentrations of 0, 0.1, 0.2, 0.4, 0.8, 1.2, 1.6 and 2 mg/ml. Protein concentrations were determined as follows: 5 μl of each sample or standard was aliquoted in duplicate into a bacteriological 96-well plate (Nunc Inc., Naperville, IL) and mixed with 25 μl of Bio-Rad reagent B and with 200 μl of active A solution, obtained by mixing 1ml of reagent A with 20 μl of reagent S. After 15 min of incubation, protein concentrations were read on an absorbance microplate reader (Labtech International Ltd., East Sussex, UK) set at 650 nm wavelength and the results analysed using Stringray software (Dazdaq Ltd., East Sussex, UK). When necessary high concentration lysates, especially whole kidney and bone marrow lysates were diluted 1 in 10 before used in protein assay. This was performed to avoid having concentrations too high that were no longer in the linearity range of the protein assay and though could not be calculated accurately.

2.8.3. Preparation of lysates for Western blot

A. Whole kidney lysates

Whole kidney lysates prepared in **2.8.1A** were thawed at RT, added 1/10 of bromophenol blue and supplemented with 250 μl/ml β-mercaptoethanol.

B. Whole bone marrow lysates

Whole bone marrow lysates prepared in **2.8.1B** were thawed at RT, added 1/10 of bromophenol blue and supplemented with 250 μl/ml β-mercaptoethanol.

C. Chicken FAK immunoprecipitation (IP)

Endothelial cells isolated from Pdgfb-iCreER+;$FAK^{fl/fl}$;$R26^{FAK861F/861F}$ and control $FAK^{fl/fl}$;$R26^{FAK861F/861F}$ mice were seeded in 15 cm petri dishes at approximately 50-60% of confluency and grown in MLEC medium with or without 500 nM of hydroxitamoxifen for 48h. The cells were then positive sorted (see **2.6.3D**) before being lysed with 1 ml of RIPA buffer. 0.8 – 1 mg of protein was immunoprecipitated with Rabbit anti-chicken FAK antibody using the Immunoprecipitation kit – Dynabeads Protein G (Invitrogen, Paisley, UK), according with the manufacturer's instructions. Briefly 5 μl anti-chicken FAK antibody per lysate was bound to 50 μl of Dynabeads for 10 min at RT with rotation. 0.8 – 1 mg of protein lysate in 1 ml total volume were then incubated overnight at 4°C with the antibody-bound Dynabeads with rotation. Supernatant was removed from the Dynabeads using a magnetic holder and to test the non-immunoprecipitated (non-IP) samples, 24 μl of each supernatant were then added to 6μl of NUPAGE sample buffer (Invitrogen, Paisley, UK) and 3 μl

of NUPAGE reducing agent (Invitrogen, Paisley, UK) to run in gel. The remaining supernatant was stored at -20°C. The Dynabeads were washed and chicken FAK imunoprecipitated (IP) protein eluted each in 5 μl sample buffer, 6 μl reducing agent, and distilled water to a total volume of 20 μl. The IP and non-IP (supernatants) samples were boiled at 100°C for 10 min and the Dynabeads were removed from the IP samples before running in a pre-cast gel.

D. Lysate preparation for c-myc Western blotting

Endothelial cells isolated from Pdgfb-iCreER+;$FAK^{fl/fl}$;$R26^{FAK861F/861F}$ and control $FAK^{fl/fl}$;$R26^{FAK861F/861F}$ mice were seeded into 6 cm petri dishes at approximately 50-60% of confluency and grown in MLEC medium with or without 500 nM of hydroxitamoxifen for 48h. The cells were then positive sorted (see **2.6.3D**) before being lysed with 50 μl of cell lysis buffer for c-myc western blotting. The protein concentration was measured and 50 μg of protein were run in non-precast 8% polycarylamide gels as described below (**2.8.4**). Lysates were diluted to the desired concentration in equal volume of lysis buffer and 1:5 of 5X sample buffer (10% (w/v) SDS, 20% glycerol (v/v), 312.5 mM Tris and a few crystals of bromophenol blue) supplemented with 250 μl/ml β-mercaptoethanol.

2.8.4. Gel electrophoresis

A. SDS-polyacrylamide gel electrophoresis – non-precast gels

8% polyacrylamide gels 1.0-1.5 mm thick were used for resolving protein lysates.

8% Acrylamide Gel Recipe:

30% Acrylamide (National Diagnostics, UK)	2.7 ml
4X Resolving Buffer (National Diagnostics, UK)	2.5 ml
Distilled Water	4.8 ml
Ammonium persulphate (APS) 10% (w/v) (National Diagnostics, UK)	100 µl
TEMED (National Diagnostics, UK)	6 µl

This resolving gel was poured into pre-formed cassettes (Invitrogen, Paisley, UK) and overlaid with isopropanol, to prevent gel-air contact, which inhibits polymerisation. Gels were polymerised for 30 min at RT, the isopropanol was discarded, stacking gel was poured on top and a lane comb was introduced.

Stacking Gel Recipe:

30% Acrylamide (National Diagnostics, UK)	330 µl
Stacking Buffer (National Diagnostics, UK)	0.5 ml
Distilled Water	1.15 ml
Ammonim persulphate (APS) 10% (w/v) (National Diagnostics, UK)	20 µl
TEMED (National Diagnostics, UK)	2 µl

The well comb was inserted after pouring the stacking gel and the gel left to polymerise for further 30 min. The comb was then removed and the gel was placed in a gel tank (Invitrogen, Paisley, UK) and covered totally with 1X running buffer (0.025M Tris base, 0.192M glycine, 0.1% sodium dodecyl sulfate, Fisher Biotech, New Jersey, USA). Lysates prepared in **2.8.3** were boiled for 10 min at 100°C and loaded into the gel together with 10 μl of rainbow marker ladder (GE, Paisley, UK). The gel was run at 125 volts at RT until the desired separation was achieved.

B. Precast gels

Samples from chicken FAK imunoprecipitations (**2.8.3C**) were run in NUPAGE 1.5 mm polyacrylamide precast (Invitrogen, Paisley, UK) 4-12% gradient gels run in NUPAGE running buffer (Invitrogen, Paisley, UK). NUPAGE running buffer in direct contact with the gels was supplemented with 2.5% of NUPAGE antioxidant (Invitrogen, Paisley, UK) in order to maintain proteins in a reduced form. 10 μl of the rainbow marker ladder were used and the gel was run at 120 volts in the cold room until the desired separation was achieved.

2.8.5. Transfer

Resolved proteins were then transferred from gels to Hybond nitrocellulose transfer membranes (GE, Paisley, UK) using the transfer set up as shown in **Fig.18**. All sponges, Whatman paper and membranes were cut to the size of the gels and prewet in transfer buffer before assembling the transfer "sandwich". Air bubbles were removed by rolling a plastic pipette over the "sandwich" and the transfer "sandwich" placed in the transfer apparatus (Invitrogen, Paisley, UK). The transfer apparatus was

closed, placed in a transfer tank and immersed in transfer buffer. In the case of the precast gels the transfer buffer used was NUPAGE transfer buffer (Invitrogen, Paisley, UK) and the transfer was performed at 30 volts for 2h in the cold room (4°C) while in the case of non-precast gels the transfer buffer used was composed by 0.025M Tris, 0.192M glycine (National Diagnostics, UK), 20% methanol (Fisher Scientific, Leicestershire, UK) and the transfer was performed at 30 volts for 1.5h at RT. These conditions were optimised for transferring proteins ranging from 100-250 KDa.

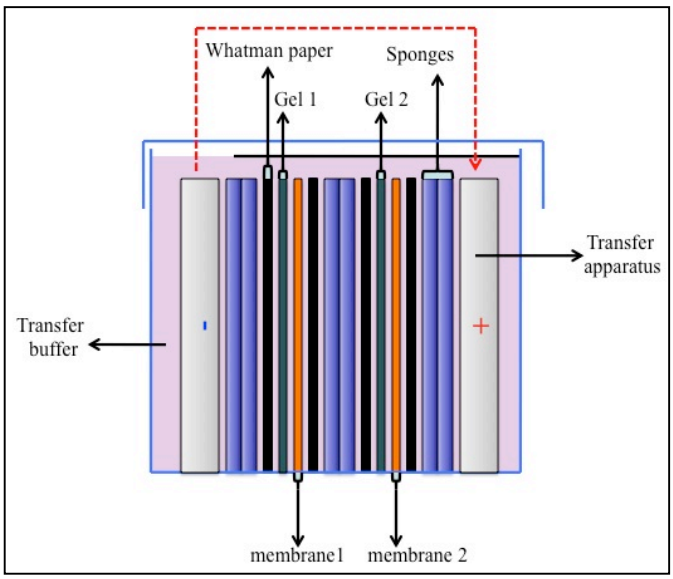

Figure 18: Diagram representing transfer set up of proteins from polyacrylamide gels to Hybond nitrocellulose membranes.

The transfer 'sandwich' is built with all the components immersed in transfer buffer from the negative to positive pole of the transfer apparatus on the following order: two sponges, one Whatman paper, gel 1, membrane 1, one Whatman paper, two sponges, one Whatman paper, gel 2, membrane 2, one Whatman paper and two sponges. Transfer apparatus is closed, placed in a tank filled with transfer buffer and proteins transferred from the negative to positive electrode (gel to membrane) by electric field.

After the transfer the membranes were immersed in Ponceau S (Sigma, Dorset, UK) and washed briefly in distilled water to access the efficiency of the transfer and dried until performing the Western Blot.

2.8.6. Western blot

A. Western blotting to detect FAK

Membranes were blocked in 5% BSA (w/v) in 0.1% Tween-20 (Sigma, Dorset, UK) in PBS (PBS-T) for 1 hour; incubated with mouse monoclonal anti-FAK diluted 1:1000 in blocking solution overnight at 4°C; washed 3 times for 5 min each in PBS-T; incubated for 1 hour at RT with horseradish peroxidase (HRP)- conjugated anti-mouse IgG diluted 1:1000 in 5% milk (Marvel, UK) in PBS-T; washed 3 times for 5 min each in PBS-T and bands detected by chemiluminescence as detailed below (**2.8.7**).

B. Western blotting to detect c-myc

Membranes were blocked in 5% milk in PBS-T for 1 hour at RT; incubated overnight 4°C with mouse monoclonal anti-myc diluted 1:1000 in 5% milk in PBS-T; washed 3 times for 5 min each in PBS-T; incubated for 1 hour at RT with HRP- conjugated anti-mouse IgG diluted 1:1000 in 5% milk in PBS-T; washed 3 times for 5 min each in PBS-T and bands detected by chemiluminescence as detailed below (**2.8.7**).

C. Western blotting to detect HSC70

HSC70 protein detection was used as a loading control. After probing and stripping (see **2.8.8**) membranes were blocked in 5% milk in PBS-T for 1h; incubated for 1hour in mouse monoclonal anti-HSC70 diluted 1:5000 in 5% milk in PBS-T for 1h; washed 3 times for 5 min each in PBS-T; incubated in HRP- conjugated anti-mouse IgG diluted 1:1000 in 5% milk in PBS-T; washed 3 times for 5 min each in PBS-T and bands detected by chemiluminescence as detailed below (**2.8.7**).

2.8.7. Enhanced chemiluminescence

ECL is a light emitting non-radioactive method for detection of immobilised specific antigens conjugated with HRP labelled antibodies. HRP oxidises luminol present in the ECL reagents in the presence of enhancer such as phenol. Luminol becomes excited and decay to the normal state by chemiluminescence. Immunoreactive bands were visualised by incubating the membranes with ECL chemiluminescence reagents (GE, Paisley, UK) for 2 min and then exposing the membrane in an autoradiographic film (Fujifilm, PYSER-SGI Limited, UK) for several seconds to 20 minutes. After exposing, the films were developed with a Kodak X-OMAT 1000A film processor (East Kodak Company, New York, NY, USA).

2.8.8. Stripping Western blot membranes

Membranes that had been previously probed and developed were incubated with Re-Blot Plus Mild Solution 10x (Millipore, Watford, UK) diluted 1:10 in distilled water in a shaking tray for 5 minutes at room temperature. After stripping, the blot was treated with ECL to confirm that the antibodies had been removed. Finally, the membrane was washed in PBS-T and blocked again ready for re-probing with a new primary antibody.

2.8.9. Storage of Western blot membranes

For short-term storage (one week) membranes were kept in PBS at 4°C. For long-term storage membranes were enveloped in plastic and kept at -20°C.

2.8.10. Densitometry

Densitometric analysis of Western blot bands was performed using Image J software.

2.9. Animal experiments

2.9.1. Tamoxifen treatment

A. Tamoxifen formulations

I. Tamoxifen for gavage

Tamoxifen for gavage is a 0.03 mg/µl tamoxifen solution in ethanol and corn oil. To prepare tamoxifen for gavage for approximately twenty mice 750 mg of tamoxifen free base (Sigma-Aldrich, Dorset, UK) were first suspended in 2 ml of 100% ethanol and 22 ml of corn oil (Sigma-Aldrich, Dorset, UK). This suspension was then dissolved in a water bath at 55°C with intermittent vortexing. Tamoxifen solution was then stored in 1.5-2 ml aliquots at -20°C. Due to possible tamoxifen precipitation tamoxifen solution was always heated at 37°C before administration.

II. Tamoxifen and low oestrogen clearing diet

Tamoxifen diet and low oestrogen clearing diet were purchased from Harlan Laboratories, Indianapolis, USA. Mice generally need a washout period of one week with low oestrogen clearing diet before starting the tamoxifen diet. The dosage of tamoxifen diet is around 400 mg/Kg animal.

III. Tamoxifen pellets

Slow release (25mg/pellet, 21-day release) tamoxifen pellets were purchased from Innovative Research America, Sarasota, Florida, USA.

B. Tamoxifen treatment in RERTn$^{ERT/ERT}$Cre;FAK$^{fl/fl}$ and control FAK$^{fl/fl}$ or control RERTn$^{ERT/ERT}$Cre mice

Mice were given 100µl of tamoxifen solution prepared in **2.9.1A-I** via gavage for 5 consecutive days before the start of any tumour experiment. During the gavage period mice were given low oestrogen tamoxifen diet. After gavage mice were switched onto daily tamoxifen diet until the animals were killed at the endpoint of the experiment.

C. Tamoxifen treatment of bone marrow chimeras

Since some bone marrow chimeras were found to die suddenly after gavage and subcutaneous pellets caused severe irritation to the irradiated mice a particular strategy with the diet was adopted for tamoxifen treatment. Mice were given low oestrogen clearing diet for one week and daily tamoxifen diet for 1-2 weeks before starting any tumour experiment. This was done 2-6 weeks after the initial bone marrow transplant (see **2.9.3.**). Tamoxifen diet was maintained daily until the animals were killed at the endpoint of the experiment.

D. Pdgfb-iCreER+;FAK$^{fl/fl}$;R26FAK$^{861F/861F}$ and control FAK$^{fl/fl}$;R26FAK$^{861F/861F}$ mice tamoxifen treatment

Mice were anaesthetised and slow release (25mg/pellet, 21-day release) tamoxifen pellets were implanted subcutaneously via trochar into the scruff of the neck. Previous experiments in our laboratory have shown efficient FAK knockout in Pdgfb-iCreER+;FAK$^{fl/fl}$ mice after two days of tamoxifen pellet implantation (Tavora *et al*., 2010). For this reason all the tumour injections were performed at least 2 days after tamoxifen pellet implantation.

2.9.2. Subcutaneous tumour growth and experimental metastasis assays

Syngeneic mouse tumour cell line B16F0 (melanoma, derived from C57black6) was used in subcutaneous tumour growth assays whilst both B16F0 and B16F10 cell lines were used in experimental metastasis assays. Tamoxifen-treated mice were given $1x10^6$ cells (B16F0), resuspended in 100μl of PBS, injected subcutaneously into the scruff of the neck or flank for the subcutaneous tumour growth or $0.5x10^6$ cells (B16F0 or B16F10) resuspended in 100μl of PBS injected via the tail vein of the mouse for experimental metastasis assays. Subcutaneous tumour size was measured with digital callipers at 12 days post inoculation. For the experimental metastasis assays mice were culled by cervical dislocation at 15-19 days post tumour inoculation, organs removed and examined for macroscopic metastasis. Tissues were either fixed in 4% formaldehyde in PBS or snap-frozen in isopentane cooled in liquid nitrogen for subsequent immunohistochemical analysis (see **2.10**).

2.9.3. Bone marrow transplant (BMT) experiments

A. Irradiaton of recipient mice

Since irradiation causes myelosupression making the mice prone to infection WT mice (recipients) were given 10% Baytril antibiotic in their drinking water before full body lethal irradiation. Irradiation consisted of 1000 rads of γ-radiation in 2 split doses of 500 rads each, 3-4 hours apart, in a gamma irradiator (IBL 437C gamma irradiator, Schering Health Care, Berkshire, UK). This dose ablates endogenous bone marrow.

B. Donor bone marrow harvesting

RERTn$^{ERT/ERT}$Cre;FAK$^{fl/fl}$ or control RERTn$^{ERT/ERT}$Cre donor mice were culled and rinsed in 70% ethanol. Under sterile conditions, the skin of the lower limbs was removed, femurs dissected and muscle trimmed away from the bone. Femur heads were removed with sharp scissors and the bone marrow was gently flushed out in 20 ml of DMEM supplemented with 10% FCS into a 50 ml Falcon tube using a 20 ml syringe and a 25 gauge needle. The bone marrow suspension was passed through a 70 μm cell strainer. Bone marrow from 3-4 donor mice was used for transplant into 10 recipient mice; centrifuged at 1200 rpm for 3 min; mixed together in 50 ml of DMEM supplemented with 10% FCS; cells were counted by adding 1 ml of cell suspension to 1 ml of methylene blue and using a counting chamber; centrifuged at 1200 rpm for 3 min; washed twice in PBS and finally ressuspended in PBS to a final concentration of $1x10^6$ cells/100 μl PBS.

C. Bone marrow transplant (BMT)

Lethally irradiated WT mice (recipient mice) were injected intravenously (tail vein) with approximately $1x10^6$ donor bone marrow cells/ 100μl PBS. The mice were then maintained on antibiotic water until two weeks after transplant and allowed to recover for 2-6 weeks after transplant.

D. Subcutaneous and experimental metastasis tumour experiments

Four to six weeks post-transplant mice were treated with tamoxifen and tumour experiments were performed as described in **2.9.1C** and **2.9.2** respectively.

E. RIP-Tag2 model

Lethally irradiated RIP-Tag2/+ mice were transplanted with bone marrow cells from male $RERTn^{ERT/ERT}Cre;FAK^{fl/fl}$ or $RERTn^{ERT/ERT}Cre$ control mice at 6 weeks of age and started low estrogen clearing diet soon after transplant. Mice were given daily tamoxifen diet treatment from 8 weeks of age (2 weeks post-transplant) and were culled at 16 weeks of age. At necropsy pancreas, liver, lung, mesentery and spleen were fixed in 4% formaldehyde in PBS for subsequent immunohistochemical analysis.

2.9.4. Dextran/FITC perfusion

Mice were anaesthetised by using 200 μl IP injection of 1.5% w/v sodium pentabarbiton in PBS. The thoracic cavity was opened and the auricle of the right atrium was cut to allow circulating blood to extravasate. The apex of the left ventricle was then cannulated using a 25 g needle and 1 ml of dextran/FITC (Sigma, Dorset, UK) was hand injected using a 1 ml syringe. 30 min following injection tumours were excised and snap frozen as described in **2.9.2**.

2.9.5. In vivo homing/colonisation assays

Red cell tracker red CMPTX (Invitrogen, Paisley, UK – 50 μg ressuspend in 14.7 μl of DMSO) was used for B16F0 cell labelling for *in vivo* homing/colonisation assays. Cells were trypsinised and washed 2 times in Serum Free Media (SFM). A maximum of 2 x 10^6 cells/1ml SFM was ressuspended and 1μl CMPTX/1ml media (in 15 ml falcons) was used. Cells were incubated at 37 ºC for 10 min. Finally 10 ml of DMEM+10% FBS were added and cells washed 3 times in PBS. Cells were ressuspended at a concentration of 0.5 x 10^6 cells/100 μl of PBS and injected via the tail vein into mice (100 μl/mouse). This procedure was performed after tamoxifen treatment of RERTn$^{ERT/ERT}$Cre;FAK$^{fl/fl}$ and control RERT$^{ERT/ERT}$ mice or WT mice that had received bone marrow transplant (from RERTn$^{ERT/ERT}$Cre;FAK$^{fl/fl}$ or control RERTn$^{ERT/ERT}$Cre mice) as described in **2.9.1** and **2.9.3** At 2-5h or 48h post inoculation, mice were sacrificed and lungs fixed in 4% paraformaldehyde. Lungs were dissected, photographed using a Leica MZ16F fluorescence stereomicroscope, snap frozen in OCT (OCT Killik, Bio-Optica, IT) and 5 μm cryosections prepared for analysis. Total numbers of red fluorescent tumour cells were quantified and

normalised for the total number of DAPI positive nuclei for each section using a Zeiss Axioplan microscope (Zeiss).

2.9.6. In vivo Gr1^{+} cell depletion

RERTn$^{ERT/ERT}$Cre;FAK$^{fl/fl}$ or control RERTn$^{ERT/ERT}$Cre mice received tamoxifen treatment as described in **2.9.1B** and were given 50μg of rat anti-mouse Gr1 antibody (eBiosciences, Hatfield, UK) or rat anti-mouse IgG2b κ isotype control antibody (eBiosciences, Hatfield, UK) in 100μl PBS one day before and in the day of tumour cell injection. Homing/colonisation assays were performed as described in **2.9.5** for both antibody groups.

2.9.7. Home office regulations

All animals were used in accord with United Kingdom Coordination Committee on Cancer Research guidelines and Home Office Regulations.

2.10. Tumour quantitation

2.10.1. Subcutaneous tumour quantitation

Subcutaneous tumour size was assessed after necropsy of animals by measuring length, width and depth of each tumour using digital callipers.

2.10.2. Experimental metastasis assays

The number of metastases per organ was counted by eye under a dissecting microscope (Zeiss Stemi SV11).

2.10.3. RIP-Tag2 model

Primary tumour, invasion grading and metastasis quantifications were all performed in large T antigen stained sections as described in **2.11.5** Six step wise sections, 100μm apart were analysed per tissue for all mice in all analysis.

Total primary tumour area was assessed by calculating the sum of all individual tumour areas per pancreas using the 5X objective of a Zeiss Axioplan microscope.

To determine invasion grading pancreatic tumours in RIP-Tag2 mice were classified into three levels of progression: encapsulated, least aggressive; invasive type I, where the invasive front of the tumour is beginning to penetrate into the surrounding pancreas; and invasive type II, where the invasive front of the tumour engulfs islands of normal pancreas as described previously (Lopez and Hanahan, 2002; Paez-Ribes *et al*., 2009). The results were presented as % of tumours in each invasion grading out of total tumours per animal. The incidence of lymph node, liver and lung metastasis was determined by scoring for presence or absence in each animal.

2.11. Histological analysis

2.11.1. Tissue sections preparation

A. Frozen tissue sections

Mouse tissue previously snap frozen in OCT was sectioned on a cryostat and 5 μm thick sections were mounted onto glass slides and frozen at - 80 °C. Frozen sections were only used up to 3 months after being cut.

B. Paraffin-embedded tissue sections

Tissues previously fixed in 4% formaldehyde for 24h at RT were transferred to 70% ethanol before being embedded in paraffin (procedures performed by Barts Cancer Institute Pathology Department). Paraffin blocks were sectioned on a microtome (Leica) and 5 μm thick sections were mounted onto glass slides and dried for 1-10h at 37 °C. Slides were stored at room temperature until ready to use.

2.11.2. Tumour blood vessel quantitation

A. Blood vessel staining in frozen tumour sections

Blood vessel quantitation in frozen tumours was performed by counting the number of PECAM positive vessels in 5 μm frozen tumour sections from age and size-matched tumours grown in test and control mice. Sections were fixed in cold acetone for 10 minutes at 4 °C and blocked in 1% BSA (PAA, Somerset, UK), 3% normal goat serum (NGS) (Sigma, Dorset, UK) in PBS for 1 hour at room temperature (RT). The sections were incubated with anti-PECAM antibody (BD Biosciences, San Jose,

CA, USA) diluted 1:100 in 0.3% NGS and 0.1% BSA in PBS overnight at 4°C, washed 3 times in PBS 0.02% triton X-100 (Sigma, Dorset, UK), and incubated with the secondary antibody, Alexa fluor 546 goat anti-rat (Invitrogen, Paisley, UK) diluted 1:100 in 0.3% NGS and 0.1% BSA in PBS for 40 minutes at RT. Finally, sections were washed 3 times in PBS 0.02% triton X-100, 1 time in distilled water and mounted in Prolong Gold antifade reagent with DAPI (Invitrogen, Paisley, UK).

B. Blood vessel staining in paraffin-embedded tumour sections

Blood vessel quantification in paraffin embedded tumour sections was performed by counting the number of endomucin positive vessels in 5 μm tumour sections from age and size-matched tumours grown in test and control mice. Paraffin sections were de-waxed in xylene (BDH Laboratory Supplies, Poole, UK) in 2 changes of 5 min each and rehydrated in graded ethanol (2 min in each 100%, 80%, 70% and 50%) before being blocked in 5% normal goat serum (NGS) in PBS for 1 hour at room temperature (RT). The sections were incubated with rat anti-mouse endomucin antibody (clone V.7C7, Santa Cruz Biotechnology, CA, USA) diluted 1:200 in 0.5% NGS in PBS overnight at 4°C, washed 3 times in PBS 0.02% triton X-100 and incubated with the secondary antibody, Alexa fluor 546 goat anti-rat diluted 1:200 in 0.5% NGS in PBS for 40 minutes at RT. Finally, sections were washed 3 times in PBS 0.02% triton X-100, 1 time in distilled water and mounted in Prolong Gold antifade reagent with DAPI.

C. Blood vessel quantitation

Tumour blood vessel density was calculated by counting the total number of blood vessels across midline tumour sections and dividing this by the area of the section. Volumes were given as number of blood vessels/mm^2 of tumour section. Representative fields were photographed using a Hamamatsu Digital Camera (Improvision, London, UK) on a Zeiss Axioplan microscope (Zeiss, HERTS, UK). Identical settings were used for all the tissue samples.

D. Quantitation of functional blood vessels in frozen tumour sections

Tumour sections from **2.9.4** where mice had been injected with dextran FITC to identify blood vessels with flow were imunostained for PECAM as described in **2.11.2A** and total number PECAM positive blood vessels and number of PECAM blood vessels that were also FITC positive (fluorescence from dextran FITC dye) were counted across the entire section and normalised for the total area of the section. Results were presented as % of FITC positive vessels over total PECAM positive blood vessels per mm^2 of tumour. Representative fields were photographed using a Hamamatsu Digital Camera on a Zeiss Axioplan microscope. Identical settings were used for all the tissue samples.

E. Quantitation of blood vessel laminin coverage in paraffin tumour sections

Paraffin embedded tumour sections were stained double stained for endomucin and laminin. Briefly paraffin tumour sections were de-waxed and re-hydrated as described in **2.11.2B** before being blocked in 5% normal goat serum (NGS) in PBS for 1 hour at room temperature (RT). The sections were incubated with rat anti-mouse endomucin antibody (clone V.7C7, Santa Cruz Biotechnology, CA, USA) and rabbit anti-mouse laminin diluted 1:200 in 0.5% NGS in PBS overnight at 4°C, washed 3 times in PBS 0.02% triton X-100 and incubated with the secondary antibody, Alexa fluor 488 goat anti-rat and Alexa fluor 546 goat anti-rabbit diluted 1:200 in 0.5% NGS in PBS for 40 minutes at RT. Finally, sections were washed 3 times in PBS 0.02% triton X-100, 1 time in distilled water and mounted in Prolong Gold antifade reagent with DAPI.

Total number endomucin positive blood vessels and number of endomucin blood vessels that had laminin coverage (basement membrane) were counted across the entire section and normalised for the total area of the section. Results were presented as % of laminin positive vessels over total endomucin positive blood vessels per mm^2 of tumour. Representative fields were photographed using a Hamamatsu Digital Camera on a Zeiss Axioplan microscope. Identical settings were used for all the tissue samples.

F. Quantitation of blood vessel supporting cell coverage in paraffin tumour sections

Paraffin embedded tumour sections were stained double stained for endomucin and alpha-smooth actin (α-SMA). Briefly paraffin tumour sections were de-waxed and re-hydrated as described in **2.11.2B** before being blocked in 5% normal goat serum (NGS) in PBS for 1 hour at room temperature (RT). The sections were incubated with rat anti-mouse endomucin antibody (clone V.7C7, Santa Cruz Biotechnology, CA, USA) and rabbit anti-mouse α-SMA-cy3 (Sigma, Dorset, UK) conjugated diluted 1:200 in 0.5% NGS in PBS overnight at 4°C, washed 3 times in PBS 0.02% triton X-100 and incubated with the secondary antibody, Alexa fluor 488 goat anti-rat diluted 1:200 in 0.5% NGS in PBS for 40 minutes at RT. Finally, sections were washed 3 times in PBS 0.02% triton X-100, 1 time in distilled water and mounted in Prolong Gold antifade reagent with DAPI.

Total number endomucin positive blood vessels and number of endomucin blood vessels that had supporting cell coverage (α-SMA positive) were counted across the entire section and normalised for the total area of the section. Results were presented as % of α-SMA positive vessels over total endomucin positive blood vessels per mm^2 of tumour. Representative fields were photographed using a Hamamatsu Digital Camera on a Zeiss Axioplan microscope. Identical settings were used for all the tissue samples.

2.11.3. Haematoxylin and eosin (H&E) staining

H&E staining was performed in Barts Cancer Institute Pathology Department using the Sakura RS-601 staining machine using Harris's haematoxylin for 5 min and 1% eosin for 5 min followed by rinsing in tap water. Sections were rehydrated in increasing concentrations of ethanol (50%, 70%, 80%, 100%), 2 min in each before clearing in xylene and mounting in DPX (Sigma, Dorset, UK).

2.11.4. $Gr1^+$cell and tumour-$Gr1^+$ cell interaction quantitation in frozen sections

A. Gr1 staining in frozen lung sections

For immunofluorescent staining for Gr1, 5 μm frozen lung sections were fixed in 100% acetone for 10min, blocked in 5% normal goat serum for 1 h at RT, incubated with rat anti-mouse Gr1 (clone RB68C5 - BD pharmigen, Oxford, UK) primary antibody (1:50 dilution) overnight at 4°C and anti-rat Alexa-Fluor-488 (Invitrogen, Paisley, UK) secondary antibody (1:200 dilution) for 45 min at room temperature and finally mounted with Prolong anti-fade with DAPI.

B. $Gr1^+$ cell quantitation in frozen lung sections

Number of Gr1 positive cells/mm2 lung was quantified using the 20X objective of a Zeiss Axioplan microscope (Zeiss) in at least five different fields per lung section for a minimum of 4 mice/group. The number of Gr1 positive cells was normalised for the DAPI area quantified on the same fields.

C. Tumour-Gr1$^+$ cell interaction quantitation in frozen lung sections

B16F0-Gr1$^+$ cell interactions were quantified in the sections from the 2h time point of the homing/colonisation described in **2.9.5** using the 40X objective of a Zeiss Axioplan microscope. The percentage of B16F0 interacting with at least one Gr1$^+$ cell was calculated for at least 4 different fields per section in a minimum of 4 mice/group.

2.11.5. Large T cell antigen staining

Six step-wise paraffin embedded sections of pancreas, liver and lung 5 μm thick and 100 μm apart per animal were de-waxed in xylene in 2 changes of 5 min each and after 2 min in 100% ethanol endogenous peroxidade activity was blocked by incubating the sections for 5 min at RT in 3% hydrogen peroxide (Sigma, Dorset, UK) in methanol (BDH Laboratory Supplies, Poole, UK). Sections were then rehydrated in graded ethanol (2 min in each 100%, 80%, 70% and 50%) before being microwaved for 10 min in previously boiled 10 mM citrate buffer (Sigma, Dorset, UK) pH6 (antigen retrieval step). Endogenous biotin was blocked using avidin/biotin blocking kit (Vector Labs, Peterborough, UK), 15 min in avidin D, one PBS wash and 15 min in biotin solution. After being blocked in 5% normal goat serum (previously centrifuged to avoid non-specific crystals), incubated with rabbit anti-mouse large T-cell antigen (Santa Cruz Santa Cruz Biotechnology, CA, USA) antibody (1:200 dilution) overnight at 4°C sections were incubated with anti-rabbit biotynilated secondary antibody (Sigma, Dorset, UK) (1:200 dilution) for 45 min at RT. ABC reagents (Vector Labs, Peterborough, UK) were added for 30 min at RT and staining

developed with DAB (approximately 5 min) (Vector Labs, Peterborough, UK), sections washed for 1 min in running tap water and couterstained with haematoxylin (Sigma, Dorset, UK), approximately 2 min. Sections were washed for 1 min in running tap water, 1 min in PBS and another 1 min in running tap water. Sections were rehydrated in increasing concentrations of ethanol (50%, 70%, 80%, 100%), 2 min in each before clearing in xylene and mounting in DPX.

2.11.6. In situ hybridisation for Y chromosome

Five μm paraffin sections of spleen were de-waxed in xylene in 2 changes of 5 min each and after 2 min in 100% ethanol endogenous peroxidade activity was blocked by incubating the sections for 5 min at RT in 3% hydrogen peroxide in methanol. Sections were then rehydrated in graded ethanol (2 min in each 100%, 80%, 70% and 50%) before being permeabilised by incubating in 1M sodium thiocyanate (Sigma, Dorset, UK) for 10 min at 80°C and washed 3 times in PBS. Tissue was then digested for 7 min in 0.4% pepsin (Sigma, Dorset, UK) in 0.1M HCl at 37°C. Pepsin was then quenched by immersing slides in 0.2% glycine (Merck, Nottingham, UK) in PBS and slides washed twice in PBS. Slides were post-fixed in 4% paraformaldehyde for 2 min at RT and washed in 3 changes of PBS over 15 minutes. Slides were then dehydrated by immersion in successively increasing concentrations of ethanol (50%, 70%, 80%, 100%) 2 min each before clearing in xylene and allowed to air dry. 9-15 μl of FITC-labelled Y-chromosome paint (Cambio, Cambridge, UK) was applied to each slide and sealed by placing a coverslip on the section and using rubber solution glue to prevent evaporation. DNA was denatured using a hybridisation plate at 60°C for 10 min after which probe was allowed to hybridise overnight at 37°C. On the following

day coverslips were gently removed and unbound probe removed by washing slides in 2 changes of 0.5X Standard Sodium Citrate (SSC) solution. After one PBS wash sections were incubated with peroxidase-conjugated anti-fluorescein antibody (Boehringer, Mannheim, Germany) diluted 1:50 in PBS for 1 hour at RT. After 3 PBS and one water wash staining was developed with DAB (approximately 5 min), sections washed for 1 min in running tap water and couterstained with haematoxylin for approximately 2 min. Sections were washed for 1 min in running tap water, 1 min in PBS and another 1 min in running tap water. Sections were then rehydrated in increasing concentrations of ethanol (50%, 70%, 80%, 100%), 2 min in each before clearing in xylene and mounting in DPX.

2.12. Analysis of statistical significance

For RIP-Tag2 data and experimental metastasis set analysis, since the data were not normally distributed, nonparametric Mann-Whitney and chi-square tests were used to determine statistical significance. All other data sets were analysed for statistical significance using Student's *t* test. For both tests $P<0.05$ was considered statistically significant.

3. RESULTS PART I – Stromal and bone marrow derived FAK in tumour growth, angiogenesis and metastasis

This chapter of my PhD data describes the role of inducible FAK deficiency in the stromal compartment and specifically in the bone marrow compartment in tumour growth, angiogenesis and metastasis where I have demonstrated that loss of bone marrow focal adhesion kinase is sufficient to enhance tumour metastasis.

The upregulation of FAK within tumour cells has directed studies to investigate the requirement for this molecule in cancer progression (Furuyama *et al*., 2006; Judson *et al*., 1999; Lark *et al*., 2005). Indeed investments have focused on the development of FAK inhibitors in the treatment of cancer and such inhibitors are in clinical trials for the treatment of this disease (Halder *et al*., 2007; Kurio *et al*., 2011; Stokes *et al*., 2011). These agents are likely to affect both the tumour cell compartment and the stromal compartment, but the effect of the loss of FAK in the stromal compartment, especially in metastasis is poorly understood.

3.1. Stromal FAK deficiency decreases subcutaneous tumour growth and angiogenesis

3.1.1. Generation of ubiquitous inducible FAK deficient mice

Constitutive deletion of FAK results in a phenotype where the embryos die at E8.5 due to severe defects in late gastrulation (Ilic *et al*, 1995). Therefore, to examine the effect of the stromal-deletion of FAK in mice I have used a tamoxifen inducible model for the ubiquitous deletion of FAK in adult mice. For that purpose I have crossed $FAK^{fl/fl}$ mice with $RERTn^{ERT/ERT}Cre$ mice where Cre-ERT2 is under the control of the large subunit of RNA polymerase II promoter (Barriere *et al*., 2007; Guerra *et al*., 2003) to first generate $RERTn^{ERT/+}Cre;FAK^{fl/+}$ mice. These mice were intercrossed to generate $RERTn^{ERT/ERT}Cre;FAK^{fl/fl}$ mice that allow FAK deletion in the majority of the cells after tamoxifen treatment in adult mice. Examples of RERTnCre and FAK floxed PCR performed using DNA extracted from ear snips are shown in **Fig. 19**. RERTnCre PCR (**Fig. 19A**) indentifies genotypes homozygous ($RERTn^{ERT/ERT}Cre$) and heterozygous ($RERTn^{ERT/+}Cre$) for RERTnCre, and WT mice that do not express RERTnCre in either allele ($RERTn^{+/+}Cre$). FAK floxed PCR (**Fig. 19B**) identifies genotypes with one ($FAK^{fl/+}$) or both ($FAK^{fl/fl}$) FAK floxed alleles, and WT mice non-floxed ($FAK^{+/+}$).

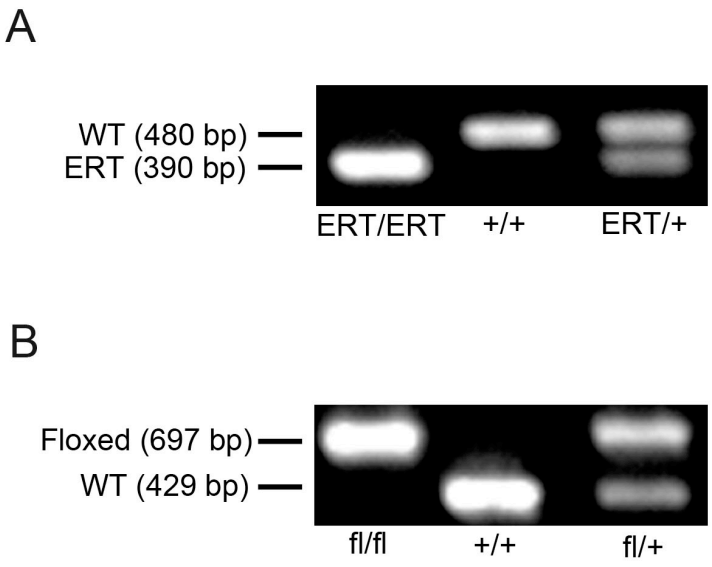

Figure 19: RERTn and FAK floxed PCR.

PCR results from DNA extracted from mice ear snips. (**A**) PCR for RERTnCre shows mice homozygous ($RERTn^{ERT/ERT}Cre$), WT ($RERTn^{+/+}Cre$) and heterozygous ($RERTn^{ERT/+}Cre$) for RERTnCre. (**B**) FAK floxed PCR shows mice with both FAK floxed alleles ($FAK^{fl/fl}$), WT mice non-floxed ($FAK^{+/+}$), and mice heterozygous for the floxed allele ($FAK^{fl/+}$).

RERTn$^{ERT/ERT}$Cre;FAK$^{fl/fl}$ mice and respective controls appeared normal without any visible adverse effects after tamoxifen treatment. FAK deletion was observed by Western blotting in whole kidney and bone marrow lysates from RERTn$^{ERT/ERT}$Cre;FAK$^{fl/fl}$ mice after tamoxifen treatment when compared with similarly treated non-floxed RERTn$^{ERT/ERT}$Cre controls (**Fig. 20).** In some of the tumour experiments presented in my thesis I have injected mouse melanoma cells that express FAK into tamoxifen treated RERTn$^{ERT/ERT}$Cre;FAK$^{fl/fl}$ mice. Thus for brevity RERTn$^{ERT/ERT}$Cre;FAK$^{fl/fl}$ were called StrFAK^{KO} (stromal FAK knockouts) and the control non-floxed RERTn$^{ERT/ERT}$Cre or Cre- FAK$^{fl/fl}$ mice called StrFAK^{WT} (stromal FAK *wild type*).

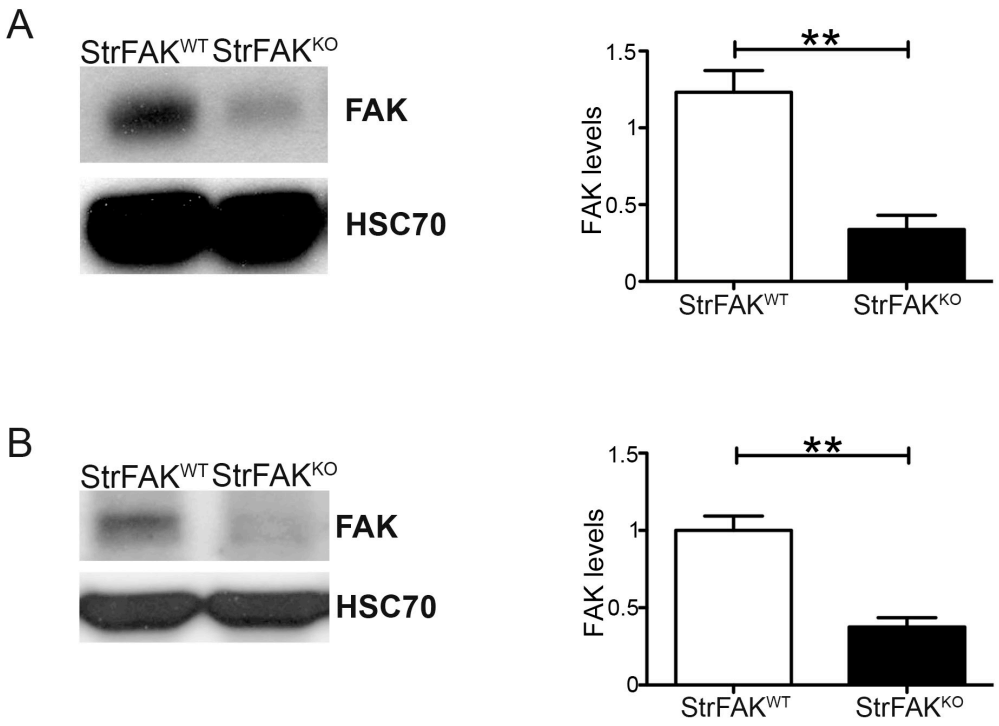

Figure 20: Evidence for FAK deficiency in StrFAK^{KO} mice.

StrFAK^{KO} mice show efficient stromal FAK deficiency after tamoxifen treatment when compared with control StrFAK^{WT}. Western blot analysis of kidney **(A)** and whole BM (**B**) isolated from StrFAK^{KO} and StrFAK^{WT} mice show depletion of FAK in StrFAK^{KO} when compared with StrFAK^{WT} mice. HSC70 was used as a loading control. Bar charts represent mean densitometric results of FAK levels relative to HSC70 + s.e.m.; n, 4-5 mice/genotype $^{**}P<0.01$.

3.1.2. Stromal FAK deficiency in adult mice inhibits subcutaneous tumour growth and angiogenesis

To study effect of stromal FAK deficiency on tumour growth and angiogenesis $StrFAK^{KO}$ and $StrFAK^{WT}$ mice were injected subcutaneously with B16F0 mouse melanoma cells. Ten days post-tumour cell injection $StrFAK^{KO}$ mice showed significantly decreased subcutaneous B16F0 tumour size when compared with control $StrFAK^{WT}$ (**Fig. 21A**). Age and size matched tumours were processed for histological analysis of PECAM-positive blood vessels of midline tumour sections. Tumour blood vessel density was decreased significantly in $StrFAK^{KO}$ mice when compared with similarly treated controls (**Fig. 21B**). These results suggest that stromal-deficiency of FAK in adult mice is sufficient to inhibit tumour growth and indicate that stromal FAK, likely including the endothelium is important for supporting tumour angiogenesis. This in line with our previously published work showing that endothelial FAK is important for tumour growth and angiogenesis (Tavora *et al*., 2010).

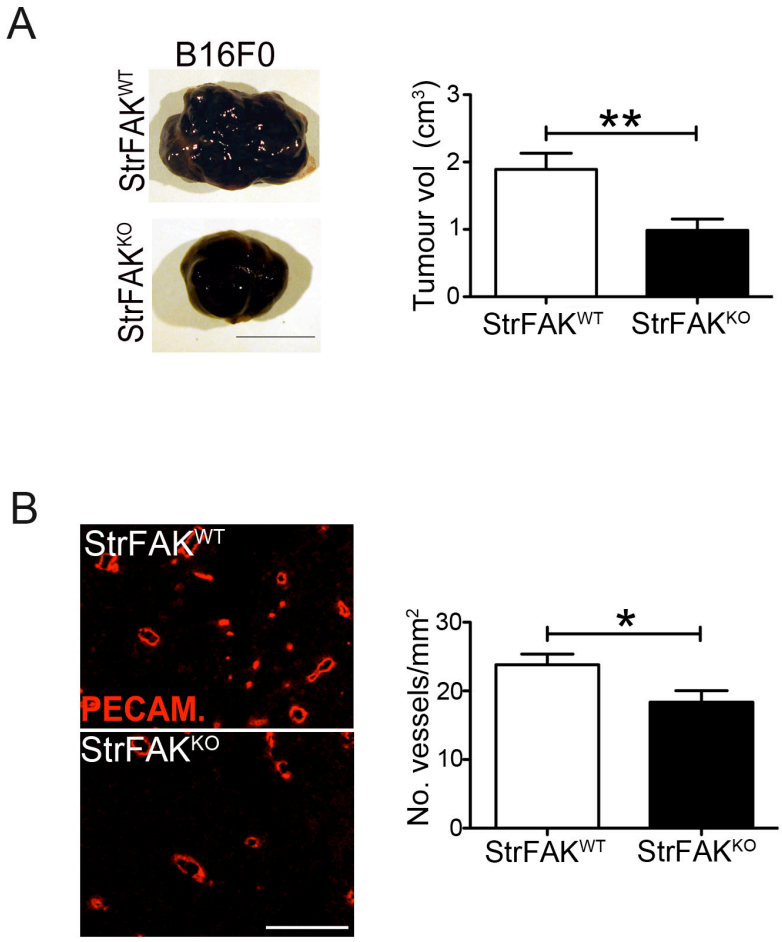

Figure 21: Stromal FAK deficiency in mice decreases subcutaneous tumour growth and angiogenesis

$StrFAK^{WT}$ and $StrFAK^{KO}$ mice were given subcutaneous injections of syngeneic tumour cell line B16F0 melanoma. 10 day old tumour size was decreased significantly in $StrFAK^{KO}$ mice when compared with $StrFAK^{WT}$ controls. (**A**) Pictures of representative tumours are given. Bar charts show mean tumour volume +s.e.m.; n, 10 mice/genotype; (**B**) Tumour blood vessel density is reduced in $StrFAK^{KO}$ mice. Representative immunofluorescence micrographs identifying PECAM-positive blood vessels in midline sections of tumours are shown. Blood vessel density was assessed by counting the total number of blood vessels per mm^2 across entire midline sections of size-matched tumours. Bar charts represent mean tumour blood vessel density +s.e.m; n, 4 mice/genotype. **A**, 1cm; **B**, 200μm. $^{**}P<0.01$; $^{*}P<0.05$.

3.2. Deficiency of bone marrow FAK is not sufficient to affect subcutaneous tumour growth or angiogenesis

Stromal cells can be derived from the organ in which the tumour has formed or from other compartments such as the bone marrow (BM). There are several reports describing BM contribution to tumour growth and angiogenesis. Some studies suggest that circulating endothelial progenitor cells (CEPs) that are derived from the BM are capable of differentiating into mature endothelial cells, recruit to angiogenic sites, and incorporate newly forming blood vessels (Lyden *et al*., 2001; Ruzinova *et al*., 2003). Recent evidence has highlighted a role of bone marrow derived mesenchymal cells in supporting tumour angiogenesis as they have been shown to be precursors of pericytes and cancer-associated fibroblasts (De Palma *et al*., 2005; Mishra *et al*., 2008). These cells are recruited to sites of tumour growth and have been shown to enhance angiogenesis by secreting VEGF (Beckermann *et al*., 2008).

3.2.1. Generation of inducible bone marrow FAK deficient mice

To dissect the requirement of FAK within the bone marrow compartment from FAK in non-bone marrow derived cells in tumour growth, angiogenesis and metastasis we carried out a series of BM transplant (BMT) experiments. Briefly, female *wild type* (WT) recipient mice were lethally irradiated, to ablate endogenous BM, and transplanted immediately with either RERTn$^{ERT/ERT}$Cre;FAK$^{fl/fl}$ or control FAK non-floxed RERTn$^{ERT/ERT}$Cre male BM to generate bone marrow chimeras (**Fig. 22A**). Tamoxifen-treatment, four to six weeks post-transplant, induced efficient FAK deletion specifically in the bone marrow compartment of mice transplanted with RERTn$^{ERT/ERT}$Cre;FAK$^{fl/fl}$ BM (BMFAK^{KO}) and not in control transplanted animals (BMFAK^{WT}). Given that spleen is a main reservoir for bone marrow derived cells I have accessed the efficiency of bone marrow repopulation after transplant in spleen. *In situ* hybridisation for the Y chromosome confirmed engraftment of bone marrow derived cells in both genotypes (**Fig. 22B**). In addition, Western blot analysis of whole bone marrow established the efficiency of FAK deletion in the bone marrow compartment in BMFAK^{KO} mice, when compared with BMFAK^{WT} controls (**Fig. 22C**).

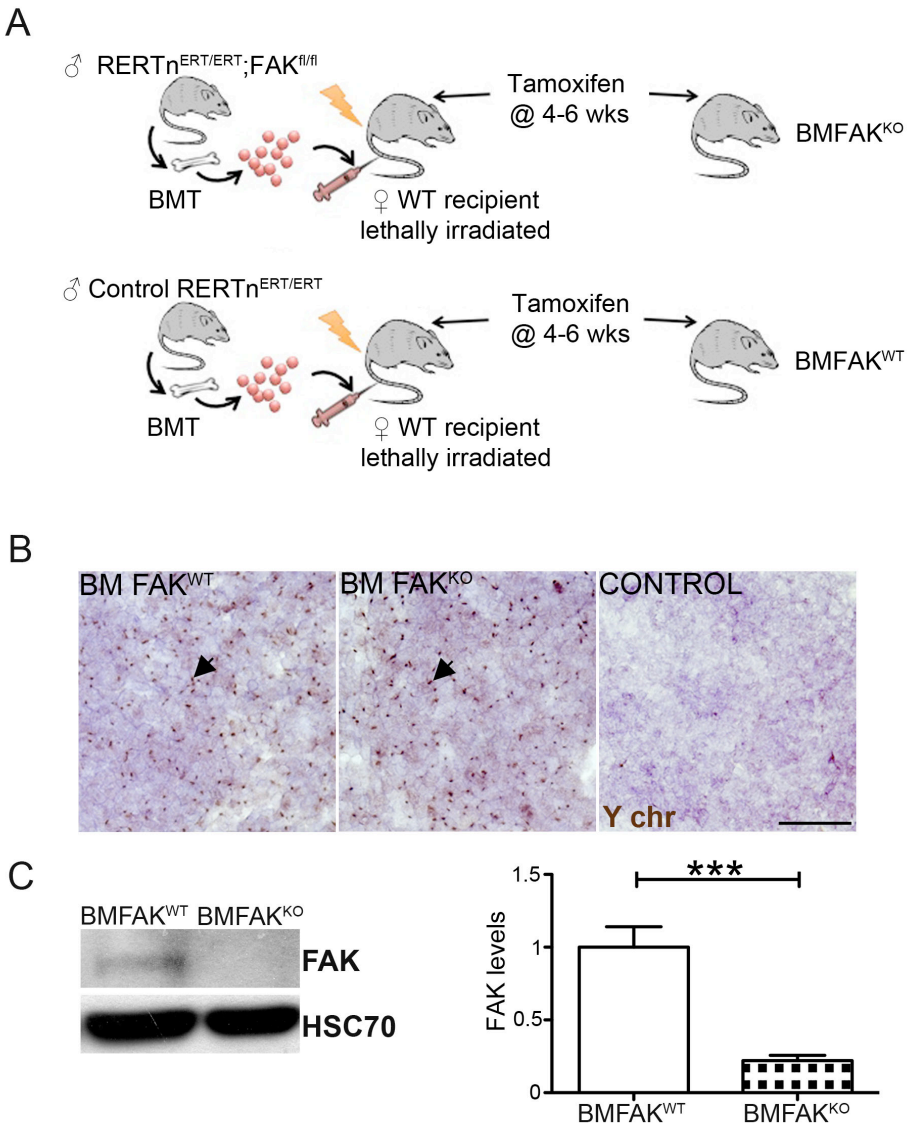

Figure 22: Generation of BMFAK^{WT} and BMFAK^{KO} mice

Schematic of BMFAK^{WT} and BMFAK^{KO} generation. (**A**) Female WT recipient mice were lethally irradiated to ablate the endogenous BM and received a BM transplant (BMT) from BM derived from either RERTn$^{ERT/ERTCre}$;FAK$^{fl/fl}$ or control RERTn$^{ERT/ERT}$Cre male donor mice. 4-6 weeks post-transplant all mice received tamoxifen treatment to generate bone marrow FAK deficient mice (BMFAK^{KO}) and bone marrow FAK *wild type* mice (BMFAK^{WT}), respectively. (**B**) *In situ* hybridization for Y chromosome (black arrow) in spleens from BMFAK^{WT} and BM FAK^{KO} mice shows repopulation of the spleen by male donor BM cells. Non-engrafted transplant (Control) shows no Y-chromosome signal. (**C**) Western blot analysis of whole BM isolated from BMFAK^{KO} mice show depletion of FAK when compared with BMFAK^{WT} mice. Bar chart represents mean densitometric results of FAK levels relative to HSC70 + s.e.m. Scale bar, 50μm. ***P<0.001.

3.2.2. Bone marrow FAK deficiency does not affect subcutaneous tumour growth or angiogenesis

To study effect of FAK deficiency specifically in the BM compartment in tumour growth and angiogenesis $BMFAK^{KO}$ and $BMFAK^{WT}$ mice were injected subcutaneously with B16F0 cells. Fourteen days post tumour cell injection $BMFAK^{KO}$ mice showed no significant difference in B16F0 tumour growth when compared with controls (**Fig. 23A**). Age and size matched tumours were processed for histological analysis of endomucin-positive blood vessels. Blood vessel density was not changed between $BMFAK^{WT}$ and $BMFAK^{KO}$ mice (**Fig. 23B**). These results suggest that FAK expression in bone marrow cells is not sufficient tumour growth or tumour angiogenesis.

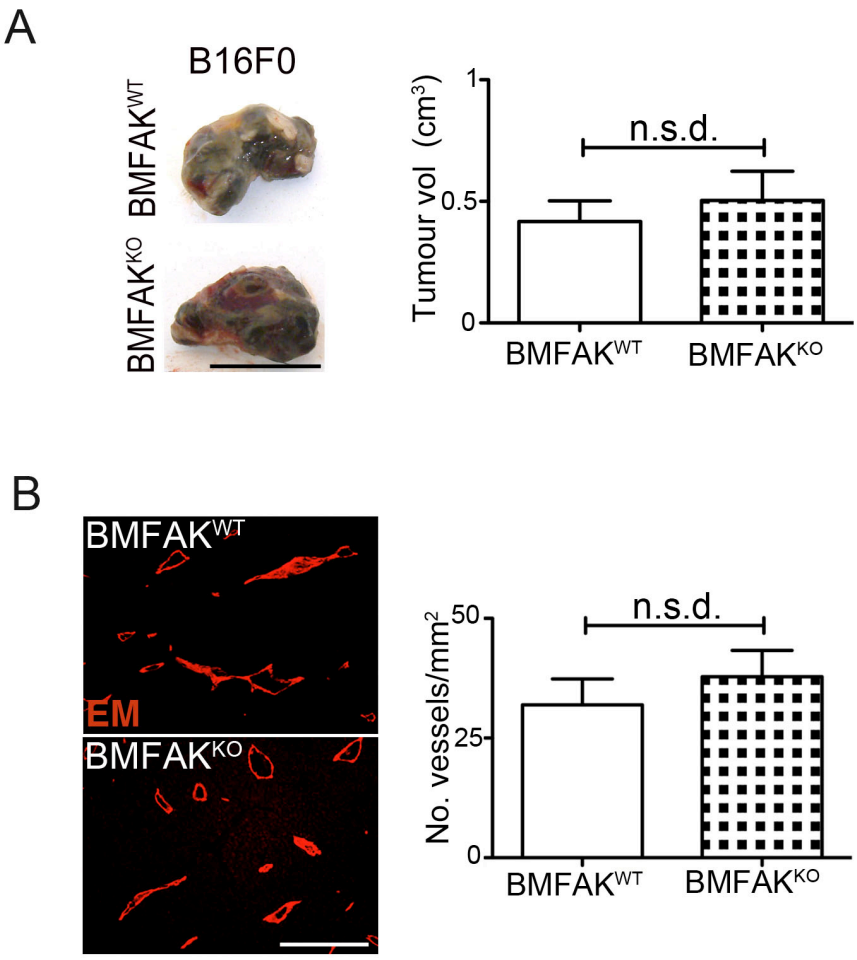

Figure 23: Bone marrow FAK deficiency in mice does not affect subcutaneous tumour growth or angiogenesis

$BMFAK^{WT}$ and $BMFAK^{KO}$ mice were given subcutaneous injections of syngeneic tumour cell line B16F0 melanoma. 14 day old tumour size was similar in $BMFAK^{KO}$ mice when compared with $BMFAK^{WT}$ controls. (**A**) Pictures of representative tumours are given. Bar charts show mean tumour volume +s.e.m.; n, 10 mice/genotype. (**B**) Tumour blood vessel density was similar for tumours grown in $BMFAK^{WT}$ and $BMFAK^{KO}$ mice. Representative immunofluorescence micrographs identifying endomucin (EM) positive blood vessels in midline sections of tumours are shown. Blood vessel density was assessed by counting the total number of blood vessels per mm^2 across entire midline sections of size-matched tumours. Bar chart represents mean tumour blood vessel density +s.e.m; n, 4 mice/genotype. **A**, 1cm; **B**, 200μm. n.s.d. (no significant difference).

3.2.3. Bone marrow FAK deficiency does not affect blood vessel function

Although tumour blood vessel density seemed unaffected in $BMFAK^{KO}$ mice evidence for bone marrow derived pericytes and blood vessel function have been described (De Palma *et al*., 2005; Mishra *et al*., 2008). To assess the effect of BM FAK deficiency in vessel function I have perfused a high molecular weight fluorescent dye (2 million KDa dextran-FITC) into tumour burdened mice. Thirty minutes post-perfusion mice were killed, tumours snap frozen and cryosections stained for the blood vessel marker PECAM. The percentage of dextran-FITC positive blood vessels was assessed histologically. $BMFAK^{WT}$ and $BMFAK^{KO}$ mice showed no change in the number of functional tumour blood vessels (**Fig. 24A**). Similar tumour sections were also double-stained for laminin and endomucin and the percentage of laminin covered blood vessels calculated. No changes in laminin positive blood vessels were observed between genotypes (**Fig. 24B**). Furthermore tumour sections were double-stained for α-SMA and endomucin and the percentage of blood vessels with supporting cell association was not changed between $BMFAK^{WT}$ and $BMFAK^{KO}$ mice (**Fig. 24C**). These results suggest that FAK deficiency in the bone marrow compartment is not sufficient to affect B16F0 tumour blood vessel function or supporting cell coverage. Together my results show that loss of bone marrow FAK is not sufficient to affect subcutaneous tumour growth and angiogenesis.

A

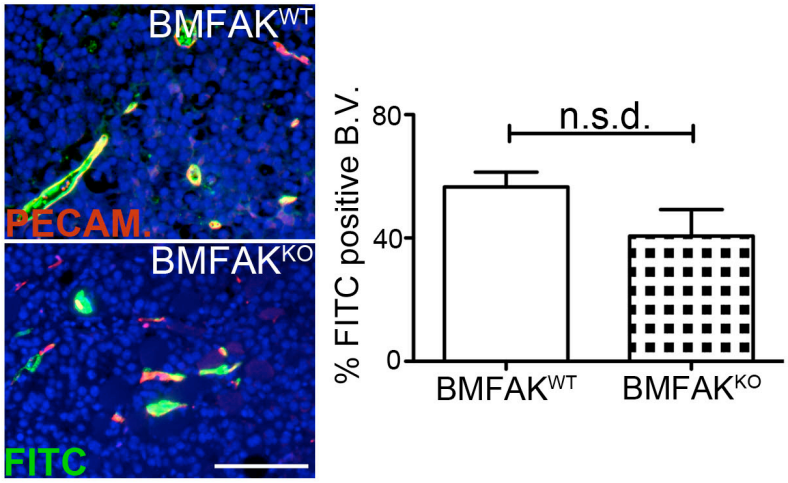
BMFAK^WT
PECAM
BMFAK^KO
FITC
% FITC positive B.V.
80
40
0
n.s.d.
BMFAK^WT
BMFAK^KO

B

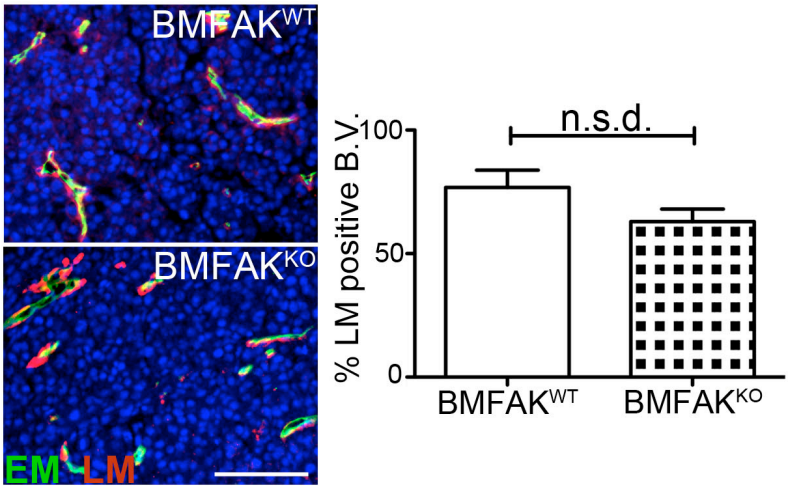
BMFAK^WT
BMFAK^KO
EM LM
% LM positive B.V.
100
50
0
n.s.d.
BMFAK^WT
BMFAK^KO

C

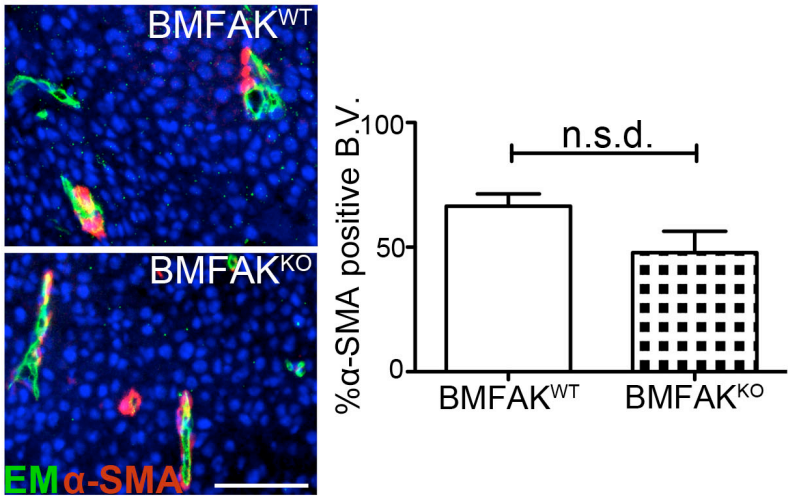
BMFAK^WT
BMFAK^KO
EM α-SMA
%α-SMA positive B.V.
100
50
0
n.s.d.
BMFAK^WT
BMFAK^KO

Figure 24: Bone marrow FAK deficiency in mice does not affect subcutaneous B16 vessel function

(**A**) $BMFAK^{WT}$ and $BMFAK^{KO}$ mice were given subcutaneous injections of B16F0 melanoma cells. 14 days post-tumour cell inoculation mice were perfused with high molecular weight dextran-FITC. Representative immunofluorescence micrographs identifying PECAM positive blood vessels (red) and dextran-FITC perfused blood vessels (green) in midline sections of tumours are shown. Vessel function was assessed by counting and number of FITC-positive blood vessels over the total number of blood vessels across entire midline sections of size-matched tumours. Bar charts represent mean % of FITC-positive blood vessels +s.e.m; n, 4 mice/genotype. (**B**) Laminin deposition of tumour blood vessels is not affected by BM FAK deficiency. 14 day old tumours were immunostained for laminin and endomuncin. Representative immunofluorescence micrographs identifying endomucin (EM) positive blood vessels (green) and laminin (red) in midline sections of tumours are shown. Blood vessel laminin deposition was assessed by counting the number of laminin positive blood vessels over the total number of blood vessels across entire midline sections of size-matched tumours. Bar charts represent mean % of laminin positive blood vessels +s.e.m; n, 4 mice/genotype. (**C**) Supporting cell coverage of tumour blood vessels is not affected when BM is FAK deficient. 14 day old tumours were immunostained for α-SMA and endomuncin. Representative immunofluorescence micrographs identifying endomucin (EM) positive blood vessels (green) and α-SMA (red) in midline sections of tumours are shown. Supporting cell coverage of blood vessels was assessed by counting the number of α-SMA positive blood vessels over the total number of blood vessels across entire midline sections of size-matched tumours. Bar charts represent mean % of α-SMA positive blood vessels +s.e.m; n, 4 mice/genotype. Scale bar, 200μm. n.s.d. (no significant difference).

3.3. Deficiency of bone marrow FAK enhances tumour metastasis

Several lines of evidence have identified that stromal cells can affect metastasis. In this context bone marrow derived cells have also been identified as important in tumour invasiveness and implicated in organ-specific tumour metastasis (Du *et al*., 2008; Kaplan *et al*., 2005). However role of FAK in this process is not clear.

3.3.1. Stromal FAK deficiency in adult mice increases experimental B16F10 metastasis

To study the effect of stromal FAK deletion in tumour metastasis $StrFAK^{WT}$ and $StrFAK^{KO}$ mice were injected, via the tail vein, B16F10 melanoma cells and examined metastasis. $StrFAK^{KO}$ mice showed a significant increase in tumour nodules 19 days post-tail vein injection when compared with $StrFAK^{WT}$ mice. Gross observations (**Fig. 25A**) of organs at necropsy revealed an elevated number of tumour nodules in the lungs, liver and bone of $StrFAK^{KO}$ mice when compared with controls. The presence of these increased numbers of metastases was confirmed in H&E stained sections of these tissues (**Fig. 25B**) and quantification of the numbers of B16F10 nodules per animal showed that this difference was statistically significant (**Fig. 25C** and **D**). These data suggest that stromal FAK deficiency leads to an increase number of metastases.

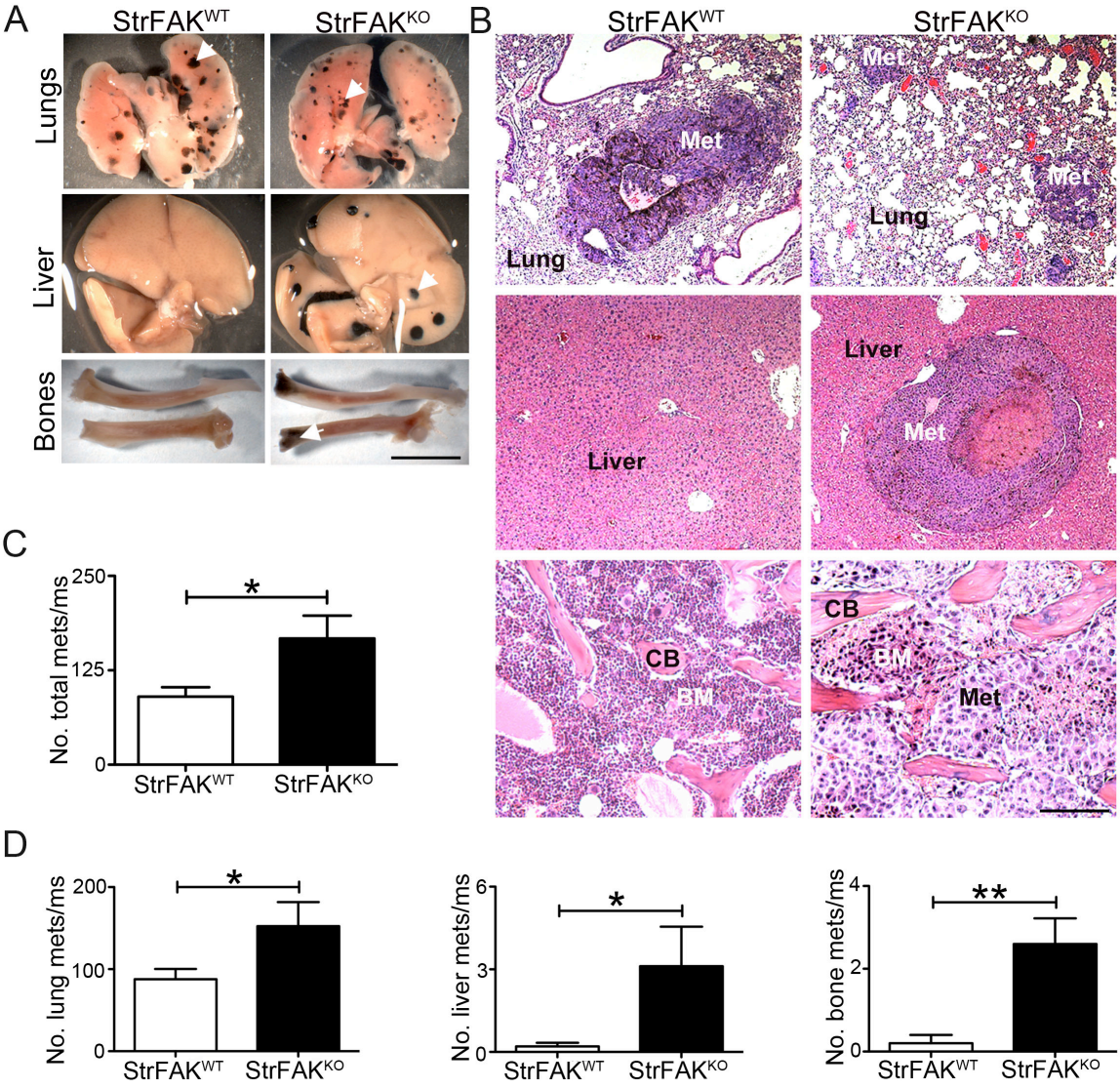

Figure 25: Stromal FAK deficiency in mice increases experimental B16F10 metastasis

StrFAK^{WT} and StrFAK^{KO} mice were injected via the tail vein with B16F10 melanoma cells. **(A)** Macroscopic images of metastases in lungs, liver and bones 19 days post-tumour inoculation and **(B)** representative images of H&E stained sections from lung, liver and bone metastases (Met) from StrFAK^{WT} and StrFAK^{KO} mice are given. **(C)** The total number of metastasis was increased significantly in StrFAK^{KO} mice when compared with StrFAK^{WT} controls. Bar chart represents mean number of metastases / mouse + s.e.m. **(D)** Bar charts show mean number of lung, liver or bone metastasis/mouse+ s.e.m., n,10-12 mice/genotype. *White arrows*, metastases; *CB*, calcified bone; *BM*, bone marrow. Scale bars: **A** ,1cm; **B**, 200mm. *P<0.05, **P<0.01.

3.3.2. Bone marrow FAK deficiency is sufficient to increase B16F0 metastasis

To dissect the requirement of FAK within the bone marrow compartment from FAK in non-bone marrow derived cells in tumour metastasis, $BMFAK^{WT}$ and $BMFAK^{KO}$ were injected via the tail vein with B16F0 tumour cells. Results showed that deficiency of FAK in the bone marrow compartment alone was sufficient to increase significantly the total number of tumour nodules in $BMFAK^{KO}$ mice when compared with controls (**Fig. 26A**). The presence of this increased number of metastases was confirmed in histological analysis of the lungs, liver and bones from $BMFAK^{KO}$ mice and respective controls (**Fig. 26B**). Quantification revealed a significant in increase in the number of B16F0 nodules not only in $BMFAK^{KO}$ lungs, but also in the livers and bones of these mice when compared with controls (**Figs. 26C** and **D**). Together, these data indicate that the loss of stromal FAK, even within the bone marrow compartment alone is sufficient to control of tumour metastasis in experimental metastasis models.

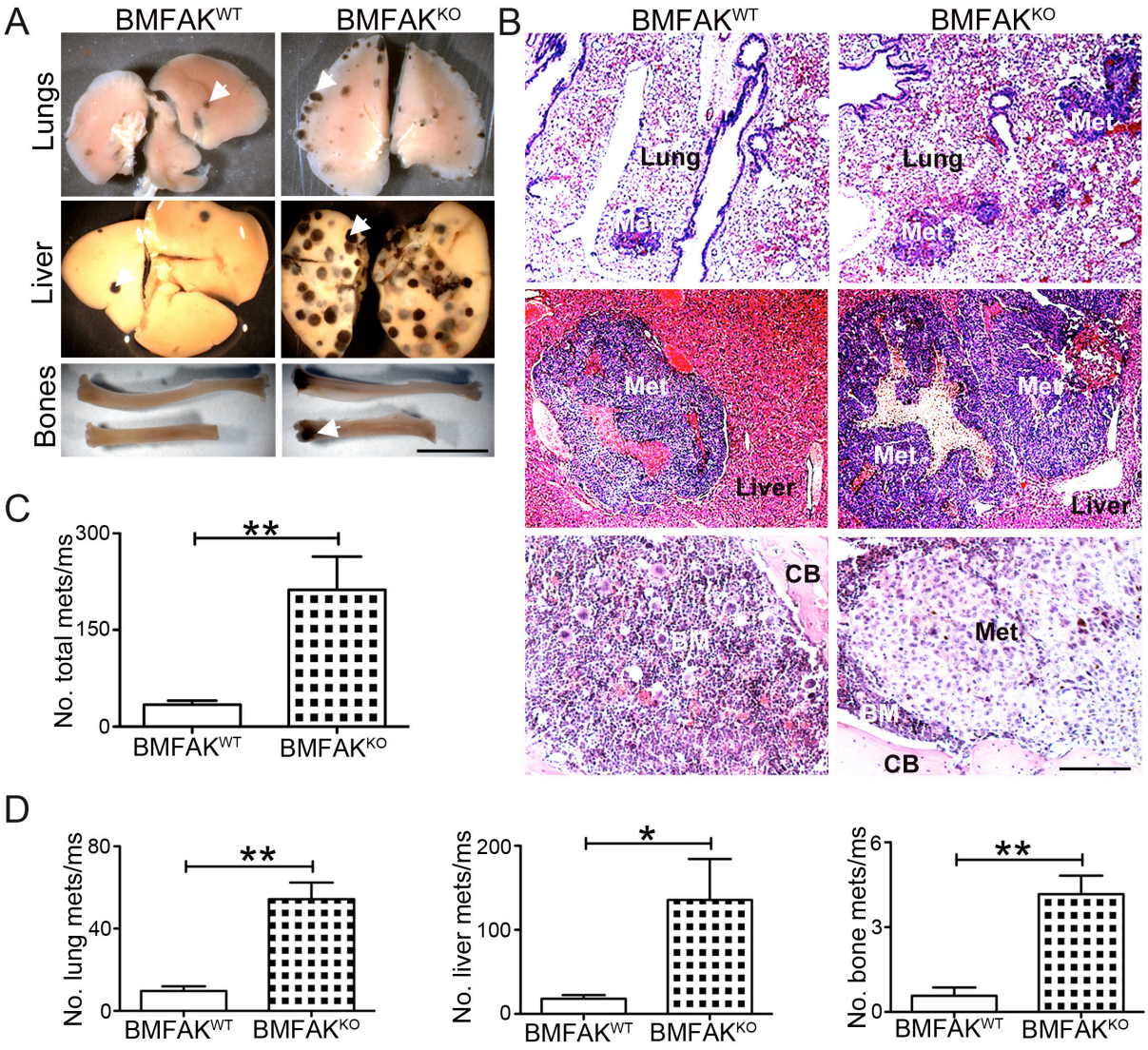

Figure 26: Bone marrow FAK deficiency in mice increases experimental B16F10 metastasis

BMFAK^{WT} and BMFAK^{KO} mice were injected with B16F0 tumour cells via the tail vein in experimental metastasis assays. Increased numbers of metastases were observed in the lungs, liver and bones of BMFAK^{KO} mice. **(A)** Macroscopic images of metastases in lungs, liver and bones 15-17 days post-tumour inoculation and **(B)** representative images of H&E stained sections of metastases (Met) in lung, liver and bone from BMFAK^{WT} and BMFAK^{KO} mice are shown. **(C)** Bar chart shows mean number of metastasis/ mouse + s.e.m. for all organs in BMFAK^{KO} mice when compared with BMFAK^{WT} controls. **(D)** Bar charts show mean numbers of lung, liver and bone metastasis/mouse+ s.e.m., n,9 mice/genotype. *White arrows*, metastasis *CB*, calcified bone; *BM*, bone marrow. Scale bars: **A**, 1cm; **B** 200mm. *P<0.05, **P<0.01.

3.3.3. Bone marrow FAK deficiency does not affect primary tumour growth or invasion in the RIP-Tag2 model of cancer

RIP-Tag2 mice are a well-studied, spontaneous model of pancreatic cancer that express the SV40 large T antigen (Tag) under the control of the rat insulin promoter (Hanahan, 1985). Expression of Tag in pancreatic islets β-cells leads to development of hyperplasic lesions at 6-8 weeks of age from which a fraction will progress into highly vascularised β-cell tumours in mice of 10-14 weeks of age. These tumours have been reported to invade and spread to lymph nodes and liver thereafter (Lopez and Hanahan, 2002). Insulin secretion by these highly metabolic tumour cells leads to death due to hypoglycemia between 12-16 weeks of age (Hanahan, 1985).

To test the effect of bone marrow FAK–deficiency in a spontaneous model of metastatic cancer I have transplanted lethally irradiated 6-week-old female RIP-Tag2/+ (**Fig. 27A**) mice with bone marrow from either male RERTn$^{ERT/ERT}$Cre;FAK$^{fl/fl}$ (BMFAK^{KO}) or control FAK non-floxed RERTn$^{ERT/ERT}$Cre (BMFAK^{WT}). Two weeks after bone marrow transplant mice were treated with tamoxifen, to induce FAK deletion in the bone marrow compartment, and at 16 weeks of age necropsy performed. BMFAK^{KO} mice showed no significant difference burden of pancreatic tumours (**Fig. 27B**) corroborating the data obtained for subcutaneous B16F0 tumour growth (see **Fig. 23A**). It is noteworthy that the tumour burden in both genotypes was lower than predicted for this age of RIP-Tag2 mice most likely because the animals were irradiated. Previous work has shown that total body irradiation and BMT prolonged average mouse survival by 1 to 2 weeks without

affecting incidence or progression of adenomas to invasive tumours (De Palma *et al*., 2005).

The pancreatic tumours in RIP-Tag2 mice can be classified into three levels of progression: encapsulated, least aggressive; invasive type I, where the invasive front of the tumour is beginning to penetrate into the surrounding pancreas; and invasive type II, where the invasive front of the tumour engulfs islands of normal pancreas (Lopez and Hanahan, 2002; Paez-Ribes *et al*., 2009) (**Fig. 27C**). Quantification of large Tag immunostained pancreas sections revealed that $BMFAK^{KO}$ mice displayed no significant differences in tumour invasiveness (**Fig. 27D**). These results suggest that BM FAK is not sufficient to modulate primary tumour growth and invasion.

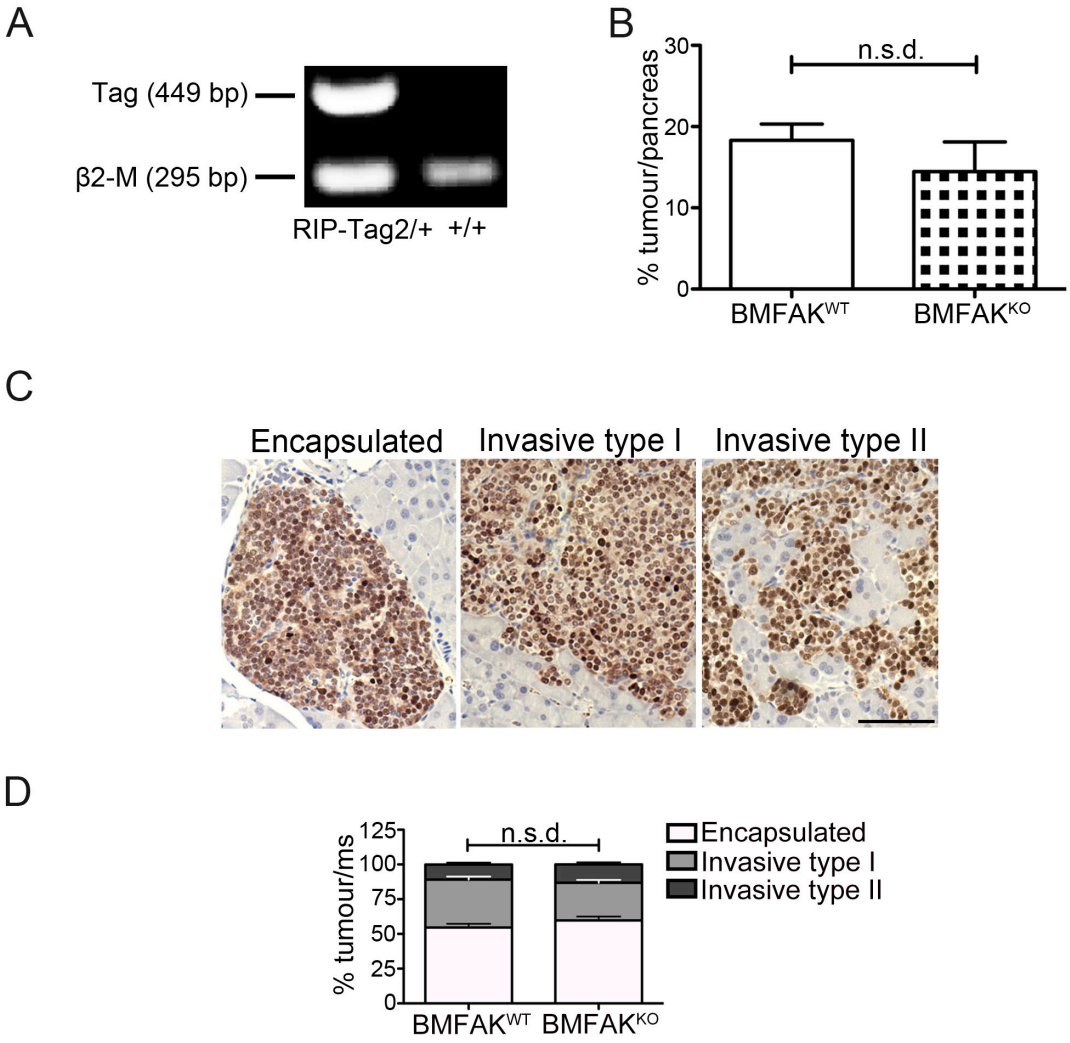

Figure 27: Bone marrow FAK deficiency in mice does not affect tumour burden or invasiveness in the RIP-Tag2 model of cancer

RIP-Tag2/+ mice were transplanted at 6 weeks of age, tamoxifen treated at 8-9 weeks generating BMFAK^{WT} and BMFAK^{KO} chimeras and necropsied at 16 weeks of age. Histological analysis was performed in 6 different levels of the pancreas, liver and lungs after immunohistochemical staining for the tumour marker SV40 T antigen. (**A**) PCR performed in DNA extracted from mice ear snips. RIP-Tag2 PCR shows mice hemizygous (RIP-Tag2/+) and WT (+/+) for the SV40 T antigen (Tag). β2-microglobulin (β2-M) was used as a DNA-loading control. (**B**) No difference in tumour burden was observed between BMFAK^{WT} and BMFAK^{KO} mice. Bar chart represent % tumour area normalised to total pancreas area per animal +s.e.m, n, 7-13 mice per genotype. (**C**) Histological images of tumour sections stained for large T-antigen at different states of invasiveness are shown. (**D**) Quantification of tumour invasiveness represented as the percentage of encapsulated islet tumours (encapsulated), microinvasive carcinomas (Invasive type I), and fully invasive carcinomas (Invasive type II) + s.e.m. shows no difference between BMFAK^{WT} and BMFAK^{KO} mice. Scale bar, 200μm, n.s.d (no significant difference).

3.3.4. Bone marrow FAK deficiency in adult mice is sufficient to increase liver and lung metastasis in the RIP-Tag2 model of cancer

I have also analysed metastasis in the RIP-Tag2 model. Dissemination of tumour cells can be through lymphatic or blood vessels. Histological analysis the 2 peri-pancreatic lymph nodes showed that metastasis to this site was low and not statistically different between both genotypes (**Fig. 28A-C**). In contrast, the incidence of liver metastasis was significantly higher in $BMFAK^{KO}$ when compared with $BMFAK^{WT}$ mice (**Fig. 29A, B**). Unexpectedly $BMFAK^{KO}$ mice also presented an increased incidence of lung metastases, an organ that has previously never been reported to display RIP-Tag2 metastasis (**Fig. 29A,B**). Total metastasis incidence was statistically increased in $BMFAK^{KO}$ mice when compared with $BMFAK^{WT}$ controls as assessed by the chi-square test (**Fig. 29B**). These data identify, using a spontaneous models of cancer, that deficiency of BM-derived FAK is sufficient to enhance tumour metastasis and that the effect is probably blood dissemination of the tumour cells similarly to the experimental metastasis model.

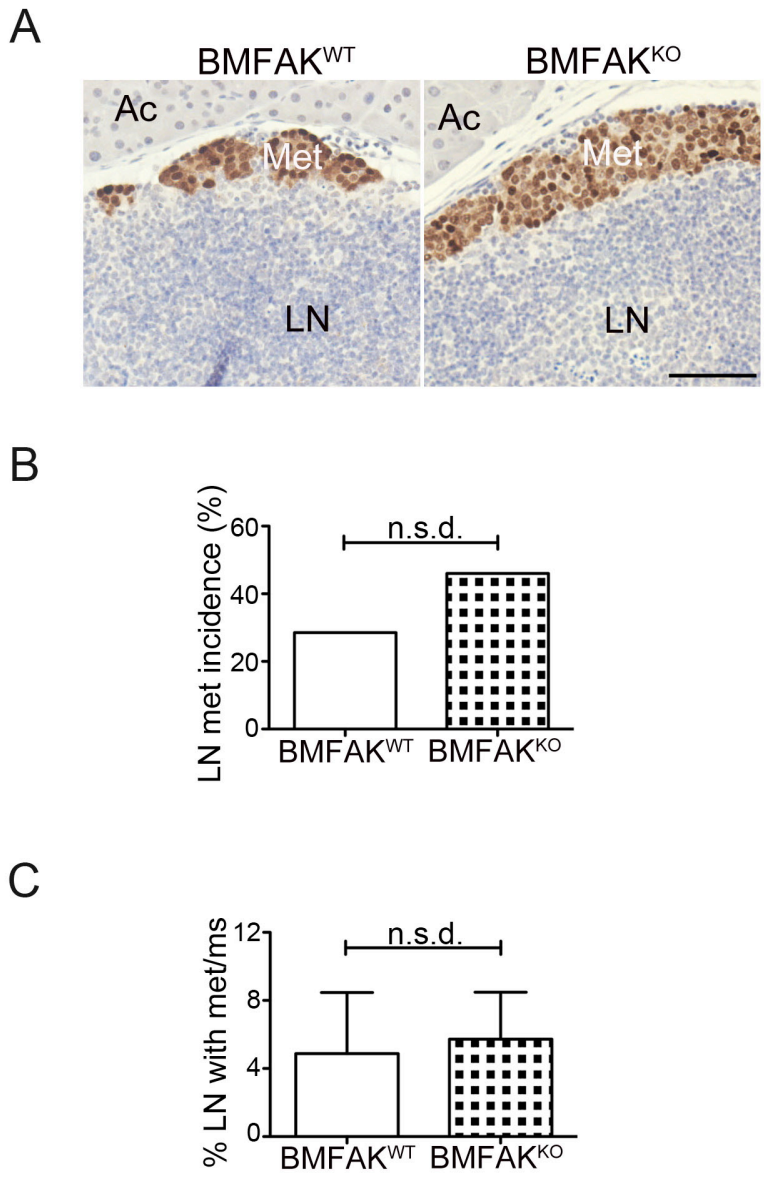

Figure 28: Bone marrow FAK deficiency in mice does not affect lymph node metastasis in the RIP-Tag2 model of cancer

RIP-Tag2/+ mice were transplanted at 6 weeks of age, tamoxifen treated at 8-9 weeks generating $BMFAK^{WT}$ and $BMFAK^{KO}$ chimeras and necropsied at 16 weeks of age. Histological analysis was performed in 6 different levels of pancreas with peri-pancreatic lymph nodes after immunohistochemical staining for the tumour marker SV40 T antigen. (**A**) Histological analysis of lymph node (LN) metastasis show tumour cells infiltrating (Met) into the LN adjacent to pancreatic acinar tissue (Ac). (**B**) Bar charts show no difference in the incidence of LN metastasis or in % of LN with metastasis (**C**) +s.e.m. between $BMFAK^{WT}$ and $BMFAK^{KO}$ mice. Scale bar, 200μm. n.s.d (no significant difference).

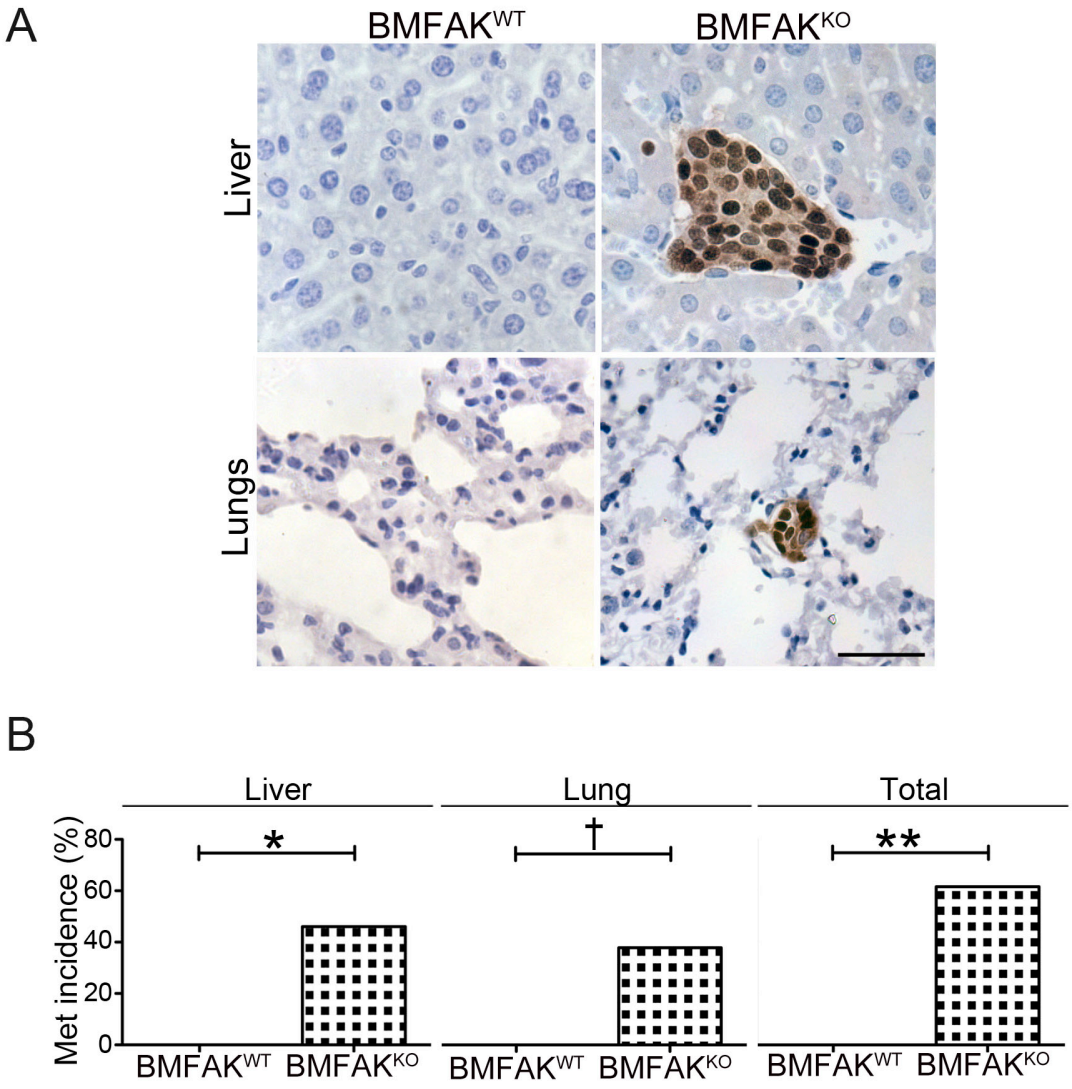

Figure 29: Bone marrow FAK deficiency in mice is sufficient to increase liver and lung metastasis in the RIP-Tag2 model of cancer

RIP-Tag2/+ mice were transplanted at 6 weeks of age, tamoxifen treated at 8-9 weeks generating BMFAK^{WT} and BMFAK^{KO} chimeras and necropsied at 16 weeks of age. Histological analysis was performed in 6 different levels of liver and lungs after immunohistochemical staining for the tumour marker SV40 T antigen. BMFAK^{KO} mice have increased incidence of metastasis. (**A**) Representative images of liver and lung metastasis are shown. (**B**) Bar charts represent percentage of animals with liver, lung and total percentage of animals with metastasis. Scale bar, 50μm. †P<0.06, *P<0.05, **P<0.01.

3.4. Increased $Gr1^+$ cell numbers increase tumour cell colonisation in $StrFAK^{KO}$ and $BMFAK^{KO}$ mice

Survival in the circulation, seeding at distant sites, invasion and dissemination of tumour cells are all dependent on the stromal environment. Many of the cells recruited from the bone marrow compartment are known to contribute to tumour metastasis. Some studies have suggested that tumour cells can direct formation of bone marrow derived cell pre-metastatic niches that render selected target organ microenvironments permissive for the implantation and subsequent outgrowth of disseminating tumour cells (Hiratsuka *et al*., 2006; Kaplan *et al*., 2005).

3.4.1. StrFAK^{KO} mice show increased peripheral blood and spleen numbers of myeloid cells

To dissect whether stromal FAK deficiency induced an immune phenotype that could contribute for the increased metastasis burden I have first analysed the mobilisation of myeloid immune cells into circulation. I have analysed myeloid peripheral blood numbers in StrFAK^{KO} and StrFAK^{WT} unchallenged (non-metastasis burden animals), 2-5h after tumour cell injection (to analyse tumour cell seeding), 24-48h after tumour cell injection (to analyse tumour cell colonisation) and at the endpoint of experiment. I observed significantly higher numbers of myeloid CD11b^{+}Gr1^{+} cells especially of granulocytic-neutrophil like (PMN) origin (CD11b^{+}Gr1^{hi}Ly6C^{lo}) in blood of unchallenged StrFAK^{KO} mice when compared with controls. The numbers of PMN cells were elevated at 2-5h and 24h post-tumour cell injection in the StrFAK^{KO} mice with less increase in the controls. Furthermore, an increase in this peripheral blood PMN population was observed at the experimental endpoint of the experiment in StrFAK^{KO} mice when metastases were established (**Fig. 30A**). The spleen is a main reservoir of these myeloid cells and I have observed a similar profile of increased PMN cells in the spleens of StrFAK^{KO} mice when compared with controls (**Fig. 30B**). I have also observed a similar enhancement in the monocytic fraction (Mon) of CD11b^{+}Gr1^{+} cells (CD11b^{+}Gr1^{lo+int}Ly6C^{hi}) in peripheral blood and spleen of StrFAK^{KO} mice when compared with controls (**Fig. 31A, B**).

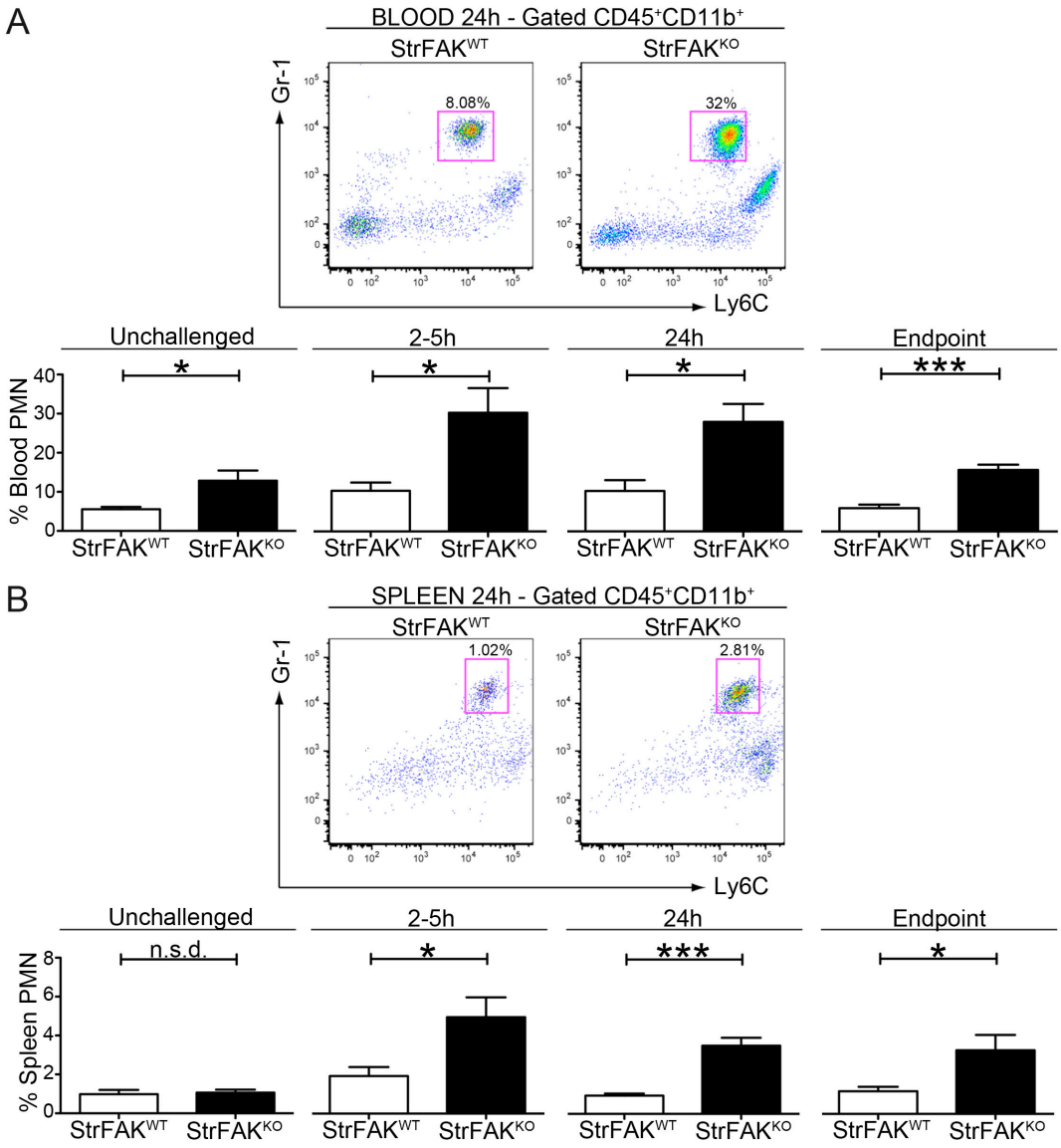

Figure 30: Stromal FAK deficiency enhances the numbers of peripheral blood and spleen CD11b^{+}Gr1^{+} granulocytes

Levels of CD11b^{+}Gr1^{hi}Ly6C^{lo} (PMN) cells were analysed by flow cytometry the in the blood (**A**) and spleen (**B**) blood and spleen of either unchallenged StrFAK^{WT} and StrFAK^{KO} mice, or 2-5h, 24h and 15 days post-tumour cell injection into the tail vein. Representative dot blots 24h post-tumour injection are shown. Bar charts represent live percentages CD11b^{+}Gr1^{hi}Ly6C^{lo} cells from CD45^{+} cells in all time points in blood and spleen + s.e.m., n, 3-4 mice/genotype. n.s.d. (no significant difference) **P*<0.05, ****P*<0.001.

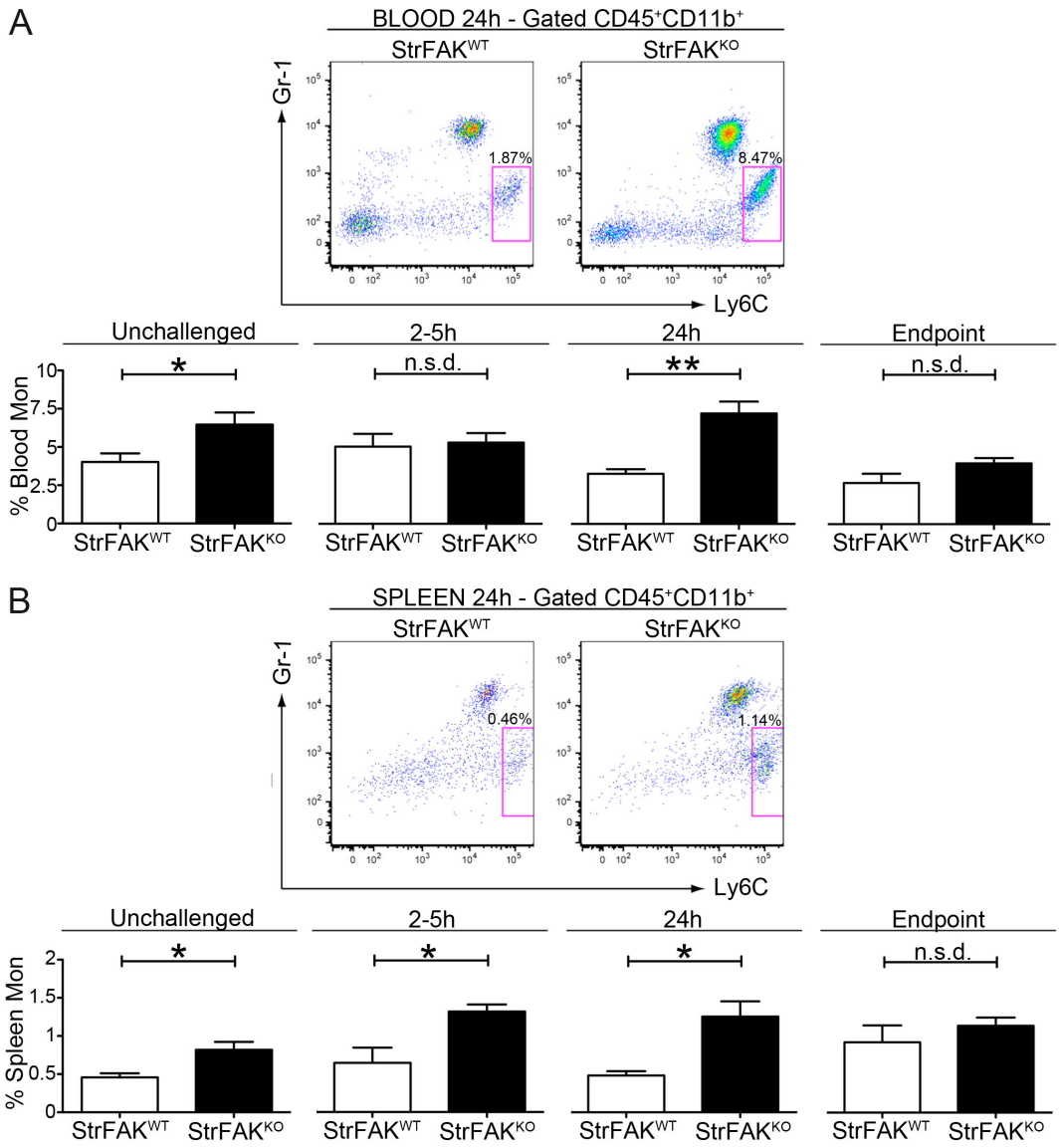

Figure 31: Stromal FAK deficiency enhances the numbers of peripheral blood and spleen CD11b^{+}Gr1^{+} monocytes

Levels of CD11b^{+}Gr1^{lo+int}Ly6C^{hi} (Mon) cells were analysed by flow cytometry the in the blood (**A**) and spleen (**B**) blood and spleen of either unchallenged StrFAK^{WT} and StrFAK^{KO} mice, or 2-5h, 24h and 15 days post-tumour cell injection into the tail vein. Representative dot blots 24h post-tumour injection are shown. Bar charts represent live percentages CD11b^{+}Gr1^{lo+int}Ly6C^{hi} cells from CD45^{+} cells in all time points in blood and spleen + s.e.m., n, 3-4 mice/genotype. n.s.d. (no significant difference), **P*<0.05, ***P*<0.01.

3.4.2. Stromal FAK deficiency induces an increase in bone marrow haematopoietic stem cells

Circulating myeloid cells, especially granulocytes are a good indicator of haematopoietic stem cell (HSC) numbers or function (Bhattacharya *et al*., 2006; Wright *et al*., 2001). Disrupting interactions between HSCs and bone marrow stroma leads to HSC activation and mobilisation from bone marrow (Cheshier *et al*., 1999; Mercier *et al*., 2012; Wilson *et al*., 2008). To analyse bone marrow progenitors I have used the strategy shown in **Fig.32**. Haematopoietic progenitors were identified within the lineage mix negative population, i.e., that do not express any markers for B-cells (CD45R or B220), granulocytes (Ly6G), myelomonocytic cells (CD11b), T lymphocytes (CD3) and erythroid cells (Ter119). HSCs are negative for the lineage markers, but express the growth factor receptor c-Kit and the cell surface antigen Sca ($Lin^-cKit^+Sca^+$) (Ashman *et al*., 1991; Mercier *et al*., 2012; Spangrude *et al*., 1988). Within the Sca^- population, expression of cell surface markers CD16/32 (also know as FCγIII/ FCγIII) and Flt3 and low or intermediate levels of cKit defined common dendritic progenitor and macrophage/dendritic progenitors (CDP/MDP) ($Lin^-cKit^{lo+int}Sca^-$ $CD16/32^+$ $Flt3^+$) (D'Amico and Wu, 2003). Unfortunately staining for cell surface marker CD34, which is important for characterisation of common myeloid progenitors (CMP) and granulocyte/monocyte progenitors (GMP) (Akashi *et al*., 2000), was too weak and analysis of this marker was not possible. Instead we have identified common myeloid progenitors (CMP) by $Lin^-cKit^+Sca^-$ $CD16/32^-$ and granulocyte/monocyte progenitors by expression of $Lin^-cKit^-Sca^-$ $CD16/32^+$ within the population with lower expression of Flt3 (D'Amico and Wu, 2003).

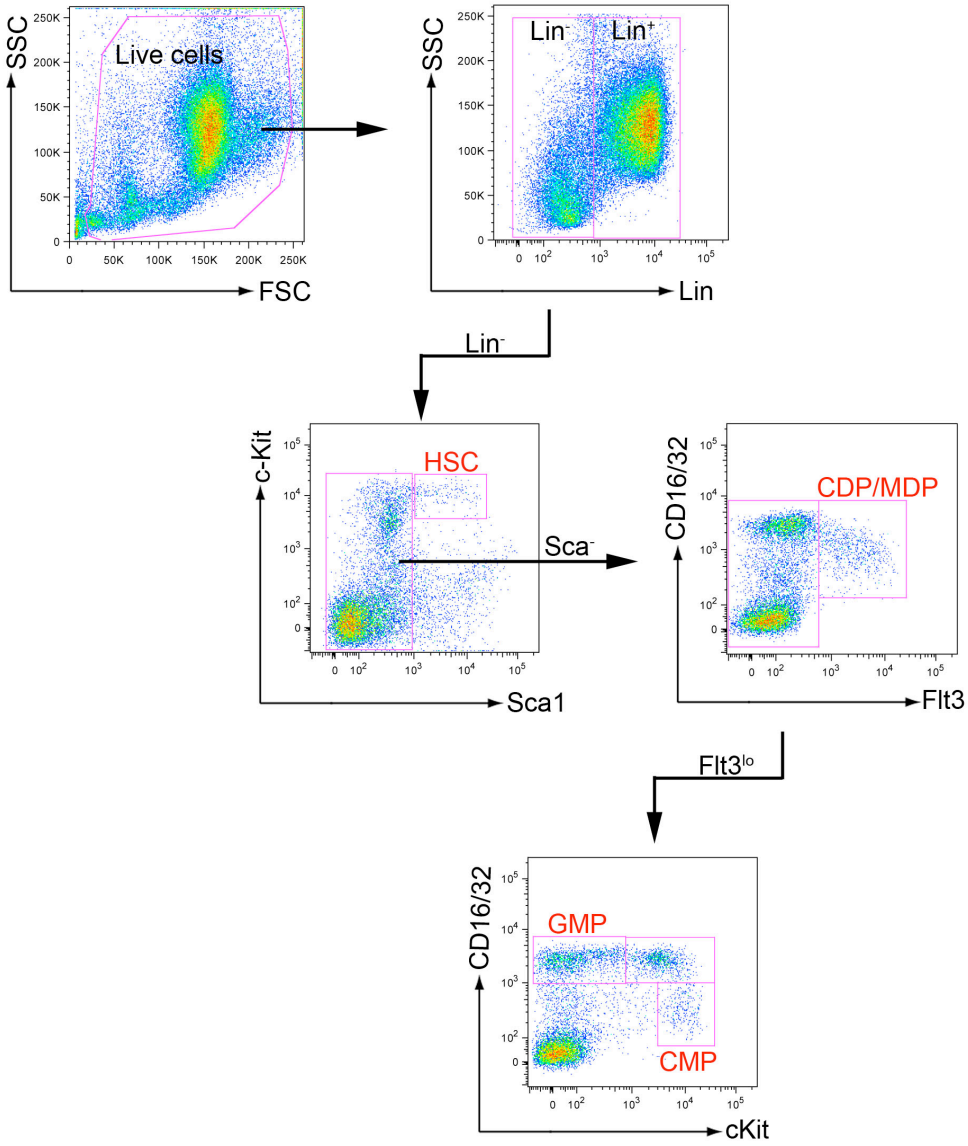

Figure 32: Schematic of bone marrow progenitor analysis strategy by flow cytometry

Bone marrow progenitors were analysed by flow cytometry. Representative dot blots are shown. A lineage mix of antibodies was used to distinguish progenitors (Lin^-) from committed cells (Lin^+) within bone marrow live cells. Haematopoietic stem cells (HSC) are characterised by $Lin^-cKit^+Sca^+$. Within the Sca^- population common dendritic progenitor and macrophage/dendritic progenitor (CDP/MDP) were identified by expression low or intermediate levels of cKit and expression of cell surface markers CD16/32 and Flt3 ($Lin^-cKit^{lo+int}Sca^-$ $CD16/32^+$ $Flt3^+$). Within the $Lin^-Sca^-Flt3^{lo}$ population common myeloid progenitors (CMP) were characterised by $Lin^-cKit^+Sca^-$ $CD16/32^-$ whereas granulocyte/monocyte progenitors were identified by expression of $Lin^-cKit^-Sca^-$ $CD16/32^+$.

In order to test whether the increased peripheral blood $CD11b^{+}Gr1^{+}$ cell numbers could be a consequence of HSC changes I have analysed HSC numbers in bone marrow of unchallenged $StrFAK^{WT}$ and $StrFAK^{KO}$ mice. I have observed increased numbers of bone HSCs in $StrFAK^{KO}$ mice when compared with controls (**Fig.33 A**). These results suggest that stromal FAK deficiency might have an effect in haematopoiesis or HSC activation. Analysis of the frequency of bone marrow committed myeloid progenitors, such CMP, GMP and CDP/MDP and also $CD11b^{+}Gr1^{+}$ cells in the bone marrow of unchallenged $StrFAK^{WT}$ vs $StrFAK^{KO}$ mice showed no significant differences between genotypes (**Fig. 33B-E**). This suggests there might be an increased mobilisation of these myeloid populations from the bone marrow compartment. Interestingly unchallenged $BMFAK^{KO}$ animals also showed increased circulating and spleen expansion of myeloid granulocytic $CD11b^{+}Gr1^{+}$ cells when compared with controls suggesting bone marrow FAK might be important for haematopoietic homeostasis (**Fig.34**).

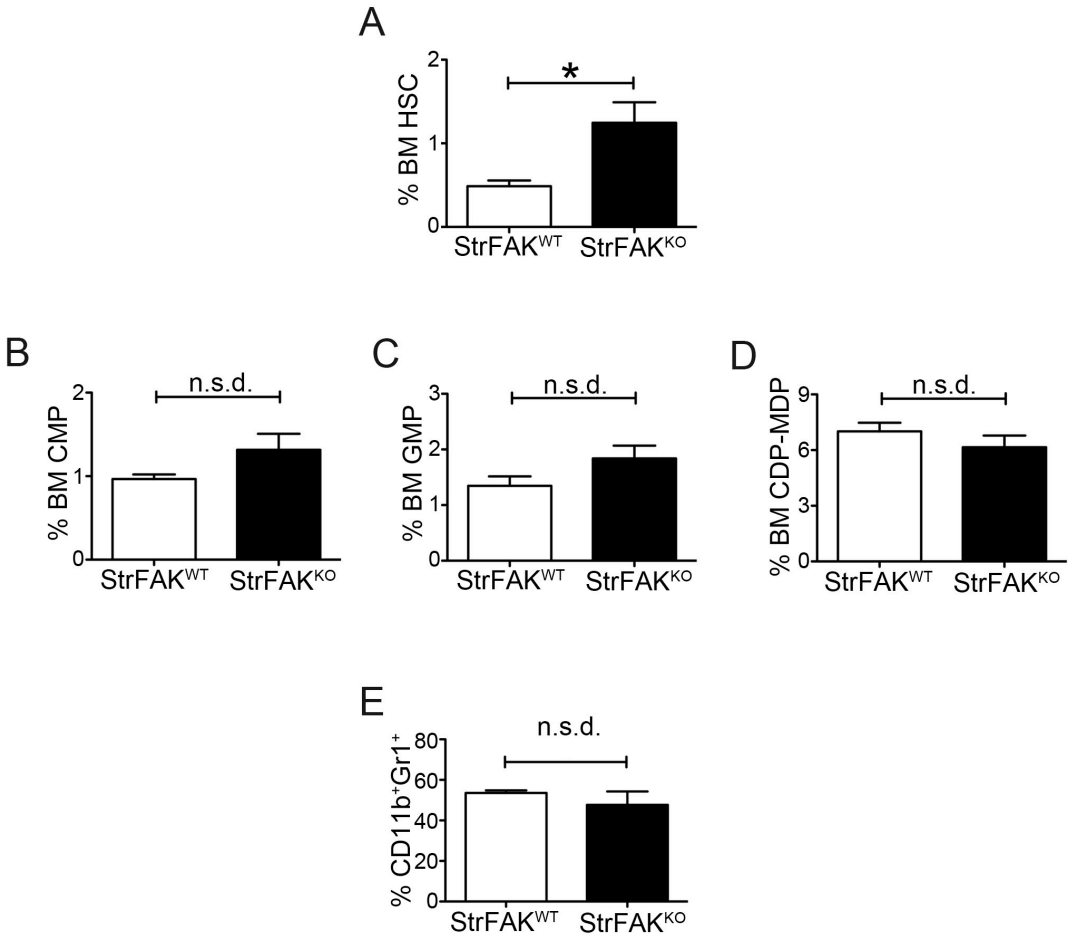

Figure 33: Stromal FAK deficiency induces an increase in bone marrow haematopoietic stem cells.

Unchallenged StrFAK^{WT} and StrFAK^{KO} mice single cells suspensions of bone marrow were analysed by flow cytometry. (**A**) StrFAK^{KO} mice showed increased numbers of bone marrow haematopoietic stem cells when compared with StrFAK^{KO} mice. Bar chart shows live cell percentages + s.e.m. No differences in the numbers of bone marrow progenitors such as common myeloid progenitor (CMP), (**B**) granulocytic-monocytic progenitor (GMP), (**C**) common dendritic and macrophage-dendritic cell progenitors (CDP-MDP) (**D**) were observed between bone marrow isolated from unchallenged StrFAK^{WT} and StrFAK^{KO} mice. Bar charts show live cell percentages + s.e.m. (**E**) CD11b^{+}Gr1^{+} bone marrow numbers were also similar between StrFAK^{WT} and StrFAK^{KO} mice. Bar chart represents live percentages CD11b^{+}Gr1^{+} cells from CD45^{+} cells in bone marrow + s.e.m. n,5 mice/genotype. n.s.d. (no significant difference), *P<0.05.

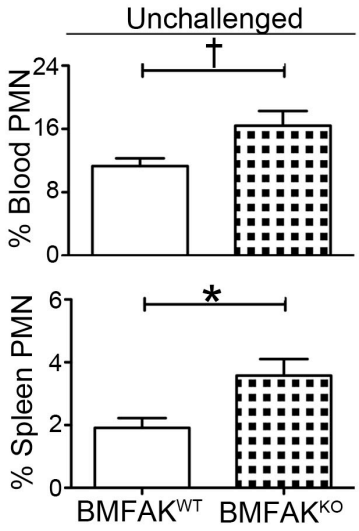

Figure 34: Bone marrow FAK deficiency is sufficient to increase numbers of peripheral blood and spleen $CD11b^{+}Gr1^{+}$ granulocytes (PMN)

Unchallenged $BMFAK^{WT}$ and $BMFAK^{KO}$ mice single cells suspensions of blood and spleen were analysed by flow cytometry. $BMFAK^{KO}$ mice show increased numbers of $CD45^{+}CD11b^{+}Gr1^{+}Ly6C^{lo}$ (PMN) in blood and spleen. Bar charts show live percentages from $CD45^{+}$ cells in blood and spleen +s.e.m., n, 3-4 mice/genotype. †P<0.051 *P<0.05.

3.4.3. Numbers of Gr1^{+}-tumour cell interactions in StrFAK^{KO} and BMFAK^{KO} mice reflect the increase in Gr1^{+} cell numbers in the lung

Given the increased mobilisation and expansion of the CD11b^{+}Gr1^{+} cells in the spleen at early time points after tumour cell injection I next analysed whether an increase of these cells was observed at metastatic sites such as the lung. I stained lung sections for Gr1^{+} cells 2-5h after tumour cell injection and have observed a similar increase in the number of Gr1^{+} cells infiltrating lungs in StrFAK^{KO} and BMFAK^{KO} mice when compared with controls (**Fig. 35A, B**). Given that these cells are known to suppress immune response I went on to analyse lung lymphoid infiltration (Connolly *et al*., 2010; Sceneay *et al*., 2012). I observed a decrease in infiltration of CD4^{+} and CD8^{+} T cells (**Fig. 36A, B**) in the lungs at early time points after tumour cell injection but no differences in NK cell infiltrate in StrFAK^{KO} mice when compared with controls at the same time points (**Fig. 36C, D**). Taken together, the enhanced Gr1^{+} cell numbers and decreased T-cell numbers correlate with the enhanced metastasis in StrFAK^{KO} and BMFAK^{KO} mice. Granulocytic cells have been shown interact with tumour cells and facilitate their entrapment and survival in the lung (Huh *et al*., 2010; Spicer *et al*., 2012). Given that the frequency of granulocytic cells in StrFAK^{KO} and BMFAK^{KO} mice was elevated I sought to examine if these cells were interacting with the tumour cells. I labelled the tumour cells with a red cell tracker and analysed whether at the same early time points these Gr1^{+} cells was in close association with tumour cells. An increased percentage of B16F0 cells were found to interact with Gr1^{+} cells in the lungs of StrFAK^{KO} and BMFAK^{KO} when compared with control mice **(Fig. 37A, B)**.

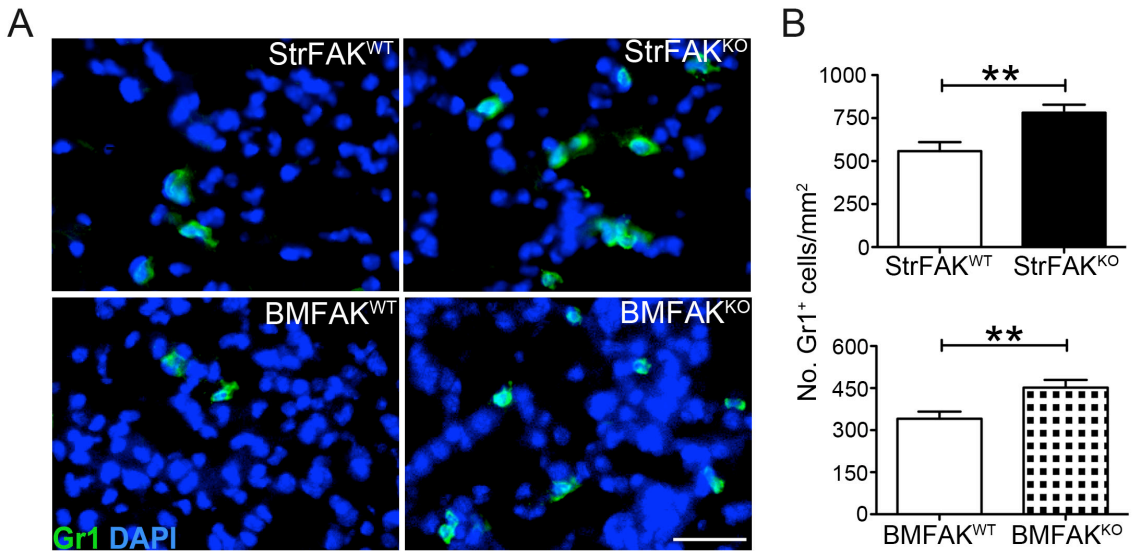

Figure 35: StrFAK^{KO} and BMFAK^{KO} mice show increased Gr1^{+} cell infiltration in lung at early time points after tumour cell injection.

B16F0 cells were injected via the tail vein into StrFAK^{WT}, StrFAK^{KO}, BMFAK^{WT} and BMFAK^{KO} mice. Gr1^{+} cell numbers were increased in the lungs of StrFAK^{KO} and BMFAK^{KO} mice 2h-5h after tumour cell injection when compared with similarly treated control mice. **(A)** Representative images of Gr1^{+} cells (green) in all genotypes 2-5 hrs after tumour cell injection. (**B**) Bar chart represents number of Gr1^{+} cell per mm^{2} of lung DAPI area +s.e.m. n, 4-5 mice per genotype Scale bar, 50μm. ***P*<0.01.

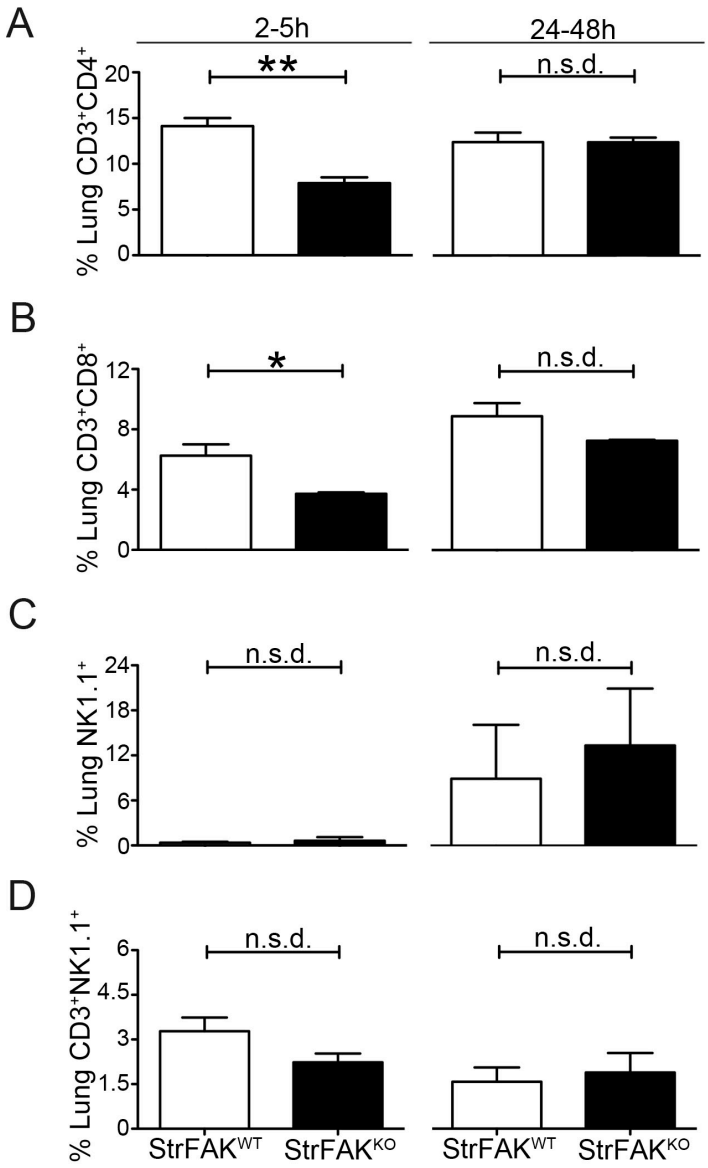

Figure 36: Stromal FAK deficiency decreases numbers of CD4 and CD8 T cells infiltrating lung at early time points after tumour cell injection

$StrFAK^{WT}$ and $StrFAK^{KO}$ mice single cells suspensions of lung were analysed by flow cytometry. $StrFAK^{KO}$ mice show decreased numbers of CD4 T cells ($CD3^+CD4^+$) (**A**) and CD8 T cells ($CD3^+CD8^+$) (**B**) cells infiltrating the lung at 2-5h post tumour injection. No significant differences were observed at 24h post tumour injection. Live percentages from $CD45^+$ cells in all time points in are shown, n, 3-4 mice/genotype. No differences in the numbers NK ($NK1.1^+$) (**C**) and NK T-cells ($CD3^+NK1.1^+$) (**D**) infiltrating the lung were observed $StrFAK^{WT}$ and $StrFAK^{KO}$ mice by flow cytometry. Bar charts show live cell percentages from $CD45^+$ cells + s.e.m., n,3-4 mice/genotype. n.s.d. (no significant difference), $*P<0.05$, $**P<0.01$.

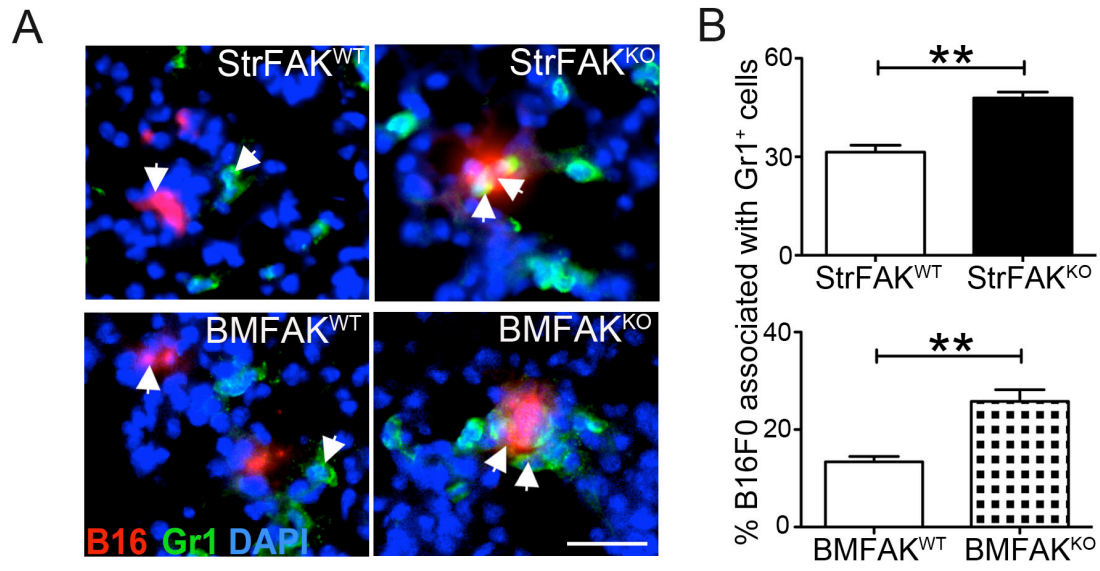

Figure 37: StrFAK^{KO} and BMFAK^{KO} mice show increased numbers of tumour cells associated with Gr1^{+} cells in the lung at early time points after tumour cell injection.

B16F0 cells, previously labelled with red cell tracker CMTPX, were injected via the tail vein into StrFAK^{WT}, StrFAK^{KO}, BMFAK^{WT} and BMFAK^{KO} mice. **(A)** The percentage of B16F0 cells associated with Gr1^{+} cell was increased in StrFAK^{KO} and BMFAK^{KO} mice 2-5h after tumour cell injection. Representative images of B16F0 (red) and Gr1+ cells (green) in StrFAK^{WT} , StrFAK^{KO}, BMFAK^{WT} and BMFAK^{KO} mice 2-5h after tumour cell injection. **(B)** Bar chart represents percentage of B16F0 cells associated with Gr1^{+} complexes +s.e.m. in all genotypes. n, 4-5 mice per genotype. Scale bar, 50μm. ***P*<0.01.

3.4.4. StrFAK^{KO} and BMFAK^{KO} mice show increased tumour cell colonisation

Given that the changes in the immune phenotype were observed at early time points after tumour cell injection and that Gr1^{+} cells were in close association with tumour cells at the same time points I asked whether FAK deficiency in the stromal, and specifically, bone marrow compartment affects the initial steps of tumour metastasis, i.e., seeding and colonisation. Red cell tracker labelled tumour cells were injected into the tail vein of StrFAK^{WT} and StrFAK^{KO}, BMFAK^{WT} and BMFAK^{KO} mice and lungs harvested 2-5h and 48h thereafter. Although there were no differences in the numbers of tumour cells seeding in the lungs 2-5h post injection a significant increase in tumour cell colonisation was observed in StrFAK^{KO} and BMFAK^{KO} mice when compared with controls (**Fig. 38A-C**).

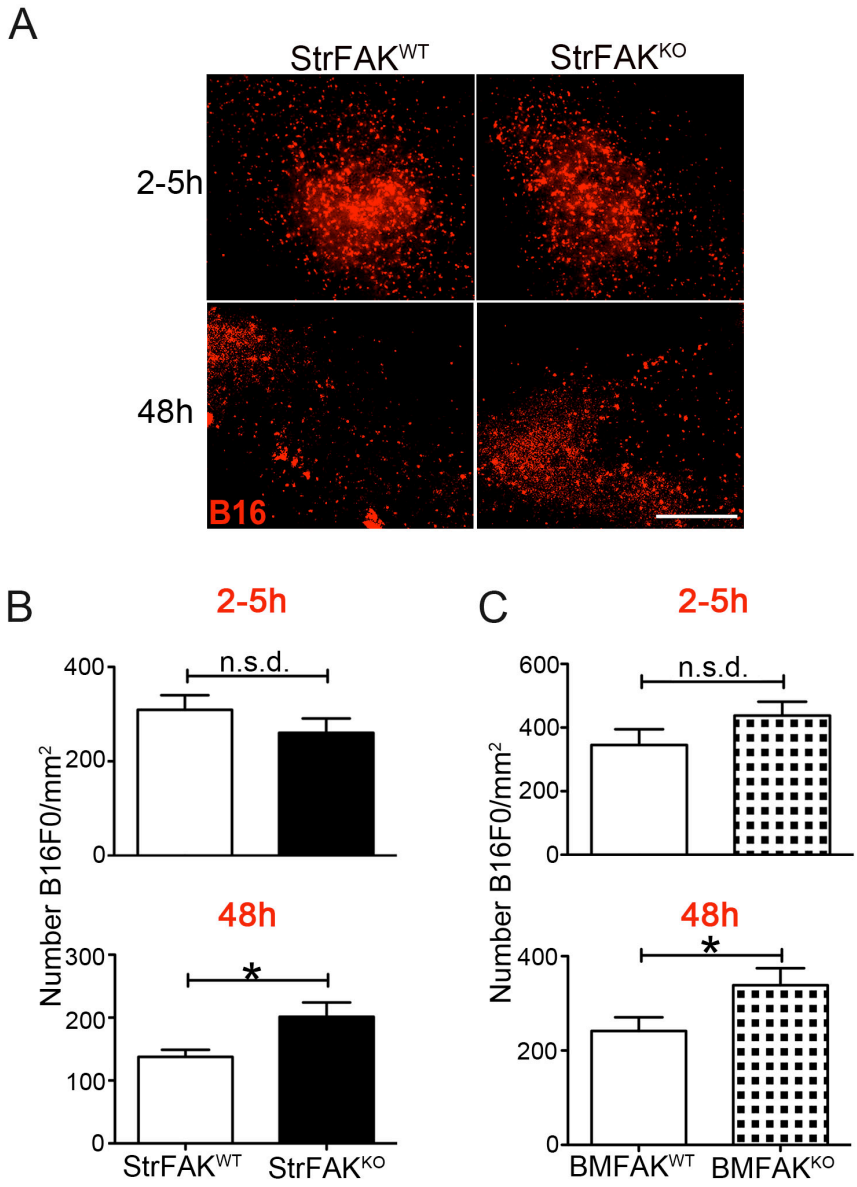

Figure 38: StrFAK^{KO} and BMFAK^{KO} mice show increased tumour cell colonisation in lungs.

B16F0 cells, previously labelled with red cell tracker CMTPX, were injected via the tail vein into StrFAK^{WT}, StrFAK^{KO}, BMFAK^{WT} and BMFAK^{KO} mice. **(A)** Lungs were harvested 2-5h and 48h after tumour cell injection to measure the numbers of tumour cells homing and colonising respectively. Representative immunofluorescence stereomicroscope images of lung surfaces from StrFAK^{WT}, StrFAK^{KO} mice are given. **(B)** Tumour cell numbers in lung sections from StrFAK^{WT} and StrFAK^{KO} mice 2-5h and 48h after tumour cell injection were counted across entire sections and normalised to lung DAPI area. **(C)** Tumour cell numbers in lung sections from BMFAK^{WT} and BMFAK^{KO} mice 2-5h and 48h after tumour cell injection were counted across entire sections and normalised to lung DAPI area. Bar charts represent mean number of B16F0 cells/mm^2 lung DAPI area +s.e.m. n, 5 mice per genotype. Scale bar**,** 500mm. n.s.d. (no significant difference), *P<0.05.

3.4.5. Gr1^{+} cell depletion is sufficient to rescue the increased tumour cell colonisation in StrFAK^{KO} mice

In order to test the requirement of Gr1^{+} cells in the enhanced tumour cell colonisation in StrFAK^{KO} mice I depleted these cells before tumour cell injection. Briefly, StrFAK^{WT} and StrFAK^{KO} mice were given two doses of a Gr1-blocking antibody, to deplete Gr1^{+} cells one day before and on the day of B16F0 injection via the tail vein. An isotype-matched control antibody was used as a negative control. The seeding and colonisation of the lung by tumour cells was tested and the efficient depletion of Gr1^{+} cells was confirmed in both time points (**Fig. 39A**). As expected tumour cell lung colonisation was decreased in StrFAK^{WT} after Gr1^{+} cell depletion (Huh *et al*., 2010; Spicer *et al*., 2012). Importantly, although the control antibody treatment had not effect in the increased colonisation observed previously in StrFAK^{KO} mice, the number of B16F0 cells that colonised in the lungs after Gr1^{+} cell-depletion was decreased in StrFAK^{KO} mice to levels similar to that found in StrFAK^{WT} mice **(Fig. 39B)**. These results indicate that the enhanced colonisation of tumour cells in the StrFAK^{KO} mice was dependent of Gr1^{+} cell infiltration in the lung.

Overall the results of this chapter demonstrated that loss stromal and specifically bone marrow derived FAK is sufficient to enhance metastasis. Furthermore this response was dependent on Gr1^{+} cells.

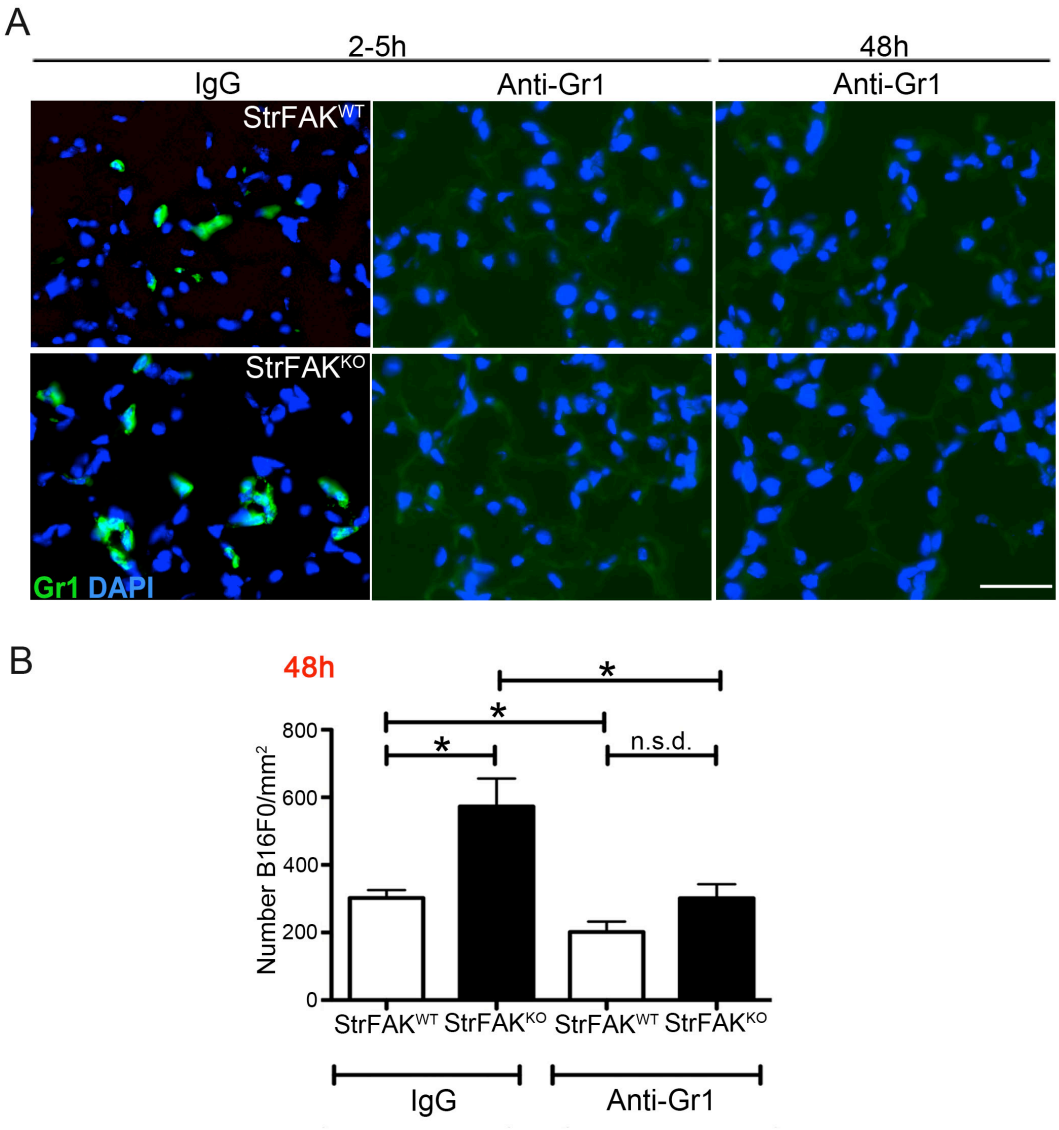

Figure 39: Depletion of Gr1^{+} cells in StrFAK^{KO} mice is sufficient to inhibit tumour cell colonisation in lungs.

Gr1+ cells were antibody depleted from StrFAK^{WT} and StrFAK^{KO} mice. Non-specific IgG was used as a control. 1 day later mice were tail vein injected with red cell tracker CMTPX labelled B16F0 cells. (**A**) Loss of Gr1^{+} cells can be observed in lung sections from mice treated with Gr1-depleting antibody. Lung sections were stained for Gr1 to detect numbers of Gr1^{+} cells. Representative images of Gr1^{+} cells (green) 2-5 hrs and 48h after tumour cell injection are given. (**B**) Although the control antibody had no effect in the increased tumour cell colonisation in the StrFAK^{KO} mice, Gr1-depletion reduced significantly numbers of B16F0 cells colonising the lungs. 48hrs post tumour cell injection B16F0 numbers in lung sections were counted. Bar chart shows mean number of B16F0 cells in lung sections of either control antibody or Gr1-depletion antibody treated StrFAK^{WT} and StrFAK^{KO} mice normalised to lung DAPI area.n, 4-5 mice/test. Scale bar, 50μm. n.s.d. (no significant difference), *P<0.05.

4. DISCUSSION PART I - Stromal and bone marrow derived FAK in tumour growth, angiogenesis and metastasis

Results from this chapter imply a role for stromal FAK, but not bone marrow derived FAK, in primary tumour growth and angiogenesis. In contrast I was able to show, in two different mouse models of cancer metastasis, that stromal, and specifically bone marrow FAK deficiency is sufficient to increase tumour metastasis. Moreover I have demonstrated that increased numbers of $CD11b^{+}Gr1^{+}$ or myeloid derived suppressor cells (MDSC) were present in the circulation or at metastatic sites when FAK was absent in the stromal, and specifically the bone marrow, compartment. This increased MDSC release and recruitment to metastatic sites, at least in part, was responsible for increased lung tumour cell colonisation and likely explains the increased metastatic burden observed in $StrFAK^{KO}$ and $BMFAK^{KO}$ animals.

4.1. Stromal and bone marrow derived FAK in tumour growth and angiogenesis

FAK is important in processes such as proliferation, survival, motility and invasion, all features of cancer cells (Hauck *et al*., 2002; Owen *et al*., 1999; Roy *et al*., 2002). FAK has been shown to be overexpressed in many human cancers and to contribute to tumour growth and metastasis in mouse models (Cance *et al*., 2000; de Heer *et al*., 2008; McLean *et al*., 2004; Provenzano *et al*., 2008). Such data concentrate predominantly on FAK expression in the cancer cells themselves and detailed examination of the expression profile of FAK in the stromal compartment is lacking. These observations have spurred the development of FAK inhibitors for anti-cancer therapy. Studies testing these drugs in animal models provided encouraging results showing decrease in tumour growth and, in some, metastasis (Kurio *et al*., 2011; Stokes *et al*., 2011; Walsh *et al*., 2010). These drugs are still in early clinical trials and information on clinical efficacy is still lacking. Importantly many of these drugs are not specific for FAK alone and therefore prevent a real understanding of how FAK inhibition works specifically (Kurio *et al*., 2011; Stokes *et al*., 2011; Walsh *et al*., 2010). What also is not clear is the relative requirement for FAK in cancer versus stromal compartments in tumourigenesis and metastasis.

Since FAK is expressed ubiquitously in mammalian cells constitutive, global genetic ablation of FAK in mice results in embryonic lethality and thus investigation of total FAK absence in adult mice especially in the stromal compartment was not possible previously (Ilic *et al*., 1995). More recently inducible deletion of endothelial FAK

using Pdgfb-iCreER;FAK$^{fl/fl}$ mice has indicated that loss of endothelial FAK can inhibit tumour angiogenesis (Tavora *et al*., 2010). In contrast using another Cre model, the tamoxifen-inducible Cre under the control of the 5'endothelial enhancer of the stem cell leukaemia locus (End-SCL-Cre-ER(T)), to induce specific FAK deletion in endothelial cells Weiss *et al* showed no significant defects in angiogenesis. However, in the latter study compensation by Pyk2 was reported and tumour angiogenesis *per se* was not examined (Weis *et al*., 2008), thus this work was not able to dissect the requirement of FAK alone in angiogenic processes. FAK null fibroblasts isolated from FAK null embryos showed defects in invasion that were not rescued by Src overexpression. In addition, Src expression in FAK null fibroblasts was sufficient to rescue motility defects presented by these cells (Hsia *et al*., 2003). This study suggests that FAK activates distinct signalling pathways to promote motility and invasion. In short, studies testing the requirement of FAK in the stromal compartment give varied results depending on the model utilised.

Interestingly, our laboratory has shown that mice lacking β3-integrin in the stromal compartment have increased tumour growth and angiogenesis (Reynolds *et al*., 2002) but display lower levels of FAK than WT mice. In fact, FAK heterozygous mice also show enhanced xenograft tumour growth and angiogenesis (Kostourou and Lechertier *et al*, unpublished data). This suggests a more complex effect of FAK levels, and possible differential regulation in different cell types, that can affect tumour growth and angiogenesis. Taken together these data begin to describe the complex role of stromal FAK in tumour growth but they do not reveal the role of bone marrow derived or even general tumour stromal FAK in this process.

By crossing the FAK floxed mice with RERTn$^{ERT/ERT}$Cre mice (tamoxifen-inducible Cre-ERT2 under the control of the promoter of the large subunit of RNA polymerase II) I was able to induce FAK deletion in the majority of cells in adult mice. Stromal FAK deletion in adult mice suppressed tumour growth and associated angiogenesis in agreement with the described positive role of FAK within the tumour cell compartment in tumourigenesis (McLean *et al*., 2004; Provenzano *et al*., 2008). Since in my experiments the tumour cells were not FAK deficient I asked the question: which cells in particular were contributing to the phenotype that I observed?

Given that FAK deletion in endothelial cells is sufficient to decrease tumour growth and angiogenesis (Tavora *et al*., 2010) I speculate that lack of FAK in endothelial cells is likely to be contributing toward the phenotype observed when I induce stromal FAK deletion in mice. At this stage I do not have direct proof for this hypothesis but the following bone marrow transplant experiments help to support this notion.

Several reports have described the contribution of BM derived cells in tumour angiogenesis (Beckermann *et al*., 2008; De Palma *et al*., 2005; Du *et al*., 2008; Shojaei *et al*., 2007). Bone marrow derived cells have been shown to be recruited to sites of tumour growth and have a pro-angiogenic role through production of VEGF and various other factors (Beckermann *et al*., 2008; Bergers and Song, 2005; Shojaei *et al*., 2007). In order to investigate whether the lack of FAK in BM cells was also contributing to the decreased tumour growth and angiogenesis observed in our mouse model, I transplanted BM cells from the RERTn$^{ERT/ERT}$;FAK$^{fl/fl}$ mice and induced FAK deletion in BM cells in adult mice. Deficiency of FAK in BM cells showed no effect in subcutaneous tumour growth or angiogenesis. These results suggest that lack

of FAK in BM cells is not sufficient to control angiogenesis and perhaps as a consequence it does not have an effect upon tumour growth. Given that the endothelial compartment in these experiments was likely to be FAK positive comparison of these BMT data with the stromal FAK deficiency data start to describe a different role for bone marrow FAK in tumourigenesis.

Even though angiogenesis seemed unaffected when the BM was FAK deficient there is evidence showing the bone marrow contributes to blood vessel supporting cells such as pericytes and fibroblasts (De Palma *et al*., 2005; Mishra *et al*., 2008). Poor coverage of blood vessels by these supporting cells results in leaky, haemorrhagic tumour blood vessels that, in turn, affect tumour growth (Abramsson *et al*., 2003). For this reason I have analysed blood vessel functionality and coverage by these supporting cells but found no differences when the bone marrow was FAK deficient. My data suggest that mural cell attachment to blood vessels was not affected by loss of FAK.

One of the major contributions of bone marrow derived cells to tumour growth and progression is the immune infiltrate. De Palma and colleagues described a specific type of monocyte that expresses Tie-2 and has a pro-angiogenic function (De Palma *et al*., 2003). Tumour associated macrophages (TAMs) have been associated with decreased survival and poor prognosis in some cancers (Ryder *et al*., 2008; Zhu *et al*., 2008). These TAMs are known producers of VEGF, EGF, FGF, MMPs and other molecules that can affect tumour cell proliferation, angiogenesis and extracellular matrix degradation (Sica *et al*., 2008). Pro-angiogenic functions were also attributed to granulocytes, such as neutrophils, due to their ability to produce MMP-9 (Nozawa

et al., 2006) or through expression of a mitogenic molecule (Bv8) (Shojaei and Ferrara, 2008; Shojaei *et al*., 2007). Importantly FAK deletion was shown to decrease inflammatory responses involving macrophages (Owen *et al*., 2007) and neutrophils (Kasorn *et al*., 2009). In fact some pharmacological FAK inhibitors (that also inhibit other molecules like Pyk2 though) have been associated with a decrease in the immune infiltrate in tumours (Stokes *et al*., 2011; Walsh *et al*., 2010).

When I analysed the immunophenotype of unstimulated mice I found increased numbers of $CD11b^{+}Gr1^{+}$ cells (MDSC), mainly of granulocytic-neutrophil like origin, in the blood of $StrFAK^{KO}$ and $BMFAK^{KO}$ mice when compared with controls. These results suggest that deficiency of FAK in the bone marrow compartment can regulate the generation or release of these cells into the circulation and that this might affect tumour growth. However the lack of an effect in subcutaneous B16 tumour growth and angiogenesis suggested these increases in circulating myeloid cells do not affect tumour growth or angiogenesis at this site.

Importantly, manipulation of macrophages has no effect in subcutaneous B16 tumours when compared with B16 tumours in the lungs after tail vein injection (van Deventer *et al*., 2002). On the other hand Muramatsu *et al* have shown that transplanting VEGFR1-null bone marrow decreased B16 subcutaneous tumour growth and angiogenesis and decreased also macrophage infiltrate (Muramatsu *et al*., 2010). Of note, however, in the same study, the numbers of macrophages in B16 tumours are much smaller than in similarly tested Lewis Lung Cell Carcinoma (LLC) xenografts. In fact, these cells localise more abundantly in the periphery than within the B16 tumours and the staining is patchy and difficult to analyse. Staining of $BMFAK^{WT}$ and

BMFAK^{KO} for markers such as F4/80 or Gr1 was also very inconclusive and showed that these cells were almost absent within the tumours. For this reason quantification was not performed and it was not included in my PhD thesis results (data not shown). In fact, these results highlight a limitation of these types of subcutaneous tumour models when examining immune cell infiltration and thus we turned our attentions to a spontaneous model of cancer growth, namely the RIP-Tag2 model.

I transplanted lethally irradiated 6-week-old RIP-Tag2 mice with bone marrow from RERTn$^{ERT/ERT}$Cre;FAK$^{fl/fl}$ animals and respective controls and induced FAK deletion at 8-9 weeks, i.e., when the angiogenic switch has been reported to already occur in these mice (Hanahan, 1985). Animals were sacrificed at 16 weeks of age when they were reported to have advanced disease (Hanahan, 1985). Similar to the subcutaneous tumour experiments just described, the lack of difference in pancreatic tumour sizes in the RIP-Tag2 model points towards no effect of bone marrow FAK levels in primary tumour growth. Noteworthy however is that in my RIP-Tag2 experiments the total tumour area was between 2-5 mm^2 per animal and most individual tumours were less than 1 mm^2. The reduced tumour growth correlated with previous reports of reduced tumour burden in pre-irradiated mice including the RIPTag-2 model when compared with non-irradiated mice (De Palma *et al*., 2005; Milas *et al*., 1987) and may reflect damage due to irradiation. In fact subcutaneous B16F0 tumour growth in BMFAK^{WT} and BMFAK^{KO} was also delayed in my experiments. This phenomenon, the tumour bed effect (TBE), is a result of radiation-induced damage of the tumour bed stroma (Hewitt and Blake, 1968). Irradiated tissue has been shown to have reduced ability to vascularise tumours and blood flow is also reduced in tumours grown in pre-irradiated animals (Jirtle *et al*., 1978).

Our studies are in line with those showing that inhibition of VEGFR-1, which targets most bone marrow derived cells, does not affect primary tumour growth or angiogenesis suggesting that bone marrow derived cells are not the main stromal drivers of primary tumour growth and angiogenesis in the RIP-Tag2 mouse model (Casanovas *et al*., 2005). In another study, also using RIP-Tag2 mice, increasing peripheral blood neutrophils, by administration of G-CSF, did not affect tumour angiogenesis, however depletion of the peripheral blood neutrophils prior to the angiogenic switch did decrease angiogenesis. Importantly when this depletion was done after the angiogenic switch, tumour angiogenesis was no longer affected (Nozawa *et al*., 2006). This study suggests peripheral blood neutrophils are important for the initial but not the later stages of angiogenesis. In addition, these data went on to describe that the mere presence, rather than the numbers, of neutrophils is important for the initial angiogenic switch since angiogenesis is not proportional to the numbers of circulating $CD11b^{+}Gr1^{+}$ cells. When comparing my data with this study one main conclusion can be drawn: the increase in circulating granulocytes/neutrophils in the bone marrow in FAK deficient mice is unlikely to affect angiogenesis.

It is fair to say that since B16 subcutaneous tumours do not have a predominant immune phenotype it is difficult to state categorically that the lack of a phenotype in bone marrow FAK deficient mice reflects the general role for bone marrow FAK in tumour growth and angiogenesis. For this purpose use of a xenograft model, e.g. LLC, which has a reported immune phenotype, may be better. In addition since the primary tumours in RIP-Tag2 experiments were very small, and likely poorly vascularised, I cannot comment on the role of bone marrow derived FAK in primary tumour angiogenesis.

4.2. Stromal and bone marrow derived FAK in tumour metastasis

Since FAK is important in processes such as migration and invasion it has been suggested to be a positive regulator of metastasis (de Heer *et al*., 2008; Hauck *et al*., 2001; Mitra *et al*., 2006a). Indeed, in some types of cancer such as colorectal cancer, high levels of both FAK and Src are indicative of poor prognosis and tumour recurrence (de Heer *et al*., 2008). However more recent evidence has pointed towards a negative role for FAK in tumour progression (Gabriel *et al*., 2006; Zheng *et al*., 2009). Despite high levels of FAK levels in primary cervical cancer samples when compared with normal epithelium, weak FAK expression was correlated with lymph node metastasis and poor overall survival (Gabriel *et al*., 2006). In addition, animal studies have shown inhibition of FAK by overexpression of FRNK results in increased numbers of Ras-mediated metastases. In the same article *in vitro* data suggested that ERK-dependent FAK phosphorylation at serine-910 primes FAK for dephosphorylation at FAK-P-Y397 by molecules downstream of Ras signalling (Zheng *et al*., 2009).

In contrast, few studies have actually assessed the role of stromal FAK in tumour progression. A recent study has suggested a role for endothelial FAK in metastasis. The authors showed that inhibition of FAK in endothelial cells decreased E-selectin expression, cancer cell homing and metastasis (Hiratsuka *et al*., 2011). More recently Chen *et al* have suggested that endothelial FAK is important for VEGF-induced permeability (Chen *et al*., 2012). These two studies suggest endothelial FAK might have a role in metastasis by controlling vascular permeability.

Given these observations I sought to test the role of stromal FAK in experimental tumour metastasis by injecting B16F10 cells into the tail vein of StrFAK^{KO} mice and analysing metastasis. Since injection of B16F0 cells in the tail vein of animals resulted in fewer than five metastases per mouse (data not shown) I have used a more metastatic variant B16F10 in my experiments. In contrast to my previously described anti-tumourigenic and anti-angiogenic role of FAK deficient stroma in subcutaneous B16 tumour growth, stromal FAK deficiency had a pro-metastatic effect even when the tumour cells themselves expressed normal levels of FAK. It has been shown previously that when tumour cells are injected into the circulation the first organ that will be colonised is the lung. I observed significantly increased lung metastasis in StrFAK^{KO} mice but, in addition and more surprisingly, I also have seen a significant increase in the number of bone and liver metastases in these mice. StrFAK^{WT} liver and bone were almost bereft of metastases suggesting that when the stroma is FAK deficient metastasis spreads to organs where it would otherwise be less frequent.

Bone marrow derived cells have also been identified as important in the regulation of tumour invasiveness and implicated in organ-specific tumour metastasis (Du *et al*., 2008; Kaplan *et al*., 2005). The plasticity of many bone marrow derived cells, such as macrophages and neutrophils, may make them capable of acquiring both pro- and anti-metastatic phenotypes (Fridlender and Albelda, 2012; Piccard *et al*., 2012; Qian and Pollard, 2010). I went on to test whether leukocyte FAK levels could also control metastasis.

My data have showed that the lack of FAK in the bone marrow compartment alone increased significantly the number of B16F0 metastases when compared with controls. Similar to the experiments in StrFAK^{KO} mice, enhanced metastasis was observed in the lungs and also in bone and liver. It is noteworthy that the total numbers of metastases were much higher in the bone marrow transplanted mice than in the StrFAK^{KO} mice even when I have used the less metastatic B16F0 line. This most likely reflects tissue damage and changes in the tumour bed stroma induced by radiation. It has been reported that mice that had irradiation show increased number of metastasis when compared with non-irradiated animals (Hewitt and Blake, 1968; Milas *et al*., 1987).

The experimental metastasis models that I have described only allow analyses of metastatic steps from when tumour cells are already in the circulation onwards. However this is only part of the metastatic process. To test the effect of bone marrow FAK deficiency in a model where primary tumours metastasise to other organs allows us to analyse steps such as primary tumour invasion. For this purpose I have used the RIP-Tag2 mouse model of spontaneous metastatic pancreatic cancer. I have observed that bone marrow FAK deficiency did not affect invasiveness of tumours suggesting that bone marrow derived FAK is not apparently involved in this initial step of metastasis.

After tumour cells have invaded into the peri-tumoural stroma, their dissemination to distant organs can be via lymphatic and/or vascular vessels (Chambers *et al*., 2002; Tammela and Alitalo, 2010). I analysed the peri-pancreatic lymph nodes for the presence of metastasis in BMFAK^{KO};RIP-Tag2/+ animals and respective controls. I

observed that metastasis to lymph nodes was low in both genotypes suggesting dissemination though lymphatic vessels was low at the time when the mice were killed. This is perhaps related to the small primary tumour size observed.

In stark contrast I have observed an increased incidence of liver micrometastases when the bone marrow was FAK deficient. Interestingly these $BMFAK^{KO}$ mice have also shown lung micrometastases, an organ not reported before to have observed metastatic spread in this model. These data suggest that loss of BM-derived FAK is sufficient to enhance tumour metastasis and that the effect probably is related to blood dissemination of the tumour cells similar to my experimental metastasis data. Indeed this early dissemination of tumour cells, even when the primary tumours and local lymph node dissemination is low, corroborates with the new view of the metastatic process that claims metastasis dissemination can occur even before tumours are clinically detectable. Using two mouse models of invasive mammary carcinomas (BALB-NeuT and MMTV-PyMT) Husemann *et al*, have observed dissemination of tumour cells even before disruption of basement membrane in the primary hyperplastic lesions (Husemann *et al*., 2008). Another study has shown that epithelial to mesenchymal transition, tumour cell migration, bloodstream entry and seeding in the liver can occur in parallel or even before tumour formation at the primary site in a mouse model of PDAC (Rhim *et al*., 2012). My data suggest that stromal, and specifically bone marrow derived FAK, might act as a negative regulator of metastatic dissemination and raise the question of which cells are being regulated by FAK and acting as pro-metastatic in its absence.

4.3. Bone marrow FAK in haematopoiesis homeostasis

The role of myeloid cells in metastasis has been studied extensively. For example, it has been described that tumour cell extravasation and pulmonary seeding by tumour cells are dependent on the production of VEGF by $Gr1^{+}CCR2^{+}$ monocytes in a mouse model of spontaneous breast cancer (Qian *et al*., 2011). Another study has highlighted that cancer cell survival is extended via tumour cell VCAM-1 macrophage $\alpha4\beta1$ interactions. Authors claim this interaction triggers anti-apoptotic signals in cancer cells and thus facilitates their seeding and metastasis (Chen *et al*., 2011). These are just a few examples of how myeloid cells can regulate tumour metastasis. Here I have shown that non-tumour burden $StrFAK^{KO}$ mice have an increase in circulating and splenic $CD11b^{+}Gr1^{+}$ cells from granulocytic/neutrophil-like and monocytic origins as described before. This result suggests at least two things: (1) FAK deficiency enhances haematopoiesis and myeloid lineage commitment and/or; (2) loss of FAK increases the release of these cells into circulation. Haematopoietic homeostasis is dependent on haematopoietic stem cells (HSCs) that have the ability to self renew and maintain lineage differentiation potential (Becker *et al*., 1963; Till and McCulloch, 1961). Progenitor cells that retain lymphoid and myeloid differentiation potential but lack self renewal capacity can reconstitute lymphocytes but not granulocytes in immunodeficient mice (Bhattacharya *et al*., 2006). Peripheral blood granulocytes are considered a good indicator of HSC numbers or activation (Bhattacharya *et al*., 2006; Wright *et al*., 2001). I have observed an increase in bone marrow numbers of HSCs in $StrFAK^{KO}$ mice even in unstimulated animals which was consistent with peripheral and spleen numbers of granulocytes. However no significant differences in bone

marrow lineage progenitors, such as common myeloid progenitor (CMP), granulocytic-monocytic progenitor (GMP) and common dendritic cell and macrophage-dendritic cell progenitors (CDP-MDP) were observed. Interestingly numbers of $CD11b^{+}Gr1^{+}$ cells also did not change in the bone marrow compartment. This suggested haematopoiesis might be increased in $StrFAK^{KO}$ mice and that these cells were probably being constantly released into the circulation. It is noteworthy that the analysis of bone marrow committed progenitors, such as CMP and GMP, should be repeated since some of the markers such as CD34 were not included in the analysis for technical reasons. It will also be useful to add IL7-Rα to exclude lymphoid progenitors and provide a more accurate analysis. Nevertheless one of the questions that has arisen from these data is: How are FAK levels regulating HSC and $CD11b^{+}Gr1^{+}$ cell numbers?

A recent study by Lu *et al* has shown that FAK is preferentially expressed in HSCs when compared with more differentiated committed progenitors in the bone marrow. Importantly the authors also observed an increase in HSC numbers when FAK was deleted specifically in the bone marrow compartment by using a Cre inducible conditional knockout under the expression of an interferon- inducible promoter (Mx1-Cre). These mice showed more dividing and fewer quiescent HSCs (Lu *et al*., 2012). Other studies have shown that HSCs can reversibly change from dormancy to a self-renewal state. Dormancy is important to maintain HSC homeostasis and protect them from exhaustion (Takizawa *et al*., 2011; Wilson *et al*., 2008). These data raise the question of whether FAK could regulate the dormancy self-renewal state? It would be interesting, in future studies, to examine HSC cycling and HSC exhaustion after transplant, i.e., their self-renewal capacity. This can be done by transplanting bone

marrow into a first recipient and from that transplanted animal re-transplant into another recipient and so on. By analysing bone marrow reconstitution after serial bone marrow transplants I should be able to test whether FAK affects HSC self-renewal ability.

Lu *et al* have also observed that FAK depleted bone marrow cells showed increased long-term haematopoietic reconstitution when half of these cells were transplanted with competitor WT cells into lethally irradiated WT mice. However reverse transplant, using a similar assay of WT cells into lethally irradiated FAK deleted recipients did not show the same engraftment advantage or increase in HSC numbers suggesting that deficiency of FAK in the bone marrow stroma is not sufficient to affect the HSC homeostasis. In addition transplantation of FAK depleted HSCs into lethally irradiated WT recipients was not sufficient to affect the numbers of HSCs and *in vitro* proliferation of HSCs was not affected by FAK levels. These data suggest that FAK levels in both the HSCs and bone marrow stroma together are necessary to regulate the numbers of HSCs. The result of the increase in numbers of HSCs was increased peripheral blood granulocytes similar to what I observed in $StrFAK^{KO}$ and $BMFAK^{KO}$ mice (Lu *et al*., 2012).

The fact that stromal FAK deficiency increased the numbers of HSCs in my studies might suggest that by altering adhesion to the bone marrow stroma the proportion of activated HSC cells have increased, resulting in increased peripheral blood and spleen granulocytes. The release of HSCs from the bone marrow compartment has been suggested to require c-Myc repression of N-cadherin and integrin adhesion (Wilson *et al*., 2004). Interestingly FAK had already been shown to be involved in adhesive

responses from haematopoietic precursor cells downstream of CXCR4 and integrins (Glodek *et al*., 2007). Thus in future studies it would be of interest to analyse the molecular profile of HSC and $CD11b^{+}Gr1^{+}$ cell adhesion receptors and also study the mobilisation of HSCs, lineage committed progenitors and $CD11b^{+}Gr1^{+}$ cells by analysing their numbers in bone marrow and peripheral blood.

4.4. Identifying $Gr1^{+}$ cells as drivers of metastasis in stromal and bone marrow FAK deficient mice

$CD11b^{+}Gr1^{+}$ cells are also referred to as myeloid-derived suppressor cells (MDSCs) and increased numbers of blood MDSCs have been clinically correlated with metastasis burden (Diaz-Montero *et al*., 2009). The increased numbers of $CD11b^{+}Gr1^{+}$ cells in blood and spleen of $StrFAK^{KO}$ mice were further enhanced at early time points after tumour cell injection. After circulating through the blood bone marrow derived cells will also home to sites of metastasis as described earlier (Huh *et al*., 2010; Qian *et al*., 2011; Spicer *et al*., 2012). $Gr1^{+}$ cell numbers were also increased 2-5 hrs after tumour cell injection at sites of metastases, such as in the lung, when either the whole stroma or bone marrow were FAK deficient.

The differences in the immune infiltrate at metastatic sites after tumour cell injection suggested these cells could play a role in the phenotype observed. Some studies suggest that MDSC can decrease CD8 and CD4 T cell proliferation and cytotoxicity (Connolly *et al*., 2010). On the other hand they were implicated in decreased NK cell cytotoxicity without changing their numbers (Sceneay *et al*., 2012). In my study,

analysis of lung lymphoid numbers at early time points (2-5 hrs and 24 hrs) after tumour cell injection showed a decrease in CD8 and CD4 T cells with no alterations in NK or NKT cell numbers when the stroma was FAK deficient. Thus my work shows that loss of stromal FAK correlates with increased numbers of $CD11b^{+}Gr1^{+}$ cells and a partially immune suppressive phenotype.

On the other hand I cannot exclude that FAK deficiency in CD8 and CD4 T cells and NK cells *per se* could affect their recruitment or anti-tumour capability and further analysis is necessary. Related to this issue, previously published work has shown that FAK deficiency alone does not affect CD4 and CD8 thymocyte development (Kanazawa *et al*., 1996). A recent study implied FAK plays a role in CXCL12-driven human thymocyte migration (Garcia *et al*., 2012). But to date the role of FAK in the activity and anti-tumour functions of these cells has not been reported.

In addition to their immune suppressive functions $CD11b^{+}Gr1^{+}$ cells also have non-immunosuppressive functions. For example it has been suggested that granulocytic/neutrophil-like $Gr1^{+}$ cells could form complexes with tumour cells that facilitate cancer cell interaction with target metastatic tissue (Huh *et al*., 2010; Qian *et al*., 2011; Spicer *et al*., 2012). I tested whether $Gr1^{+}$ cells indeed were interacting with tumour cells at metastatic sites. I observed increased numbers of tumour cells in close association with $Gr1^{+}$ cells in $StrFAK^{KO}$ and $BMFAK^{KO}$ mice when compared with controls. The extent of the increase in interactions is similar to the increase in $Gr1^{+}$ cell numbers in the same tissue suggesting FAK deficiency might not intrinsically be regulating $Gr1^{+}$ interactions with tumour cells but rather might reflect a proportional increase in tumour cell-$Gr1^{+}$ cell complexes. Despite this, my data show that the actual number of tumour cell-$Gr1^{+}$ cell complexes is increased in the lungs of both

StrFAK^{KO} and BMFAK^{KO} mice when compared with controls and this may be contributing to the overall enhanced metastasis in these mice.

Given that tumour cell-Gr1^{+} cell interaction could lead to changes in tumour cell seeding, colonisation and metastasis (Huh *et al*., 2010; Qian *et al*., 2011; Spicer *et al*., 2012), I then went on to examine these events further. Tumour cell seeding in the lung did not seem to be regulated by increased numbers of Gr1^{+} cells associated with tumour cells. However, and in contrast, the colonisation of tumour cells was increased in StrFAK^{KO} and BMFAK^{KO} mice corroborating the studies from Huh *et al*, 2010 and Spicer *et al*, 2012.

My results so far point towards a positive role for FAK deficient Gr1^{+} cells in the enhanced metastasis. To test directly the requirement of Gr1^{+} cells in this process I have depleted them in StrFAK^{WT} and StrFAK^{KO} mice before tumour cell injection and observed the effect in tumour cell colonisation in the lungs. Gr1^{+} cell depletion reduced tumour cell colonisation in StrFAK^{WT} animals. Importantly Gr1^{+} cell depletion in StrFAK^{KO} mice also resulted in a decreased tumour cell colonisation. These data suggest that the increase in Gr1^{+} cells that are recruited to metastatic sites in StrFAK^{KO} mice is a major driver of the elevated tumour cell colonisation observed. I can also infer from this result that the intrinsic effect of FAK deficiency in CD4 and CD8 T cells and NK cells is not sufficient to affect lung tumour cell colonisation.

It is tempting to speculate that the enhanced tumour cell colonisation that is observed in StrFAK^{KO} and BMFAK^{KO} mice is key to the increased metastatic burden observed in these animals. In order to clarify this in future experiments it will be important to repeat the same Gr1^{+} cell depletion in order to decrease tumour cell colonisation and

analyse the effect in the number of metastases when the stroma and specifically bone marrow are FAK deficient.

In future studies I also intend to dissect the mechanism by which increased recruitment of $Gr1^+$ cells affects colonisation and metastatic burden. To distinguish between immune suppression and other pro-metastatic functions of $CD11b^+Gr1^+$ cells in the metastatic burden it will be interesting to cross $RERTn^{ERT/ERT}Cre;FAK^{fl/fl}$ mice with RAG1 or RAG2 KO animals. These animals lack mature B and T cells but show normal levels of myeloid cells (Mombaerts *et al*., 1992; Shinkai *et al*., 1992). This will allow analysis of the role of myeloid FAK in metastasis independently in T and B cells. One limitation of these experiments is that since RAG1 or RAG2 KO animals have NK cells I will not be able to analyse the role of myeloid FAK in metastasis independently of NK cells using this model. *In vitro* NK cytotoxicty assays and NK cell depletion might reveal the role of FAK in NK cell function and the role of NK cells in the metastatic burden observed in my experiments.

When comparing my data with published work, FAK deletion in myeloid cells was reported to attenuate myeloid immune response *in vivo* due to decreased infiltration into sites of inflammation (Kasorn *et al*., 2009; Owen *et al*., 2007) however I found increased infiltration at metastatic sites. In previous studies FAK was depleted specifically in the mature myeloid population and committed progenitors thereby not affecting the FAK levels in haematopoietic stem cells and bone marrow stroma. Importantly by depleting FAK in the whole bone marrow I have affected the interactions between haematopoietic cells and bone marrow stroma resulting, for example, in increased haematopoietic stem cell numbers in line with other studies (Lu

et al., 2012). Since blood granulocytes are the main indicator of the total HSC pool (Takizawa *et al*., 2011; Wilson *et al*., 2008) I hypothesise the increased $Gr1^+$ cell numbers that I observed is a consequence of an alteration in HSC numbers.

Another important point is that the role of FAK depletion in the recruitment of myeloid cells has only been tested in response to pathogens or inflammatory stimuli and never in the context of tumours (Kasorn *et al*., 2009; Owen *et al*., 2007; Vemula *et al*., 2010). Tumour cells themselves produce growth and migratory stimuli to increase the recruitment of immune cells to metastatic sites and elicit different cellular responses than the ones required during an infection (Hiratsuka *et al*., 2006). In fact myeloid cells recruited during tumour metastasis have general immune response defects (Connolly *et al*., 2010; Sceneay *et al*., 2012; Yan *et al*., 2010). For example skewing TAM polarisation from the M2, less inflammatory phenotype, to the M1, activated inflammatory phenotype, can increase macrophage anti-tumour effects and decrease tumour metastasis (Rolny *et al*., 2011). The increased recruitment of $Gr1^+$ cells to metastatic sites in my studies, rather than being contradictory to other reports, perhaps just represents a complementary description of the phenotype adopted by a FAK deficient myeloid cell. I hypothesise FAK deficient $CD11b^+Gr1^+$ cells might have defects in inflammatory response and tumour killing capabilities themselves, acquiring instead a pro-metastatic phenotype that facilitates tumour cell colonisation. In addition increased numbers of FAK deficient $CD11b^+Gr1^+$ cells in the blood and metastatic sites might also suppress immune responses generating a pro-metastatic microenvironment. In order to clarify this, in future experiments, I will perform molecular analyses of FAK deficient $CD11b^+Gr1^+$ cells sorted from lung after tumour cell injection. It will be interesting to test whether FAK deficiency results in cytokine

profile or cell adhesion changes in $CD11b^{+}Gr1^{+}$ cells that are recruited to the lung after tumour cell injection. This will reveal whether FAK deficient $CD11b^{+}Gr1^{+}$ cells, in the context of tumours, can themselves produce pro-metastatic cytokines and whether there is any compensation in adhesion pathways that might regulate their recruitment to metastatic sites and interaction with tumour cells. It will also be interesting to test whether bone marrow FAK deficiency, in my mouse model, also shows decreased infiltration to sites of inflammation *in vivo*.

Importantly FAK inhibitors that are in early clinical trials will affect FAK levels in the stromal compartment as well. Some of these inhibitors have been shown to decrease inflammatory recruitment to primary tumours (Stokes *et al*., 2011; Walsh *et al*., 2010). However these drugs are not specific for FAK, they inhibit also Pyk2 and some growth factor receptors and analysis of myeloid infiltrate was not performed in these studies. It will be extremely interesting to analyse the immune phenotype, specifically $Gr1^{+}$ cell infiltration, in primary tumour and metastasis of tumour burdened mice treated with FAK inhibitors *in vivo*. It will also be interesting to see whether the inhibitor studies result in any changes in metastatic burden.

In conclusion in this Chapter I have shown that by decreasing FAK levels in the stromal compartment I have generated a pro-metastatic microenvironment. Bone marrow FAK deficiency was sufficient to increase metastatic burden implying a bone marrow derived cell in the phenotype observed. I have demonstrated that colonisation might be the key metastatic step affected in the absence of stromal FAK. Stromal and bone marrow FAK deficiency resulted in increased $Gr1^+$ cell numbers that had a major influence on the enhanced metastatic phenotype observed (**Fig. 40**).

I hypothesise that FAK expression, by controlling HSC and myeloid cell numbers in the circulation, can control organ tumour cell colonisation at metastatic sites. I also hypothesise that FAK expression in myeloid cells might affect their pro or anti-metastatic functions (**Fig. 40**). By altering stromal FAK levels we might affect intrinsic molecular functions but also cellular numbers by changing their interaction with their microenvironment. Further studies are necessary to clarify the mechanism by which bone marrow derived FAK can control tumour metastasis

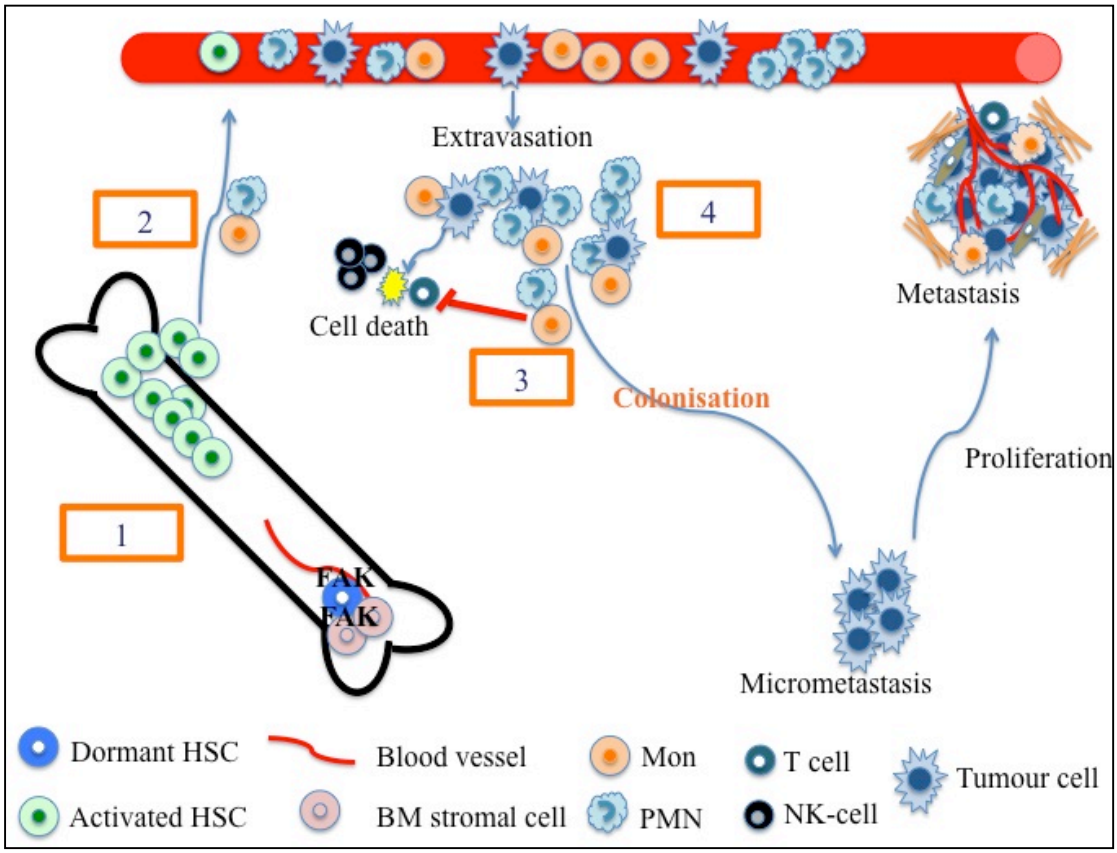

Figure 40: Model for a role for bone marrow FAK in tumour metastasis

Haematopoietic stem cells (HSCs) are usually in a dormant state through interactions with bone marrow stroma. (**1**) Bone marrow FAK deficiency might disrupt HSC-bone marrow stroma interactions resulting in activated and proliferative HSCs. (**2**) Increased HSC numbers give rise to increased granulocytic (PMN) and monocytic (Mon) $CD11b^{+}Gr1^{+}$ cell numbers in peripheral blood. (**3**) $CD11b^{+}Gr1^{+}$ cells induce an immune suppressive phenotype decreasing T cell numbers and possibly T and NK cell anti-tumor activity. (**4**) $CD11b^{+}Gr1^{+}$ cells also form complexes with tumour cells at metastatic sites facilitating their colonisation of organs. This ultimately results in increased formation of micrometastases that proliferate into detectable metastases.

5. RESULTS PART II – Point-mutant FAK knockin/knockout mice

5.1. Generation of FAK knockin mice

In the previous Chapter I tested the effect of FAK deficiency in metastasis. In future studies it will be necessary to develop point-mutant FAK knockin mice in order to dissect the molecular mechanisms that underlie FAK's role in tumour progression.

For this purpose our laboratory has generated point-mutant FAK knockin-knockout mice where mutant-FAK will be inducibly expressed (knockin) and endogenous-FAK deleted (knockout) in specific cell types. FAK has multiple phosphorylation sites and a kinase domain. We have been generating the following knockin mice:

1. WT – Control;
2. 397F – the major phosphorylation site required for FAK activity is the tyrosine 397 which was mutated to phenylalnine such that it cannot be phosphorylated;
3. 397E – tyrosine 397 was replaced with glutamic acid creating a phosphorylated mimic site (constitutive phosphorylation);
4. Kinase dead (KD) – lysine 454 in the ATP binding site was mutated to arginine disrupting the kinase activity necessary for Y397 autophosphorylation and phosphorylation of other proteins;
5. 397E/KD – double mutation where Y397 is constitutively phosphorylated but the catalytic activity of FAK is disrupted;
6. 861F – tyrosine 861 that has been implicated in VEGF signalling (Eliceiri *et al*., 2002) was replaced by a phenylalanine that cannot be phosphorylated.

The generation of these FAK mutant mice comprised the following steps: cloning constructs into targeting vectors; electroporation of mouse embryonic stem (ES) cells with targeting constructs; screen for homologous recombinant ES cell clones; Generation and breeding of chimeric mice for germline transmission; knockin/knockout breeding strategy.

I. Cloning constructs into targeting vectors

My predecessor, Dr. Bernardo Távora, performed all the cloning of point-mutant FAK constructs into targeting vectors with homology for the mouse Rosa26 locus prior to my arrival. He has also generated the FAK 861F knockin-knockout mice.

II. Electroporation of mouse embryonic stem (ES) cells with targeting constructs

WT, 397F, 397E, KD and 397E/KD constructs were electroporated into hybrid 129S6.C57BL6J ES cells (Transgenic facility CRUK). Around 100-500 neomycin-resistant clones per mutation were selected for DNA extraction.

III. Screening for homologous recombinant ES cell clones

I have been responsible for screening the homologous recombinants and the further steps of developing the WT, 397F, 397E, KD and 397E/KD point-mutant FAK mice. Southern blot analysis was used to screen for homologous recombination of the targeting vector into ES cell clones. DNA was digested with restriction enzymes

(EcoRV or AvrII), run on agarose gels, transferred to Hybond-nylon membranes and hybridised with probes to confirm homologous recombination and remove any clones with random insertions (see **Fig.9-12** of **Materials and Methods**).

The first screen was performed on EcoRV digested DNA using the 5'R26 probe (probe A), an external probe to the targeting vector that lies 5' of the Rosa26 locus (Soriano, 1999). Clones that displayed both WT and targeted band (indicative of homologous recombination in the Rosa 26 locus) (see **Table 5** and **Fig.41**) as well as their immediate gel neighbours were expanded and DNA extracted for a confirmation screen.

Table 5: Expected band sizes for Southern blot screen with 3 different probes for EcoRV and AvrII restrictions.

EcoRV	**WT Rosa 26 locus**	**Targeted Rosa 26 locus**
Probe A	11 Kb	4 Kb
Probe B	-	9 Kb
Probe C	-	4 Kb
Avr II	**WT Rosa 26 locus**	**Targeted Rosa 26 locus**
Probe A	5.5 Kb	8.4 Kb
Probe B	-	4.2 Kb
Probe C	-	8.4 Kb

Confirmation screens were performed on EcoRV and AvrII digested DNA using the external probe A as well as internal probes for GFP (probe B) and neomycin (probe C) to exclude the possibility of random integrations in other parts of the genome. With the internal probes B and C only the homologous recombinants should display a

band (**Table 5**). Appearance of other bands is indicative of random integrations and those clones cannot be used to produce chimeras (see examples in **Fig.42**) due to the possibility that the random integration has disrupted other essential genes that might account for any phenotype observed. **Fig. 42** shows the different clones from each mutation selected for injection into the blastocyst according to the bands obtained in the Southern blot analysis with EcoRV and AvrII restrictions, respectively. The total number of clones screened for each mutation as well as the number of positive clones selected to inject into the blastocyst is represented in **Table 6**.

Table 6: Number of neomycin resistant clones screened and positive clones for homologous recombination for each mutation selected to inject into the blastocyst of pseudo-pregnant female mice.

Mutation	Number clones screened	Number positive clones
WT - Control	288	2
397F	384	1
397E	96	2
KD	480	1
397E/KD	288	1

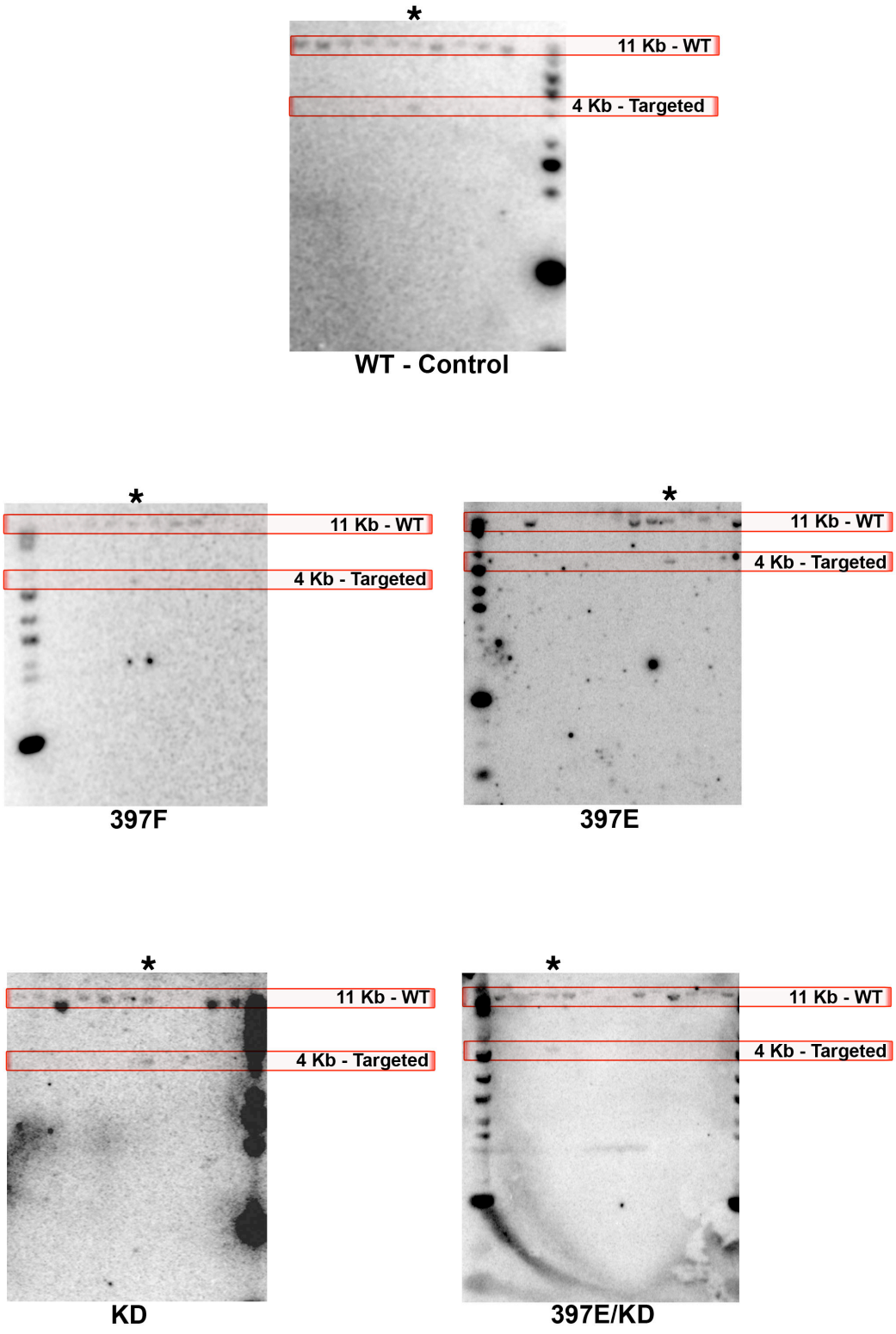

Figure 41: Southern blot analysis of external Probe A.

Examples of Southern blot analysis on EcoRV digested DNA of ES clones from WT, 397F, 397E, KD and 397E/KD. The first screen was performed using an external probe (probe A) that gives a 11Kb band for the WT allele and a 4 Kb band for the targeted allele. * identifies positive clones that screened positive for both the wild type and targeted allele.

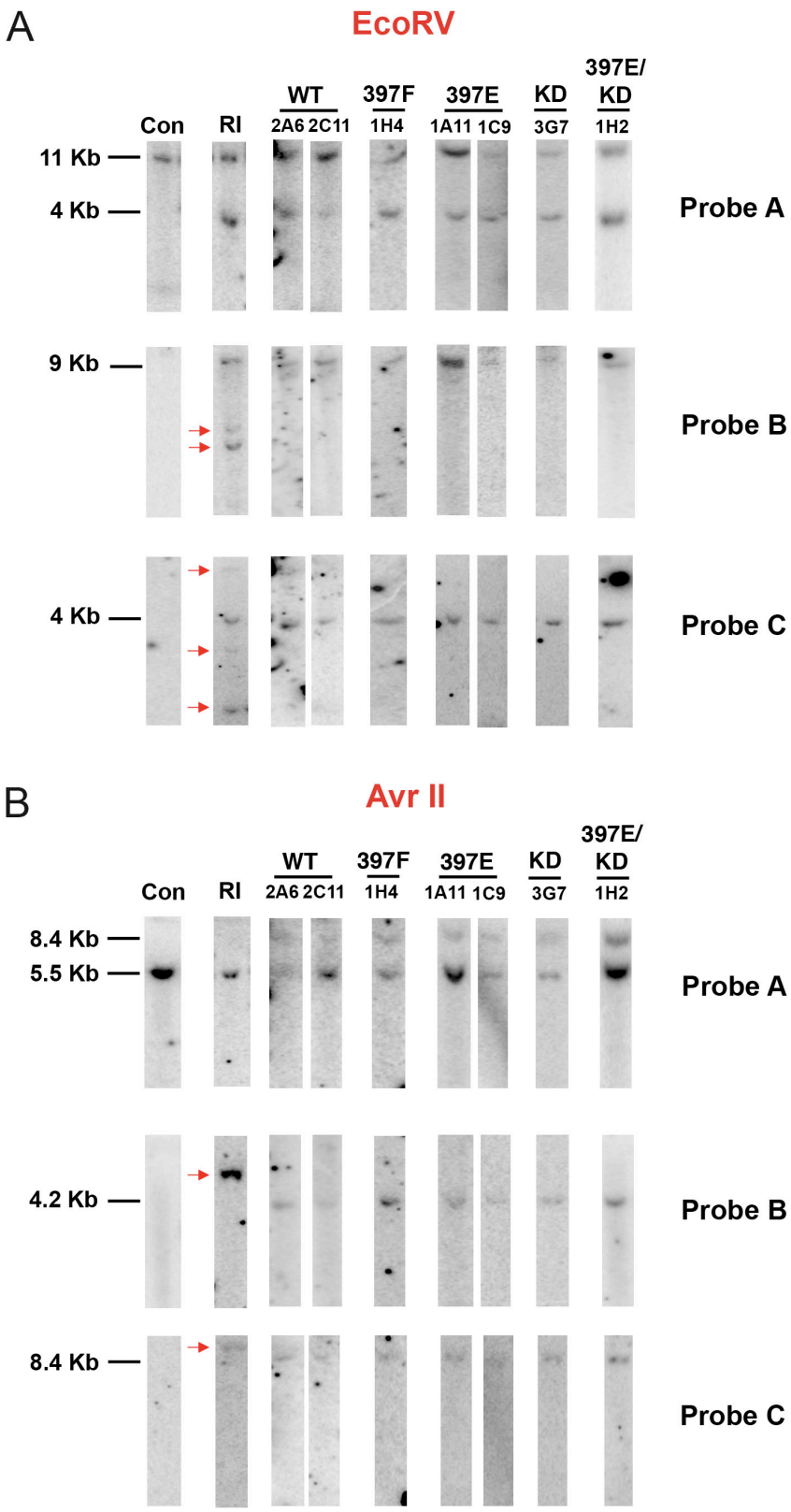
A
EcoRV
Con
RI
WT
2A6 2C11
397F
1H4
397E
1A11 1C9
KD
3G7
397E/
KD
1H2
11 Kb
4 Kb
Probe A
9 Kb
Probe B
4 Kb
Probe C
B
Avr II
Con
RI
WT
2A6 2C11
397F
1H4
397E
1A11 1C9
KD
3G7
397E/
KD
1H2
8.4 Kb
5.5 Kb
Probe A
4.2 Kb
Probe B
8.4 Kb
Probe C

Figure 42: Confirmation of Southern blot screen for homologous recombinants in targeted ES cells for the mouse Rosa 26 locus

Confirmation Southern blot analysis of EcoRV and AvrII digested DNA of ES clones selected to inject into blastocysts from WT, 397F, 397E, KD and 397E/KD using probes A, B and C. (**A**) EcoRV digested DNA Southern blot screen using Probe A shows the 11 Kb WT band in the control (Con) and both WT and targeted band (4 Kb) in the positive clones of WT, 397F, 397E, KD and 397E/KD targeted ES cells. With internal probes B and C only the Rosa 26 homologous recombinants show the expected bands (9 Kb with probe B and 4 Kb with probe C) as opposed to control (Con) that display no bands. (**B**) AvrII digested DNA Southern blot screen using Probe A shows the 5.5 Kb WT band in the control (C) and both WT and targeted band (8.4 Kb) in the positive clones of WT, 397F, 397E, KD and 397E/KD targeted ES cells. With internal probes B and C only the Rosa 26 homologous recombinants show the expected bands (4.2 Kb with probe B and 8.4 Kb with probe C) as opposite to control (Con) that display no bands. RI describes an example of random integrant clone. In (**A**) although homologous recombination has occurred in the Rosa26 locus (WT and targeted band with Probe A), a random integration has also occurred elsewhere in the genome. In (**B**) the targeted construct has only integrated in other parts of the genome that not the Rosa 26 locus (only WT band with Probe A). This gives rise to unexpected bands with probes B or C (red arrows). These clones were discarded.

IV. Generation of chimeric mice for germline transmission

The karyotype of individual clones is an important predictor of successful germline transmission. The confirmed positive ES clones were then karyotyped. Only those containing more than 70% of cells with normal chromosome counts were injected into blastocysts. 15 – 20 targeted ES cells were microinjected into day 4 fertilised mouse embryos (blastocysts). Following injection, embryos were transferred into plugged pseudopregnant foster mice, which gave birth 18 days later. Coat colour could be determined one week after birth. Given that the ES clones were from male 129S6.C57BL6J (agouti/black) mice and the recipient blastocysts were C57 black chimerism can be predicted in male with agouti/black coat colour.

High percentage chimeras (95-100%) were bred to C57/BL6 mice (black) to generate offspring. Because hybrid 129S6.C57BL6J ES cells (agouti/black) were used to generate the chimeras, germline transmission can occur in either agouti or black mice in colour. However an agouti progeny is likely to have germline transmission given that only the ES cells had the agouti colour. These mice were tail snipped and DNA genotyped by Southern blot analysis for homologous recombination using probes A, B and C. 50% of the mice screened are expected to be heterozygous for the targeted gene. **Table 7** shows a summary of the progression in the generation of point-mutant FAK knockin mice. In **Fig. 43** there are examples of the Southern blot screen and confirmation of the germline transmission in 2 males (1 agouti and 1 black in colour) for the $R26^{FAKWT/+}$ (**Fig. 43A**), 2 males (both black) (**Fig. 43B**) for the $R26^{FAK397F/+}$ and 2 males (1 black and 1 agouti in colour) for $R26^{FAK397E/KD/+}$ (**Fig.43C**). In the case of $R26^{FAK397F/+}$ and $R26^{FAK397E/KD/+}$ confirmation Southern blot screens I found more

mice that presented the expected band sizes indicative of homologous recombination with one of the internal probes. However, most of them also displayed another non-predicted bands with probes A, B and C (**Fig.43B, C**). These mice were not used due to the possibility of either random integrations in another parts of the genome or some extra recombinational events in the Rosa 26 locus. The 2 heterozygous mice for $R26^{FAKWT/+}$, $R26^{FAK397F/+}$ and $R26^{FAK397E/KD/+}$ were considered the founders and were mated with C57/BL6 mice in order to expand the colony. As I have confirmed both germline transmission and the absence of random integrations, future progeny can now be screened for Rosa 26 targeting by PCR. Heterozygous progeny for Rosa 26 targeting will then be mated in order to generate mice homozygous for the targeted gene. The ultimate goal is to generate an inducible knockin-knockout system. A post-doc in our laboratory has continued the breeding and characterisation of colonies $R26FAK^{KD/+}$; $R26FAK^{397E/+}$ and $R26FAK^{397E/KD/+}$ whereas I have continued with the generation of $R26FAK^{WT/+}$ and $R26FAK^{397F/+}$ mice.

Table 7: Summary of the progression in the generation of point mutant FAK knockin mice

Mutation	ES clone injected	Number of chimeric mice generated	Germline transmission
WT	2A6	7	2 mice
	2C11	5	-
397F	1H4	8	2 mice
397E	1A11	5	2 mice (being bred)
	1C9	4	2 mice (being bred)
KD	3G7	4	6 mice
397E/KD	1H2	2	2 mice

V. Knockin/knockout strategy

The ultimate goal of these experiments is to produce an inducible knockin/knockout system that allows the mutant FAK expression and simultaneously endogenous FAK deletion in endothelial cells, after tamoxifen treatment in adult mice so that I can test the effect of the different FAK phosphorylation sites on pathological angiogenesis, tumour progression and spread. For this purpose the different mutant point-mutant FAK knockin mice will be breed with inducible endothelial-specific FAK knockout mice. Pdgfb (platelet-derived growth factor b) is produced predominantly by endothelial cells (Hellstrom *et al*., 1999). The efficiency of tamoxifen induced Cre recombinase activity under the control of Pdgfb promoter (Pdgfb-iCreER) was tested in the ROSA26-lacZ reporter mice system and has been shown to be endothelial specific (Claxton 2008).

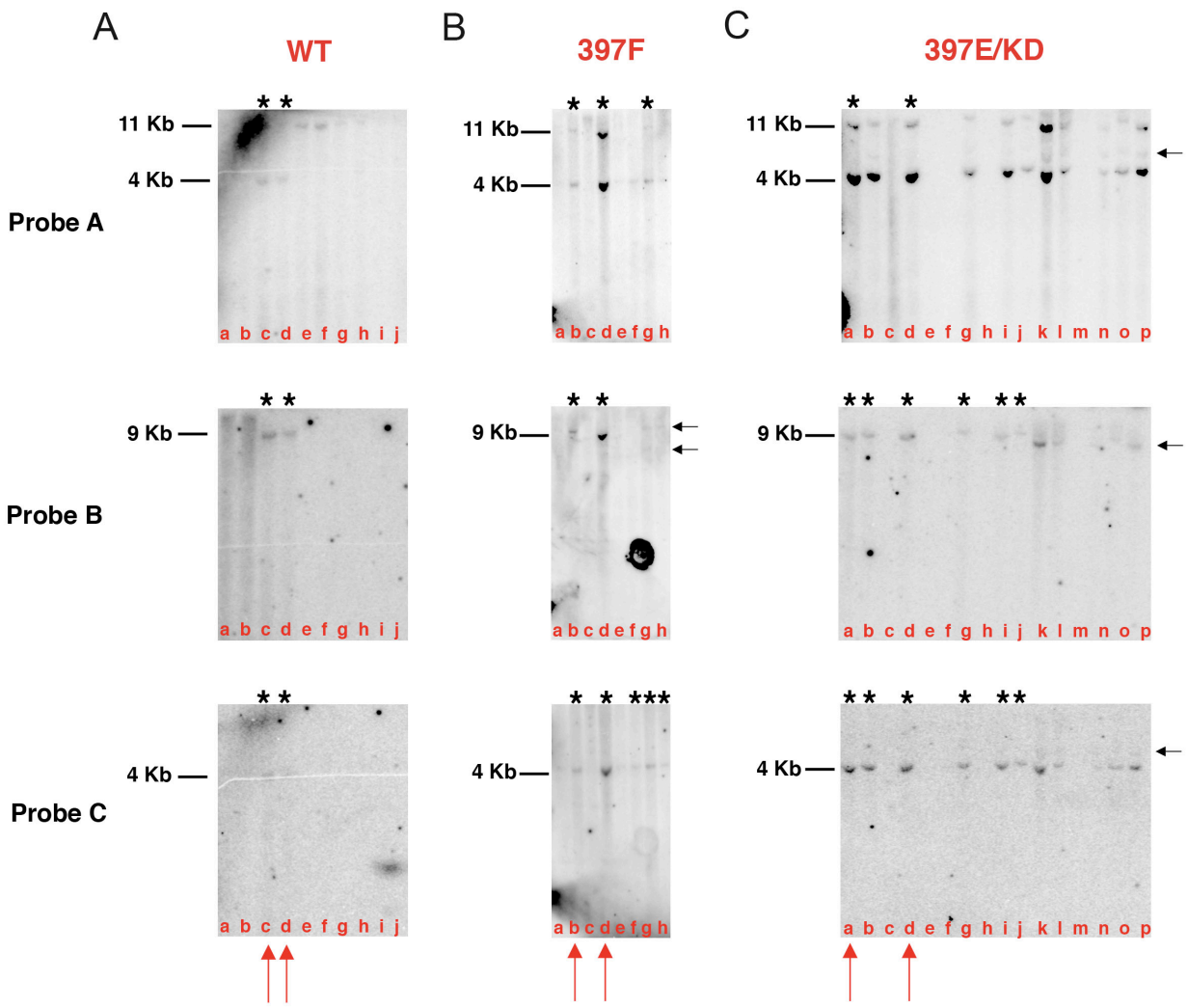
A
WT
B
397F
C
397E/KD
11 Kb
4 Kb
Probe A
9 Kb
Probe B
4 Kb
Probe C
a b c d e f g h i j
a b c d e f g h
a b c d e f g h i j k l m n o p

Southern blot analysis of germline transmission of $R26^{FAKWT}$, $R26^{FAK397F}$ and $R26^{FAK397E/KD}$ mice.

Southern blot on EcorV digested DNA extracted from tails of WT, 397F and 397E/KD chimeras progeny using probes A, B and C. (**A**) Southern blot screen for WT chimeras progeny using probes A, B and C. * identifies mice with the expected 11 Kb WT and 4 Kb targeted band with probe A, 9 Kb with probe B and 4 Kb with probe C. Mice c and d that only displayed the expected bands for Rosa 26 targeting with the 3 probes were considered the founder mice for $R26^{FAKWT}$ (red arrows) and selected for breeding. (**B**) Southern blot screen for 397F chimeras progeny using probes A, B and C. * identifies mice with the expected 11 Kb WT and 4 Kb targeted band with probe A, 9 Kb with probe B and 4 Kb with probe C. Black arrows identify bands of sizes different from expected that suggest integration in another parts of the genome or extra recombination events in the Rosa 26 locus as shown by the extra bands seen with internal probes B and C. Mice b and d that only displayed the expected bands for Rosa 26 targeting with the 3 probes were considered the founder mice for $R26^{FAK397F}$ (red arrows) and selected for breeding. (**C**) Southern blot screen for 397E/KD chimeras progeny using probes A, B and C. * identifies mice with the expected 11 Kb WT and 4 Kb targeted band with probe A, 9 Kb with probe B and 4 Kb with probe C. Black arrows identify bands of sizes different from expected that suggest integration in another parts of the genome or extra recombination events in the Rosa 26 locus as shown by the extra bands seen with internal probes B and C. Mice a and d that only displayed the expected bands for Rosa 26 targeting with the 3 probes were considered the founder mice for $R26^{FAK397E/KD}$ (red arrows) and selected for breeding.

5.2. Pdgfb-iCreER;FAK$^{fl/fl}$;R26FAK$^{861F/861F}$

Before I started my PhD, Dr. Bernardo Távora had generated Pdgfb-iCreER;FAK$^{fl/fl}$;R26$^{FAK861F/861F}$ mice: briefly founder R26$^{FAK861F/+}$ were bred with Pdgfb-iCreER;FAK$^{fl/fl}$ in order to generate mice with tamoxifen-inducible FAK 861F knockin and endogenous FAK knockout specifically in endothelial cells (Pdgfb-iCreER;FAK$^{fl/fl}$;R26$^{FAK861F/+}$). These mice were mated in order to generate mice homozygous for the FAK 861F knockin (Pdgfb-iCreER;FAK$^{fl/fl}$;R26$^{FAK861F/861F}$) (**Fig.44**). I have used the same strategy for the breeding of R26^{FAKWT} and R26^{FAK397F} and more recently generated Pdgfb-iCreER;FAK$^{fl/fl}$;R26$^{FAKWT/WT}$ and Pdgfb-iCreER;FAK$^{fl/fl}$;R26$^{FAK397F/397F}$ mice.

Given the immediate availability of the Pdgfb-iCreER;FAK$^{fl/fl}$;R26$^{FAK861F/861F}$ mice I have used this line for preliminary experiments. PCR examples for Pdgfb-iCreER, FAK floxed and Rosa 26 targeting are shown in **Fig.45**. Pdgfb-iCreER PCR (**Fig.45A**) shows mice positive (Pdgfb-iCreER+) or negative (Pdgfb-iCreER-) for CreER in the Pdgfb locus. FAK floxed PCR (**Fig. 45B**) shows mice with one (FAK$^{fl/+}$) or both (FAK$^{fl/fl}$) FAK floxed alleles and WT mice non-floxed (FAK$^{+/+}$). Rosa 26 PCR (**Fig.45C**) shows mice homozygous (R26$^{FAK861F/861F}$) and heterozygous (R26$^{FAK861F/+}$) for Rosa 26 targeting and mice non-targeted in the Rosa 26 locus (R26$^{FAK+/+}$). Pdgfb-iCreER+;FAK$^{fl/fl}$;R26$^{FAK861F/861F}$ (EC$^{861F/861F}$) and control FAK$^{fl/fl}$;R26$^{FAK861F/861F}$ (EC^{Cre-}) were used for all the experiments shown. All the mice appeared normal without any visible adverse effects after the tamoxifen treatment.

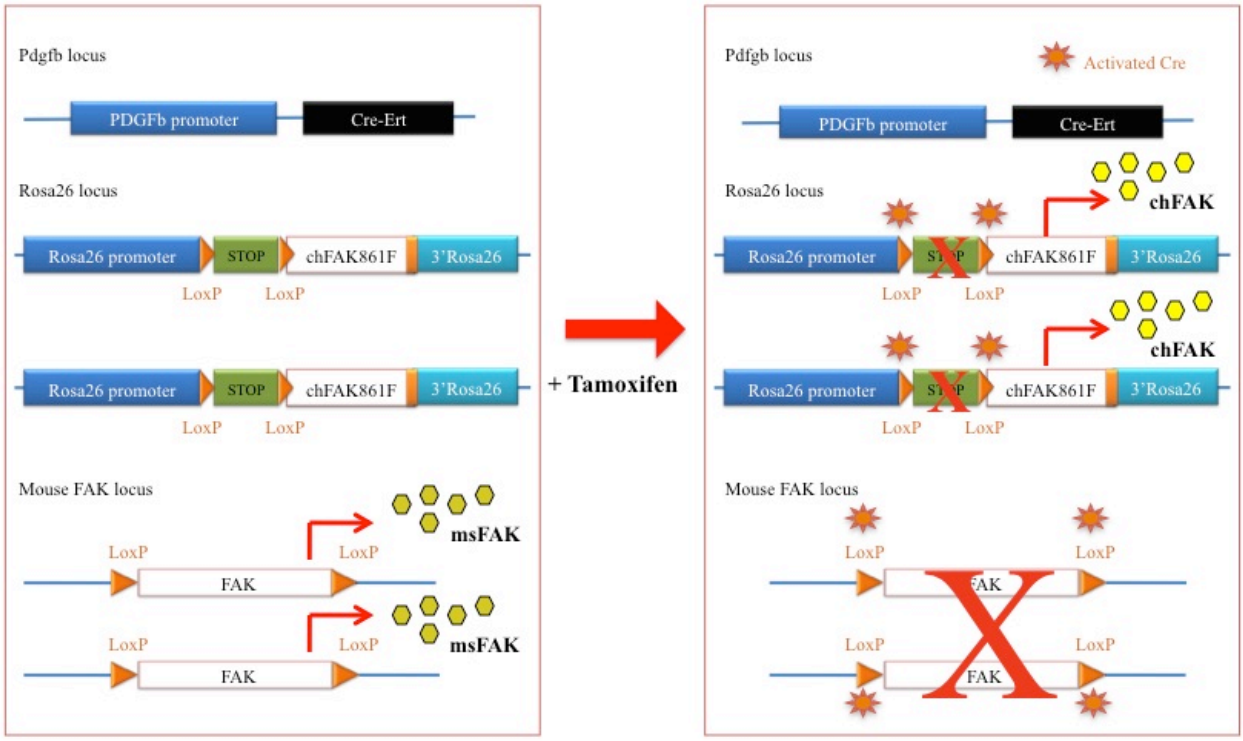

Figure 44: Pdgfb-iCreER;FAK$^{fl/fl}$;R26$^{FAK861F/861F}$ mice knockin/knockout approach.

Upon tamoxifen treatment, Cre recombinase expression under the specific endothelial promoter Pdgfb allows the recombination of the LoxP sites. This allows for the simultaneous excision of endogenous mouse FAK (msFAK) and of the STOP codon that precedes both alleles of mutant chFAK 861F. The ultimate result is the simultaneous deletion of mouse endogenous FAK and induction of homozygous expression of the mutant chFAK-861F in endothelial cells.

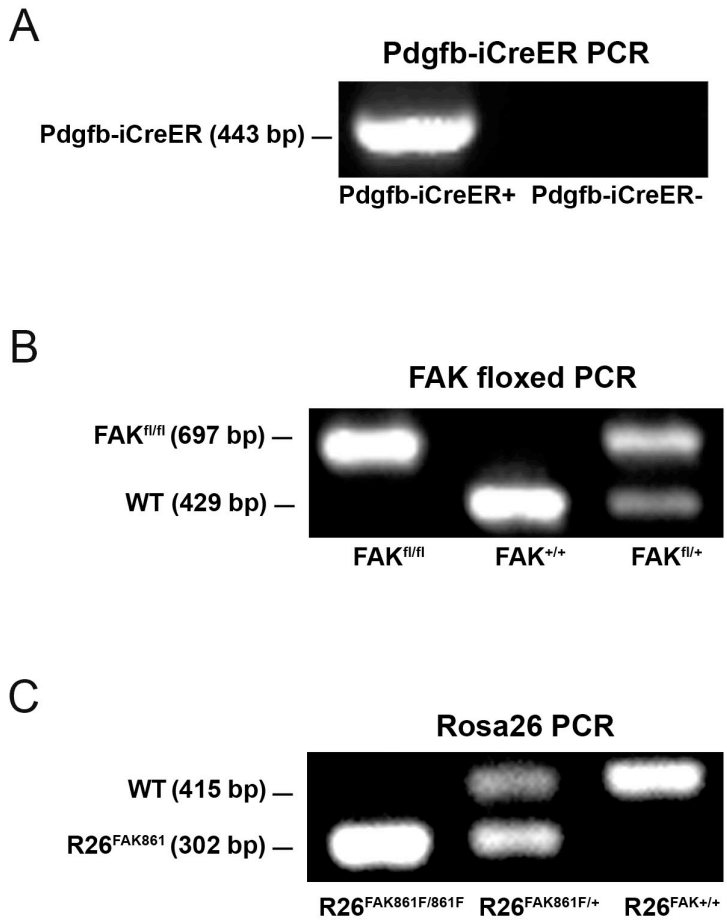

Figure 45: Genotyping for Pdgfb-iCreER, FAKfloxed and Rosa 26 targeting.

PCR performed using DNA extracted from ear snips. (**A**) Pdgfb-iCreER PCR shows mice positive (Pdgfb-iCreER+) or negative (Pdgfb-iCreER-) for CreER in the Pdgfb locus (**B**) FAK floxed PCR shows mice with both FAK floxed alleles ($FAK^{fl/fl}$), WT mice non-floxed ($FAK^{+/+}$) and mice heterozygous for the floxed allele ($FAK^{fl/+}$) (**C**) Rosa 26 PCR shows mice with both ($R26^{FAK861/861F}$) or just one ($R26^{FAK861/+}$) of the alleles targeted in Rosa 26 locus with FAK 861F or WT mice non-targeted in the Rosa26 locus ($R26^{FAK+/+}$).

*5.2.1. Efficient deletion of mouse FAK and expression of chicken FAK in tamoxifen-treated endothelial cells isolated from Pdgfb-iCre*ER;FAK$^{fl/fl}$;R26FAK$^{861F/861F}$*

In order to characterise these mice we have isolated endothelial cells from Pdgfb-iCreER+;FAK$^{fl/fl}$;R26$^{FAK861F/861F}$ (EC$^{861F/861F}$) and control FAK$^{fl/fl}$;R26$^{FAK861F/861F}$ (EC^{Cre-}) mice, treated them with 4-hydroxitamoxifen (OHT) for 2 days and extracted RNA to perform a RT-PCR or protein for Western blotting analysis. I have shown that after OHT treatment in the EC$^{861F/861F}$, the expression of endogenous mouse FAK decreased and the expression of the mutant chFAK-861F increased at the mRNA level (**Fig.46A,B**).

I have also performed a chicken FAK imunoprecipitation with antibody attached to magnetic beads and a Western blot with an antibody that recognises both mouse and chicken FAK. Using this approach I was able to detect a band that corresponds to the expected size of FAK only in EC$^{861F/861F}$ after tamoxifen treatment (even though there seems to be an unspecific band in all extracts) (**Fig.47A**). Moreover when I took the supernatant, that contained the proteins not attached to the beads, and did not imunoprecipitated with chicken FAK antibody and performed a Western blot with the FAK antibody that recognises both chicken and mouse FAK it was possible to observe that FAK protein levels had decreased after tamoxifen treatment in EC$^{861F/861F}$ as opposed to control EC^{Cre-} (**Fig.47A**). In theory after chicken FAK imunoprecipitation the supernatant should only contain msFAK suggesting that the

system is efficiently working. Furthermore since chFAK-861F contains a myc-tag I have analysed the total myc tag protein by Western blot and found that it was only expressed in $EC^{861F/861F}$ after tamoxifen treatment (**Fig.47B**). This is another indication that chFAK-861F is being expressed. This preliminary data is encouraging, however these experiments require further optimisation and quantification of protein levels to be able to make a comparison between levels of msFAK protein normally produced and the levels of chFAK-861F achieved with this system.

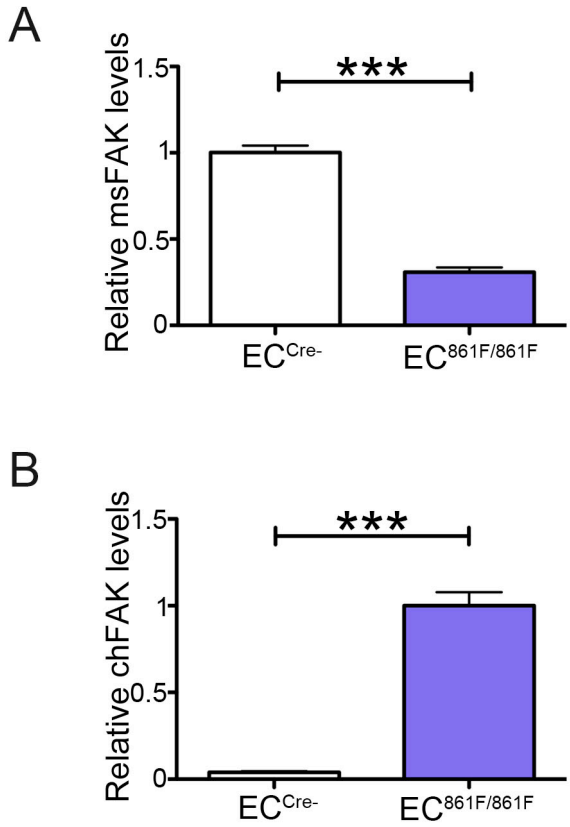

Figure 46: Loss of mouse FAK and expression of mutant chicken FAK at mRNA level in endothelial cells isolated from Pdgfb-iCreER;FAK$^{fl/fl}$;R26$^{FAK861F/861F}$ mice

Real time PCR using mouse-specific **(A)** and chicken-specific (**B**) primers in isolated endothelial cells from Pdgf-iCreER+;FAK$^{fl/fl}$;R26$^{FAK861F/861F}$ (EC$^{861F/861F}$) and control FAK$^{fl/fl}$;R26$^{FAK861F/861F}$ (EC^{Cre-}) mice. Bar charts show that mRNA levels of endogenous mouse FAK (msFAK) are decreased and mutant chicken FAK increased in OHT-treated EC$^{861F/861F}$. *P<0.05.

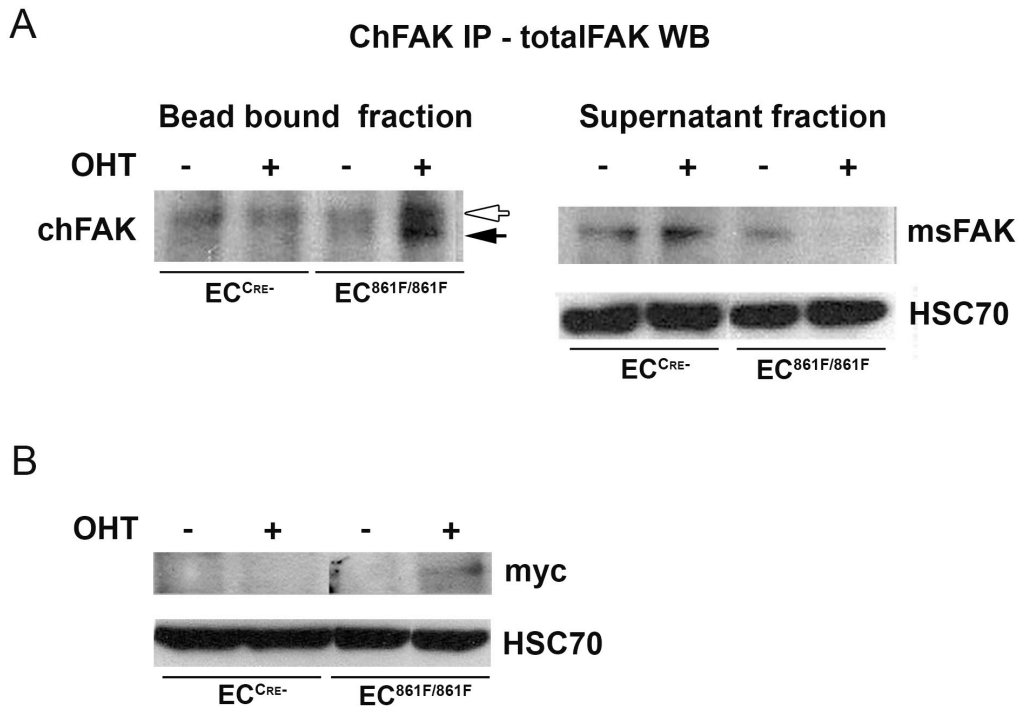

Figure 47: Loss of mouse FAK and expression of mutant chicken FAK in endothelial cells isolated from Pdgfb-iCreER;FAK$^{fl/fl}$;R26$^{FAK861F/861F}$ mice.

(A) Chicken FAK imunoprecipitation (IP) in endothelial cells isolated either from Pdgf-iCreER+;FAK$^{fl/fl}$;R26$^{FAK861F/861F}$ (EC$^{861F/861F}$) or control FAK$^{fl/fl}$;R26$^{FAK861F/861F}$ (EC^{Cre-}) mice treated (+) or not (-) with OHT and Western blot (WB) for total FAK levels using an antibody that recognises both chicken (chFAK) and mouse FAK (msFAK). Bead-bound fraction represents the protein that was imunoprecipitated with the anti-chFAK antibody. Total FAK WB in the bead fraction shows an increase in chFAK in EC$^{861F/861F}$ after tamoxifen treatment and when compared undetected levels of EC^{Cre-} controls as demonstrated by the band at around 125 Kd (expected size of FAK) (black arrow) in EC$^{861F/861F}$ after tamoxifen treatment. A non-specific band appears in all samples (open arrow). The supernatant fraction represents the proteins that were not imunoprecipitated with the anti-chFAK antibody. Total FAK WB in the supernatant fraction to detect msFAK shows a decrease in msFAK in EC$^{861F/861F}$ after tamoxifen treatment and when compared unchanged levels in EC^{Cre-}. **(B)** Total myc-tag Western blot in endothelial cells isolated either from Pdgf-iCreER;FAK$^{fl/fl}$;R26$^{FAK861F/861F}$ (EC$^{861F/861F}$) or control FAK$^{fl/fl}$; R26$^{FAK861F/861F}$ (EC^{Cre-}) mice treated (+) or not (-) with OHT. Western blot shows an increase in the myc-tag of chFAK-861F in EC$^{861F/861F}$ after tamoxifen treatment and when compared with undetected levels in EC^{Cre-} controls. HSC70 levels were used as a loading control and were similar between all the samples compared.

5.2.2. chFAK861F mutation in endothelial cells was sufficient to decrease *tumour growth and angiogenesis in vivo*

In order to determine the effect of FAK 861F mutation in tumour growth we injected B16F0 tumour cells subcutaneously into Pdgfb-iCreER+;$FAK^{fl/fl}$;$R26^{FAK861F/861F}$ and $FAK^{fl/fl}$; $R26^{FAK861F/861F}$ mice after tamoxifen treatment (21-days tamoxifen pellets). Tumour size was decreased significantly when mutant chFAK-861F was expressed in endothelial cells when compared with the EC^{Cre-} controls (P<0.05) (**Fig. 48A**). Moreover, tumours from these $EC^{861F/861F}$ mice were significantly less vascularised when compared with EC^{Cre-} controls (P < 0.05) as measured by the number of PECAM-1 positive vessels within the tumours (**Fig. 48B**). These preliminary data suggest that FAK-P-Y861 phosphorylation can support the growth of tumours and associated blood vessels. It will be important in the future to validate these preliminary results and to investigate further mechanism by which FAK-P-Y861 phosphorylation controls tumour growth and angiogenesis.

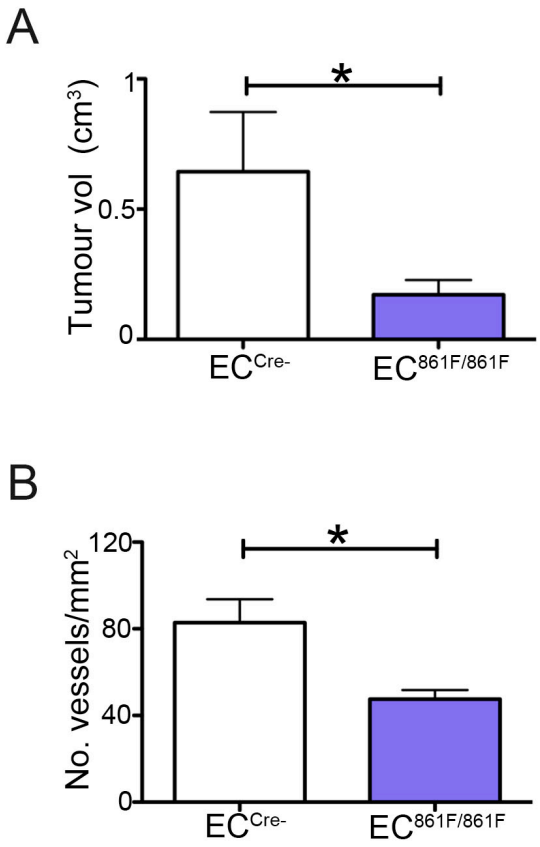

Figure 48: Endothelial-specific FAK 861F mutation is sufficient to reduce tumour growth and angiogenesis *in vivo*.

(A) Pdgfb-iCreER+;$FAK^{fl/fl}$;$R26^{FAK861F/861F}$ and control $FAK^{fl/fl}$;$R26^{FAK861F/861F}$ mice were all injected subcutaneously with B16F0 cells after tamoxifen treatment (21-days tamoxifen pellets). 10 day old tumour size was reduced significantly when mutant chFAK-861F was expressed in endothelial cells when compared with the EC^{Cre-} controls. Bar charts show mean tumour volume in cm^3 +s.e.m; n=10 mice/genotype. **(B)** Blood vessel density in subcutaneous B16F0 tumours grown in $EC^{861F/861F}$ was also reduced significantly when compared with the EC^{Cre-} controls. Bar charts represent mean tumour blood vessel density/mm^2 + s.e.m, n= 4 tumours/genotype. *P<0.05.

5.2.3. chFAK861F mutation in endothelial cells was sufficient to decrease *angiogenesis ex vivo*

Further analysis of VEGF-induced neovascularization responses was carried out using *ex vivo* aortic ring assays. Aortas from Pdgfb-iCreER+;$FAK^{fl/fl}$;$R26^{FAK861F/861F}$ and control $FAK^{fl/fl}$;$R26^{FAK861F/861F}$ mice were isolated and cut in rings. These aortic rings were embedded in collagen in the presence or absence of VEGF or serum and in the presence or absence of 4-hydroxitamoxifen. Numbers of vascular sprouts per aortic ring over a period of 18 days in culture were assessed. In the absence of VEGF, very little vessel outgrowth was detected in either $EC^{861F/861F}$ or EC^{Cre-} controls, whereas serum induced neovascularisation to a similar extent in both (data not shown). However, in the presence of VEGF, the total number of vessel sprouts was significantly reduced for $EC^{861F/861F}$ aortic rings when compared with EC^{Cre-} controls ($P < 0.05$) (**Fig.49**). These results give further evidence for the involvement of FAK-P-Y861 phosphorylation in angiogenesis.

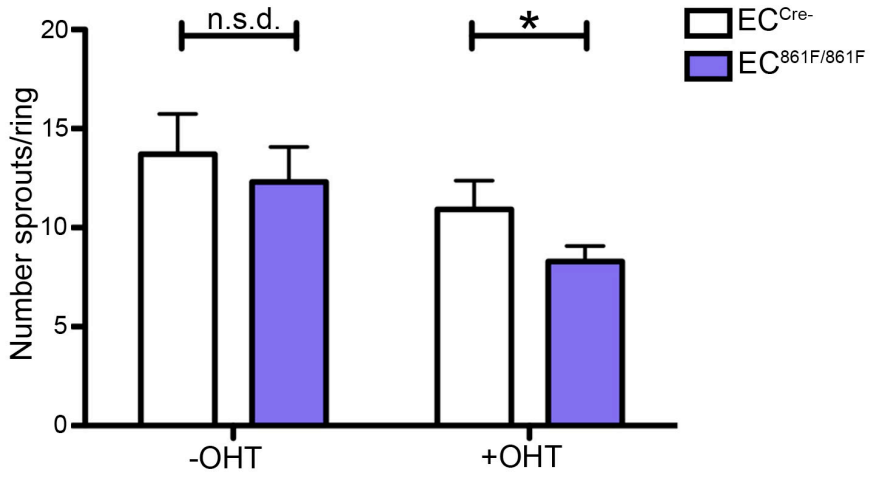

Figure 49: Endothelial-specific FAK 861F mutation

Aortas were isolated from Pdgfb-iCreER+;$FAK^{fl/fl}$;$R26^{FAK861F/861F}$ and control $FAK^{fl/fl}$;$R26^{FAK861F/861F}$ mice and cut in rings. Aortic rings were grown in 3D collagen culture and microvessel outgrowth examined after stimulation with 30 ng/ml of VEGF and in the presence or absence of 1 μm OHT. Endothelial-specific chFAK-861F expression was sufficient to inhibit VEGF-induced microvessel sprouting when compared with no difference after tamoxifen treatment in EC^{Cre-} controls. Bar chart represents mean number of microvessels/aortic ring +s.e.m. n=14-22 aortic rings/genotype; **P*<0.05, n.s.d. (no significant difference).

6. DISCUSSION PART II – FAK phosphorylation sites in tumour progression

Understanding the role of FAK in tumour growth and metastasis *in vivo* is important because data from several laboratories, including ours, suggest that the pleotropic effects of this molecule are spatially and temporally regulated. The next generation of investigation requires understanding of how FAK regulates these processes *in vivo*.

For this reason our laboratory has generated inducible point-mutant FAK knockin-knockout mice. The point-mutation constructs are from chicken FAK in order to distinguish them from endogenous mouse FAK, and comprise: the FAK-P-Y397 site (397F that cannot be phosphorylated and 397E that mimics constitutive phosphorylation) at which autophosphorylation represents the major event in FAK activation and induces binding and activation of Src (Schaller *et al*., 1994); the kinase domain (KD that has a disruption in the ATP-binding site generating a kinase dead mutation) that is responsible for the catalytic activity of FAK important in processes such as cell migration (Owen *et al*., 1999); a double point mutant that mimics constitutive FAK-P-Y397 phosphorylation important for Src binding but in which catalytic activity of FAK is disrupted (397E/KD); the FAK-P-Y861 (861F that cannot be phosphorylated) important for Cas binding and H-Ras-mediated transformation (Lim *et al*., 2004) and that has been implicated in VEGF signalling (Abu-Ghazaleh *et al*., 2001).

We decided to use the ubiquitously active Rosa 26 gene promoter to generate the point-mutant FAK knockin in the Rosa 26 locus (Soriano, 1999; Zambrowicz *et al*., 1997). This locus has been utilised for knockin expression reporters such as GFP and lacZ and has been shown to be effective in global or tissue-specific CreER or mycER mice (Jager *et al*., 2004; Soriano, 1999; Srinivas *et al*., 2001; Vooijs *et al*., 2001).

All chimeras were generated successfully. Point mutant mice 397E are being crossed with FAK floxed mice and with specific Cre lines (such as the endothelial specific Pdgfb-iCreER) in order to generate tamoxifen-inducible point-mutant FAK knockin/knockout mice that will allow for simultaneous point-mutant FAK expression and endogenous FAK deletion in a specific cell type (such as endothelial cells) after tamoxifen treatment. All the other lines (WT, 397F, 397E/KD, KD and 861F) are already crossed into Pdgfb-iCreER;$FAK^{fl/fl}$;$R26FAK^{KI/KI}$. Other post-docs in our laboratory are also crossing these $FAK^{fl/fl}$;$R26FAK^{KI/KI}$ to other Cre lines such as PDGFRβ, a pericyte marker to enquire about the role of FAK phosphorylation sites in these cells.

I have also just crossed the $R26FAK^{WT/WT}$ knockin with $RERTn^{ERT/ERT}$Cre to generate $RERTn^{ERT/ERT}$Cre;$R26FAK^{WT/+}$ and $RERTn^{ERT/ERT}$Cre;$R26FAK^{WT/WT}$ mice. These mice have inducible chFAK knockin in the Rosa 26 promoter but still maintain msFAK in the endogenous promoter after tamoxifen treatment. Transplant of bone marrow cells from $RERTn^{ERT/ERT}$Cre;$R26FAK^{WT/+}$ and $RERTn^{ERT/ERT}$Cre;$R26FAK^{WT/WT}$ mice into lethally irradiated WT mice and tamoxifen treatment will allow me to analyse the effect of overexpression with one or two extra copies of FAK respectively in the phenotypes observed in Results Part I.

This constitutes a powerful system that permits a temporal control of the knockin/knockout as well as tissue-specific activation by crossing with different Cre lines. Temporal control of knockin/knockout will avoid any lethality during development; the knockin approach engineers single copy point-mutant FAK, reducing any overexpression artefacts; and by simultaneously knocking-out FAK and knocking-in point-mutant FAK we will avoid possible transphosphorylation between endogenous and mutant FAK.

Noteworthy is that the mutant knockin expression is under the control of Rosa26 rather than FAK promoter. This is of particular importance in cancer studies because FAK promoter contains p53 and nuclear factor kappa B (NF-κB) binding sites (Golubovskaya *et al*., 2004). The p53 binding to FAK promoter was shown to repress FAK activity both *in vitro* and *in vivo* (Golubovskaya *et al*., 2004; Golubovskaya *et al*., 2008). In contrast, NF-κB has been shown to induce FAK expression (Golubovskaya *et al*., 2004). A recent study has demonstrated that proteosome inhibitor bortezomib can downregulate FAK promoter activity though a mechanism dependent on NF-κB inhibition and thereby affect cancer cell migration and apoptosis (Ko *et al*., 2010). In this context the control chFAK WT knockin/FAK knockout line plays a crucial role. It will be extremely important to always have this control in parallel in all the *in vitro* and *in vivo* analysis to take in account any effect of FAK promoter interactions in the phenotypes observed.

Dr. Bernardo Távora from our laboratory has successfully finished generating the first point-mutant chFAK-861F knockin/FAK knockout line where Cre recombinase is under the expression of the endothelial-specific Pdgfb-iCreER promoter (Claxton *et al*., 2008). I was able to show preliminary evidence that the chFAK-861F mutant is expressed at the same time that msFAK is deleted in endothelial cells. More recently another post-doc in our laboratory has evidence that mutant ch-FAK861F is being expressed at levels that are comparable with endogenous msFAK levels, at least at the mRNA level. Thus we hope that this system will provide mutant FAK expression at physiological levels, an important feature when exploring their functions *in vivo*.

Even though further characterisation is necessary I performed some preliminary experiments in order to investigate the effect of chFAK-861F mutation in endothelial cells in tumour growth and angiogenesis *in vivo*. PdgfbiCreER+;$FAK^{fl/fl}$;$R26FAK^{861F/861F}$ mice and respective controls were injected with B16 tumour cells subcutaneously, and I found that both tumour growth and tumour angiogenesis were decreased when mutant FAK was expressed. These preliminary results suggest that FAK-P-Y861 phosphorylation site is important for both tumour growth and angiogenesis *in vivo*. I was also able to show that FAK-P-861F mutation decreased VEGF-induced angiogenesis *ex vivo*. These results are in line with previous studies in which FAK-P-Y861 phosphorylation has been implicated in VEGF signalling (Abu-Ghazaleh *et al*., 2001; Eliceiri *et al*., 2002). An important point to take in account is that deletion of FAK in endothelial cells also decreases tumour growth and angiogenesis *in vivo* (Tavora *et al*., 2010). So until further characterisation of mutant FAK expression levels *in vivo* I cannot exclude the possibility that this phenotype might also be due to low levels of expression of

chFAK-861F mutant. However if we can confirm the role of FAK tyrosine 861 in tumour angiogenesis this can represent an interesting anti-angiogenic target.

One of the explanations appointed as responsible for anti-angiogenic therapy resistance is hypoxia-dependent up-regulation of other pro-angiogenic factors such as bFGF (Casanovas *et al*., 2005). FAK has also been shown to be involved in bFGF/FGFR signalling dependent migration of endothelial cells (Shi *et al*., 2011). It would be of particular relevance to test the effect of chFAK-861F mutation in endothelial cells in bFGF-induced angiogenesis *ex vivo*. It will be interesting to investigate in the future if by manipulating FAK phosphorylation sites we can overcome antiangiogenic therapy resistance *in vivo*.

7. CONCLUDING REMARKS

During my PhD I was able to show, for the first time, that stromal FAK even though important for tumour growth and angiogenesis seems to be a negative regulator of tumour metastasis. I have also demonstrated that although FAK levels can still have a positive role in some cells such as endothelial cells, at least in the context of tumour growth, bone marrow derived FAK plays an important negative role in tumour cell colonisation and metastasis. Even though many questions still need clarification I was also able to generate mouse model tools that will allow more directed studies on the mechanism of FAK regulation in different cell types and different processes of tumour progression.

Cancer therapy often relies on combinations of more than one drug. If we can understand which pathways are being activated by FAK deficiency in myeloid cells that drive the metastatic process we can perhaps give valuable information on which drugs can be combined with FAK inhibitors to achieve the best treatment outcome. On the other hand by dissecting how different FAK phosphorylation sites affect its function *in vivo* we might find a common regulation in primary tumours and metastasis that can be used for the development of new and more efficient FAK inhibitors.

ACKNOWLEDGMENTS

I want to thank my first supervisor Professor Kairbaan Hodivala-Dilke for all the teaching, support and advice during my PhD. I want to thank also Professor Ian Hart, my second supervisor, for all the help, support and important advice. They were both truly inspiring and motivating during these years.

I also have to thank my supervisor for establishing crucial collaborations for my experiments. In that sense I am really grateful to Dr. Thorsten Hagemman and Dr. Eleni Maniatti for all the help and advice in the immunology and also Dr. Oriol Casanovas for the expert advice in the RIP-Tag2 mouse model analysis.

I want to acknowledge in special 2 members of Adhesion and Angiogenesis Laboratory that have been my Lab mentors throughout my PhD: Stephen Robinson and Bernardo Távora. I could have not done it without you! A very special thanks goes to Louise Reynolds for all the enormous help and advice in my experiments. Many of my results had also the Lab help of other post-docs (Delphine Lees, Tanguy Lechertier, Dylan Jones, Isabelle Fernandez). And thanks to everyone else in the group: Ping Pui Wong, Marianne Baker, Annika Alexopoulous, Alan Watson.

Many thanks to the animal house staff: Ian Roswell and all members of Transgenic Unit; Peter Miller and Janet MacDonald; Hagen and Julie; Julie Bee and Clare in LIF; Anthony Price and Danny in Whitechapel. A very special thanks goes to Garry Saunders, Colin Pegrum and Colin Wren in Clare Hall and Bruce Williams and Julie Holdsworth in Charterhouse Square that helped me in all animal experiments of my PhD. I definitely could not have done it without you!

I want to thank all members of Tumour Biology Department for making my integration in the laboratory so easy and for all the help, advice and support. Also here a very special thanks to George Elia for all the enormous help and advice in all the histology based work.

For all the friendship and for making my PhD years so much fun and easy thank you so much Bernardo Távora and Fieke Froeling but also Antonio Saha, Chia Yu Chen, Ping Pui Wong, Sabarinath Vallath and Maria Monterubio-Acebes.

A very special thanks to my flatmates with whom I have shared my last and more complicated years of PhD: Maria Cary and Luís Casanova. Your support and friendship were very important. The only way is Faraday!!! And also many thanks to all my friends in London that made these years so much fun and easy.

Back home all the friendship and support were not forgotten. Lena Maria for sharing all the PhD and non-PhD problems and for all the friendship and also Pedro Ferreira: We did it (well hurry up Pedro!)! And to my best friends Aninhas, Nila, Joana, Ines e Nana…..I don't need to say much…you know! Thank you to my cousin and oldest friend Ricardo and also to Antonio, Joao, Osvaldo, Tiago, Laura, Maria Leonor, etc!

To my family I reserved the last and biggest thank you: Madrinha, Tio Manuel, Ricardo, Carina, Bianca, Paulo, Tio Ze, Beatriz, Tia Barbara, Orlando, Helia, Rodrigo, Tio Chico OBRIGADA!

And to the 3 people I most love in my life my parents and my brother. Mae, Pai, Mano: OBRIGADA! ADORO-VOS!

BIBLIOGRAPHY

Aberle, H., H. Schwartz, and R. Kemler. 1996. Cadherin-catenin complex: protein interactions and their implications for cadherin function. *Journal of cellular biochemistry*. 61:514-523.

Abramsson, A., P. Lindblom, and C. Betsholtz. 2003. Endothelial and nonendothelial sources of PDGF-B regulate pericyte recruitment and influence vascular pattern formation in tumors. *The Journal of clinical investigation*. 112:1142-1151.

Abshire, M.Y., K.S. Thomas, K.A. Owen, and A.H. Bouton. 2011. Macrophage motility requires distinct alpha5beta1/FAK and alpha4beta1/paxillin signaling events. *J Leukoc Biol*. 89:251-257.

Abu-Ghazaleh, R., J. Kabir, H. Jia, M. Lobo, and I. Zachary. 2001. Src mediates stimulation by vascular endothelial growth factor of the phosphorylation of focal adhesion kinase at tyrosine 861, and migration and anti-apoptosis in endothelial cells. *Biochem J*. 360:255-264.

Adams, R.H., and K. Alitalo. 2007. Molecular regulation of angiogenesis and lymphangiogenesis. *Nature reviews. Molecular cell biology*. 8:464-478.

Agochiya, M., V.G. Brunton, D.W. Owens, E.K. Parkinson, C. Paraskeva, W.N. Keith, and M.C. Frame. 1999. Increased dosage and amplification of the focal adhesion kinase gene in human cancer cells. *Oncogene*. 18:5646-5653.

Ahn, G.O., and J.M. Brown. 2009. Role of endothelial progenitors and other bone marrow derived cells in the development of the tumor vasculature. *Angiogenesis*. 12:159-164.

Akashi, K., D. Traver, T. Miyamoto, and I.L. Weissman. 2000. A clonogenic common myeloid progenitor that gives rise to all myeloid lineages. *Nature*. 404:193-197.

Al-Hajj, M., M.S. Wicha, A. Benito-Hernandez, S.J. Morrison, and M.F. Clarke. 2003. Prospective identification of tumorigenic breast cancer cells. *Proceedings of the National Academy of Sciences of the United States of America*. 100:3983-3988.

Almand, B., J.I. Clark, E. Nikitina, J. van Beynen, N.R. English, S.C. Knight, D.P. Carbone, and D.I. Gabrilovich. 2001. Increased production of immature myeloid cells in cancer patients: a mechanism of immunosuppression in cancer. *J Immunol*. 166:678-689.

Alva, A., S. Slovin, S. Daignault, M. Carducci, R. Dipaola, K. Pienta, D. Agus, K. Cooney, A. Chen, D.C. Smith, and M. Hussain. 2012. Phase II study of cilengitide (EMD 121974, NSC 707544) in patients with non-metastatic castration resistant prostate cancer, NCI-6735. A study by the DOD/PCF prostate cancer clinical trials consortium. *Invest New Drugs*. 30:749-757.

Ambati, B.K., M. Nozaki, N. Singh, A. Takeda, P.D. Jani, T. Suthar, R.J. Albuquerque, E. Richter, E. Sakurai, M.T. Newcomb, M.E. Kleinman, R.B. Caldwell, Q. Lin, Y. Ogura, A. Orecchia, D.A. Samuelson, D.W. Agnew, J. St Leger, W.R. Green, P.J. Mahasreshti, D.T. Curiel, D. Kwan, H. Marsh, S. Ikeda, L.J. Leiper, J.M. Collinson, S. Bogdanovich, T.S. Khurana, M. Shibuya, M.E. Baldwin, N. Ferrara, H.P. Gerber, S. De Falco, J. Witta, J.Z. Baffi, B.J. Raisler, and J. Ambati. 2006. Corneal avascularity is due to soluble VEGF receptor-1. *Nature*. 443:993-997.

Ambati, B.K., E. Patterson, P. Jani, C. Jenkins, E. Higgins, N. Singh, T. Suthar, N. Vira, K. Smith, and R. Caldwell. 2007. Soluble vascular endothelial growth factor receptor-1 contributes to the corneal antiangiogenic barrier. *The British journal of ophthalmology*. 91:505-508.

Aronsohn, M.S., H.M. Brown, G. Hauptman, and L.J. Kornberg. 2003. Expression of focal adhesion kinase and phosphorylated focal adhesion kinase in squamous cell carcinoma of the larynx. *The Laryngoscope*. 113:1944-1948.

Ashman, L.K., A.C. Cambareri, L.B. To, R.J. Levinsky, and C.A. Juttner. 1991. Expression of the YB5.B8 antigen (c-kit proto-oncogene product) in normal human bone marrow. *Blood*. 78:30-37.

Auffray, C., M.H. Sieweke, and F. Geissmann. 2009. Blood monocytes: development, heterogeneity, and relationship with dendritic cells. *Annu Rev Immunol*. 27:669-692.

Avraham, H., S.Y. Park, K. Schinkmann, and S. Avraham. 2000. RAFTK/Pyk2-mediated cellular signalling. *Cell Signal*. 12:123-133.

Avraham, S., R. London, Y. Fu, S. Ota, D. Hiregowdara, J. Li, S. Jiang, L.M. Pasztor, R.A. White, J.E. Groopman, and *et al*. 1995. Identification and characterization of a novel related adhesion focal tyrosine kinase (RAFTK) from megakaryocytes and brain. *The Journal of biological chemistry*. 270:27742-27751.

Ayaki, M., K. Komatsu, M. Mukai, K. Murata, M. Kameyama, S. Ishiguro, J. Miyoshi, M. Tatsuta, and H. Nakamura. 2001. Reduced expression of focal adhesion kinase in liver metastases compared with matched primary human colorectal adenocarcinomas. *Clinical cancer research : an official journal of the American Association for Cancer Research*. 7:3106-3112.

Bakewell, S.J., P. Nestor, S. Prasad, M.H. Tomasson, N. Dowland, M. Mehrotra, R. Scarborough, J. Kanter, K. Abe, D. Phillips, and K.N. Weilbaecher. 2003. Platelet and osteoclast beta3 integrins are critical for bone metastasis. *Proceedings of the National Academy of Sciences of the United States of America*. 100:14205-14210.

Banerjee, E.R., Y.E. Latchman, Y. Jiang, G.V. Priestley, and T. Papayannopoulou. 2008. Distinct changes in adult lymphopoiesis in Rag2-/- mice fully reconstituted by alpha4-deficient adult bone marrow cells. *Experimental hematology*. 36:1004-1013.

Barleon, B., S. Sozzani, D. Zhou, H.A. Weich, A. Mantovani, and D. Marme. 1996. Migration of human monocytes in response to vascular endothelial growth factor (VEGF) is mediated via the VEGF receptor flt-1. *Blood*. 87:3336-3343.

Barreda, D.R., P.C. Hanington, and M. Belosevic. 2004. Regulation of myeloid development and function by colony stimulating factors. *Developmental and comparative immunology*. 28:509-554.

Barriere, C., D. Santamaria, A. Cerqueira, J. Galan, A. Martin, S. Ortega, M. Malumbres, P. Dubus, and M. Barbacid. 2007. Mice thrive without Cdk4 and Cdk2. *Mol Oncol*. 1:72-83.

Bates, R.C., D.I. Bellovin, C. Brown, E. Maynard, B. Wu, H. Kawakatsu, D. Sheppard, P. Oettgen, and A.M. Mercurio. 2005. Transcriptional activation of integrin beta6 during the epithelial-mesenchymal transition defines a novel prognostic indicator of aggressive colon carcinoma. *The Journal of clinical investigation*. 115:339-347.

Baumann, C.I., A.S. Bailey, W. Li, M.J. Ferkowicz, M.C. Yoder, and W.H. Fleming. 2004. PECAM-1 is expressed on hematopoietic stem cells throughout ontogeny and identifies a population of erythroid progenitors. *Blood*. 104:1010-1016.

Beck, L., Jr., and P.A. D'Amore. 1997. Vascular development: cellular and molecular regulation. *Faseb J*. 11:365-373.

Becker, A.J., C.E. Mc, and J.E. Till. 1963. Cytological demonstration of the clonal nature of spleen colonies derived from transplanted mouse marrow cells. *Nature*. 197:452-454.

Beckermann, B.M., G. Kallifatidis, A. Groth, D. Frommhold, A. Apel, J. Mattern, A.V. Salnikov, G. Moldenhauer, W. Wagner, A. Diehlmann, R. Saffrich, M. Schubert, A.D. Ho, N. Giese, M.W. Buchler, H. Friess, P. Buchler, and I. Herr. 2008. VEGF expression by mesenchymal stem cells contributes to angiogenesis in pancreatic carcinoma. *British journal of cancer*. 99:622-631.

Bergers, G., and L.E. Benjamin. 2003. Tumorigenesis and the angiogenic switch. *Nat Rev Cancer*. 3:401-410.

Bergers, G., and S. Song. 2005. The role of pericytes in blood-vessel formation and maintenance. *Neuro Oncol*. 7:452-464.

Bertout, J.A., S.A. Patel, and M.C. Simon. 2008. The impact of O2 availability on human cancer. *Nat Rev Cancer*. 8:967-975.

Bexell, D., S. Gunnarsson, A. Tormin, A. Darabi, D. Gisselsson, L. Roybon, S. Scheding, and J. Bengzon. 2009. Bone marrow multipotent mesenchymal stroma cells act as pericyte-like migratory vehicles in experimental gliomas. *Mol Ther*. 17:183-190.

Bhaskar, V., D. Zhang, M. Fox, P. Seto, M.H. Wong, P.E. Wales, D. Powers, D.T. Chao, R.B. Dubridge, and V. Ramakrishnan. 2007. A function blocking anti-mouse integrin alpha5beta1 antibody inhibits angiogenesis and impedes tumor growth in vivo. *J Transl Med*. 5:61.

Bhattacharya, D., D. Bryder, D.J. Rossi, and I.L. Weissman. 2006. Rapid lymphocyte reconstitution of unconditioned immunodeficient mice with non-self-renewing multipotent hematopoietic progenitors. *Cell Cycle*. 5:1135-1139.

Birchmeier, W., and J. Behrens. 1994. Cadherin expression in carcinomas: role in the formation of cell junctions and the prevention of invasiveness. *Biochim Biophys Acta*. 1198:11-26.

Boisset, J.C., and C. Robin. 2012. On the origin of hematopoietic stem cells: progress and controversy. *Stem Cell Res*. 8:1-13.

Bonnet, D., and J.E. Dick. 1997. Human acute myeloid leukemia is organized as a hierarchy that originates from a primitive hematopoietic cell. *Nat Med*. 3:730-737.

Brabletz, T., A. Jung, S. Reu, M. Porzner, F. Hlubek, L.A. Kunz-Schughart, R. Knuechel, and T. Kirchner. 2001. Variable beta-catenin expression in colorectal cancers indicates tumor progression driven by the tumor environment. *Proceedings of the National Academy of Sciences of the United States of America*. 98:10356-10361.

Brabletz, T., A. Jung, S. Spaderna, F. Hlubek, and T. Kirchner. 2005. Opinion: migrating cancer stem cells - an integrated concept of malignant tumour progression. *Nat Rev Cancer*. 5:744-749.

Brakebusch, C., S. Fillatreau, A.J. Potocnik, G. Bungartz, P. Wilhelm, M. Svensson, P. Kearney, H. Korner, D. Gray, and R. Fassler. 2002. Beta1 integrin is not essential for hematopoiesis but is necessary for the T cell-dependent IgM antibody response. *Immunity*. 16:465-477.

Bronte, V., E. Apolloni, A. Cabrelle, R. Ronca, P. Serafini, P. Zamboni, N.P. Restifo, and P. Zanovello. 2000. Identification of a CD11b(+)/Gr-1(+)/CD31(+) myeloid progenitor capable of activating or suppressing CD8(+) T cells. *Blood*. 96:3838-3846.

Broxterman, H.J., J. Lankelma, and K. Hoekman. 2003. Resistance to cytotoxic and anti-angiogenic anticancer agents: similarities and differences. *Drug Resist Updat*. 6:111-127.

Burns, J.M., B.C. Summers, Y. Wang, A. Melikian, R. Berahovich, Z. Miao, M.E. Penfold, M.J. Sunshine, D.R. Littman, C.J. Kuo, K. Wei, B.E. McMaster, K. Wright, M.C. Howard, and T.J. Schall. 2006. A novel chemokine receptor for SDF-1 and I-TAC involved in cell survival, cell adhesion, and tumor development. *The Journal of experimental medicine*. 203:2201-2213.

Butler, J.M., D.J. Nolan, E.L. Vertes, B. Varnum-Finney, H. Kobayashi, A.T. Hooper, M. Seandel, K. Shido, I.A. White, M. Kobayashi, L. Witte, C. May, C. Shawber, Y. Kimura, J. Kitajewski, Z. Rosenwaks, I.D. Bernstein, and S. Rafii. 2010. Endothelial cells are essential for the self-renewal and repopulation of Notch-dependent hematopoietic stem cells. *Cell stem cell*. 6:251-264.

Cai, L., J. Han, X. Zhuo, Y. Xiong, J. Dong, and X. Li. 2009. Overexpression and significance of focal adhesion kinase in hepatocellular carcinoma and its relationship with HBV infection. *Med Oncol*. 26:409-414.

Calalb, M.B., T.R. Polte, and S.K. Hanks. 1995. Tyrosine phosphorylation of focal adhesion kinase at sites in the catalytic domain regulates kinase activity: a role for Src family kinases. *Mol Cell Biol*. 15:954-963.

Calvani, M., A. Rapisarda, B. Uranchimeg, R.H. Shoemaker, and G. Melillo. 2006. Hypoxic induction of an HIF-1alpha-dependent bFGF autocrine loop drives angiogenesis in human endothelial cells. *Blood*. 107:2705-2712.

Cance, W.G., J.E. Harris, M.V. Iacocca, E. Roche, X. Yang, J. Chang, S. Simkins, and L. Xu. 2000. Immunohistochemical analyses of focal adhesion kinase expression in benign and malignant human breast and colon tissues: correlation with preinvasive and invasive phenotypes. *Clinical cancer research : an official journal of the American Association for Cancer Research*. 6:2417-2423.

Carlson, T.R., Y. Feng, P.C. Maisonpierre, M. Mrksich, and A.O. Morla. 2001. Direct cell adhesion to the angiopoietins mediated by integrins. *The Journal of biological chemistry*. 276:26516-26525.

Carmeliet, P. 2000. Mechanisms of angiogenesis and arteriogenesis. *Nature medicine*. 6:389-395.

Carmeliet, P. 2003. Angiogenesis in health and disease. *Nature medicine*. 9:653-660.

Carmeliet, P. 2005. VEGF as a key mediator of angiogenesis in cancer. *Oncology*. 69 Suppl 3:4-10.

Carmeliet, P., V. Ferreira, G. Breier, S. Pollefeyt, L. Kieckens, M. Gertsenstein, M. Fahrig, A. Vandenhoeck, K. Harpal, C. Eberhardt, C. Declercq, J. Pawling, L. Moons, D. Collen, W. Risau, and A. Nagy. 1996. Abnormal blood vessel development and lethality in embryos lacking a single VEGF allele. *Nature*. 380:435-439.

Carragher, N.O., B. Levkau, R. Ross, and E.W. Raines. 1999. Degraded collagen fragments promote rapid disassembly of smooth muscle focal adhesions that correlates with cleavage of pp125(FAK), paxillin, and talin. *The Journal of cell biology*. 147:619-630.

Casanovas, O., D.J. Hicklin, G. Bergers, and D. Hanahan. 2005. Drug resistance by evasion of antiangiogenic targeting of VEGF signaling in late-stage pancreatic islet tumors. *Cancer Cell*. 8:299-309.

Ceccarelli, D.F., H.K. Song, F. Poy, M.D. Schaller, and M.J. Eck. 2006. Crystal structure of the FERM domain of focal adhesion kinase. *The Journal of biological chemistry*. 281:252-259.

Chambers, A.F., A.C. Groom, and I.C. MacDonald. 2002. Dissemination and growth of cancer cells in metastatic sites. *Nat Rev Cancer*. 2:563-572.

Chan, K.T., D.A. Bennin, and A. Huttenlocher. 2010. Regulation of adhesion dynamics by calpain-mediated proteolysis of focal adhesion kinase (FAK). *The Journal of biological chemistry*. 285:11418-11426.

Chen, H.C., P.A. Appeddu, J.T. Parsons, J.D. Hildebrand, M.D. Schaller, and J.L. Guan. 1995. Interaction of focal adhesion kinase with cytoskeletal protein talin. *The Journal of biological chemistry*. 270:16995-16999.

Chen, J.J., Y.C. Lin, P.L. Yao, A. Yuan, H.Y. Chen, C.T. Shun, M.F. Tsai, C.H. Chen, and P.C. Yang. 2005. Tumor-associated macrophages: the double-edged sword in cancer progression. *J Clin Oncol*. 23:953-964.

Chen, Q., X.H. Zhang, and J. Massague. 2011. Macrophage binding to receptor VCAM-1 transmits survival signals in breast cancer cells that invade the lungs. *Cancer Cell*. 20:538-549.

Chen, X.L., J.O. Nam, C. Jean, C. Lawson, C.T. Walsh, E. Goka, S.T. Lim, A. Tomar, I. Tancioni, S. Uryu, J.L. Guan, L.M. Acevedo, S.M. Weis, D.A. Cheresh, and D.D. Schlaepfer. 2012. VEGF-induced vascular permeability is mediated by FAK. *Dev Cell*. 22:146-157.

Cheshier, S.H., S.J. Morrison, X. Liao, and I.L. Weissman. 1999. In vivo proliferation and cell cycle kinetics of long-term self-renewing hematopoietic stem cells. *Proceedings of the National Academy of Sciences of the United States of America*. 96:3120-3125.

Chioda, M., E. Peranzoni, G. Desantis, F. Papalini, E. Falisi, S. Solito, S. Mandruzzato, and V. Bronte. 2011. Myeloid cell diversification and complexity: an old concept with new turns in oncology. *Cancer metastasis reviews*. 30:27-43.

Chodniewicz, D., and R.L. Klemke. 2004. Regulation of integrin-mediated cellular responses through assembly of a CAS/Crk scaffold. *Biochim Biophys Acta*. 1692:63-76.

Choi, K. 1998. Hemangioblast development and regulation. *Biochem Cell Biol*. 76:947-956.
Choi, W.T., S. Duggineni, Y. Xu, Z. Huang, and J. An. 2012. Drug discovery research targeting the CXC chemokine receptor 4 (CXCR4). *Journal of medicinal chemistry*. 55:977-994.
Church, G.M., and W. Gilbert. 1984. Genomic sequencing. *Proceedings of the National Academy of Sciences of the United States of America*. 81:1991-1995.
Clauss, M., H. Weich, G. Breier, U. Knies, W. Rockl, J. Waltenberger, and W. Risau. 1996. The vascular endothelial growth factor receptor Flt-1 mediates biological activities. Implications for a functional role of placenta growth factor in monocyte activation and chemotaxis. *The Journal of biological chemistry*. 271:17629-17634.
Claxton, S., V. Kostourou, S. Jadeja, P. Chambon, K. Hodivala-Dilke, and M. Fruttiger. 2008. Efficient, inducible Cre-recombinase activation in vascular endothelium. *Genesis*. 46:74-80.
Cobb, B.S., M.D. Schaller, T.H. Leu, and J.T. Parsons. 1994. Stable association of pp60src and pp59fyn with the focal adhesion-associated protein tyrosine kinase, pp125FAK. *Mol Cell Biol*. 14:147-155.
Coghlin, C., and G.I. Murray. 2010. Current and emerging concepts in tumour metastasis. *J Pathol*. 222:1-15.
Conacci-Sorrell, M., I. Simcha, T. Ben-Yedidia, J. Blechman, P. Savagner, and A. Ben-Ze'ev. 2003. Autoregulation of E-cadherin expression by cadherin-cadherin interactions: the roles of beta-catenin signaling, Slug, and MAPK. *The Journal of cell biology*. 163:847-857.
Connolly, M.K., J. Mallen-St Clair, A.S. Bedrosian, A. Malhotra, V. Vera, J. Ibrahim, J. Henning, H.L. Pachter, D. Bar-Sagi, A.B. Frey, and G. Miller. 2010. Distinct populations of metastases-enabling myeloid cells expand in the liver of mice harboring invasive and preinvasive intra-abdominal tumor. *J Leukoc Biol*. 87:713-725.
Conway, E.M., D. Collen, and P. Carmeliet. 2001. Molecular mechanisms of blood vessel growth. *Cardiovascular research*. 49:507-521.
Cooper, L.A., T.L. Shen, and J.L. Guan. 2003. Regulation of focal adhesion kinase by its amino-terminal domain through an autoinhibitory interaction. *Mol Cell Biol*. 23:8030-8041.
Curiel, T.J., G. Coukos, L. Zou, X. Alvarez, P. Cheng, P. Mottram, M. Evdemon-Hogan, J.R. Conejo-Garcia, L. Zhang, M. Burow, Y. Zhu, S. Wei, I. Kryczek, B. Daniel, A. Gordon, L. Myers, A. Lackner, M.L. Disis, K.L. Knutson, L. Chen, and W. Zou. 2004. Specific recruitment of regulatory T cells in ovarian carcinoma fosters immune privilege and predicts reduced survival. *Nature medicine*. 10:942-949.
D'Amico, A., and L. Wu. 2003. The early progenitors of mouse dendritic cells and plasmacytoid predendritic cells are within the bone marrow hemopoietic precursors expressing Flt3. *The Journal of experimental medicine*. 198:293-303.
da Silva, R.G., B. Tavora, S.D. Robinson, L.E. Reynolds, C. Szekeres, J. Lamar, S. Batista, V. Kostourou, M.A. Germain, A.R. Reynolds, D.T. Jones, A.R. Watson, J.L. Jones, A. Harris, I.R. Hart, M.L. Iruela-Arispe, C.M. Dipersio, J.A. Kreidberg, and K.M. Hodivala-Dilke. 2010. Endothelial alpha3beta1-integrin represses pathological angiogenesis and sustains endothelial-VEGF. *The American journal of pathology*. 177:1534-1548.
Dawson, M.R., D.G. Duda, D. Fukumura, and R.K. Jain. 2009. VEGFR1-activity-independent metastasis formation. *Nature*. 461:E4; discussion E5.
De Bock, K., S. Cauwenberghs, and P. Carmeliet. 2011. Vessel abnormalization: another hallmark of cancer? Molecular mechanisms and therapeutic implications. *Curr Opin Genet Dev*. 21:73-79.
de Heer, P., M.M. Koudijs, C.J. van de Velde, R.I. Aalbers, R.A. Tollenaar, H. Putter, J. Morreau, B. van de Water, and P.J. Kuppen. 2008. Combined expression of the non-

receptor protein tyrosine kinases FAK and Src in primary colorectal cancer is associated with tumor recurrence and metastasis formation. *Eur J Surg Oncol*. 34:1253-1261.

De Palma, M., M.A. Venneri, R. Galli, L. Sergi Sergi, L.S. Politi, M. Sampaolesi, and L. Naldini. 2005. Tie2 identifies a hematopoietic lineage of proangiogenic monocytes required for tumor vessel formation and a mesenchymal population of pericyte progenitors. *Cancer Cell*. 8:211-226.

De Palma, M., M.A. Venneri, C. Roca, and L. Naldini. 2003. Targeting exogenous genes to tumor angiogenesis by transplantation of genetically modified hematopoietic stem cells. *Nature medicine*. 9:789-795.

de Vicente, J.C., P. Rosado, P. Lequerica-Fernandez, E. Allonca, L. Villallain, and G. Hernandez-Vallejo. 2012. Focal adhesion kinase overexpression: Correlation with lymph node metastasis and shorter survival in oral squamous cell carcinoma. *Head & neck*.

Del Fattore, A., M. Capannolo, and N. Rucci. 2010. Bone and bone marrow: the same organ. *Arch Biochem Biophys*. 503:28-34.

Desgrosellier, J.S., L.A. Barnes, D.J. Shields, M. Huang, S.K. Lau, N. Prevost, D. Tarin, S.J. Shattil, and D.A. Cheresh. 2009. An integrin alpha(v)beta(3)-c-Src oncogenic unit promotes anchorage-independence and tumor progression. *Nature medicine*. 15:1163-1169.

Desgrosellier, J.S., and D.A. Cheresh. 2010. Integrins in cancer: biological implications and therapeutic opportunities. *Nat Rev Cancer*. 10:9-22.

Diaz-Montero, C.M., M.L. Salem, M.I. Nishimura, E. Garrett-Mayer, D.J. Cole, and A.J. Montero. 2009. Increased circulating myeloid-derived suppressor cells correlate with clinical cancer stage, metastatic tumor burden, and doxorubicin-cyclophosphamide chemotherapy. *Cancer Immunol Immunother*. 58:49-59.

Dickson, P.V., J.B. Hamner, T.L. Sims, C.H. Fraga, C.Y. Ng, S. Rajasekeran, N.L. Hagedorn, M.B. McCarville, C.F. Stewart, and A.M. Davidoff. 2007. Bevacizumab-induced transient remodeling of the vasculature in neuroblastoma xenografts results in improved delivery and efficacy of systemically administered chemotherapy. *Clinical cancer research : an official journal of the American Association for Cancer Research*. 13:3942-3950.

Djonov, V., M. Schmid, S.A. Tschanz, and P.H. Burri. 2000. Intussusceptive angiogenesis: its role in embryonic vascular network formation. *Circulation research*. 86:286-292.

Du, R., K.V. Lu, C. Petritsch, P. Liu, R. Ganss, E. Passegue, H. Song, S. Vandenberg, R.S. Johnson, Z. Werb, and G. Bergers. 2008. HIF1alpha induces the recruitment of bone marrow derived vascular modulatory cells to regulate tumor angiogenesis and invasion. *Cancer Cell*. 13:206-220.

Duda, D.G., and R.K. Jain. 2010. Premetastatic lung "niche": is vascular endothelial growth factor receptor 1 activation required? *Cancer research*. 70:5670-5673.

Duda, D.G., S.V. Kozin, N.D. Kirkpatrick, L. Xu, D. Fukumura, and R.K. Jain. 2011. CXCL12 (SDF1alpha)-CXCR4/CXCR7 pathway inhibition: an emerging sensitizer for anticancer therapies? *Clinical cancer research : an official journal of the American Association for Cancer Research*. 17:2074-2080.

Dunty, J.M., and M.D. Schaller. 2002. The N termini of focal adhesion kinase family members regulate substrate phosphorylation, localization, and cell morphology. *The Journal of biological chemistry*. 277:45644-45654.

Eagle, H., and E.M. Levine. 1967. Growth regulatory effects of cellular interaction. *Nature*. 213:1102-1106.

Eash, K.J., A.M. Greenbaum, P.K. Gopalan, and D.C. Link. 2010. CXCR2 and CXCR4 antagonistically regulate neutrophil trafficking from murine bone marrow. *The Journal of clinical investigation*. 120:2423-2431.

Ebos, J.M., C.R. Lee, W. Cruz-Munoz, G.A. Bjarnason, J.G. Christensen, and R.S. Kerbel. 2009. Accelerated metastasis after short-term treatment with a potent inhibitor of tumor angiogenesis. *Cancer Cell*. 15:232-239.

Eliceiri, B.P., and D.A. Cheresh. 1999. The role of alphav integrins during angiogenesis: insights into potential mechanisms of action and clinical development. *The Journal of clinical investigation*. 103:1227-1230.

Eliceiri, B.P., X.S. Puente, J.D. Hood, D.G. Stupack, D.D. Schlaepfer, X.Z. Huang, D. Sheppard, and D.A. Cheresh. 2002. Src-mediated coupling of focal adhesion kinase to integrin alpha(v)beta5 in vascular endothelial growth factor signaling. *The Journal of cell biology*. 157:149-160.

Eyles, J., A.L. Puaux, X. Wang, B. Toh, C. Prakash, M. Hong, T.G. Tan, L. Zheng, L.C. Ong, Y. Jin, M. Kato, A. Prevost-Blondel, P. Chow, H. Yang, and J.P. Abastado. 2010. Tumor cells disseminate early, but immunosurveillance limits metastatic outgrowth, in a mouse model of melanoma. *The Journal of clinical investigation*. 120:2030-2039.

Felding-Habermann, B., T.E. O'Toole, J.W. Smith, E. Fransvea, Z.M. Ruggeri, M.H. Ginsberg, P.E. Hughes, N. Pampori, S.J. Shattil, A. Saven, and B.M. Mueller. 2001. Integrin activation controls metastasis in human breast cancer. *Proceedings of the National Academy of Sciences of the United States of America*. 98:1853-1858.

Feng, W., N.P. McCabe, G.H. Mahabeleshwar, P.R. Somanath, D.R. Phillips, and T.V. Byzova. 2008. The angiogenic response is dictated by beta3 integrin on bone marrow derived cells. *The Journal of cell biology*. 183:1145-1157.

Ferrara, N., H.P. Gerber, and J. LeCouter. 2003. The biology of VEGF and its receptors. *Nature medicine*. 9:669-676.

Fidler, I.J., and L.M. Ellis. 1994. The implications of angiogenesis for the biology and therapy of cancer metastasis. *Cell*. 79:185-188.

Fiedler, K., and C. Brunner. 2012. The role of transcription factors in the guidance of granulopoiesis. *Am J Blood Res*. 2:57-65.

Folkman, J. 2006. Antiangiogenesis in cancer therapy--endostatin and its mechanisms of action. *Experimental cell research*. 312:594-607.

Fong, G.H., J. Rossant, M. Gertsenstein, and M.L. Breitman. 1995. Role of the Flt-1 receptor tyrosine kinase in regulating the assembly of vascular endothelium. *Nature*. 376:66-70.

Frame, M.C., H. Patel, B. Serrels, D. Lietha, and M.J. Eck. 2010. The FERM domain: organizing the structure and function of FAK. *Nature reviews. Molecular cell biology*. 11:802-814.

Franco, S., B. Perrin, and A. Huttenlocher. 2004. Isoform specific function of calpain 2 in regulating membrane protrusion. *Experimental cell research*. 299:179-187.

Fridlender, Z.G., and S.M. Albelda. 2012. Tumor-associated neutrophils: friend or foe? *Carcinogenesis*. 33:949-955.

Fridlender, Z.G., J. Sun, S. Kim, V. Kapoor, G. Cheng, L. Ling, G.S. Worthen, and S.M. Albelda. 2009. Polarization of tumor-associated neutrophil phenotype by TGF-beta: "N1" versus "N2" TAN. *Cancer Cell*. 16:183-194.

Funahashi, Y., N.H. Sugi, T. Semba, Y. Yamamoto, S. Hamaoka, N. Tsukahara-Tamai, Y. Ozawa, A. Tsuruoka, K. Nara, K. Takahashi, T. Okabe, J. Kamata, T. Owa, N. Ueda, T. Haneda, M. Yonaga, K. Yoshimatsu, and T. Wakabayashi. 2002. Sulfonamide derivative, E7820, is a unique angiogenesis inhibitor suppressing an expression of integrin alpha2 subunit on endothelium. *Cancer research*. 62:6116-6123.

Furuta, Y., D. Ilic, S. Kanazawa, N. Takeda, T. Yamamoto, and S. Aizawa. 1995. Mesodermal defect in late phase of gastrulation by a targeted mutation of focal adhesion kinase, FAK. *Oncogene*. 11:1989-1995.

Furuyama, K., R. Doi, T. Mori, E. Toyoda, D. Ito, K. Kami, M. Koizumi, A. Kida, Y. Kawaguchi, and K. Fujimoto. 2006. Clinical significance of focal adhesion kinase in resectable pancreatic cancer. *World J Surg*. 30:219-226.

Gabriel, B., A. zur Hausen, E. Stickeler, C. Dietz, G. Gitsch, D.C. Fischer, J. Bouda, C. Tempfer, and A. Hasenburg. 2006. Weak expression of focal adhesion kinase (pp125FAK) in patients with cervical cancer is associated with poor disease outcome. *Clinical cancer research : an official journal of the American Association for Cancer Research*. 12:2476-2483.

Gabrilovich, D.I., and S. Nagaraj. 2009. Myeloid-derived suppressor cells as regulators of the immune system. *Nat Rev Immunol*. 9:162-174.

Gale, N.W., and G.D. Yancopoulos. 1999. Growth factors acting via endothelial cell-specific receptor tyrosine kinases: VEGFs, angiopoietins, and ephrins in vascular development. *Genes Dev*. 13:1055-1066.

Gao, D., N. Joshi, H. Choi, S. Ryu, M. Hahn, R. Catena, H. Sadik, P. Argani, P. Wagner, L.T. Vahdat, J.L. Port, B. Stiles, S. Sukumar, N.K. Altorki, S. Rafii, and V. Mittal. 2012. Myeloid progenitor cells in the premetastatic lung promote metastases by inducing mesenchymal to epithelial transition. *Cancer research*. 72:1384-1394.

Garcia, F., Y. Lepelletier, S. Smaniotto, R. Hadj-Slimane, M. Dardenne, O. Hermine, and W. Savino. 2012. Inhibitory effect of semaphorin-3A, a known axon guidance molecule, in the human thymocyte migration induced by CXCL12. *J Leukoc Biol*. 91:7-13.

Geiger, B., A. Bershadsky, R. Pankov, and K.M. Yamada. 2001. Transmembrane crosstalk between the extracellular matrix--cytoskeleton crosstalk. *Nature reviews. Molecular cell biology*. 2:793-805.

Geissmann, F., M.G. Manz, S. Jung, M.H. Sieweke, M. Merad, and K. Ley. 2010. Development of monocytes, macrophages, and dendritic cells. *Science*. 327:656-661.

Gerber, H.P., A. McMurtrey, J. Kowalski, M. Yan, B.A. Keyt, V. Dixit, and N. Ferrara. 1998. Vascular endothelial growth factor regulates endothelial cell survival through the phosphatidylinositol 3'-kinase/Akt signal transduction pathway. Requirement for Flk-1/KDR activation. *The Journal of biological chemistry*. 273:30336-30343.

Germain, M., A. De Arcangelis, S.D. Robinson, M. Baker, B. Tavora, G. D'Amico, R. Silva, V. Kostourou, L.E. Reynolds, A. Watson, J.L. Jones, E. Georges-Labouesse, and K. Hodivala-Dilke. 2009. Genetic ablation of the alpha 6-integrin subunit in Tie1Cre mice enhances tumour angiogenesis. *J Pathol*.

Ginsberg, M.H., A. Partridge, and S.J. Shattil. 2005. Integrin regulation. *Curr Opin Cell Biol*. 17:509-516.

Glodek, A.M., Y. Le, D.M. Dykxhoorn, S.Y. Park, G. Mostoslavsky, R. Mulligan, J. Lieberman, H.E. Beggs, M. Honczarenko, and L.E. Silberstein. 2007. Focal adhesion kinase is required for CXCL12-induced chemotactic and pro-adhesive responses in hematopoietic precursor cells. *Leukemia*. 21:1723-1732.

Golubovskaya, V., A. Kaur, and W. Cance. 2004. Cloning and characterization of the promoter region of human focal adhesion kinase gene: nuclear factor kappa B and p53 binding sites. *Biochim Biophys Acta*. 1678:111-125.

Golubovskaya, V.M., and W.G. Cance. 2011. FAK and p53 Protein Interactions. *Anti-cancer agents in medicinal chemistry*. 11:617-619.

Golubovskaya, V.M., R. Finch, and W.G. Cance. 2005. Direct interaction of the N-terminal domain of focal adhesion kinase with the N-terminal transactivation domain of p53. *The Journal of biological chemistry*. 280:25008-25021.

Golubovskaya, V.M., R. Finch, F. Kweh, N.A. Massoll, M. Campbell-Thompson, M.R. Wallace, and W.G. Cance. 2008. p53 regulates FAK expression in human tumor cells. *Mol Carcinog*. 47:373-382.

Gothert, J.R., S.E. Gustin, J.A. van Eekelen, U. Schmidt, M.A. Hall, S.M. Jane, A.R. Green, B. Gottgens, D.J. Izon, and C.G. Begley. 2004. Genetically tagging endothelial cells

in vivo: bone marrow derived cells do not contribute to tumor endothelium. *Blood*. 104:1769-1777.

Graham, K., K. Moran-Jones, O.J. Sansom, V.G. Brunton, and M.C. Frame. 2011. FAK deletion promotes p53-mediated induction of p21, DNA-damage responses and radio-resistance in advanced squamous cancer cells. *PloS one*. 6:e27806.

Greco, F.A., and J.D. Hainsworth. 2009. Introduction: unknown primary cancer. *Semin Oncol*. 36:6-7.

Gruber, G., J. Hess, C. Stiefel, D.M. Aebersold, Y. Zimmer, R.H. Greiner, U. Studer, H.J. Altermatt, R. Hlushchuk, and V. Djonov. 2005. Correlation between the tumoral expression of beta3-integrin and outcome in cervical cancer patients who had undergone radiotherapy. *British journal of cancer*. 92:41-46.

Guerra, C., N. Mijimolle, A. Dhawahir, P. Dubus, M. Barradas, M. Serrano, V. Campuzano, and M. Barbacid. 2003. Tumor induction by an endogenous K-ras oncogene is highly dependent on cellular context. *Cancer Cell*. 4:111-120.

Gupta, K., S. Kshirsagar, W. Li, L. Gui, S. Ramakrishnan, P. Gupta, P.Y. Law, and R.P. Hebbel. 1999. VEGF prevents apoptosis of human microvascular endothelial cells via opposing effects on MAPK/ERK and SAPK/JNK signaling. *Experimental cell research*. 247:495-504.

Halder, J., Y.G. Lin, W.M. Merritt, W.A. Spannuth, A.M. Nick, T. Honda, A.A. Kamat, L.Y. Han, T.J. Kim, C. Lu, A.M. Tari, W. Bornmann, A. Fernandez, G. Lopez-Berestein, and A.K. Sood. 2007. Therapeutic efficacy of a novel focal adhesion kinase inhibitor TAE226 in ovarian carcinoma. *Cancer research*. 67:10976-10983.

Hamaguchi, I., X.L. Huang, N. Takakura, J. Tada, Y. Yamaguchi, H. Kodama, and T. Suda. 1999. In vitro hematopoietic and endothelial cell development from cells expressing TEK receptor in murine aorta-gonad-mesonephros region. *Blood*. 93:1549-1556.

Hanahan, D. 1985. Heritable formation of pancreatic beta-cell tumours in transgenic mice expressing recombinant insulin/simian virus 40 oncogenes. *Nature*. 315:115-122.

Hanahan, D., and L.M. Coussens. 2012. Accessories to the crime: functions of cells recruited to the tumor microenvironment. *Cancer Cell*. 21:309-322.

Hanahan, D., and R.A. Weinberg. 2000. The hallmarks of cancer. *Cell*. 100:57-70.

Hanahan, D., and R.A. Weinberg. 2011. Hallmarks of cancer: the next generation. *Cell*. 144:646-674.

Haruta, H., Y. Nagata, and K. Todokoro. 2001. Role of Flk-1 in mouse hematopoietic stem cells. *FEBS letters*. 507:45-48.

Haskell, H., M. Natarajan, T.P. Hecker, Q. Ding, J. Stewart, Jr., J.R. Grammer, and C.L. Gladson. 2003. Focal adhesion kinase is expressed in the angiogenic blood vessels of malignant astrocytic tumors in vivo and promotes capillary tube formation of brain microvascular endothelial cells. *Clinical cancer research : an official journal of the American Association for Cancer Research*. 9:2157-2165.

Hattori, K., B. Heissig, Y. Wu, S. Dias, R. Tejada, B. Ferris, D.J. Hicklin, Z. Zhu, P. Bohlen, L. Witte, J. Hendrikx, N.R. Hackett, R.G. Crystal, M.A. Moore, Z. Werb, D. Lyden, and S. Rafii. 2002. Placental growth factor reconstitutes hematopoiesis by recruiting VEGFR1(+) stem cells from bone-marrow microenvironment. *Nature medicine*. 8:841-849.

Hauck, C.R., D.A. Hsia, D. Ilic, and D.D. Schlaepfer. 2002. v-Src SH3-enhanced interaction with focal adhesion kinase at beta 1 integrin-containing invadopodia promotes cell invasion. *The Journal of biological chemistry*. 277:12487-12490.

Hauck, C.R., D.J. Sieg, D.A. Hsia, J.C. Loftus, W.A. Gaarde, B.P. Monia, and D.D. Schlaepfer. 2001. Inhibition of focal adhesion kinase expression or activity disrupts epidermal growth factor-stimulated signaling promoting the migration of invasive human carcinoma cells. *Cancer research*. 61:7079-7090.

Hellstrom, M., M. Kalen, P. Lindahl, A. Abramsson, and C. Betsholtz. 1999. Role of PDGF-B and PDGFR-beta in recruitment of vascular smooth muscle cells and pericytes

during embryonic blood vessel formation in the mouse. *Development*. 126:3047-3055.

Hercus, T.R., D. Thomas, M.A. Guthridge, P.G. Ekert, J. King-Scott, M.W. Parker, and A.F. Lopez. 2009. The granulocyte-macrophage colony-stimulating factor receptor: linking its structure to cell signaling and its role in disease. *Blood*. 114:1289-1298.

Hewitt, H.B., and E.R. Blake. 1968. The growth of transplanted murine tumours in pre-irradiated sites. *British journal of cancer*. 22:808-824.

Hildebrand, J.D., M.D. Schaller, and J.T. Parsons. 1993. Identification of sequences required for the efficient localization of the focal adhesion kinase, pp125FAK, to cellular focal adhesions. *The Journal of cell biology*. 123:993-1005.

Hildebrand, J.D., M.D. Schaller, and J.T. Parsons. 1995. Paxillin, a tyrosine phosphorylated focal adhesion-associated protein binds to the carboxyl terminal domain of focal adhesion kinase. *Mol Biol Cell*. 6:637-647.

Hinton, C.V., S. Avraham, and H.K. Avraham. 2010. Role of the CXCR4/CXCL12 signaling axis in breast cancer metastasis to the brain. *Clinical & experimental metastasis*. 27:97-105.

Hiratsuka, S., S. Goel, W.S. Kamoun, Y. Maru, D. Fukumura, D.G. Duda, and R.K. Jain. 2011. Endothelial focal adhesion kinase mediates cancer cell homing to disCrete regions of the lungs via E-selectin up-regulation. *Proceedings of the National Academy of Sciences of the United States of America*. 108:3725-3730.

Hiratsuka, S., K. Nakamura, S. Iwai, M. Murakami, T. Itoh, H. Kijima, J.M. Shipley, R.M. Senior, and M. Shibuya. 2002. MMP9 induction by vascular endothelial growth factor receptor-1 is involved in lung-specific metastasis. *Cancer Cell*. 2:289-300.

Hiratsuka, S., A. Watanabe, H. Aburatani, and Y. Maru. 2006. Tumour-mediated upregulation of chemoattractants and recruitment of myeloid cells predetermines lung metastasis. *Nat Cell Biol*. 8:1369-1375.

Hodivala-Dilke, K.M., A.R. Reynolds, and L.E. Reynolds. 2003. Integrins in angiogenesis: multitalented molecules in a balancing act. *Cell Tissue Res*. 314:131-144.

Hosotani, R., M. Kawaguchi, T. Masui, T. Koshiba, J. Ida, K. Fujimoto, M. Wada, R. Doi, and M. Imamura. 2002. Expression of integrin alphaVbeta3 in pancreatic carcinoma: relation to MMP-2 activation and lymph node metastasis. Pancreas. 25:e30-35.

Hsia, D.A., S.K. Mitra, C.R. Hauck, D.N. Streblow, J.A. Nelson, D. Ilic, S. Huang, E. Li, G.R. Nemerow, J. Leng, K.S. Spencer, D.A. Cheresh, and D.D. Schlaepfer. 2003. Differential regulation of cell motility and invasion by FAK. *The Journal of cell biology*. 160:753-767.

Huh, S.J., S. Liang, A. Sharma, C. Dong, and G.P. Robertson. 2010. Transiently entrapped circulating tumor cells interact with neutrophils to facilitate lung metastasis development. *Cancer research*. 70:6071-6082.

Hurwitz, H., L. Fehrenbacher, W. Novotny, T. Cartwright, J. Hainsworth, W. Heim, J. Berlin, A. Baron, S. Griffing, E. Holmgren, N. Ferrara, G. Fyfe, B. Rogers, R. Ross, and F. Kabbinavar. 2004. Bevacizumab plus irinotecan, fluorouracil, and leucovorin for metastatic colorectal cancer. *N Engl J Med*. 350:2335-2342.

Husemann, Y., J.B. Geigl, F. Schubert, P. Musiani, M. Meyer, E. Burghart, G. Forni, R. Eils, T. Fehm, G. Riethmuller, and C.A. Klein. 2008. Systemic spread is an early step in breast cancer. *Cancer Cell*. 13:58-68.

Hynes, R.O. 1999. Cell adhesion: old and new questions. *Trends Cell Biol*. 9:M33-37.

Hynes, R.O. 2002. Integrins: bidirectional, allosteric signaling machines. *Cell*. 110:673-687.

Ilic, D., Y. Furuta, S. Kanazawa, N. Takeda, K. Sobue, N. Nakatsuji, S. Nomura, J. Fujimoto, M. Okada, and T. Yamamoto. 1995. Reduced cell motility and enhanced focal adhesion contact formation in cells from FAK deficient mice. *Nature*. 377:539-544.

Jager, R., J. Maurer, A. Jacob, and H. Schorle. 2004. Cell type-specific conditional regulation of the c-myc proto-oncogene by combining Cre/loxP recombination and tamoxifen-mediated activation. *Genesis*. 38:145-150.

Jain, R.K. 2005. Normalization of tumor vasculature: an emerging concept in antiangiogenic therapy. *Science*. 307:58-62.

Jensen, R.L., B.T. Ragel, K. Whang, and D. Gillespie. 2006. Inhibition of hypoxia inducible factor-1alpha (HIF-1alpha) decreases vascular endothelial growth factor (VEGF) seCretion and tumor growth in malignant gliomas. *J Neurooncol*. 78:233-247.

Jin, D.K., K. Shido, H.G. Kopp, I. Petit, S.V. Shmelkov, L.M. Young, A.T. Hooper, H. Amano, S.T. Avecilla, B. Heissig, K. Hattori, F. Zhang, D.J. Hicklin, Y. Wu, Z. Zhu, A. Dunn, H. Salari, Z. Werb, N.R. Hackett, R.G. Crystal, D. Lyden, and S. Rafii. 2006a. Cytokine-mediated deployment of SDF-1 induces revascularization through recruitment of CXCR4+ hemangiocytes. *Nature medicine*. 12:557-567.

Jin, H., A. Aiyer, J. Su, P. Borgstrom, D. Stupack, M. Friedlander, and J. Varner. 2006b. A homing mechanism for bone marrow derived progenitor cell recruitment to the neovasculature. *The Journal of clinical investigation*. 116:652-662.

Jin, H., J. Su, B. Garmy-Susini, J. Kleeman, and J. Varner. 2006c. Integrin alpha4beta1 promotes monocyte trafficking and angiogenesis in tumors. *Cancer research*. 66:2146-2152.

Jirtle, R., J.H. Rankin, and K.H. Clifton. 1978. Effect of x-irradiation of tumour bed on tumour blood flow and vascular response to drugs. *British journal of cancer*. 37:1033-1038.

Jones, G., J. Machado, Jr., M. Tolnay, and A. Merlo. 2001. PTEN-independent induction of caspase-mediated cell death and reduced invasion by the focal adhesion targeting domain (FAT) in human astrocytic brain tumors which highly express focal adhesion kinase (FAK). *Cancer research*. 61:5688-5691.

Joyce, J.A., and J.W. Pollard. 2009. Microenvironmental regulation of metastasis. *Nat Rev Cancer*. 9:239-252.

Judson, P.L., X. He, W.G. Cance, and L. Van Le. 1999. Overexpression of focal adhesion kinase, a protein tyrosine kinase, in ovarian carcinoma. *Cancer*. 86:1551-1556.

Kaipainen, A., J. Korhonen, T. Mustonen, V.W. van Hinsbergh, G.H. Fang, D. Dumont, M. Breitman, and K. Alitalo. 1995. Expression of the fms-like tyrosine kinase 4 gene becomes restricted to lymphatic endothelium during development. *Proceedings of the National Academy of Sciences of the United States of America*. 92:3566-3570.

Kalluri, R. 2003. Basement membranes: structure, assembly and role in tumour angiogenesis. *Nat Rev Cancer*. 3:422-433.

Kanazawa, S., D. Ilic, M. Hashiyama, T. Noumura, T. Yamamoto, T. Suda, and S. Aizawa. 1996. p59fyn-p125FAK cooperation in development of CD4+CD8+ thymocytes. *Blood*. 87:865-870.

Kanner, S.B., A.B. Reynolds, R.R. Vines, and J.T. Parsons. 1990. Monoclonal antibodies to individual tyrosine-phosphorylated protein substrates of oncogene-encoded tyrosine kinases. *Proceedings of the National Academy of Sciences of the United States of America*. 87:3328-3332.

Kaplan, R.N., R.D. Riba, S. Zacharoulis, A.H. Bramley, L. Vincent, C. Costa, D.D. MacDonald, D.K. Jin, K. Shido, S.A. Kerns, Z. Zhu, D. Hicklin, Y. Wu, J.L. Port, N. Altorki, E.R. Port, D. Ruggero, S.V. Shmelkov, K.K. Jensen, S. Rafii, and D. Lyden. 2005. VEGFR1-positive haematopoietic bone marrow progenitors initiate the pre-metastatic niche. *Nature*. 438:820-827.

Karsan, A., E. Yee, G.G. Poirier, P. Zhou, R. Craig, and J.M. Harlan. 1997. Fibroblast growth factor-2 inhibits endothelial cell apoptosis by Bcl-2-dependent and independent mechanisms. *The American journal of pathology*. 151:1775-1784.

Kasorn, A., P. Alcaide, Y. Jia, K.K. Subramanian, B. Sarraj, Y. Li, F. Loison, H. Hattori, L.E. Silberstein, W.F. Luscinskas, and H.R. Luo. 2009. Focal adhesion kinase regulates pathogen-killing capability and life span of neutrophils via mediating both adhesion-dependent and -independent cellular signals. *J Immunol*. 183:1032-1043.

Keck, P.J., S.D. Hauser, G. Krivi, K. Sanzo, T. Warren, J. Feder, and D.T. Connolly. 1989. Vascular permeability factor, an endothelial cell mitogen related to PDGF. *Science*. 246:1309-1312.

Khajah, M., B. Millen, D.C. Cara, C. Waterhouse, and D.M. McCafferty. 2011. Granulocyte-macrophage colony-stimulating factor (GM-CSF): a chemoattractive agent for murine leukocytes in vivo. *J Leukoc Biol*. 89:945-953.

Kim, H.K., M. De La Luz Sierra, C.K. Williams, A.V. Gulino, and G. Tosato. 2006. G-CSF down-regulation of CXCR4 expression identified as a mechanism for mobilization of myeloid cells. *Blood*. 108:812-820.

Kim, I., O.H. Yilmaz, and S.J. Morrison. 2005. CD144 (VE-cadherin) is transiently expressed by fetal liver hematopoietic stem cells. *Blood*. 106:903-905.

Kim, S., K. Bell, S.A. Mousa, and J.A. Varner. 2000. Regulation of angiogenesis in vivo by ligation of integrin alpha5beta1 with the central cell-binding domain of fibronectin. *The American journal of pathology*. 156:1345-1362.

Klingbeil, C.K., C.R. Hauck, D.A. Hsia, K.C. Jones, S.R. Reider, and D.D. Schlaepfer. 2001. Targeting Pyk2 to beta 1-integrin-containing focal contacts rescues fibronectin-stimulated signaling and haptotactic motility defects of focal adhesion kinase-null cells. *The Journal of cell biology*. 152:97-110.

Ko, B.S., T.C. Chang, C.H. Chen, C.C. Liu, C.C. Kuo, C. Hsu, Y.C. Shen, T.L. Shen, V.M. Golubovskaya, C.C. Chang, S.K. Shyue, and J.Y. Liou. 2010. Bortezomib suppresses focal adhesion kinase expression via interrupting nuclear factor-kappa B. *Life Sci*. 86:199-206.

Kortylewski, M., M. Kujawski, T. Wang, S. Wei, S. Zhang, S. Pilon-Thomas, G. Niu, H. Kay, J. Mule, W.G. Kerr, R. Jove, D. Pardoll, and H. Yu. 2005. Inhibiting Stat3 signaling in the hematopoietic system elicits multicomponent antitumor immunity. *Nature medicine*. 11:1314-1321.

Kren, A., V. Baeriswyl, F. Lehembre, C. Wunderlin, K. Strittmatter, H. Antoniadis, R. Fassler, U. Cavallaro, and G. Christofori. 2007. Increased tumor cell dissemination and cellular senescence in the absence of beta1-integrin function. *EMBO J*. 26:2832-2842.

Kume, A., H. Nishiura, J. Suda, and T. Suda. 1997. Focal adhesion kinase upregulated by granulocyte-macrophage colony-stimulating factor but not by interleukin-3 in differentiating myeloid cells. *Blood*. 89:3434-3442.

Kurio, N., T. Shimo, T. Fukazawa, M. Takaoka, T. Okui, N.M. Hassan, T. Honami, S. Hatakeyama, M. Ikeda, Y. Naomoto, and A. Sasaki. 2011. Anti-tumor effect in human breast cancer by TAE226, a dual inhibitor for FAK and IGF-IR in vitro and in vivo. *Experimental cell research*. 317:1134-1146.

Lark, A.L., C.A. Livasy, L. Dressler, D.T. Moore, R.C. Millikan, J. Geradts, M. Iacocca, D. Cowan, D. Little, R.J. Craven, and W. Cance. 2005. High focal adhesion kinase expression in invasive breast carcinomas is associated with an aggressive phenotype. *Mod Pathol*. 18:1289-1294.

Larrivee, B., K. Niessen, I. Pollet, S.Y. Corbel, M. Long, F.M. Rossi, P.L. Olive, and A. Karsan. 2005. Minimal contribution of marrow-derived endothelial precursors to tumor vasculature. *J Immunol*. 175:2890-2899.

Larsen, M., V.V. Artym, J.A. Green, and K.M. Yamada. 2006. The matrix reorganized: extracellular matrix remodeling and integrin signaling. *Curr Opin Cell Biol*. 18:463-471.

Lawler, J. 2002. Thrombospondin-1 as an endogenous inhibitor of angiogenesis and tumor growth. *Journal of cellular and molecular medicine*. 6:1-12.

Le Blanc, K., and D. Mougiakakos. 2012. Multipotent mesenchymal stromal cells and the innate immune system. *Nat Rev Immunol*. 12:383-396.

Leung, D.W., G. Cachianes, W.J. Kuang, D.V. Goeddel, and N. Ferrara. 1989. Vascular endothelial growth factor is a secreted angiogenic mitogen. *Science*. 246:1306-1309.

Levesque, J.P., J. Hendy, Y. Takamatsu, P.J. Simmons, and L.J. Bendall. 2003. Disruption of the CXCR4/CXCL12 chemotactic interaction during hematopoietic stem cell mobilization induced by GCSF or cyclophosphamide. *The Journal of clinical investigation*. 111:187-196.

Li, H., Y. Han, Q. Guo, M. Zhang, and X. Cao. 2009. Cancer-expanded myeloid-derived suppressor cells induce anergy of NK cells through membrane-bound TGF-beta 1. *J Immunol*. 182:240-249.

Li, W., S.A. Johnson, W.C. Shelley, and M.C. Yoder. 2004. Hematopoietic stem cell repopulating ability can be maintained in vitro by some primary endothelial cells. *Experimental hematology*. 32:1226-1237.

Liao, D., and R.S. Johnson. 2007. Hypoxia: a key regulator of angiogenesis in cancer. *Cancer metastasis reviews*. 26:281-290.

Lietha, D., X. Cai, D.F. Ceccarelli, Y. Li, M.D. Schaller, and M.J. Eck. 2007. Structural basis for the autoinhibition of focal adhesion kinase. *Cell*. 129:1177-1187.

Lim, J.A., S.H. Hwang, M.J. Kim, S.S. Kim, and H.S. Kim. 2012. N-terminal cleavage fragment of focal adhesion kinase is required to activate survival signaling pathway in cultured myoblasts under oxidative stress. *The FEBS journal*.

Lim, S.T., X.L. Chen, Y. Lim, D.A. Hanson, T.T. Vo, K. Howerton, N. Larocque, S.J. Fisher, D.D. Schlaepfer, and D. Ilic. 2008a. Nuclear FAK promotes cell proliferation and survival through FERM-enhanced p53 degradation. *Mol Cell*. 29:9-22.

Lim, S.T., D. Mikolon, D.G. Stupack, and D.D. Schlaepfer. 2008b. FERM control of FAK function: implications for cancer therapy. *Cell Cycle*. 7:2306-2314.

Lim, Y., I. Han, J. Jeon, H. Park, Y.Y. Bahk, and E.S. Oh. 2004. Phosphorylation of focal adhesion kinase at tyrosine 861 is crucial for Ras transformation of fibroblasts. *The Journal of biological chemistry*. 279:29060-29065.

Liotta, L.A. 1986. Tumor invasion and metastases--role of the extracellular matrix: Rhoads Memorial Award lecture. *Cancer research*. 46:1-7.

Liu, C., S. Yu, J. Kappes, J. Wang, W.E. Grizzle, K.R. Zinn, and H.G. Zhang. 2007. Expansion of spleen myeloid suppressor cells represses NK cell cytotoxicity in tumor-bearing host. *Blood*. 109:4336-4342.

Lopez, T., and D. Hanahan. 2002. Elevated levels of IGF-1 receptor convey invasive and metastatic capability in a mouse model of pancreatic islet tumorigenesis. *Cancer Cell*. 1:339-353.

Lu, J., Y. Sun, C. Nombela-Arrieta, K.P. Du, S.Y. Park, L. Chai, C. Walkley, H.R. Luo, and L.E. Silberstein. 2012. Fak depletion in both hematopoietic and nonhematopoietic niche cells leads to hematopoietic stem cell expansion. *Experimental hematology*. 40:307-317 e303.

Lu, X., E. Mu, Y. Wei, S. Riethdorf, Q. Yang, M. Yuan, J. Yan, Y. Hua, B.J. Tiede, X. Lu, B.G. Haffty, K. Pantel, J. Massague, and Y. Kang. 2011. VCAM-1 promotes osteolytic expansion of indolent bone micrometastasis of breast cancer by engaging alpha4beta1-positive osteoclast progenitors. *Cancer Cell*. 20:701-714.

Lu, Y., Z. Cai, G. Xiao, Y. Liu, E.T. Keller, Z. Yao, and J. Zhang. 2007. CCR2 expression correlates with prostate cancer progression. *Journal of cellular biochemistry*. 101:676-685.

Lu, Z., G. Jiang, P. Blume-Jensen, and T. Hunter. 2001. Epidermal growth factor-induced tumor cell invasion and metastasis initiated by dephosphorylation and downregulation of focal adhesion kinase. *Mol Cell Biol*. 21:4016-4031.

Luo, M., H. Fan, T. Nagy, H. Wei, C. Wang, S. Liu, M.S. Wicha, and J.L. Guan. 2009. Mammary epithelial-specific ablation of the focal adhesion kinase suppresses mammary tumorigenesis by affecting mammary cancer stem/progenitor cells. *Cancer research*. 69:466-474.

Luzzi, K.J., I.C. MacDonald, E.E. Schmidt, N. Kerkvliet, V.L. Morris, A.F. Chambers, and A.C. Groom. 1998. Multistep nature of metastatic inefficiency: dormancy of solitary

cells after successful extravasation and limited survival of early micrometastases. *The American journal of pathology*. 153:865-873.

Lyden, D., K. Hattori, S. Dias, C. Costa, P. Blaikie, L. Butros, A. Chadburn, B. Heissig, W. Marks, L. Witte, Y. Wu, D. Hicklin, Z. Zhu, N.R. Hackett, R.G. Crystal, M.A. Moore, K.A. Hajjar, K. Manova, R. Benezra, and S. Rafii. 2001. Impaired recruitment of bone-marrow-derived endothelial and hematopoietic precursor cells blocks tumor angiogenesis and growth. *Nature medicine*. 7:1194-1201.

Lynch, L., P.I. Vodyanik, D. Boettiger, and M.A. Guvakova. 2005. Insulin-like growth factor I controls adhesion strength mediated by alpha5beta1 integrins in motile carcinoma cells. *Mol Biol Cell*. 16:51-63.

Malanchi, I., A. Santamaria-Martinez, E. Susanto, H. Peng, H.A. Lehr, J.F. Delaloye, and J. Huelsken. 2012. Interactions between cancer stem cells and their niche govern metastatic colonization. *Nature*. 481:85-89.

Martinez, P., and M.A. Blasco. 2011. Telomeric and extra-telomeric roles for telomerase and the telomere-binding proteins. *Nat Rev Cancer*. 11:161-176.

Matthews, W., C.T. Jordan, M. Gavin, N.A. Jenkins, N.G. Copeland, and I.R. Lemischka. 1991. A receptor tyrosine kinase cDNA isolated from a population of enriched primitive hematopoietic cells and exhibiting close genetic linkage to c-kit. *Proceedings of the National Academy of Sciences of the United States of America*. 88:9026-9030.

Max, R., R.R. Gerritsen, P.T. Nooijen, S.L. Goodman, A. Sutter, U. Keilholz, D.J. Ruiter, and R.M. De Waal. 1997. Immunohistochemical analysis of integrin alpha vbeta3 expression on tumor-associated vessels of human carcinomas. *International journal of cancer. Journal international du cancer*. 71:320-324.

Mazo, I.B., J.C. Gutierrez-Ramos, P.S. Frenette, R.O. Hynes, D.D. Wagner, and U.H. von Andrian. 1998. Hematopoietic progenitor cell rolling in bone marrow microvessels: parallel contributions by endothelial selectins and vascular cell adhesion molecule 1. *The Journal of experimental medicine*. 188:465-474.

Mazzieri, R., F. Pucci, D. Moi, E. Zonari, A. Ranghetti, A. Berti, L.S. Politi, B. Gentner, J.L. Brown, L. Naldini, and M. De Palma. 2011. Targeting the ANG2/TIE2 axis inhibits tumor growth and metastasis by impairing angiogenesis and disabling rebounds of proangiogenic myeloid cells. *Cancer Cell*. 19:512-526.

Mazzoni, A., V. Bronte, A. Visintin, J.H. Spitzer, E. Apolloni, P. Serafini, P. Zanovello, and D.M. Segal. 2002. Myeloid suppressor lines inhibit T cell responses by an NO-dependent mechanism. *J Immunol*. 168:689-695.

McLean, G.W., N.H. Komiyama, B. Serrels, H. Asano, L. Reynolds, F. Conti, K. Hodivala-Dilke, D. Metzger, P. Chambon, S.G. Grant, and M.C. Frame. 2004. Specific deletion of focal adhesion kinase suppresses tumor formation and blocks malignant progression. *Genes Dev*. 18:2998-3003.

Mendez-Ferrer, S., T.V. Michurina, F. Ferraro, A.R. Mazloom, B.D. Macarthur, S.A. Lira, D.T. Scadden, A. Ma'ayan, G.N. Enikolopov, and P.S. Frenette. 2010. Mesenchymal and haematopoietic stem cells form a unique bone marrow niche. *Nature*. 466:829-834.

Meng, S., D. Tripathy, E.P. Frenkel, S. Shete, E.Z. Naftalis, J.F. Huth, P.D. Beitsch, M. Leitch, S. Hoover, D. Euhus, B. Haley, L. Morrison, T.P. Fleming, D. Herlyn, L.W. Terstappen, T. Fehm, T.F. Tucker, N. Lane, J. Wang, and J.W. Uhr. 2004. Circulating tumor cells in patients with breast cancer dormancy. *Clinical cancer research : an official journal of the American Association for Cancer Research*. 10:8152-8162.

Mercier, F.E., C. Ragu, and D.T. Scadden. 2012. The bone marrow at the crossroads of blood and immunity. *Nat Rev Immunol*. 12:49-60.

Miao, Z., K.E. Luker, B.C. Summers, R. Berahovich, M.S. Bhojani, A. Rehemtulla, C.G. Kleer, J.J. Essner, A. Nasevicius, G.D. Luker, M.C. Howard, and T.J. Schall. 2007. CXCR7 (RDC1) promotes breast and lung tumor growth in vivo and is expressed on

tumor-associated vasculature. *Proceedings of the National Academy of Sciences of the United States of America*. 104:15735-15740.

Milas, L., N. Hunter, and L.J. Peters. 1987. The tumor bed effect: dependence of tumor take, growth rate, and metastasis on the time interval between irradiation and tumor cell transplantation. *International journal of radiation oncology, biology, physics*. 13:379-383.

Mishra, P.J., R. Humeniuk, D.J. Medina, G. Alexe, J.P. Mesirov, S. Ganesan, J.W. Glod, and D. Banerjee. 2008. Carcinoma-associated fibroblast-like differentiation of human mesenchymal stem cells. *Cancer research*. 68:4331-4339.

Mitra, S.K., D.A. Hanson, and D.D. Schlaepfer. 2005. Focal adhesion kinase: in command and control of cell motility. *Nature reviews. Molecular cell biology*. 6:56-68.

Mitra, S.K., S.T. Lim, A. Chi, and D.D. Schlaepfer. 2006a. Intrinsic focal adhesion kinase activity controls orthotopic breast carcinoma metastasis via the regulation of urokinase plasminogen activator expression in a syngeneic tumor model. *Oncogene*. 25:4429-4440.

Mitra, S.K., D. Mikolon, J.E. Molina, D.A. Hsia, D.A. Hanson, A. Chi, S.T. Lim, J.A. Bernard-Trifilo, D. Ilic, D.G. Stupack, D.A. Cheresh, and D.D. Schlaepfer. 2006b. Intrinsic FAK activity and Y925 phosphorylation facilitate an angiogenic switch in tumors. *Oncogene*. 25:5969-5984.

Mitra, S.K., and D.D. Schlaepfer. 2006. Integrin-regulated FAK Src signaling in normal and cancer cells. *Curr Opin Cell Biol*. 18:516-523.

Mombaerts, P., J. Iacomini, R.S. Johnson, K. Herrup, S. Tonegawa, and V.E. Papaioannou. 1992. RAG-1-deficient mice have no mature B and T lymphocytes. *Cell*. 68:869-877.

Muller, A., B. Homey, H. Soto, N. Ge, D. Catron, M.E. Buchanan, T. McClanahan, E. Murphy, W. Yuan, S.N. Wagner, J.L. Barrera, A. Mohar, E. Verastegui, and A. Zlotnik. 2001. Involvement of chemokine receptors in breast cancer metastasis. *Nature*. 410:50-56.

Muramatsu, M., S. Yamamoto, T. Osawa, and M. Shibuya. 2010. Vascular endothelial growth factor receptor-1 signaling promotes mobilization of macrophage lineage cells from bone marrow and stimulates solid tumor growth. *Cancer research*. 70:8211-8221.

Narayana, A., P. Kelly, J. Golfinos, E. Parker, G. Johnson, E. Knopp, D. Zagzag, I. Fischer, S. Raza, P. Medabalmi, P. Eagan, and M.L. Gruber. 2009. Antiangiogenic therapy using bevacizumab in recurrent high-grade glioma: impact on local control and patient survival. *J Neurosurg*. 110:173-180.

Naumov, G.N., L.A. Akslen, and J. Folkman. 2006. Role of angiogenesis in human tumor dormancy: animal models of the angiogenic switch. *Cell Cycle*. 5:1779-1787.

Naumov, G.N., J.L. Townson, I.C. MacDonald, S.M. Wilson, V.H. Bramwell, A.C. Groom, and A.F. Chambers. 2003. Ineffectiveness of doxorubicin treatment on solitary dormant mammary carcinoma cells or late-developing metastases. *Breast Cancer Res Treat*. 82:199-206.

Nefedova, Y., M. Huang, S. Kusmartsev, R. Bhattacharya, P. Cheng, R. Salup, R. Jove, and D. Gabrilovich. 2004. Hyperactivation of STAT3 is involved in abnormal differentiation of dendritic cells in cancer. *J Immunol*. 172:464-474.

Nelson, A.R., B. Fingleton, M.L. Rothenberg, and L.M. Matrisian. 2000. Matrix metalloproteinases: biologic activity and clinical implications. *J Clin Oncol*. 18:1135-1149.

Neufeld, G., T. Cohen, S. Gengrinovitch, and Z. Poltorak. 1999. Vascular endothelial growth factor (VEGF) and its receptors. *Faseb J*. 13:9-22.

Nolan, K., J. Lacoste, and J.T. Parsons. 1999. Regulated expression of focal adhesion kinase-related nonkinase, the autonomously expressed C-terminal domain of focal adhesion kinase. *Mol Cell Biol*. 19:6120-6129.

Nozawa, H., C. Chiu, and D. Hanahan. 2006. Infiltrating neutrophils mediate the initial angiogenic switch in a mouse model of multistage carcinogenesis. *Proceedings of the National Academy of Sciences of the United States of America*. 103:12493-12498.

O'Brien, C.A., A. Pollett, S. Gallinger, and J.E. Dick. 2007. A human colon cancer cell capable of initiating tumour growth in immunodeficient mice. *Nature*. 445:106-110.

Okigaki, M., C. Davis, M. Falasca, S. Harroch, D.P. Felsenfeld, M.P. Sheetz, and J. Schlessinger. 2003. Pyk2 regulates multiple signaling events crucial for macrophage morphology and migration. *Proceedings of the National Academy of Sciences of the United States of America*. 100:10740-10745.

Ortega, N., F. Jonca, S. Vincent, C. Favard, M.M. Ruchoux, and J. Plouet. 1997. Systemic activation of the vascular endothelial growth factor receptor KDR/flk-1 selectively triggers endothelial cells with an angiogenic phenotype. *The American journal of pathology*. 151:1215-1224.

Ossovskaya, V., S.T. Lim, N. Ota, D.D. Schlaepfer, and D. Ilic. 2008. FAK nuclear export signal sequences. *FEBS letters*. 582:2402-2406.

Ostrand-Rosenberg, S., and P. Sinha. 2009. Myeloid-derived suppressor cells: linking inflammation and cancer. *J Immunol*. 182:4499-4506.

Owen, J.D., P.J. Ruest, D.W. Fry, and S.K. Hanks. 1999. Induced focal adhesion kinase (FAK) expression in FAK null cells enhances cell spreading and migration requiring both auto- and activation loop phosphorylation sites and inhibits adhesion-dependent tyrosine phosphorylation of Pyk2. *Mol Cell Biol*. 19:4806-4818.

Owen, K.A., F.J. Pixley, K.S. Thomas, M. Vicente-Manzanares, B.J. Ray, A.F. Horwitz, J.T. Parsons, H.E. Beggs, E.R. Stanley, and A.H. Bouton. 2007. Regulation of lamellipodial persistence, adhesion turnover, and motility in macrophages by focal adhesion kinase. *The Journal of cell biology*. 179:1275-1287.

Owens, L.V., L. Xu, G.A. Dent, X. Yang, G.C. Sturge, R.J. Craven, and W.G. Cance. 1996. Focal adhesion kinase as a marker of invasive potential in differentiated human thyroid cancer. *Annals of surgical oncology*. 3:100-105.

Paez-Ribes, M., E. Allen, J. Hudock, T. Takeda, H. Okuyama, F. Vinals, M. Inoue, G. Bergers, D. Hanahan, and O. Casanovas. 2009. Antiangiogenic therapy elicits malignant progression of tumors to increased local invasion and distant metastasis. *Cancer Cell*. 15:220-231.

Paget, S. 1889. The distribution of secondary growths in cancer of the breast. *Lancet*. 1:571-573.

Pai, R.K., A.H. Beck, J. Mitchem, D.C. Linehan, D.T. Chang, J.A. Norton, and R.K. Pai. 2011. Pattern of lymph node involvement and prognosis in pancreatic adenocarcinoma: direct lymph node invasion has similar survival to node-negative disease. *Am J Surg Pathol*. 35:228-234.

Pantel, K., R.H. Brakenhoff, and B. Brandt. 2008. Detection, clinical relevance and specific biological properties of disseminating tumour cells. *Nat Rev Cancer*. 8:329-340.

Papayannopoulou, T., G.V. Priestley, B. Nakamoto, V. Zafiropoulos, and L.M. Scott. 2001. Molecular pathways in bone marrow homing: dominant role of alpha(4)beta(1) over beta(2)-integrins and selectins. *Blood*. 98:2403-2411.

Park, J.H., B.L. Lee, J. Yoon, J. Kim, M.A. Kim, H.K. Yang, and W.H. Kim. 2010. Focal adhesion kinase (FAK) gene amplification and its clinical implications in gastric cancer. *Human pathology*. 41:1664-1673.

Parsons, S.A., R. Sharma, D.L. Roccamatisi, H. Zhang, B. Petri, P. Kubes, P. Colarusso, and K.D. Patel. 2012. Endothelial paxillin and focal adhesion kinase (FAK) play a critical role in neutrophil transmigration. *European journal of immunology*. 42:436-446.

Pear, W.S., and F. Radtke. 2003. Notch signaling in lymphopoiesis. *Semin Immunol*. 15:69-79.

Peng, X., H. Ueda, H. Zhou, T. Stokol, T.L. Shen, A. Alcaraz, T. Nagy, J.D. Vassalli, and J.L. Guan. 2004. Overexpression of focal adhesion kinase in vascular endothelial cells promotes angiogenesis in transgenic mice. *Cardiovascular research*. 64:421-430.

Perl, A.K., P. Wilgenbus, U. Dahl, H. Semb, and G. Christofori. 1998. A causal role for E-cadherin in the transition from adenoma to carcinoma. *Nature*. 392:190-193.

Peters, B.A., L.A. Diaz, K. Polyak, L. Meszler, K. Romans, E.C. Guinan, J.H. Antin, D. Myerson, S.R. Hamilton, B. Vogelstein, K.W. Kinzler, and C. Lengauer. 2005. Contribution of bone marrow derived endothelial cells to human tumor vasculature. *Nature medicine*. 11:261-262.

Petty, J.M., C.C. Lenox, D.J. Weiss, M.E. Poynter, and B.T. Suratt. 2009. Crosstalk between CXCR4/stromal derived factor-1 and VLA-4/VCAM-1 pathways regulates neutrophil retention in the bone marrow. *J Immunol*. 182:604-612.

Piccard, H., R.J. Muschel, and G. Opdenakker. 2012. On the dual roles and polarized phenotypes of neutrophils in tumor development and progression. *Crit Rev Oncol Hematol*. 82:296-309.

Polte, T.R., and S.K. Hanks. 1997. Complexes of focal adhesion kinase (FAK) and Crk-associated substrate (p130(Cas)) are elevated in cytoskeleton-associated fractions following adhesion and Src transformation. Requirements for Src kinase activity and FAK proline-rich motifs. *The Journal of biological chemistry*. 272:5501-5509.

Polte, T.R., A.J. Naftilan, and S.K. Hanks. 1994. Focal adhesion kinase is abundant in developing blood vessels and elevation of its phosphotyrosine content in vascular smooth muscle cells is a rapid response to angiotensin II. *Journal of cellular biochemistry*. 55:106-119.

Polyak, K., and R.A. Weinberg. 2009. Transitions between epithelial and mesenchymal states: acquisition of malignant and stem cell traits. *Nat Rev Cancer*. 9:265-273.

Provenzano, P.P., D.R. Inman, K.W. Eliceiri, H.E. Beggs, and P.J. Keely. 2008. Mammary epithelial-specific disruption of focal adhesion kinase retards tumor formation and metastasis in a transgenic mouse model of human breast cancer. *The American journal of pathology*. 173:1551-1565.

Qi, J.H., and L. Claesson-Welsh. 2001. VEGF-induced activation of phosphoinositide 3-kinase is dependent on focal adhesion kinase. *Experimental cell research*. 263:173-182.

Qian, B.Z., J. Li, H. Zhang, T. Kitamura, J. Zhang, L.R. Campion, E.A. Kaiser, L.A. Snyder, and J.W. Pollard. 2011. CCL2 recruits inflammatory monocytes to facilitate breast-tumour metastasis. *Nature*. 475:222-225.

Qian, B.Z., and J.W. Pollard. 2010. Macrophage diversity enhances tumor progression and metastasis. *Cell*. 141:39-51.

Rafii, S., D. Lyden, R. Benezra, K. Hattori, and B. Heissig. 2002. Vascular and haematopoietic stem cells: novel targets for anti-angiogenesis therapy? *Nat Rev Cancer*. 2:826-835.

Rahimi, N. 2006. Vascular endothelial growth factor receptors: molecular mechanisms of activation and therapeutic potentials. *Experimental eye research*. 83:1005-1016.

Rajantie, I., M. Ilmonen, A. Alminaite, U. Ozerdem, K. Alitalo, and P. Salven. 2004. Adult bone marrow derived cells recruited during angiogenesis comprise precursors for periendothelial vascular mural cells. *Blood*. 104:2084-2086.

Ramjaun, A.R., and K. Hodivala-Dilke. 2009. The role of cell adhesion pathways in angiogenesis. *Int J Biochem Cell Biol*. 41:521-530.

Ramsay, A.G., J.F. Marshall, and I.R. Hart. 2007. Integrin trafficking and its role in cancer metastasis. *Cancer metastasis reviews*. 26:567-578.

Reardon, D.A., K.L. Fink, T. Mikkelsen, T.F. Cloughesy, A. O'Neill, S. Plotkin, M. Glantz, P. Ravin, J.J. Raizer, K.M. Rich, D. Schiff, W.R. Shapiro, S. Burdette-Radoux, E.J. Dropcho, S.M. Wittemer, J. Nippgen, M. Picard, and L.B. Nabors. 2008. Randomized

phase II study of cilengitide, an integrin-targeting arginine-glycine-aspartic acid peptide, in recurrent glioblastoma multiforme. *J Clin Oncol*. 26:5610-5617.

Reynolds, A.R., I.R. Hart, A.R. Watson, J.C. Welti, R.G. Silva, S.D. Robinson, G. Da Violante, M. Gourlaouen, M. Salih, M.C. Jones, D.T. Jones, G. Saunders, V. Kostourou, F. Perron-Sierra, J.C. Norman, G.C. Tucker, and K.M. Hodivala-Dilke. 2009. Stimulation of tumor growth and angiogenesis by low concentrations of RGD-mimetic integrin inhibitors. *Nature medicine*. 15:392-400.

Reynolds, L.E., and K.M. Hodivala-Dilke. 2006. Primary mouse endothelial cell culture for assays of angiogenesis. *Methods Mol Med*. 120:503-509.

Reynolds, L.E., L. Wyder, J.C. Lively, D. Taverna, S.D. Robinson, X. Huang, D. Sheppard, R.O. Hynes, and K.M. Hodivala-Dilke. 2002. Enhanced pathological angiogenesis in mice lacking beta3 integrin or beta3 and beta5 integrins. *Nature medicine*. 8:27-34.

Rhim, A.D., E.T. Mirek, N.M. Aiello, A. Maitra, J.M. Bailey, F. McAllister, M. Reichert, G.L. Beatty, A.K. Rustgi, R.H. Vonderheide, S.D. Leach, and B.Z. Stanger. 2012. EMT and dissemination precede pancreatic tumor formation. *Cell*. 148:349-361.

Richardson, A., and T. Parsons. 1996. A mechanism for regulation of the adhesion-associated proteintyrosine kinase pp125FAK. *Nature*. 380:538-540.

Risau, W. 1997. Mechanisms of angiogenesis. *Nature*. 386:671-674.

Robinson, C.J., and S.E. Stringer. 2001. The splice variants of vascular endothelial growth factor (VEGF) and their receptors. *Journal of cell science*. 114:853-865.

Rolny, C., M. Mazzone, S. Tugues, D. Laoui, I. Johansson, C. Coulon, M.L. Squadrito, I. Segura, X. Li, E. Knevels, S. Costa, S. Vinckier, T. Dresselaer, P. Akerud, M. De Mol, H. Salomaki, M. Phillipson, S. Wyns, E. Larsson, I. Buysschaert, J. Botling, U. Himmelreich, J.A. Van Ginderachter, M. De Palma, M. Dewerchin, L. Claesson-Welsh, and P. Carmeliet. 2011. HRG inhibits tumor growth and metastasis by inducing macrophage polarization and vessel normalization through downregulation of PlGF. *Cancer Cell*. 19:31-44.

Romer, L.H., K.G. Birukov, and J.G. Garcia. 2006. Focal adhesions: paradigm for a signaling nexus. *Circulation research*. 98:606-616.

Rosmarin, A.G., Z. Yang, and K.K. Resendes. 2005. Transcriptional regulation in myelopoiesis: Hematopoietic fate choice, myeloid differentiation, and leukemogenesis. *Experimental hematology*. 33:131-143.

Roy, H., S. Bhardwaj, and S. Yla-Herttuala. 2006. Biology of vascular endothelial growth factors. *FEBS letters*. 580:2879-2887.

Roy, S., P.J. Ruest, and S.K. Hanks. 2002. FAK regulates tyrosine phosphorylation of CAS, paxillin, and PYK2 in cells expressing v-Src, but is not a critical determinant of v-Src transformation. *Journal of cellular biochemistry*. 84:377-388.

Ruest, P.J., N.Y. Shin, T.R. Polte, X. Zhang, and S.K. Hanks. 2001. Mechanisms of CAS substrate domain tyrosine phosphorylation by FAK and Src. *Mol Cell Biol*. 21:7641-7652.

Ruzinova, M.B., R.A. Schoer, W. Gerald, J.E. Egan, P.P. Pandolfi, S. Rafii, K. Manova, V. Mittal, and R. Benezra. 2003. Effect of angiogenesis inhibition by Id loss and the contribution of bone-marrow-derived endothelial cells in spontaneous murine tumors. *Cancer Cell*. 4:277-289.

Ryder, M., R.A. Ghossein, J.C. Ricarte-Filho, J.A. Knauf, and J.A. Fagin. 2008. Increased density of tumor-associated macrophages is associated with decreased survival in advanced thyroid cancer. *Endocr Relat Cancer*. 15:1069-1074.

Sceneay, J., M.T. Chow, A. Chen, H.M. Halse, C.S. Wong, D.M. Andrews, E.K. Sloan, B.S. Parker, D.D. Bowtell, M.J. Smyth, and A. Moller. 2012. Primary Tumor Hypoxia Recruits CD11b+/Ly6Cmed/Ly6G+ Immune Suppressor Cells and Compromises NK Cell Cytotoxicity in the Premetastatic Niche. *Cancer research*.

Schaller, M.D., C.A. Borgman, B.S. Cobb, R.R. Vines, A.B. Reynolds, and J.T. Parsons. 1992. pp125FAK a structurally distinctive protein-tyrosine kinase associated with

focal adhesions. *Proceedings of the National Academy of Sciences of the United States of America*. 89:5192-5196.

Schaller, M.D., C.A. Borgman, and J.T. Parsons. 1993. Autonomous expression of a noncatalytic domain of the focal adhesion-associated protein tyrosine kinase pp125FAK. *Mol Cell Biol*. 13:785-791.

Schaller, M.D., J.D. Hildebrand, and J.T. Parsons. 1999. Complex formation with focal adhesion kinase: A mechanism to regulate activity and subcellular localization of Src kinases. *Mol Biol Cell*. 10:3489-3505.

Schaller, M.D., J.D. Hildebrand, J.D. Shannon, J.W. Fox, R.R. Vines, and J.T. Parsons. 1994. Autophosphorylation of the focal adhesion kinase, pp125FAK, directs SH2-dependent binding of pp60src. *Mol Cell Biol*. 14:1680-1688.

Schaller, M.D., C.A. Otey, J.D. Hildebrand, and J.T. Parsons. 1995. Focal adhesion kinase and paxillin bind to peptides mimicking beta integrin cytoplasmic domains. *The Journal of cell biology*. 130:1181-1187.

Schmidt-Kittler, O., T. Ragg, A. Daskalakis, M. Granzow, A. Ahr, T.J. Blankenstein, M. Kaufmann, J. Diebold, H. Arnholdt, P. Muller, J. Bischoff, D. Harich, G. Schlimok, G. Riethmuller, R. Eils, and C.A. Klein. 2003. From latent disseminated cells to overt metastasis: genetic analysis of systemic breast cancer progression. *Proceedings of the National Academy of Sciences of the United States of America*. 100:7737-7742.

Schultze, A., S. Decker, J. Otten, A.K. Horst, G. Vohwinkel, G. Schuch, C. Bokemeyer, S. Loges, and W. Fiedler. 2010. TAE226-mediated inhibition of focal adhesion kinase interferes with tumor angiogenesis and vasculogenesis. *Invest New Drugs*. 28:825-833.

Scott, L.M., G.V. Priestley, and T. Papayannopoulou. 2003. Deletion of alpha4 integrins from adult hematopoietic cells reveals roles in homeostasis, regeneration, and homing. *Mol Cell Biol*. 23:9349-9360.

Semerad, C.L., M.J. Christopher, F. Liu, B. Short, P.J. Simmons, I. Winkler, J.P. Levesque, J. Chappel, F.P. Ross, and D.C. Link. 2005. G-CSF potently inhibits osteoblast activity and CXCL12 mRNA expression in the bone marrow. *Blood*. 106:3020-3027.

Senger, D.R., K.P. Claffey, J.E. Benes, C.A. Perruzzi, A.P. Sergiou, and M. Detmar. 1997. Angiogenesis promoted by vascular endothelial growth factor: regulation through alpha1beta1 and alpha2beta1 integrins. *Proceedings of the National Academy of Sciences of the United States of America*. 94:13612-13617.

Shalaby, F., J. Rossant, T.P. Yamaguchi, M. Gertsenstein, X.F. Wu, M.L. Breitman, and A.C. Schuh. 1995. Failure of blood-island formation and vasculogenesis in Flk-1-deficient mice. *Nature*. 376:62-66.

Shen, T.L., A.Y. Park, A. Alcaraz, X. Peng, I. Jang, P. Koni, R.A. Flavell, H. Gu, and J.L. Guan. 2005. Conditional knockout of focal adhesion kinase in endothelial cells reveals its role in angiogenesis and vascular development in late embryogenesis. *The Journal of cell biology*. 169:941-952.

Shi, C., J. Lu, W. Wu, F. Ma, J. Georges, H. Huang, J. Balducci, Y. Chang, and Y. Huang. 2011. Endothelial cell-specific molecule 2 (ECSM2) localizes to cell-cell junctions and modulates bFGF-directed cell migration via the ERK-FAK pathway. *PloS one*. 6:e21482.

Shinkai, Y., G. Rathbun, K.P. Lam, E.M. Oltz, V. Stewart, M. Mendelsohn, J. Charron, M. Datta, F. Young, A.M. Stall, and *et al*. 1992. RAG-2-deficient mice lack mature lymphocytes owing to inability to initiate V(D)J rearrangement. *Cell*. 68:855-867.

Shipitsin, M., L.L. Campbell, P. Argani, S. Weremowicz, N. Bloushtain-Qimron, J. Yao, T. Nikolskaya, T. Serebryiskaya, R. Beroukhim, M. Hu, M.K. Halushka, S. Sukumar, L.M. Parker, K.S. Anderson, L.N. Harris, J.E. Garber, A.L. Richardson, S.J. Schnitt, Y. Nikolsky, R.S. Gelman, and K. Polyak. 2007. Molecular definition of breast tumor heterogeneity. *Cancer Cell*. 11:259-273.

Shojaei, F., and N. Ferrara. 2008. Refractoriness to antivascular endothelial growth factor treatment: role of myeloid cells. *Cancer research*. 68:5501-5504.

Shojaei, F., X. Wu, C. Zhong, L. Yu, X.H. Liang, J. Yao, D. Blanchard, C. Bais, F.V. Peale, N. van Bruggen, C. Ho, J. Ross, M. Tan, R.A. Carano, Y.G. Meng, and N. Ferrara. 2007. Bv8 regulates myeloid-cell-dependent tumour angiogenesis. *Nature*. 450:825-831.

Sica, A., P. Larghi, A. Mancino, L. Rubino, C. Porta, M.G. Totaro, M. Rimoldi, S.K. Biswas, P. Allavena, and A. Mantovani. 2008. Macrophage polarization in tumour progression. *Semin Cancer Biol*. 18:349-355.

Sieg, D.J., C.R. Hauck, D. Ilic, C.K. Klingbeil, E. Schaefer, C.H. Damsky, and D.D. Schlaepfer. 2000. FAK integrates growth-factor and integrin signals to promote cell migration. *Nat Cell Biol*. 2:249-256.

Sieg, D.J., C.R. Hauck, and D.D. Schlaepfer. 1999. Required role of focal adhesion kinase (FAK) for integrin-stimulated cell migration. *Journal of cell science*. 112 (Pt 16):2677-2691.

Singh, S.K., C. Hawkins, I.D. Clarke, J.A. Squire, J. Bayani, T. Hide, R.M. Henkelman, M.D. Cusimano, and P.B. Dirks. 2004. Identification of human brain tumour initiating cells. *Nature*. 432:396-401.

Soker, S., S. Takashima, H.Q. Miao, G. Neufeld, and M. Klagsbrun. 1998. Neuropilin-1 is expressed by endothelial and tumor cells as an isoform-specific receptor for vascular endothelial growth factor. *Cell*. 92:735-745.

Soligo, D., R. Schiro, R. Luksch, G. Manara, N. Quirici, C. Parravicini, and G. Lambertenghi Deliliers. 1990. Expression of integrins in human bone marrow. *Br J Haematol*. 76:323-332.

Soriano, P. 1999. Generalized lacZ expression with the ROSA26 Cre reporter strain. *Nat Genet*. 21:70-71.

Soucek, L., E.R. Lawlor, D. Soto, K. Shchors, L.B. Swigart, and G.I. Evan. 2007. Mast cells are required for angiogenesis and macroscopic expansion of Myc-induced pancreatic islet tumors. *Nature medicine*. 13:1211-1218.

Spangrude, G.J., S. Heimfeld, and I.L. Weissman. 1988. Purification and characterization of mouse hematopoietic stem cells. *Science*. 241:58-62.

Spicer, J.D., B. McDonald, J.J. Cools-Lartigue, S.C. Chow, B. Giannias, P. Kubes, and L.E. Ferri. 2012. Neutrophils promote liver metastasis via Mac-1 mediated interactions with circulating tumor cells. *Cancer research*.

Srinivas, S., T. Watanabe, C.S. Lin, C.M. William, Y. Tanabe, T.M. Jessell, and F. Costantini. 2001. Cre reporter strains produced by targeted insertion of EYFP and ECFP into the ROSA26 locus. *BMC Dev Biol*. 1:4.

Stappert, J., and R. Kemler. 1994. A short core region of E-cadherin is essential for catenin binding and is highly phosphorylated. *Cell Adhes Commun*. 2:319-327.

Stoeltzing, O., W. Liu, N. Reinmuth, F. Fan, G.C. Parry, A.A. Parikh, M.F. McCarty, C.D. Bucana, A.P. Mazar, and L.M. Ellis. 2003. Inhibition of integrin alpha5beta1 function with a small peptide (ATN-161) plus continuous 5-FU infusion reduces colorectal liver metastases and improves survival in mice. *International journal of cancer. Journal international du cancer*. 104:496-503.

Stokes, J.B., S.J. Adair, J.K. Slack-Davis, D.M. Walters, R.W. Tilghman, E.D. Hershey, B. Lowrey, K.S. Thomas, A.H. Bouton, R.F. Hwang, E.B. Stelow, J.T. Parsons, and T.W. Bauer. 2011. Inhibition of focal adhesion kinase by PF-562,271 inhibits the growth and metastasis of pancreatic cancer concomitant with altering the tumor microenvironment. *Mol Cancer Ther*. 10:2135-2145.

Stupp, R., M.E. Hegi, B. Neyns, R. Goldbrunner, U. Schlegel, P.M. Clement, G.G. Grabenbauer, A.F. Ochsenbein, M. Simon, P.Y. Dietrich, T. Pietsch, C. Hicking, J.C. Tonn, A.C. Diserens, A. Pica, M. Hermisson, S. Krueger, M. Picard, and M. Weller. 2010. Phase I/IIa study of cilengitide and temozolomide with concomitant

radiotherapy followed by cilengitide and temozolomide maintenance therapy in patients with newly diagnosed glioblastoma. *J Clin Oncol*. 28:2712-2718.
Sugiyama, T., H. Kohara, M. Noda, and T. Nagasawa. 2006. Maintenance of the hematopoietic stem cell pool by CXCL12-CXCR4 chemokine signaling in bone marrow stromal cell niches. *Immunity*. 25:977-988.
Sun, J.C., and L.L. Lanier. 2011. NK cell development, homeostasis and function: parallels with CD8(+) T cells. *Nat Rev Immunol*. 11:645-657.
Sun, X., G. Cheng, M. Hao, J. Zheng, X. Zhou, J. Zhang, R.S. Taichman, K.J. Pienta, and J. Wang. 2010. CXCL12 / CXCR4 / CXCR7 chemokine axis and cancer progression. *Cancer metastasis reviews*. 29:709-722.
Suzuki, M., E.S. Mose, V. Montel, and D. Tarin. 2006. Dormant cancer cells retrieved from metastasis-free organs regain tumorigenic and metastatic potency. *The American journal of pathology*. 169:673-681.
Takizawa, H., R.R. Regoes, C.S. Boddupalli, S. Bonhoeffer, and M.G. Manz. 2011. Dynamic variation in cycling of hematopoietic stem cells in steady state and inflammation. *The Journal of experimental medicine*. 208:273-284.
Talmadge, J.E., and I.J. Fidler. 2010. AACR centennial series: the biology of cancer metastasis: historical perspective. *Cancer research*. 70:5649-5669.
Tammela, T., and K. Alitalo. 2010. Lymphangiogenesis: Molecular mechanisms and future promise. *Cell*. 140:460-476.
Tavora, B., S. Batista, L.E. Reynolds, S. Jadeja, S. Robinson, V. Kostourou, I. Hart, M. Fruttiger, M. Parsons, and K.M. Hodivala-Dilke. 2010. Endothelial FAK is required for tumour angiogenesis. *EMBO Mol Med*. 2:516-528.
Taylor, J.M., C.P. Mack, K. Nolan, C.P. Regan, G.K. Owens, and J.T. Parsons. 2001. Selective expression of an endogenous inhibitor of FAK regulates proliferation and migration of vascular smooth muscle cells. *Mol Cell Biol*. 21:1565-1572.
ten Dijke, P., and H.M. Arthur. 2007. Extracellular control of TGFbeta signalling in vascular development and disease. *Nature reviews. Molecular cell biology*. 8:857-869.
Thomas, E.D., H.L. Lochte, Jr., W.C. Lu, and J.W. Ferrebee. 1957. Intravenous infusion of bone marrow in patients receiving radiation and chemotherapy. *N Engl J Med*. 257:491-496.
Thomlinson, R.H. 1977. Hypoxia and tumours. *J Clin Pathol Suppl (R Coll Pathol)*. 11:105-113.
Thurston, G., J.S. Rudge, E. Ioffe, H. Zhou, L. Ross, S.D. Croll, N. Glazer, J. Holash, D.M. McDonald, and G.D. Yancopoulos. 2000. Angiopoietin-1 protects the adult vasculature against plasma leakage. *Nature medicine*. 6:460-463.
Till, J.E., and E.A. McCulloch. 1961. A direct measurement of the radiation sensitivity of normal mouse bone marrow cells. *Radiat Res*. 14:213-222.
Tong, R.T., Y. Boucher, S.V. Kozin, F. Winkler, D.J. Hicklin, and R.K. Jain. 2004. Vascular normalization by vascular endothelial growth factor receptor 2 blockade induces a pressure gradient across the vasculature and improves drug penetration in tumors. *Cancer research*. 64:3731-3736.
Tremblay, L., W. Hauck, A.G. Aprikian, L.R. Begin, A. Chapdelaine, and S. Chevalier. 1996. Focal adhesion kinase (pp125FAK) expression, activation and association with paxillin and p50CSK in human metastatic prostate carcinoma. *International journal of cancer. Journal international du cancer*. 68:164-171.
Tsou, C.L., W. Peters, Y. Si, S. Slaymaker, A.M. Aslanian, S.P. Weisberg, M. Mack, and I.F. Charo. 2007. Critical roles for CCR2 and MCP-3 in monocyte mobilization from bone marrow and recruitment to inflammatory sites. *The Journal of clinical investigation*. 117:902-909.
Turner, C.E., J.R. Glenney, Jr., and K. Burridge. 1990. Paxillin: a new vinculin-binding protein present in focal adhesions. *The Journal of cell biology*. 111:1059-1068.

Ueha, S., F.H. Shand, and K. Matsushima. 2011. Myeloid cell population dynamics in healthy and tumor-bearing mice. *Int Immunopharmacol*. 11:783-788.

Van Aarsen, L.A., D.R. Leone, S. Ho, B.M. Dolinski, P.E. McCoon, D.J. LePage, R. Kelly, G. Heaney, P. Rayhorn, C. Reid, K.J. Simon, G.S. Horan, N. Tao, H.A. Gardner, M.M. Skelly, A.M. Gown, G.J. Thomas, P.H. Weinreb, S.E. Fawell, and S.M. Violette. 2008. Antibody-mediated blockade of integrin alpha v beta 6 inhibits tumor progression in vivo by a transforming growth factor-beta-regulated mechanism. *Cancer research*. 68:561-570.

van Buul, J.D., E.C. Anthony, M. Fernandez-Borja, K. Burridge, and P.L. Hordijk. 2005. Proline-rich tyrosine kinase 2 (Pyk2) mediates vascular endothelial-cadherin-based cell-cell adhesion by regulating beta-catenin tyrosine phosphorylation. *The Journal of biological chemistry*. 280:21129-21136.

van Deventer, H.W., J.S. Serody, K.P. McKinnon, C. Clements, W.J. Brickey, and J.P. Ting. 2002. Transfection of macrophage inflammatory protein 1 alpha into B16 F10 melanoma cells inhibits growth of pulmonary metastases but not subcutaneous tumors. *J Immunol*. 169:1634-1639.

Vemula, S., B. Ramdas, P. Hanneman, J. Martin, H.E. Beggs, and R. Kapur. 2010. Essential role for focal adhesion kinase in regulating stress hematopoiesis. *Blood*. 116:4103-4115.

Vooijs, M., J. Jonkers, and A. Berns. 2001. A highly efficient ligand-regulated Cre recombinase mouse line shows that LoxP recombination is position dependent. *EMBO Rep*. 2:292-297.

Walsh, C., I. Tanjoni, S. Uryu, A. Tomar, J.O. Nam, H. Luo, A. Phillips, N. Patel, C. Kwok, G. McMahon, D.G. Stupack, and D.D. Schlaepfer. 2010. Oral delivery of PND-1186 FAK inhibitor decreases tumor growth and spontaneous breast to lung metastasis in pre-clinical models. *Cancer Biol Ther*. 9:778-790.

Wang, D., J.R. Grammer, C.S. Cobbs, J.E. Stewart, Jr., Z. Liu, R. Rhoden, T.P. Hecker, Q. Ding, and C.L. Gladson. 2000. p125 focal adhesion kinase promotes malignant astrocytoma cell proliferation in vivo. *Journal of cell science*. 113 Pt 23:4221-4230.

Wang, H., and J.A. Keiser. 1998. Vascular endothelial growth factor upregulates the expression of matrix metalloproteinases in vascular smooth muscle cells: role of flt-1. *Circulation research*. 83:832-840.

Watson, A.R., S.C. Pitchford, L.E. Reynolds, N. Direkze, M. Brittan, M.R. Alison, S. Rankin, N.A. Wright, and K.M. Hodivala-Dilke. 2009. Deficiency of bone marrow beta3-integrin enhances non-functional neovascularization. *J Pathol*.

Weinberg, R. 2007. The Biology of Cancer. Garland Science, New York.

Weis, S.M., S.T. Lim, K.M. Lutu-Fuga, L.A. Barnes, X.L. Chen, J.R. Gothert, T.L. Shen, J.L. Guan, D.D. Schlaepfer, and D.A. Cheresh. 2008. Compensatory role for Pyk2 during angiogenesis in adult mice lacking endothelial cell FAK. *The Journal of cell biology*. 181:43-50.

Weiss, L. 1990. Metastatic inefficiency. *Adv Cancer Res*. 54:159-211.

Wengner, A.M., S.C. Pitchford, R.C. Furze, and S.M. Rankin. 2008. The coordinated action of G-CSF and ELR + CXC chemokines in neutrophil mobilization during acute inflammation. *Blood*. 111:42-49.

Wilson, A., E. Laurenti, G. Oser, R.C. van der Wath, W. Blanco-Bose, M. Jaworski, S. Offner, C.F. Dunant, L. Eshkind, E. Bockamp, P. Lio, H.R. Macdonald, and A. Trumpp. 2008. Hematopoietic stem cells reversibly switch from dormancy to self-renewal during homeostasis and repair. *Cell*. 135:1118-1129.

Wilson, A., M.J. Murphy, T. Oskarsson, K. Kaloulis, M.D. Bettess, G.M. Oser, A.C. Pasche, C. Knabenhans, H.R. Macdonald, and A. Trumpp. 2004. c-Myc controls the balance between hematopoietic stem cell self-renewal and differentiation. *Genes Dev*. 18:2747-2763.

Wright, D.E., A.J. Wagers, A.P. Gulati, F.L. Johnson, and I.L. Weissman. 2001. Physiological migration of hematopoietic stem and progenitor cells. *Science*. 294:1933-1936.

Wyckoff, J.B., J.G. Jones, J.S. Condeelis, and J.E. Segall. 2000. A critical step in metastasis: in vivo analysis of intravasation at the primary tumor. *Cancer research*. 60:2504-2511.

Xing, Z., H.C. Chen, J.K. Nowlen, S.J. Taylor, D. Shalloway, and J.L. Guan. 1994. Direct interaction of v-Src with the focal adhesion kinase mediated by the Src SH2 domain. *Mol Biol Cell*. 5:413-421.

Yan, H.H., M. Pickup, Y. Pang, A.E. Gorska, Z. Li, A. Chytil, Y. Geng, J.W. Gray, H.L. Moses, and L. Yang. 2010. Gr-1+CD11b+ myeloid cells tip the balance of immune protection to tumor promotion in the premetastatic lung. *Cancer research*. 70:6139-6149.

Yancopoulos, G.D., S. Davis, N.W. Gale, J.S. Rudge, S.J. Wiegand, and J. Holash. 2000. Vascular-specific growth factors and blood vessel formation. *Nature*. 407:242-248.

Yang, J.C., L. Haworth, R.M. Sherry, P. Hwu, D.J. Schwartzentruber, S.L. Topalian, S.M. Steinberg, H.X. Chen, and S.A. Rosenberg. 2003. A randomized trial of bevacizumab, an anti-vascular endothelial growth factor antibody, for metastatic renal cancer. *N Engl J Med*. 349:427-434.

Yang, J.T., H. Rayburn, and R.O. Hynes. 1993. Embryonic mesodermal defects in alpha 5 integrin-deficient mice. *Development*. 119:1093-1105.

Yang, L., J. Huang, X. Ren, A.E. Gorska, A. Chytil, M. Aakre, D.P. Carbone, L.M. Matrisian, A. Richmond, P.C. Lin, and H.L. Moses. 2008. Abrogation of TGF beta signaling in mammary carcinomas recruits Gr-1+CD11b+ myeloid cells that promote metastasis. *Cancer Cell*. 13:23-35.

Yoder, M.C. 2002. Embryonic hematopoiesis in mice and humans. *Acta Paediatr Suppl*. 91:5-8.

Yoshida, D., K. Kim, M. Noha, and A. Teramoto. 2006. Hypoxia inducible factor 1-alpha regulates of platelet derived growth factor-B in human glioblastoma cells. *J Neurooncol*. 76:13-21.

Zachary, I., and G. Gliki. 2001. Signaling transduction mechanisms mediating biological actions of the vascular endothelial growth factor family. *Cardiovascular research*. 49:568-581.

Zambrowicz, B.P., A. Imamoto, S. Fiering, L.A. Herzenberg, W.G. Kerr, and P. Soriano. 1997. Disruption of overlapping transcripts in the ROSA beta geo 26 gene trap strain leads to widespread expression of beta-galactosidase in mouse embryos and hematopoietic cells. *Proceedings of the National Academy of Sciences of the United States of America*. 94:3789-3794.

Zhang, J., C. Niu, L. Ye, H. Huang, X. He, W.G. Tong, J. Ross, J. Haug, T. Johnson, J.Q. Feng, S. Harris, L.M. Wiedemann, Y. Mishina, and L. Li. 2003. Identification of the haematopoietic stem cell niche and control of the niche size. *Nature*. 425:836-841.

Zhang, J., L. Patel, and K.J. Pienta. 2010a. CC chemokine ligand 2 (CCL2) promotes prostate cancer tumorigenesis and metastasis. *Cytokine & growth factor reviews*. 21:41-48.

Zhang, J., L. Patel, and K.J. Pienta. 2010b. Targeting chemokine (C-C motif) ligand 2 (CCL2) as an example of translation of cancer molecular biology to the clinic. *Progress in molecular biology and translational science*. 95:31-53.

Zheng, Y., Y. Xia, D. Hawke, M. Halle, M.L. Tremblay, X. Gao, X.Z. Zhou, K. Aldape, M.H. Cobb, K. Xie, J. He, and Z. Lu. 2009. FAK phosphorylation by ERK primes ras-induced tyrosine dephosphorylation of FAK mediated by PIN1 and PTP-PEST. *Mol Cell*. 35:11-25.

Zhu, X.D., J.B. Zhang, P.Y. Zhuang, H.G. Zhu, W. Zhang, Y.Q. Xiong, W.Z. Wu, L. Wang, Z.Y. Tang, and H.C. Sun. 2008. High expression of macrophage colony-stimulating

factor in peritumoral liver tissue is associated with poor survival after curative resection of hepatocellular carcinoma. *J Clin Oncol*. 26:2707-2716.

Ziegler, B.L., M. Valtieri, G.A. Porada, R. De Maria, R. Muller, B. Masella, M. Gabbianelli, I. Casella, E. Pelosi, T. Bock, E.D. Zanjani, and C. Peschle. 1999. KDR receptor: a key marker defining hematopoietic stem cells. *Science*. 285:1553-1558.